Aspects of the plasma modification of polymeric materials

Walker, Susan Ann

A thesis entitled

ASPECTS OF THE PLASMA MODIFICATION OF POLYMERIC MATERIALS

by

Susan Ann Walker, B.Sc Hons. (Dunelm)

A candidate for the degree of Doctor of Philosophy

St. Mary's College,
University of Durham.

May 1990

To Glen and my Parents

MEMORANDUM

The work described in this thesis was carried out at the University of Durham between October 1987 and May 1990. It is the original work of the author, except where acknowledged by reference, and has not been submitted for any other degree.

Some of the work in this thesis has formed the subject of the following publication:

"An investigation of the Ageing of Plasma Oxidised PEEK," W.J. Brennan, W.J. Feast, H.S. Munro and S.A. Walker, Polymer, submitted.

Some of the work in this thesis has been presented at the following meetings:

ICI Materials Centre Symposium, Collaborative Projects in Polymers Synthesis and Properties. ICI, Wilton, Middlesbrough. 20-22 April 1988, "Plasma Modification of Carbon Fibres," H.S. Munro and S.A. Walker.

9th International Symposium on Plasma Chemistry, Pugnochiuso, Italy, 4-8 September 1989, "An Investigation of the Ageing of Plasma Oxidised Peek,"W.J. Brennan, W.J. Feast, H.S. Munro and S.A. Walker.

ABSTRACT

The effect of orientation and crystallinity of certain polymers, polyethylene, polypropylene, polyethylene terephthalate (PET) and poly (ether ether ketone) (PEEK), upon the extent and nature of plasma oxidation was studied. It was found that increasing the extent of surface ordering lessened susceptibility to plasma oxidation and reduced the subsequent decay of surface treatment.

The surface ageing of plasma oxidised PEEK was extensively studied with regards to the transient increase in hydrophilicity that has been observed after plasma modification. The decay and transient increase in hydrophilicity were found to be dependent upon crystallinity and storage temperature. An estimate of the activation energies for processes leading to the increase in contact angle after plasma modification were calculated and found to suggest that these processes were rotational reorganisations at the surface as opposed to migrational reorganisations. The decay of other plasma modified surfaces revealed that plasma oxidised PET and plasma fluorinated PEEK both underwent transitional reorganisations at the surface, however no such change was observed for ammonia plasma treated PEEK.

Plasma modification of carbon fibres was investigated with regards to improving composite performance. Microwave plasma treatments were found to be as good as standard commercial treatments. Graphitic carbon was investigated as a model for carbon fibre surfaces, however, the plasma modified surface was found to age more readily and to be too labile for useful comparison.

ACKNOWLEDGEMENTS

I wish to thank my supervisors from academia, Prof. W. J. Feast and Dr. H. S. Munro, and from industry Dr. W. J. Brennan for their help and enthusiasm during this work. Also ICI, Wilton for the provision of a research grant, many materials and use of equipment at the Wilton Materials Research Centre.

I am indebted to Drs. C. Till and C. Davis for their work on the plasma modification of carbon fibres which was the basis for the work in Chapter 5. I would also like to thank the other members of the Surface Science Group at the University of Durham, Ian McBriar, Richard Ward, Alex Shard, Jas Pal Badyal, Sonia Watkinson and Graham Eyre for their helpful discussions.

I am particularly indebted to Dr. D. Briggs for recording all the SIMS spectra shown in this thesis and to his and Dr. W.J. Brennan's advice on their interpretation. Many thanks are also due to Dr. J. Yarwood, Dr. H. Ancelin and Ms M. Vaughan for the recording of the infra-red spectra and advice on their interpretation.

Many thanks are also due to the people who provided the excellent technical support during this work: George Rowe, Tony Royston, Elizabeth Wood and Glyn Metcalfe.

Last but not least I would like to thank my husband Glen, without whose encouragement and support this thesis would never have been completed.

CONTENTS

		Page Number
MEMORANDUM		3
ABSTRACT		4
ACKNOWLEDGEMENTS		4
CONTENTS		6
CHAPTER ONE:	SURFACE MODIFICATION OF POLYMERS	11
1.1	INTRODUCTION	12
1.2	PLASMAS	17
	1.2.1 INTRODUCTION	17
	1.2.2 FUNDAMENTAL ASPECTS OF PLASMAS	22
	1.2.3 PLASMA TECHNIQUES	26
1.3	TECHNIQUES FOR SURFACE CHARACTERISATION	29
	1.3.1 CONTACT ANGLES	31
	1.3.2 SURFACE SPECTROSCOPIES	34
REFERENCES		39
CHAPTER TWO: AN INVESTIGATION INTO THE EFFECTS OF POLYMER ORIENTATION AND CRYSTALLINITY UPON THE EXTENT AND NATURE OF PLASMA OXIDATION.		44
2.1	INTRODUCTION	45
2.2	EXPERIMENTAL	46
	2.2.1 MATERIALS	46
	2.2.2 INFRA-RED SPECTROSCOPY	49
	2.2.3 XPS ANALYSIS	50
	2.2.4 PLASMA MODIFICATION	51
	2.2.5 CONTACT ANGLE MEASUREMENTS	51
	2.2.6 SEM	51
2.3	EFFECT OF ORIENTATION ON POLYETHYLENE	52

2.3.1 INFRA-RED STUDIES OF DRAWN POLYETHYLENE 52
2.3.2 PLASMA MODIFICATION OF DRAWN AND UNDRAWN POLYETHYLENE 61
2.3.3 CONCLUSIONS 65
2.4 EFFECT OF BIAXIAL ORIENTATION ON POLYPROPYLENE 66
2.4.1 INFRA-RED STUDIES OF POLYPROPYLENE 66
2.4.2 PLASMA MODIFICATION OF POLYPROPYLENE 68
2.4.3 CONCLUSIONS 70
2.5 PLASMA ETCHING OF POLYMERS 70
2.5.1 XPS ANALYSIS OF PEEK AND PET 71
2.5.2 PLASMA ETCHING OF PEEK AND PET 72
2.5.3 CONCLUSION 75
2.6 DISCUSSION 75
REFERENCES 78
CHAPTER THREE: AN INVESTIGATION INTO THE AGEING OF PLASMA MODIFIED PEEK. 80
3.1 INTRODUCTION 81
3.2 EXPERIMENTAL 82
3.2.1 MATERIALS 82
3.2.2 PLASMA TREATMENT 82
3.2.3 CONTACT ANGLES 82
3.2.4 XPS 83
3.2.5 SIMS 83
3.3 PLASMA MODIFICATION OF PEEK 84
3.3.1 INITIAL EFFECTS OF TREATMENT 84
3.3.2 CONTACT ANGLE DECAY OF PLASMA MODIFIED PEEK 86

3.3.3 XPS ANALYSIS OF THE AGEING OF PLASMA MODIFIED PEEK 88
3.3.4 SIMS ANALYSIS OF THE AGEING OF PLASMA MODIFIED PEEK 90
3.3.5 CONCLUSIONS 92
3.4 CALCULATION OF YASUDA'S MOBILITY PARAMETER 93
3.4.1 INTRODUCTION 93
3.4.2 RESULTS AND CONCLUSIONS 96
3.5 KINETIC ANALYSIS 99
3.5.1 THEORY 99
3.5.2 ANALYSIS OF DATA 105
3.5.3 CONCLUSIONS 108
3.6 DISCUSSION 108
REFERENCES 114
APPENDIX 3.1 116
APPENDIX 3.2 124
APPENDIX 3.3 135
CHAPTER FOUR: FURTHER STUDIES ON THE AGEING OF PLASMA MODIFIED SURFACES 143
4.1 INTRODUCTION 144
4.2 EXPERIMENTAL 145
4.2.1 MATERIALS 145
4.2.2 PLASMA MODIFICATION 145
4.2.3 XPS MEASUREMENTS 147
4.2.4 CONTACT ANGLE MEASUREMENTS 147
4.2.5 SIMS MEASUREMENTS 147
4.3 PLASMA OXIDATION OF PET 148
4.4 PLASMA FLUORINATION OF PEEK 150

4.5 PLASMA MODIFICATION OF PEEK USING AN AMMONIA PLASMA 156

4.6 DISCUSSION 159

REFERENCES 161

CHAPTER FIVE: PLASMA MODIFICATION OF CARBON FIBRES 162

5.1 INTRODUCTION 163

5.1.1 COMPOSITES 163

5.1.2 CARBON FIBRES 164

5.1.3 COMPOSITE TESTING 166

5.1.4 XPS STUDIES OF CARBON FIBRES 167

5.2 EXPERIMENTAL 172

5.2.1 MATERIALS 172

5.2.2 PLASMA MODIFICATION 172

5.2.3 XPS ANALYSIS 176

5.2.4 CONTACT ANGLE MEASUREMENTS 178

5.2.5 COMPOSITE MANUFACTURE AND TESTING 179

5.3 PLASMA MODIFICATION OF CARBON FIBRES 182

5.3.1 INTRODUCTION 182

5.3.2 RESULTS 183

5.3.2.1 MICROWAVE TREATMENT 183

5.3.2.2 LABELLING 185

5.3.2.3 RF PLASMA TREATMENT 187

5.4 COMPOSITE TESTING 190

5.4.1 MICROWAVE PLASMA TREATED FIBRES 190

5.4.2 RADIOFREQUENCY PLASMA TREATED FIBRES 192

5.4.3 EFFECT OF HUMIDITY 193

5.5 CONTACT ANGLE MEASUREMENTS ON CARBON FIBRES 194

5.6 PLASMA MODIFICATION OF GRAPHITE 197

5.6.1 INTRODUCTION 197

5.6.2 PLASMA MODIFICATION 200

5.7 DISCUSSION 202

REFERENCES 208

APPENDIX 1 210

APPENDIX 2 211

CHAPTER ONE

SURFACE MODIFICATION OF POLYMERS

1.1 INTRODUCTION

Before the introduction of synthetic materials for making fabrics, films and solid objects, the only available materials were natural or modified natural products. These natural materials have been selected for reasons of availability and suitable, strength, flexibility, wear and other physical properties. However the aesthetic appearance and texture of a material is important and the ability of a surface to accept dyes, paint, inks or adhesives is often a requirement.

The latter half of this century has seen the introduction on a large scale of many advanced materials, for example polymers and composites.[1,2] These have come into widespread use for several reasons including: their ease of processing and cheapness compared to conventional materials, and their bulk characteristics such as, good strength to weight ratios, which are not readily obtainable from traditional materials. Many of these materials have no inherent characteristic appearance or texture, these properties can be varied depending upon techniques employed during the manufacturing process. However many synthetic materials do not possess inherently useful surface properties, such as wettability with inks and adhesives or anti-soil, by contrast, properties. In polymers such shortcomings arise from a lack of appropriate groups, either hydrophilic[3] or hydrophobic, at the surface. This situation could be overcome by a surface treatment which introduced suitable chemical functionalities at the polymer surface. In response to the aesthetic and

technological demands outlined above, surface modification techniques have become important in a range of material applications.[4] The main thrust of the work reported aimed at increasing the polarity of the surface.

One of the first attempts to modify polymer surfaces used chlorine,[5] but due to economic and technical reasons the process was soon abandoned in favour of more efficient techniques. Exposure to ozone and ultra-violet radiation has been investigated[6] but the process was found to be rather slow. Oxidation by chromic acid solutions[7] is very effective but suffers from the drawback of the hazardous nature of the chemicals, their possible inclusion in the bulk polymer, and the need for washing and drying the treated polymer, and disposal of waste reagents. It is, therefore, not suitable for large scale use but it does have the advantage that the whole surface is treated at once and the surfaces of complicated three-dimensional objects can be treated effectively.

Treatment of hydrocarbons using chromium VI oxide in a mixture of acetic acid and acetic anhydride, has been used as a means of hydroxylating polymers in solution.[8] This reaction can be applied directly to the substrate surface, in the case of polypropylene this results in a reduction in the contact angle with water of 10° after 10 hours.[9] However this process breaks up the polymer structure and the dissolution of modified polymer causes significant weight loss during the reaction.

Even relatively inert materials can be treated using conventional chemical techniques. Polytetrafluoroethene (PTFE) has been treated using a variety of lithium reagents to insert alcohol, aldehyde and carboxylic acid groups into the surface.[10] As an alternative to direct reaction with the surface recent work[11] has utilised the reduction and crosslinking capacity of the benzoin dianion to produce a thin coating attached to the PTFE. This layer can then be reacted further to give specific functionalities such as halogen, hydroxyl, amino and carboxylic acid groups. The advantages of this technique are that the reaction time is only 15 minutes and the thickness of the modified layer can be controlled down to a minimum of 150 Å.

With solution state techniques there is always a concern that solvents or reagents may be absorbed into the polymer and may migrate or be leached out during end product usage. This will not necessarily be a problem for some end product uses, but many potential applications would be inhibited by such possibilities and a careful post treatment purification would be required.

The aim of various thermal treatments is to heat the surface of the material, using hot air, infra-red radiation or direct application of a flame, whilst keeping the bulk of the material at an ambient temperature. This is extremely difficult in the case of small objects or thin films. Additionally the extent of treatment is not easily controlled and generally causes oxidation extending into the bulk of the sample.[12-16]

The large scale method which is now commonly used for

plastic film is that of corona discharge. The actual mechanics of this technique are very simple and make it ideal for continuous processing[17,18,19] (see Figure 1.1). A corona is produced by

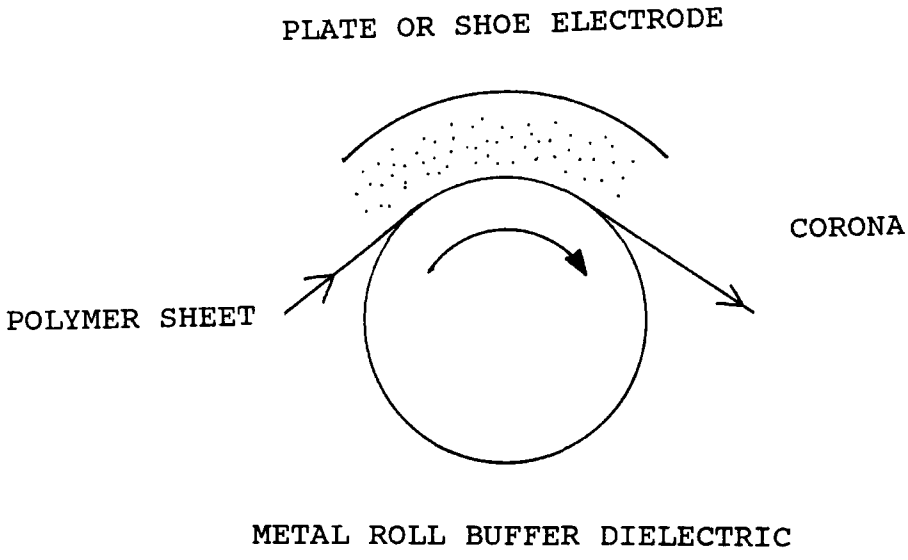

Figure 1.1 Continuous Corona Treatment of Polymer Film.

setting up an electric field between two electrodes under the appropriate power and pressure conditions. Often this means using a discharge in air at atmospheric pressure. The discharge can be induced by either a direct or alternating current and provided that the gap between the electrodes is sufficiently small these will have the same effect. Whilst this technique is quick and solvent free, control of the chemistry of the modification is difficult and heating of the substrate may occur.

The plasma treatment of polymers has been the subject of considerable research.[20] The major virtues of this technique are that it involves clean reactions and takes only seconds to

achieve the result desired, producing profound changes in the surface properties of the material. Additionally the overall bulk properties (optical and electrical characteristics, tensile strength, etc.) for which the polymer was originally chosen remain unchanged. Though a vacuum system is required the operating pressures are moderate (0.1-0.01 torr) and therefore the necessary equipment is relatively inexpensive. The lack of solvents in the process means that reactants are unlikely to be absorbed into the polymer and later released. With careful control of the plasma conditions undue heating or ablation of the substrate can be avoided and the technique can be adapted to either batch or continuous processing.[4] In the case of a plasma modification the thickness of the modified layer has been estimated to only extend up to 10um[20] depending on the conditions of the plasma (pressure, power, gas, flow rate). However the surface properties of a polymer sample are determined solely by the composition of the outermost few monolayers, which means that the surface chemistry of a treated sample is effectively governed by the modified material.

A drawback of plasma oxidation and corona discharge treatments of polymers is that after treatment it has been found that the enhanced properties initially achieved deteriorate over a period ranging from a few days to several weeks, until reaching an equilibrium value.[21,22,23] It has been suggested that this decrease in hydrophilicity is due to a combination of two processes.[21,22] One involves rotation of surface polar groups into the bulk of the material to reduce the surface energy. The

other is due to the migration of low molecular weight, polar fragments into the polymer matrix. Yasuda and Yasuda's work on the plasma fluorination of polymers[24,25] shows that after treatment, surface fluorination decreases when samples are stored in water. Subsequent drying and heating restored the surface to a similar condition to the freshly treated material, this may be interpreted on the basis that the surface modification is not lost to the external environment during the ageing process, and it is a physical not a chemical ageing.

1.2 PLASMAS

1.2.1 INTRODUCTION

A plasma is defined as a wholly or partially ionised gas, and is sometimes referred to as the fourth state of matter. A plasma generally consists of molecules, atoms and ions in both ground and excited states (including metastable states), and electrons, such that the concentration of positively and negatively charged species results in close to overall electrical neutrality. Plasmas occur in nature and in the laboratory in many different forms which can be characterised by their electron density and their average electron energy[26] (see Figure 1.2). Examples of naturally occurring plasmas include stars, such as the sun, interplanetary space, the aurora borealis and the aurora australis. In the laboratory plasmas may be produced using electrical discharges, electron beams or lasers.

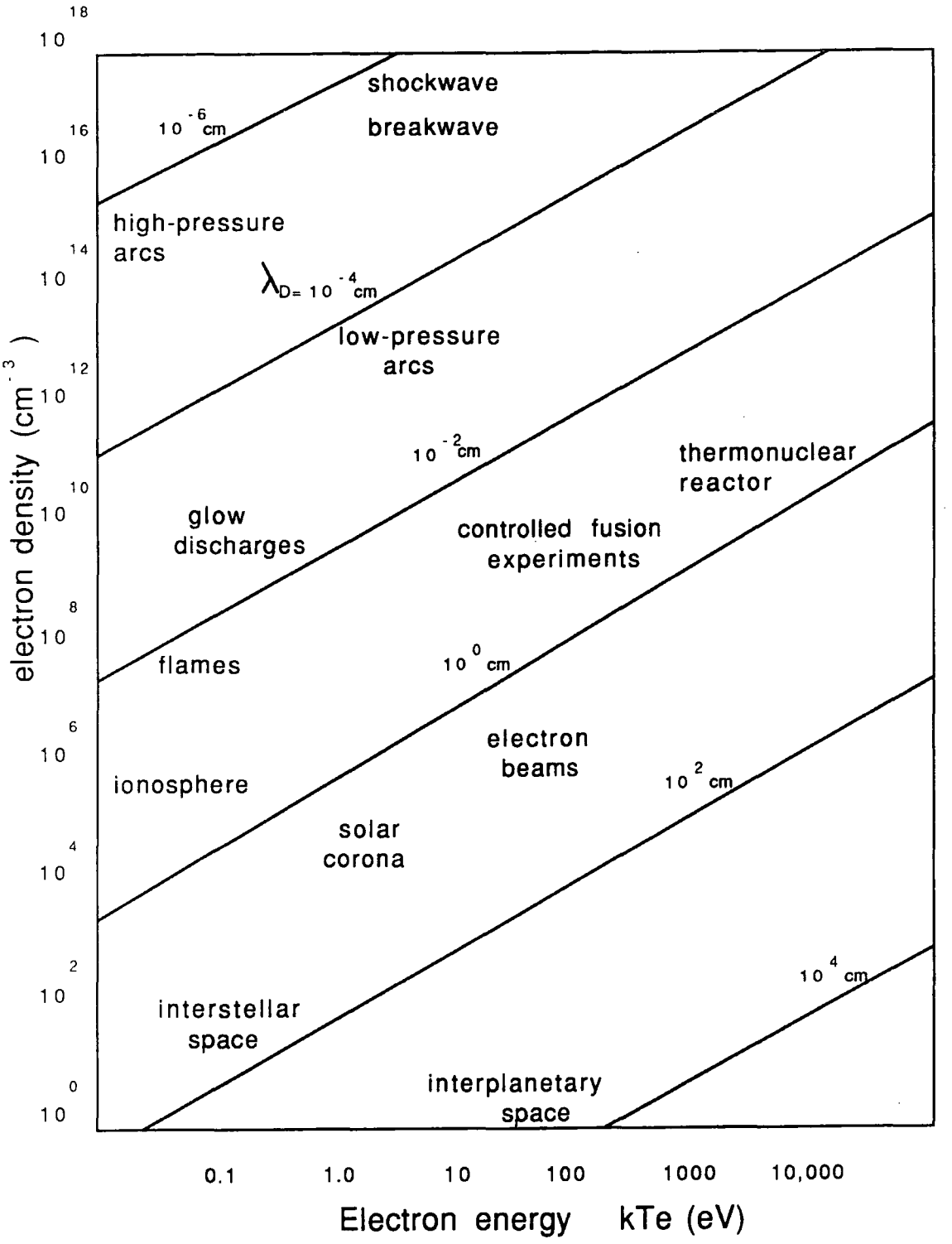

Figure 1.2 Characterisation of Plasmas by their Electron Temperatures and Electron Densities.

Plasmas can be divided into two types known as hot or cold plasmas. In a hot, or equilibrium, plasma the electron temperature is roughly equal to the gas temperature, which must be very high in order for ionisation to occur. This class of plasma can be used in metallurgy for reducing metallic ores and slag to the base metal[27] and in the analysis of materials by ICP OES (inductively coupled plasma optical emission spectrophotometry) or ICPMS[28] (inductively coupled plasma mass spectroscopy). In the high temperature of the plasma most materials are reduced to their constituent atoms, whose optical emission or mass spectra are recorded in order to give an elemental analysis. Hot plasmas have also been used in attempts to produce controlled nuclear fusion for use as a power source.

Cold, or non-equilibrium, plasmas generally have electron temperatures much higher than the temperature of the ions and molecules in the gas, typically by about 2 orders of magnitude. Cold plasmas can be formed in the laboratory by means of a gas discharge. Early investigations of gas discharges were carried out in the 18^{th} and 19^{th} centuries. The discovery of the induction coil by Ruhmkorff[28] led to investigations of cathode rays emitted from discharge tubes by Crookes (1879) and others. In 1897 Thomson showed that cathode rays consisted of electrons, and by the early 1900's it had been established by Townsend[29] and others that conductivity in electrical discharges resulted from ionisation in gas discharges by collision. The word "plasma" was coined by Langmuir in 1928 to denote the state of ionised gases

formed in an electric discharge.[30] Cold plasmas often produce visible emission from excited species in the plasma, causing them to be sometimes known as glow discharges.

Cold plasmas have found use chemically in several areas:-

(i) Synthetic Organic/Organometallic Chemistry

The energies available in a plasma are considerably greater than in conventional chemical reactions,[31] and reaction pathways not normally available can be exploited. All organic compounds undergo some reaction in a glow discharge but the product mixture may be complex and percentage yields may be low. Best results are obtained by avoiding high electron energies and elevated temperatures, which reduces the damage done to the molecules. Most of the work in this area has been done by Suhr and coworkers.[32]

(ii) Surface Modification

This can be achieved in a number of ways:

(a) Surface grafting.[33,34] A polymer is exposed to a plasma in order to create reactive sites which can be used to initiate a conventional free radical polymerisation on the surface. For example the wettability[35] and flame retardancy[36] of fibres can be improved by this method.

(b) Inert plasmas, such as argon, may be used to cross-link

polymer surfaces by direct and radiative energy transfer. This can be used for example to improve the adhesive bonding of polymers.[37]

(c) Direct chemical modification of surfaces may be achieved using more reactive gases. For example an oxygen plasma may be used to increase the wettability of a surface,[38] while CF_4 plasmas can make a surface hydrophobic.[39] Ammonia plasmas may be used to incorporate nitrogen into a surface.[40]

(d) Etching of polymeric materials can be achieved by using oxygen or halocarbon plasmas under more severe conditions, or for longer periods of time. This is of particular use in the removal of resist materials in the electronics industry.[26]

(iii) Polymerisation and Film Deposition

(a) Plasma Polymerisation. Polymer formation occurs when almost any organic compound is subjected to a glow discharge.[22] The polymer is generally different from any conventional polymer and forms as a thin film on any surface in contact with the plasma.

(b) Inorganic materials such as silicon[41] and metals[42] may be deposited as thin films from organosilicon or organometallic plasmas. This is sometimes called plasma induced chemical vapour deposition, and is of use particularly in the electronics industry.

(c) A plasma may be used to initiate a conventional polymerisation reaction in a solid or liquid monomer which is either in contact with the plasma or with reactive species generated by it.[43] This is known as plasma induced polymerisation.

1.2.2 FUNDAMENTAL ASPECTS OF PLASMAS

Theoretically a plasma, by definition, must be electrically neutral, a condition which is satisfied when the dimensions of the discharged column are greater than the Debye length λ_D,[26]

$$\lambda_D=((E_okTe)/(ne^2))^{\frac{1}{2}} \qquad 1.1$$

which defines the distance over which a charge imbalance may exist, where

E_o is the permittivity of free space

k is the Boltzmann constant

T_e is the electron temperature

n is the electron density

and e is the charge on the electron.

The ionisation of molecules within the plasma zone is essential if the discharge is to be initiated and maintained. Electrons within the plasma are accelerated by the electric field and produce further ionisation by collisions with other species. Collisions between an electron and a gas molecule result in one

of two states; an elastic collision in which very little energy

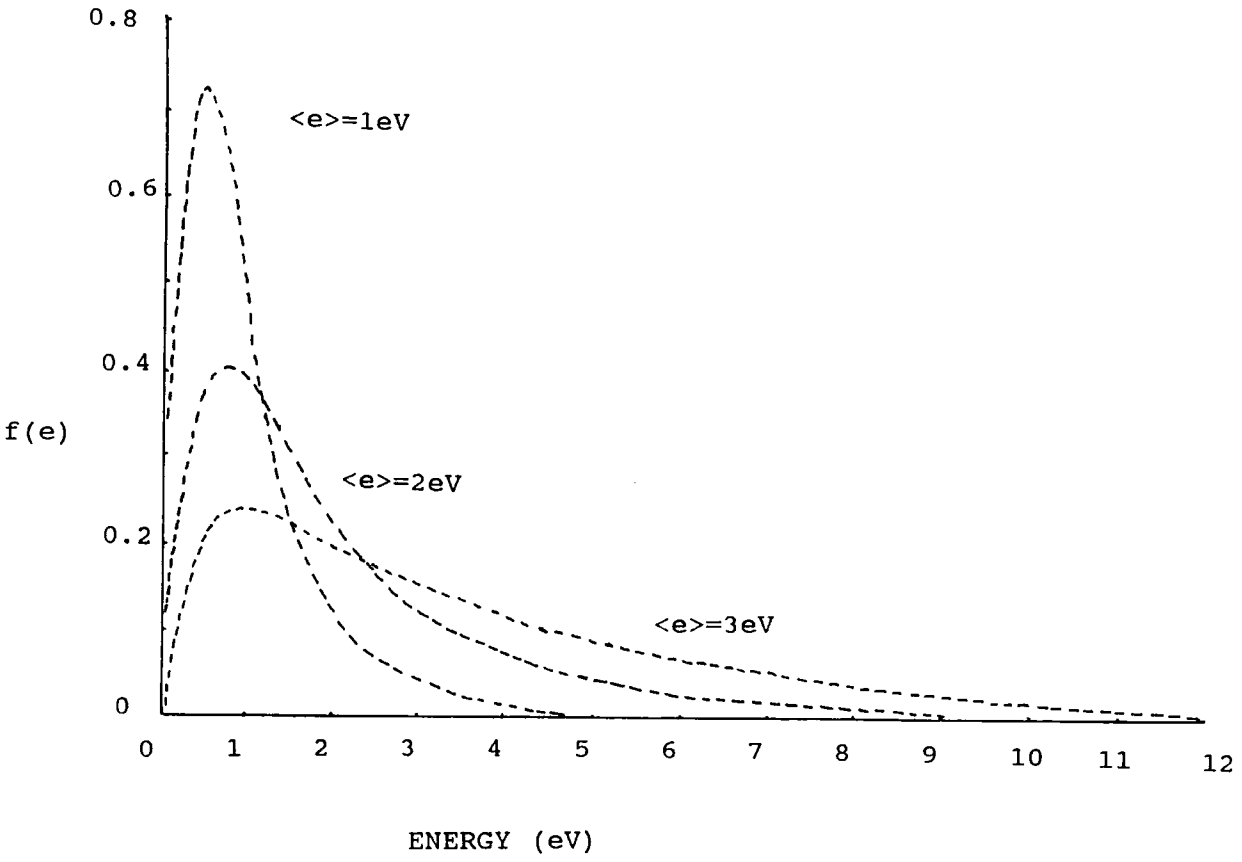

Figure 1.3 Distribution of Electron Energies in a Plasma.

is lost or transferred by the electron,[26] or an inelastic collision which results in the transfer of usable energy from the electron to the molecule. When the electron does not have enough energy to cause ionisation of the molecule, the transfer of energy in an inelastic collision results in the production of a higher energy state of the molecule where the excess energy can be stored in rotational, vibrational and/or electronic excitation. It is from such inelastic collisions that electron energy is continuously lost. After collision the electron gains

energy from the electric field, the amount of kinetic energy picked up before further collision is dependent on the mean free path of the electron in the gas[44] which is connected to the pressure of the system; at too high a pressure the mean free path is very small and the amount of energy gained is not very large. Too low a pressure results in a long mean free path such that gas collisions are not important. Consequently there is a typical working pressure range of 0.05-10 torr. At charge densities of around 10^{10} cm^{-3} it has been calculated that the average lifetime of an electron against recombination is around a millisecond[45].

The average velocity, v, of an electron between collisions is given by:[46]

$$v=((Me^2E\lambda)/m^3)^{1/4} \qquad 1.2$$

where M is the mass of the heavier particle
e is the charge on the electron
E is the electric field
λ is the electron mean free path
and m is the mass of the electron .

Expressions describing the electron energy distribution in terms of energy input, discharge dimensions and gas pressure lead to a Maxwellian distribution of electron energies as shown in Figure 1.3.[45]

Such numerical solutions are only possible for simple systems, but the form of the distribution has been analysed experimentally by probe measurements[47] and direct electron sampling.[48] From Figure 1.3 it can be seen that the average

electron energy will be in the range 2-3eV,[44] i.e. the energy distribution is such that that the electrons are more effective at producing excitation than ionisation. In fact neutral species dominate, the degree of ionisation being low, 10^{-4}-10^{-7} cm^{-3}.[33] Since only the electrons in the tail of the distribution will be effective in producing ionisation, because ionisation potentials are typically 10eV or more, it may be expected that some of the major chemistry occurring in the plasma is connected, not with ionisation but with excitation; since typical bond dissociation energies of typical gases and organic compounds lie well below 10eV, see Table 1.1.

Table 1.1 Some Typical Bond Energies for Organic Compounds and Some Gases (eV).

C-H	4.3	C-O	3.5	C=C	6.1
C-F	4.4	C=O	8.0	O=O	5.2
C-C	3.4	C-N	2.9	N-H	4.0

The collision process depicted in Figure 1.4, results in the emission of electromagnetic radiation produced during the de-excitation of the various excited species that occur. Some of this output is in the visible region giving rise to the term glow discharge and the characteristic colours of different plasmas. However most of the radiation is in the UV/vacuum UV region, as has been shown for argon plasmas.[49] This component has a role to play in the surface modification of polymers since it permits a

transfer of energy to deeper regions in the surface than those which can be accessed by direct impact transfer. Both the IR and visible components are absorbed, but the IR radiation, which can be strongly absorbed, is dissipated through thermal processes.[50]

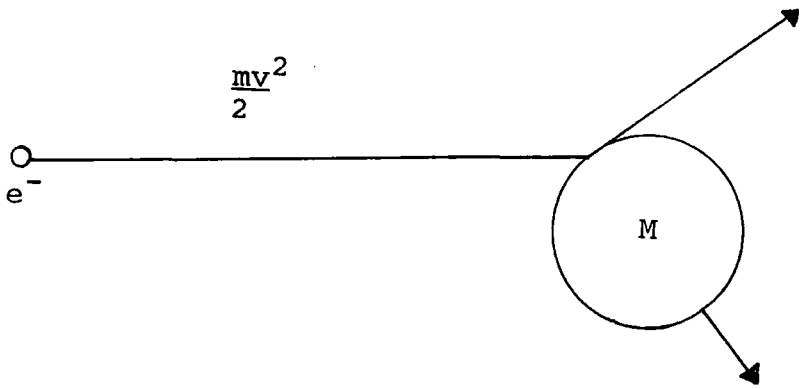

ELECTRONS

IONS - vibrational -> infra-red

ATOMS $h\nu$ - rotational -> micro-wave

METASTABLES - electronic -> ultra-violet

RADICALS

Figure 1.4 Collision Processes in a Plasma.

1.2.3 PLASMA TECHNIQUES

In general there are three aspects which are of interest; the source of the electrical power used to sustain the plasma,

the coupling mechanism and what can be described as the plasma environment. In Figure 1.5. It can be seen that there are two main types of coupling mechanisms, i.e. direct and indirect.[51] In the direct method, resistive coupling, the glow discharge is initiated between electrodes, which consequently are part of the plasma environment and may therefore be deposited on if any polymer is formed. The indirect method, inductive and capacitive coupling, allows the plasma to be formed by an apparatus which is isolated from it. This is achieved by means of a coil wound round the reactor or by use of external electrodes. Microwave discharges may also be excited inductively using a tuned cavity.

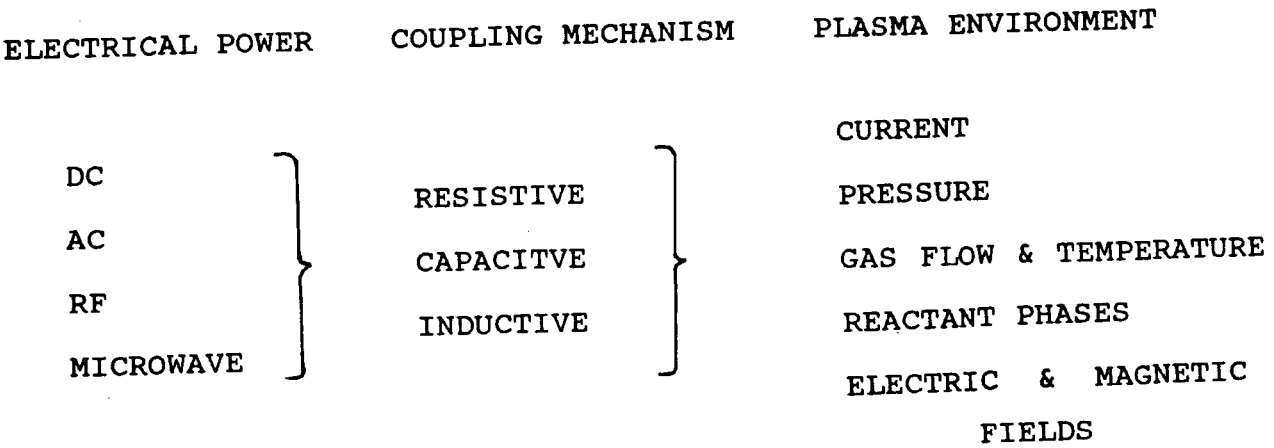

Figure 1.5 Elements in a Glow Discharge Experiment.

Indirect coupling mechanisms can only be used however with

frequencies greater than 1MHz;[32] below this frequency direct contact of the electrodes with the plasma is necessary for sufficient energy to be transferred to maintain the plasma. With internal electrodes, and low pressures, experiments have been performed over a wide range of frequencies from the acoustic to microwave region. Yasuda et al have employed frequencies of 60Hz, 10kHz and 13.56MHz,[52] though there have been comparatively few studies of the effect of the exciting frequency on the nature of the product of the plasma.[53]

The main operating parameters of a glow discharge experiment are those of power input and operating pressure. These typically vary from 0.1 watt to a few kilowatts and between 0.1 torr to one atmosphere respectively. Operating pressures using a radio frequency (RF) discharge can range from 0.05 to 1 torr whilst power input is in the region 0.1W to 150W, using commercially available equipment. Low power levels (<1.0W) are generally difficult to sustain, but when using RF power a stable plasma can be accomplished by pulsing the power input.

Microwave discharges are less stable at low pressures. The use of an increased pressure leads to an increase in the gas temperature which can cause decomposition of organic species and is therefore not a preferred method for plasma polymerisation, although it has found use in plasma modification techniques. At higher power levels cooling systems may be necessary, especially for the electrodes in a DC discharge. The use of DC does allow pressures of up to 1 atmosphere though this will again lead to an increased gas temperature. This factor together with the

acceleration which ions in a DC plasma experience limits the utility of DC discharges in plasma chemistry.

Low frequency and DC discharges are generally characterised in terms of the voltage and current supplied to the electrodes. Typical operating conditions are in the range 10-100V and 1A at pressures of 1 torr. For RF and microwave plasmas the situation is less straightforward, the requisite instrumentation is needed to measure the power in the plasma, and to match the impedance of the generator with that of the coil volume in order to maximise the power transmitted to the plasma.

1.3 TECHNIQUES FOR SURFACE CHARACTERISATION

Using plasmas the outermost surface of a material can be treated to give desirable properties. Additionally this can be achieved in such a way as to only affect these surface layers which leads to certain problems in studying the effects of such processes. Many forms of conventional analysis are of little or no use since the amount of modified material is too small to be distinguished from the bulk of the sample. In the case of a plasma polymer however a certain amount of information can be obtained if it is possible to produce a sufficient quantity of material.

Micro analysis can be performed on polymer which can be scraped from the walls of the reactor. Most analyses will, however, be hampered by the relatively insoluble nature, due to

the high degree of crosslinking, of most of these materials. Also the results of such an elemental analysis should be regarded with some caution since the inclusion of some material from the substrate during collection of the sample is possible.

Infra-red spectroscopy can be used to analyse plasma treated materials. In the case of a modified surface no difference will be seen between the untreated and treated samples using transmission infra-red unless the treatment is very extensive and has penetrated well into the bulk of the sample. However a film of plasma polymer may be studied in this manner if supported on a suitable medium. The complex structure of plasma polymers makes a precise interpretation of the spectrum difficult, though useful information concerning the general nature of the material can be derived.[54]

Nuclear magnetic resonance (NMR) is another technique which is unable to study a plasma modified surface due to the small amount of treated material and its intimate attachment to the bulk of the sample. In addition, since plasma polymers are essentially insoluble in most organic solvents, solution state NMR cannot be directly applied to the analysis of the polymer, however solid state NMR is capable of providing some data[55] such as the presence of both saturated and unsaturated environments. For example, using plasma polymers derived from monomers labelled with ^{13}C, it has been possible to distinguish the relative degrees of unsaturation of films produced from a variety of hydrocarbons.[56]

In general it is more useful to consider surface sensitive techniques when plasma modified materials are to be investigated. These range widely in complexity and usefulness and include contact angle measurements, electron microscopy and various surface spectroscopies.

1.3.1 CONTACT ANGLES

A drop of liquid resting on a surface will form a finite angle between the air liquid interface and the solid surface, this is known as the contact angle θ[57] (Figure1.6). It is one of the oldest techniques used in the characterisation of surfaces but has the advantages of simplicity, speed and low cost. It does have several disadvantages however, contact angle measurements are prone to error. Inaccuracies can be induced by contamination of the measurement liquid, by surface roughness and by penetration of the surface by the liquid or swelling of the surface caused by this. The liquid used may in fact alter the surface under study; a polar polymer with a high degree of chain mobility will undergo a configurational change to minimise the interfacial energy. However providing these factors are taken into account, contact angles measurements are a valuable guide to the surface energies of polymers.

There are several methods for measuring contact angles[58] but one of the simplest is the sessile drop technique. In this process a drop of liquid is placed on top of the dry surface and its contact angle can then be determined either directly, using a goniometer, or indirectly by taking measurements of the width and

height of the drop. The contact angle is related to these measurements via the formula:

$$\tan(\theta/2)=2H/W \qquad 1.3$$

where H and W are the height and width of the drop respectively.

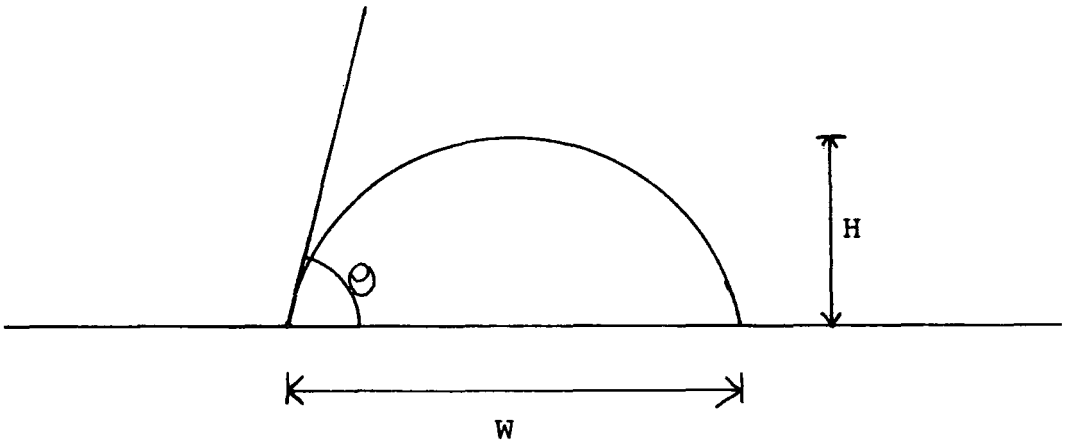

Figure 1.6 Measurement of Contact Angle Using the Sessile Drop Technique.

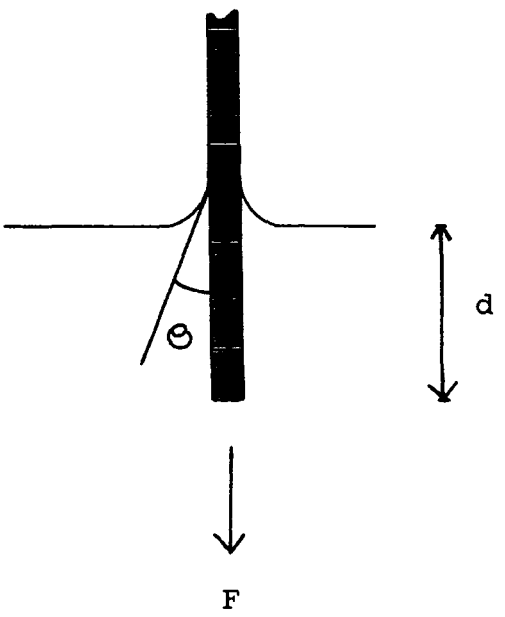

Figure 1.7 Contact Angle Measurements on Single Fibres.

This method is only suitable for the analysis of relatively flat surfaces, for fibrous samples the Wilhelmy plate method is more suitable[59] (Figure 1.7). Partial immersion of the fibre in the wetting medium subjects the fibre to forces due to surface tension and buoyancy, the resultant force, F, is given by the following equation:

$$F=p\gamma_l\cos\theta-pgAd \qquad 1.4$$

where,

- p is the perimeter of the fibre,
- γ_l is the surface tension of the liquid,
- θ is the contact angle between fibre and liquid,
- p is the density of the liquid,
- g is the acceleration due to gravity,
- A is the cross-sectional area of the fibre, and
- d is the depth of immersion.

Plotting the force, F, as the depth of immersion increases allows extrapolation to d=0, the point of immersion, such that the contact angle can be determined.

These methods have the advantage that the surface does not have to be exposed to the measuring liquid for a long time, in comparison to the sessile bubble technique where the surface may be soaked in the liquid for up to 48 hours before testing, and this minimises any reorientation of the surface structure which may be induced by the test.

By measuring the contact angles against two liquids of known surface energies it is possible to calculate the polar and dispersive components of the surface energy of the solid using the formula below.[60,61]

$$1+\cos\theta=(2/\gamma_L)\left((\gamma^d_L\gamma^d_S)^{\frac{1}{2}}+(\gamma^p_L\gamma^p_S)^{\frac{1}{2}}\right) \qquad 1.5$$

where, γ_L is the surface energy of the liquid,

γ^d_L is the dispersive component of surface tension of the liquid,

γ^p_L is the polar component of surface tension of the liquid,

γ^d_S is the dispersive component of surface tension of the solid

and γ^p_S is the polar component of the surface tension of the solid.

1.3.2 SURFACE SPECTROSCOPIES

Over the last 25 years the need for clean well characterised surfaces for the microelectronic industries has stimulated the development of a number of surface spectroscopic techniques which enable the chemistry of the surface to be probed directly. These techniques provide a variety of information from varying depths within the sample as illustrated in Figure 1.8.

Currently it is necessary to employ a number of these techniques, possibly with older methods such as contact angles to

build up a full picture of the surface. There are however two techniques which lend themselves particularly well to the study of modified polymers, these are secondary ion mass spectroscopy (SIMS) and x-ray photoelectron spectroscopy (XPS), also known as electron spectroscopy for chemical analysis (ESCA).

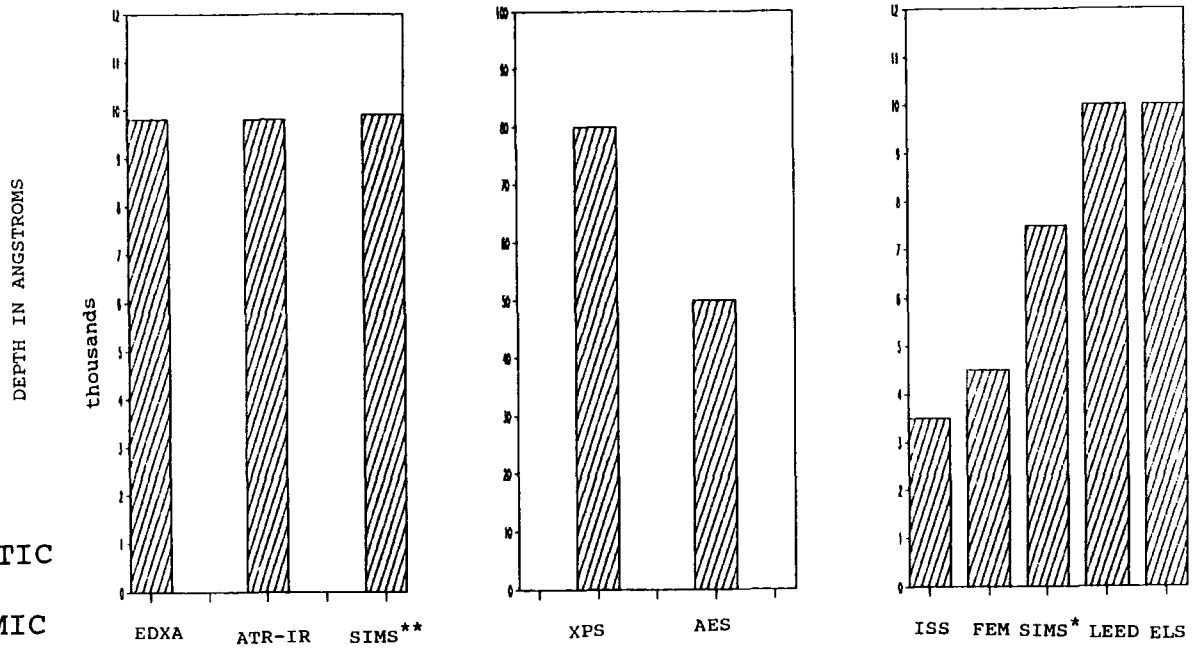

Figure 1.8 Comparison of Some Surface Analytical Techniques With Respect to Depth of Analysis.[62]

The application of SIMS to polymer surfaces[63] has not yet achieved its full potential, although some systems have been extensively studied, such as polyacrylates and polymeth-acrylates.[64,65] The SIMS process uses an ion or atomic beam to sputter ionic fragments of the sample from the surface. These are then analysed in a similar way to the fragments in a conventional mass spectrometer. One problem with the technique is that the high energy ion beam used to produce the ions from the surface

can produce a plasma like state which can alter those fragments before detection. Additionally the ion beam may induce changes in the substrate itself. These problems can however be minimised by adjusting the experimental conditions to optimise the spectrum of each sample. In practice the static SIMS mode is employed when analysing polymers, this technique uses a very low ion current which is rastered across the surface of the sample. This avoids any sampling of the surface which may have been damaged by the ion beam. Its main advantage over XPS is its superior surface sensitivity and molecular selectivity which enables a much greater level of structural information to be obtained. Disadvantages include the very high cost of the technique and the level of operator training required to optimise the conditions of the experiment in order to obtain a spectrum of high quality. The information obtained by SIMS analysis tends to be complementary to rather than alternative to XPS analysis.

The application of XPS to the study of polymer surfaces has been excellently demonstrated by Clark et al.,[66] and now is a relatively widespread technique used extensively in the analysis of polymer surfaces. In the XPS experiment a beam of x-rays of known energy is used to produce photoemission of electrons from the sample. The x-ray energy is sufficient to eject core level electrons which are collected and analysed according to their kinetic energy. From this it is possible to calculate the binding energy of the electron since the sum of the photoelectrons binding and kinetic energies must be equal to the energy of the ionising x-ray photon. It is an ideal technique for the

investigation of modified surfaces since it is highly surface sensitive and non destructive. XPS can routinely provide the following information:

1. Elemental analysis of all elements except hydrogen and helium can be calculated from the relevant peak areas together with a knowledge of the appropriate sensitivity factors.

2. Functional group analysis; structural features can be determined from a knowledge of the binding energy chemical shifts produced in a particular core level spectrum, especially the C_{1s} core level, by the different functional groups within the sample. Where two groups produce similar shifts it is sometimes possible to distinguish between them by performing a surface reaction with one of them and then analysing for the presence of the new functionality introduced.

3. Information on the presence of unsaturated or aromatic features from shake-up (π-π^*) transitions.

4. Non destructive depth profiling; by increasing take off angle surface features can be enhanced. Additionally the sampling depth can be varied by use of x-ray sources of different energies.

The disadvantages of XPS are that it is expensive and requires an ultra high vacuum system. Additionally it is not possible to study the hydrogen content of a material directly or to study the bulk of a sample without sectioning or etching it. XPS also requires trained operators to achieve its full potential. Despite

these disadvantages it is currently the best way to quickly assess the surface chemistry of a material and so it has been used throughout this work as a major investigative tool.

REFERENCES

1. J.M. McKelvey, "Polymer Processing", J. Wiley & Sons, New York, 1962.
2. H. Ulrich, "Introduction to Industrial Polymers", Hanser, Munchen, 1982.
3. T.F Mc Laughlin Jr., "Modern Packaging", p153-156, 1960.
4. D.T. Clark and W.J. Feast, "Polymer Surfaces", Wiley Interscience, New York, 1978.
5. J.R Myles & D. Whittaker, British Patent 581,717, Oct 2nd 1946.
6. I.E Wolinski, Us Patent 2,805,960, Sept 10 1957.
7. D. Briggs, D.M. Brewis and M.B. Konieczko, J. Materials Sci., 11, p1270, 1976.
8. A.E. Shilov, "Activation of Saturated Hydrocarbons by Transition Metal Complexes", D. Riedel Publishing Co., Holland, 1984.
9. K.W. Lee and T.J. McCarthy, Macromolecules, 21(2), p309, 1988.
10. A.J. Dias and T.J. McCarthy, Macromolecules, 18, p1826, 1985.
11. C.A. Costello and T.J. McCarthy, Macromolecules, 20, p2819, 1987.
12. D.T. Clark, W.J. Feast, W.K.R. Musgrave and I. Ritchie, J. Polym. Sci. Polym. Chem. Edn., 13, p857, 1975.
13. D.T. Clark, W.J. Feast, W.K.R. Musgrave and I. Ritchie, in "Advances in Polymer Friction and Wear", Vol.5A, Ed. L.H. Lee, Plenum Press, New York, 1975.

14. D.T. Clark and H.R. Thomas, J. Polym. Sci. Polym. Chem. Edn., 14, p1671, 1976.

15. D. Briggs, D.M. Brewis and M.B. Konieczko, J. Materials Sci., 12, p429, 1977.

16. D.T. Clark, A. Dilks and D. Shuttleworth, J. Materials Sci., 12, 1977.

17. H.F. Beer, Ph.D. Thesis, Durham, 1980.

18. A. Rufolo & R.R. Winans, ASTM Bull. No. 214, p53-6, 1956.

19. A. Rufolo & R.R Winans, Am. Soc. Testing Mater., No. 198, p8-14, 1957.

20. M. Hudis, in "Techniques and Applications of Plasma Chemistry", Eds. J.R. Hollahan and A.T. Bell, John Wiley and Sons, New York, 1974.

21. D. Briggs & M.P Seah, "Practical Surface Analysis", John Wiley & Sons, Chichester, pp359-392, 1983.

22. H. Yasuda, "Plasma Polymerisation", Academic Press, London, 1985.

23. P.M. Triolo & J.D. Andrade, J. Biomedical Materials Research, 17, p1013, 1987.

24. H. Yasuda, A.K. Sharma, & T. Yasuda, J. Polym. Sci. Phys. Ed., 19. p1285, 1981.

25. T. Yasuda, K. Yoshida, T. Okuno & H. Yasuda, J. Appl. Polym. Sci. Part B: Polym. Phys., 26, p2061- 74, 1988.

26. A.T. Bell, in "Techniques and Applications of Plasma Chemistry", Eds. J.R. Hollahan and A.T. Bell, Wiley, New York, 1974.

27. K. Upudhya, Trans. Ind. Ins Met., 38, p472, 1985.

28. S.C. Brown, in "Gaseous Electronics", Vol.1, Eds. M.N. Hirsh and H.J. Oskan, Academic Press, New York, 1978.

29. J. S. Townsend, Phil. Mag., 8, p733, 1904.

30. L. Tonks and I. Langmuir, Phys. Rev., 33, p195, 1929.

31. H. Suhr, Plasma Chem. Plasma Processing, 3, p1, 1983.

32. H. Suhr in "Techniques & Applications of Plasma Chemistry", Eds. J.R. Hollahan and A.T. Bell, Wiley, New York, 1974.

33. C.I. Simonesçue and F. Denes, Cellulose Chem. Technol., 14, p285, 1980.

34. A.E. Plavlath & K.E. Lee, J. Macromol. Sci. Chem., A10, p579, 1976.

35. M.M. Millard, K.S. Lee and A.E. Pavlath, Text. Res. J., 42, p307, 1972.

36. D.M. Soignet, R.J. Berni and R.R. Banerito, J. Appl. Polym. Sci., 20, p2483, 1976.

37. M.M. Millard, K.S. Lee and A.E. Pavlath, Text. Res. J., 42, p460, 1972.

38. P.M.Tricolo and J.D.Andrade, J. Biomed. Mater. Res., 17, p129, 1983.

39. M.Strobel, S.Corn, L.S.Lyon and G.A.Korba, J. Polym. Sci., Polym. Chem. Ed., 23, p1125, 1985.

40. L.T.Nguyen, N.H.Sung and N.P.Suh, J. Polym. Sci., Polym. Chem. Ed., 18, p541, 1980.

41. J.R.Hollahan and R.S.Rosler in "Thin Film Processes", Eds. J.Vossen and W.Kern, Academic Press, New York, 1979.

42. C.Oehr and H.Suhr, Appl. Phys., A45, p151, 1988.

43. Y.Osada, M.Hashidzume, E.Tsuchida and A.T.Bell, Nature, 286, p693, 1980.

44. F. Kaufman, chapter 3 in " Chemical Reactions in Electrical Discharges", Ed. R.F. Gould, American Chem. Soc. Advances in Chemistry Series 80, Washington D.C., 1969.

45. W.L. Fite, in ref. 15, chapter 1.

46. J.M. Meek and J.D. Craggs, Eds., "Electrical Breakdown of Gases", Wiley, Chichester, 1978.

47. P. Brassem and F.J.M.J. Massen, Spectrochimica Acta, 29B, p203, 1974.

48. D.T. Clark and A. Dilks, in "Charaterisation of Metal and Polymer Surfaces", Vol.2, Ed. L.H. Lee, Academic Press, New York, 1977.

49. D.T. Clark and A. Dilks, J. Polym. Sci. Polym. Chem. Edn., 18, p1233, 1980.

50. M. Hudis, in chapter 3 "Techniques and Applications of Plasma Chemistry", Eds. J.R. Hollahan and A.T. Bell, Wiley, New York, 1974.

51. F.K. McTaggart, "Plasma Chemistry in Electrical Discharges", Elsevier, Amsterdam, 1967.

52. N. Morosoff and H. Yasuda, in "Plasma Polymerisation", Eds. M. Shen and A.T. Bell, ACS Symp. Series 108, Washington D.C., 1978.

53. R. Claude, M. Moison and M.R. Wertheimer, Polymeric Materials Science and Engineering, 56, p134, 1987.

54. C. Till, Ph.D. Thesis, Durham, 1986.

55. A. Dilks and S. Kaplan, J. Polym. Sci. Polym. Chem. Edn., 21, p1819, 1983.

56. A. Dilks, S. Kaplan and A. Vanhaelen, J. Polym. Sci. Polym.

Chem. Edn., 19, p2987, 1981.

57. B.W. Cherry, "Polymer Surfaces", Cambridge University Press, Cambridge, 1981.

58. R.J. Good and R.R. Stromberg, Eds, "Surface and Colloid Science", Vol.2, Plenum Press, New York, 1979.

59. B. Miller & R. A. Young, Textile Research J., 45(5), p359-65, 1975.

60. A.M. Wrobel, Physicochemical Aspects of Polymer Surfaces, 1, p197, 1983.

61. D.H. Kaeble, J. Adhesion, 2(2), p66-81, 1970.

62. B.D. Ratner, Adv. Chem. Serv., 199, p9, 1982.

63. M.R. Ross, Diss. Abstr. Int. B., 42, p2357, 1976.

64. M.J. Hearn and D. Briggs, Surface and Interface Analysis, forthcoming.

65. D. Briggs, B.D. Ratner, to be published.

66. D.T. Clark, in "Photon, Electron, and Ion Probes of Polymer Structure and Properties", Eds. T.J. Fabish, D. Dwight and H.R. Thomas, ACS Sympossium Series, No.162, Am. Chem. Soc., Washington D.C., 1979.

CHAPTER TWO

AN INVESTIGATION INTO THE EFFECTS OF POLYMER ORIENTATION AND CRYSTALLINITY UPON THE EXTENT AND NATURE OF PLASMA OXIDATION

2.1 INTRODUCTION

Many commercial products use polymers that are not totally amorphous[1] they are often semi-crystalline and some, fibres especially,[2] are highly oriented. The physical characteristics of the material, such as tensile strength and chemical resistance are related to the degree of molecular order. Often some degree of crystallinity is an inherent property of industrial polymers such as polyethylene terephthalate (PET) and polyethylene (PE), others such as polystyrene and polymethylmethacrylate are generally considered as essentially amorphous.[3] Orientation of polymers may result from the manufacturing process for example by drawing of films and fibres or by the forces set up in other techniques such as blow molding.[4] In materials that are predisposed to some degree of crystallinity such as melt quenched PET stretching produces both molecular orientation and small regions of three dimensional order, known as crystallites.[3] A simplistic explanation of this type of behaviour is that the orientation processes have brought the molecules into a suitable position for them to order in a three dimensional arrangement and hence crystallise. It can also be argued that an increase in the molecular ordering of a polymer will lower the entropy barrier to crystallisation thus orientation induces crystallinity.[5]

Evidence has been reported which is consistent with the hypothesis that amorphous regions of polymers are more readily plasma etched than crystallites at the surface.[6] In this chapter some preliminary investigations performed in order to determine

how crystallinity and orientation effects the extent and nature of plasma oxidation of several polymeric materials are described.

2.2. EXPERIMENTAL

2.2.1 MATERIALS

Samples of low density polyethylene (LDPE) and high density polyethylene (HDPE) were supplied by the Metal Box Company. All other samples were supplied by ICI Materials Centre, Wilton.

Samples of LDPE and HDPE were washed with methanol prior to treatment and XPS investigation showed that they had oxygen to carbon atomic ratios of approximately 4 oxygen to 100 carbon atoms, no other contaminants were observed. Pristine samples were shown to have a contact angle with distilled water of 105°±2.

Two methods of drawing were used one performed at Durham the other at ICI Materials Research Centre, Wilton. At Durham samples were drawn manually using two draw ratios which proved to be reproducible, an eight-fold draw was obtained at the onset of necking[7] in the stressed portion of the polymer; a twelve-fold draw was obtained by drawing the polymer as far as possible over steam (see Figure 2.1). Samples were shown to be uniformly drawn in the necked region by graduations marked onto the polymer surface with an indelible marker before drawing. In comparative studies only material taken from one sample was used as it was felt that this method would be highly susceptible to variations between samples.

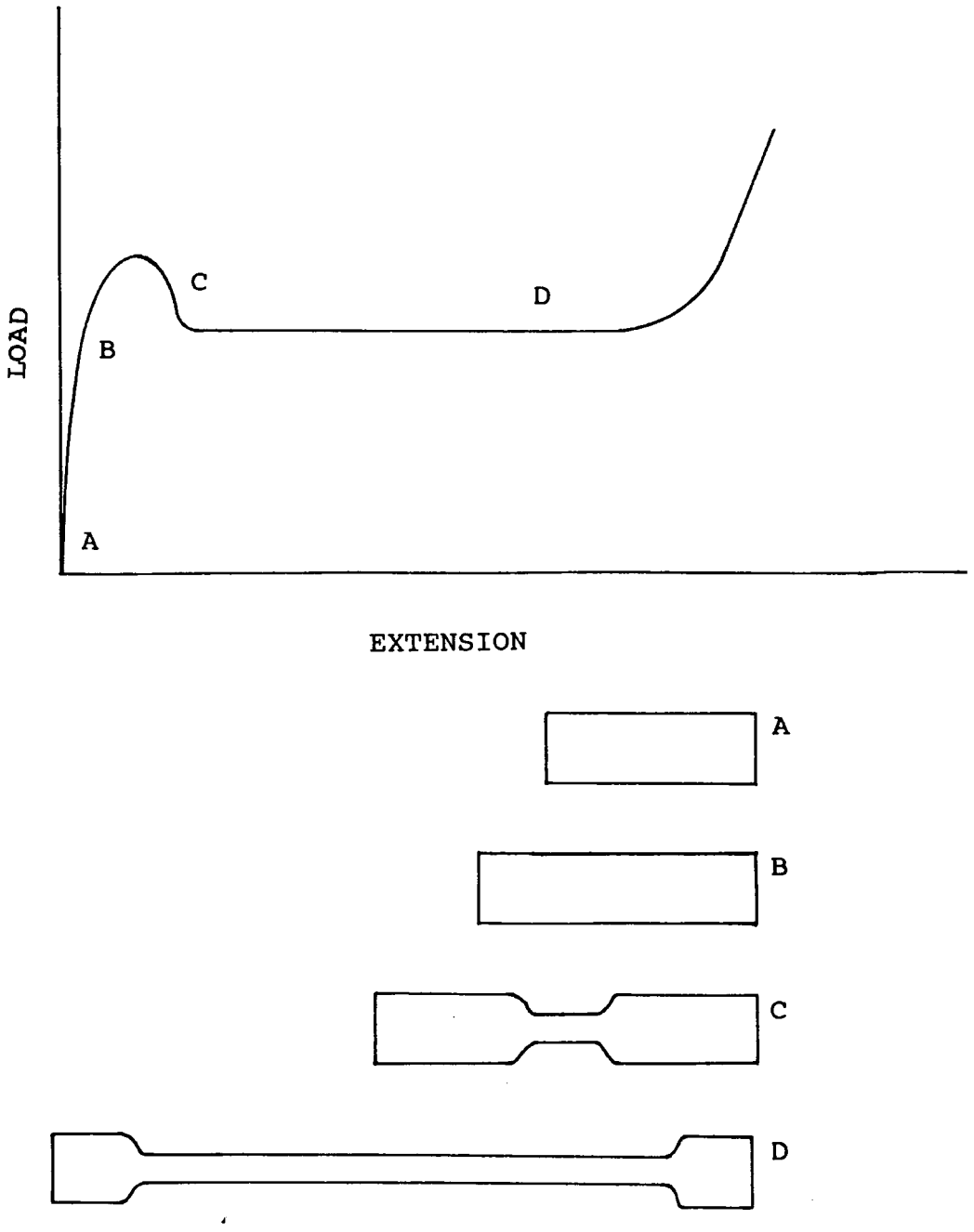

Figure 2.1. The Necking Phenomenon of Drawn Polymers.

At ICI LDPE and HDPE were drawn using an Instron tensile tester at a temperature of 90°C. With this method a wider variety of draw ratios were obtained than was possible at Durham. Using the Instron the onset of necking occurred at a draw ratio of seven, although it proved possible to draw LDPE uniformly below this threshold.

Two samples of polypropylene were provided: undrawn material thickness 25 microns and polypropylene biaxially drawn at 150°C, also of 25 microns thickness. Washing with methanol rendered the samples free from any contaminants except a small amount of oxygen, measured at two oxygen atoms per 100 carbon atoms.

Polyethylene terephthalate (PET) film in the amorphous state was also supplied by ICI (see Figure 2.2). The polymer was found to have substantial surface contamination, which was removed by washing in "Micro" detergent as supplied by the International Products Corporation, and thoroughly rinsing in water followed by hot methanol, until XPS showed that the samples were clean.

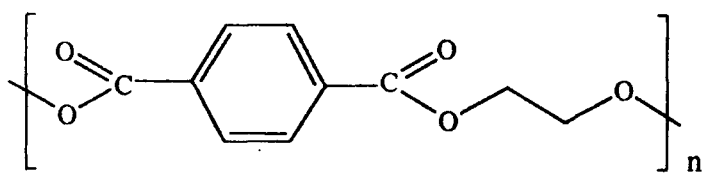

Figure 2.2 Structure of Polyethylene Terephthalate.

Semi-crystalline samples were prepared according to Tant and Wilks[8], and the 51% crystalline sample was washed with chloroform to remove the crystals of cyclic oligomers formed on the surface during the heating process. This was not an ideal method as chloroform is known to cause stress crystallisation at the surface[9].

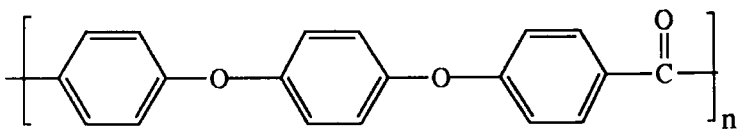

Figure 2.3 Structure of Poly (ether ether ketone).

Samples of poly (ether ether ketone) (PEEK) (see Figure 2.3) were also supplied by ICI. Four types of commercially available film were investigated, namely; amorphous, 10% crystalline with uniaxial orientation, 20-23% crystalline without orientation and 35% crystalline with biaxial orientation. Films were cleaned in the same manner as amorphous PET prior to any experimental procedure.

2.2.2 INFRA-RED SPECTROSCOPY

Transmission infra-red spectra were recorded on a Perkin

Elmer 577 and polarised transmission infra-red spectra were recorded on a Bomen Fourier Transform infra-red spectrometer. Attenuated Total Internal Reflection infra-red spectra were recorded on a Mattson Instruments Inc. Sirius 100, with a KRS-5 crystal. Infra-red spectra obtained on the Bomen infra-red spectrometer were subject to interference fringes, this problem was overcome by placing the samples to be analysed between two sodium chloride plates with Nujol. This is not an ideal solution as some of the Nujol's absorbance bands coincide with those of PE and it is also possible that the hydrocarbon oil will cause swelling and increase the disorder of the polymer matrix. It was thought however that only a small proportion of the sample would be effected by the Nujol and that the infra-red technique would not be sensitive to such small changes.

2.2.3 XPS ANALYSIS

XPS spectra were recorded on a Kratos ES200 or ES300 electron spectrometer in fixed retarding mode using Mg $K_{a1,2}$ X-rays of 1253.6 eV energy and a take off angle of 35° unless otherwise specified. All binding energies were referenced to the hydrocarbon, C-H peak with a binding energy of 285eV. Samples were mounted on a three sided probe tip measuring approximately 17mm by 8mm, using double sided Scotch adhesive tape. Series of spectra recorded for comparative purposes were recorded on one spectrometer only.

2.2.4 PLASMA MODIFICATIONS

Plasma modifications were carried out using 0.2mbar oxygen plasmas of various powers and duration in a Polaron Instruments plasma asher E2000. The apparatus was pumped down to a base pressure of about $4x10^{-2}$ torr using an Edwards ED2M2 mechanical rotary pump. The power to the plasma was supplied by a 13.56 MHz RF generator. Before each treatment the system was tuned without the sample so that the operating conditions were optimised and the reflected power minimised.

2.2.5 CONTACT ANGLE MEASUREMENTS

Contact angle measurements were performed using the sessile drop technique using a 1 microlitre drop of distilled water. Averages of at least three measurements were taken, these averages were found to be consistent within ±2°.

2.2.6 SCANNING ELECTRON MICROSCOPY.

Samples were sputtered with a thin layer of gold in a Polaron Instruments SEM Coating Unit ES100, prior to investigation with a Cambridge Stereoscan 600 scanning electron microscope.

2.3 EFFECT OF ORIENTATION ON POLYETHYLENE

2.3.1 INFRA-RED SPECTRA OF DRAWN POLYETHYLENE.

Transmission infra-red spectra were obtained from oriented and unoriented polyethylene samples, and the relative intensities of the crystalline ($730cm^{-1}$) and to amorphous ($1352cm^{-1}$) absorptions were measured to obtain an apparent degree of crystallinity,[10] see Table 2.1 and Figure 2.4.

It can be seen that drawing both low and high density polyethylene readily causes an increase in crystallinity, this effect is more pronounced in HDPE than in LDPE. It should be noted however that HDPE is always significantly more crystalline than LDPE.

Table 2.1. Crystalline to Amorphous Ratios of Drawn and Undrawn Polyethylene.

PE	DRAW RATIO	ABSORBANCE AMORPHOUS ($1352cm^{-1}$)	ABSORBANCE CRYSTALLINE ($730cm^{-1}$)	C:A
LDPE	0	0.22	0.19	0.9
	8	0.34	0.51	1.5
	12	0.24	0.44	1.8
HDPE	0	0.08	0.37	4
	8	0.06	0.45	7
	12	0.01	0.21	21

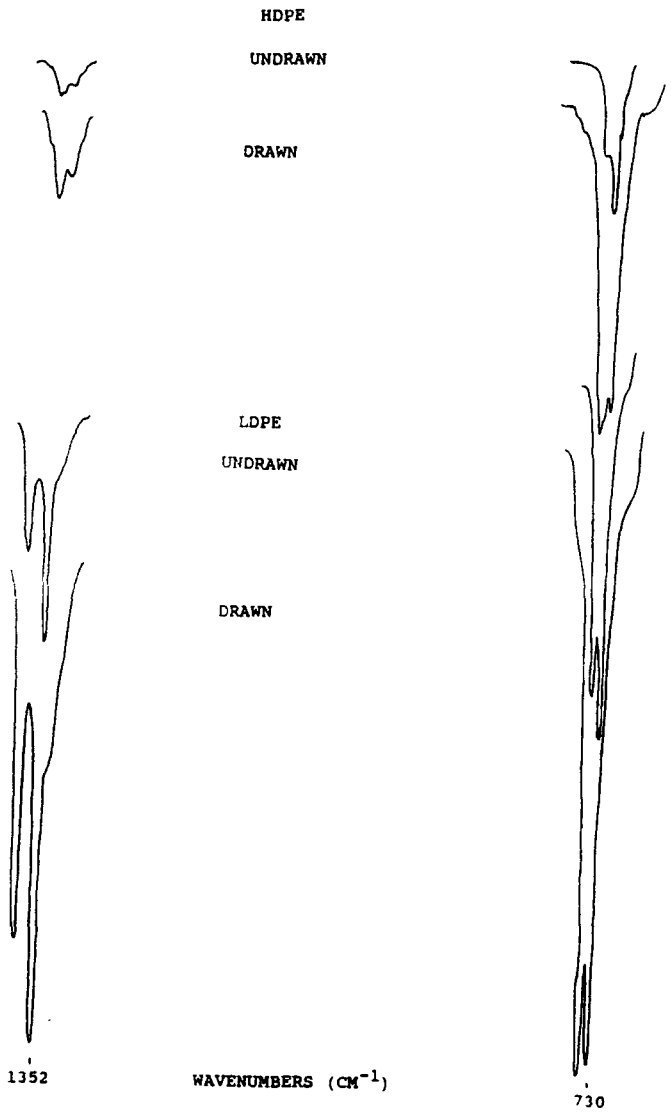

Figure 2.4 Effect of Drawing on the Infra Red Absorptions of LDPE and HDPE.

Polarised infra-red measurements have been made to determine how uniaxial stretching effects the bulk orientation within the polymer. Literature in the area suggests that the best absorbances to observe for investigations into the orientation of polyethylene are $730cm^{-1}$ and $720cm^{-1}$,[11,12] however, the spectrometer used was limited to wavenumbers above $750cm^{-1}$. The absorption bands chosen were: $1894cm^{-1}$, with change in dipole perpendicular to the polymer chain in crystalline phase and $2016cm^{-1}$, with change in dipole parallel to the polymer chain in

both the amorphous and crystalline phases (Figure 2.5). Spectra were recorded parallel (V) and perpendicular (H) to the direction of orientation; the ratio of these two absorbances, known as the dichroic ratio, were measured, see Tables 2.2a,b. The ratio of the absorbances 2016(V) to 1894(H), apparent degree of crystallinity,[10] was also determined as a comparative measure of crystallinity.

Table 2.2a. Effect of Drawing on the IR Absorbances of LDPE.

DRAW RATIO	POLARISER	ABSORBANCE 2016	ABSORBANCE 1894	DICHROIC RATIO 2016	DICHROIC RATIO 1894	DRAW RATE (mm/min)	APPARENT DEGREE OF CRYSTALLINITY
0	V	1.11	1.04	1.1	1.0	0	1
	H	1.02	1.06				
1.6	V	1.69	0.29	2.9	2.6	50	2
	H	0.59	0.77				
5	V	1.04	----	3.6	---	500	1.5
	H	0.29	0.64				
7	V	0.84	0.25	3.2	2.2	50	1.5
	H	0.26	0.56				
11	V	0.89	----	8.9	---	50	1.5
	H	0.1	0.54				
16	V	0.78	----	---	---	500	2
	H	-----	0.43				

These results show, as expected that the greater the draw ratio applied to the sample, the more highly oriented are the polymer chains within the sample. The more highly drawn samples

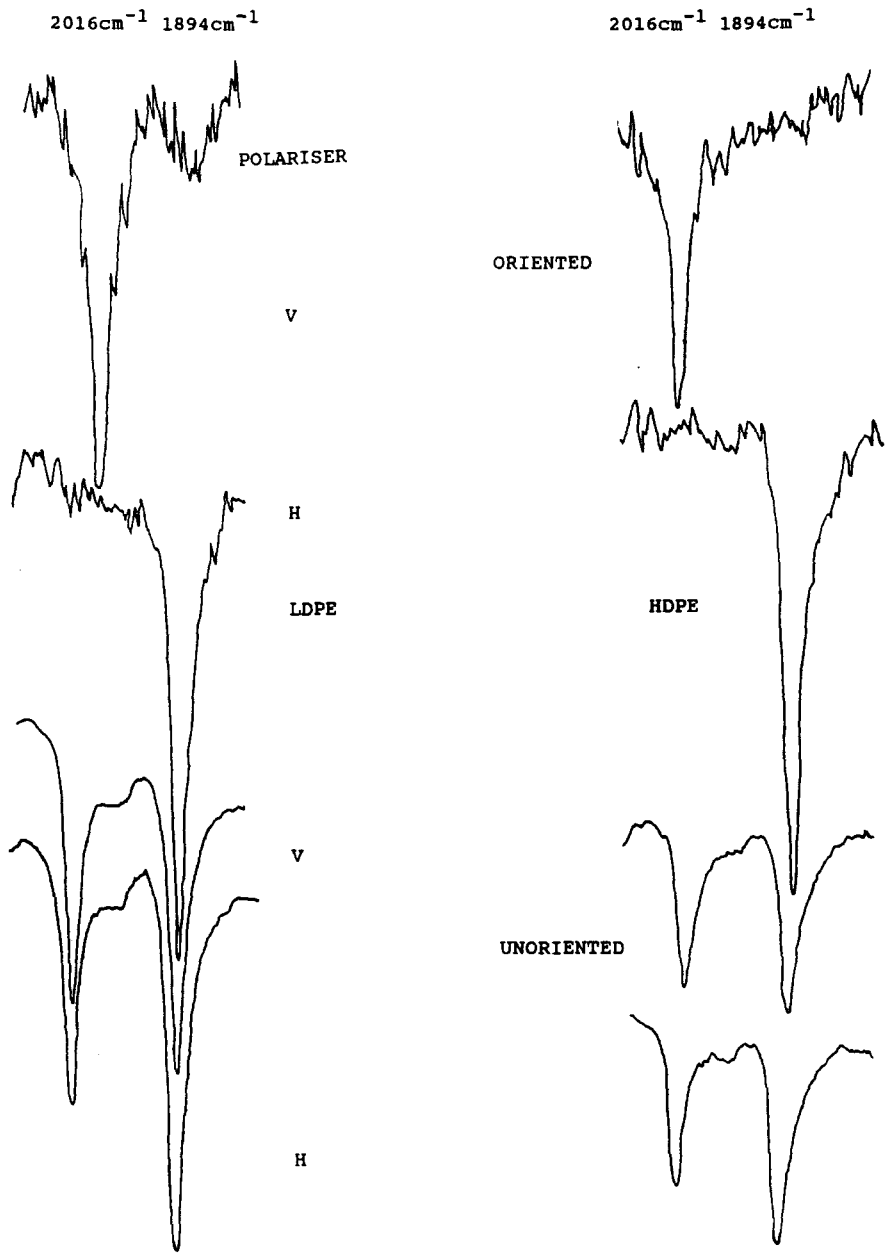

Figure 2.5 Effect of Orientation on the Polarised IR Spectra of Polyethylene.

Table 2.2a. Effect of Drawing on the IR Absorbances of LDPE.

DRAW RATIO	POLARISER	ABSORBANCE 2016	ABSORBANCE 1894	DICHROIC RATIO 2016	DICHROIC RATIO 1894	DRAW RATE (mm/min)	APPARENT DEGREE OF CRYSTALLINITY
0	V	1.98	1.16	1.2	1.4	0	1
	H	1.65	1.65				
7	V	1.60	----	4.7	---	50	1.5
	H	0.34	1.11				
	V	2.16	----	16.6	---	100	3
	H	0.13	0.73				
	V	1.85	----	18.5	---	500	4.5
	H	0.10	0.42				
8	V	1.64	----	---	---	100	2
	H	----	0.84				
	V	0.93	----	---	---	500	4.5
	H	----	0.21				
14	V	1.32	----	---	---	100	6.5
	H	----	0.21				

of both LDPE and HDPE both show "complete" orientation as seen by the infra red technique i.e. the absorption bands are only seen with one polariser orientation, further drawing appears to cause the polymer molecules to slide over one another. More interesting is the effect of draw rate on the dichroic ratio, faster draw rates appearing to cause a greater degree of orientation. Studies on polyethylene films using a variety of techniques[13] have shown that in the case of extruded films, only the crystalline regions

show any degree of orientation whereas in cold drawn material both amorphous and crystalline regions show alignment. Using the WLF time-temperature superposition procedure it can be postulated that in higher temperature, or longer time scale experiments the amorphous regions of the sample are less inclined to become ordered and adopt a more entropically preferred configuration. At a lower temperature or shorter time scale, the molecular chains do not have the thermal energy to move quickly enough to achieve a more disordered state. This somewhat simplistic explanation is supported out by the apparent increase in the ratio of the amorphous and crystalline absorbance to solely crystalline absorbance shown in Table 2.2a,b as 2016(V)/1894(H).

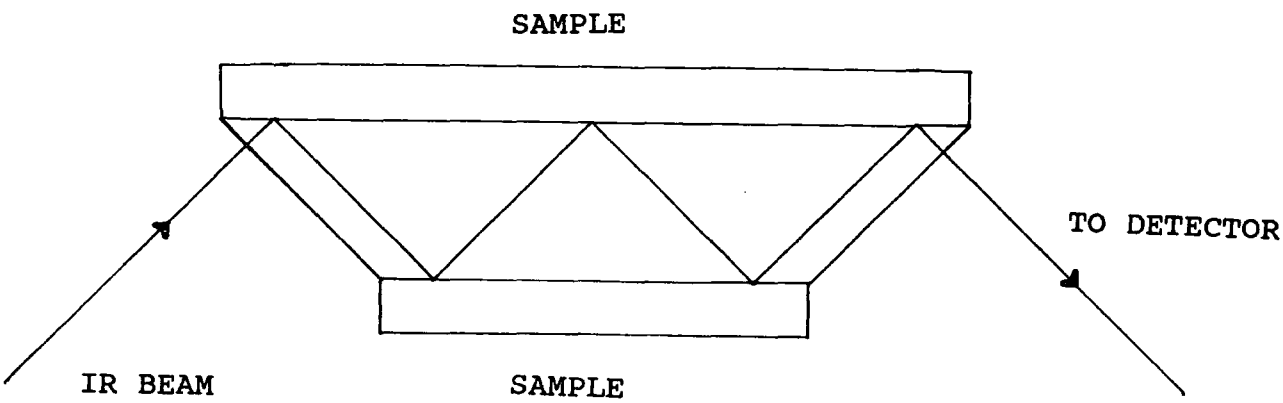

Figure 2.6 Schematic Representation of the ATR Experiment.

Fourier transform infra-red attenuated total internal reflection (FT-IR ATR), as illustrated in Figure 2.6, has been

demonstrated to be an extremely useful technique in helping to determine aspects of the surface structure of polymers.[15,16] Its surface sensitivity is somewhat limited when compared to other surface science techniques, with the sampling depth thought to be approximately half a micron.[16] Polarised FT-IR ATR measurements have been used to determine whether bulk drawing has oriented the surface molecules or introduced crystallinity in the outer regions of the bulk.

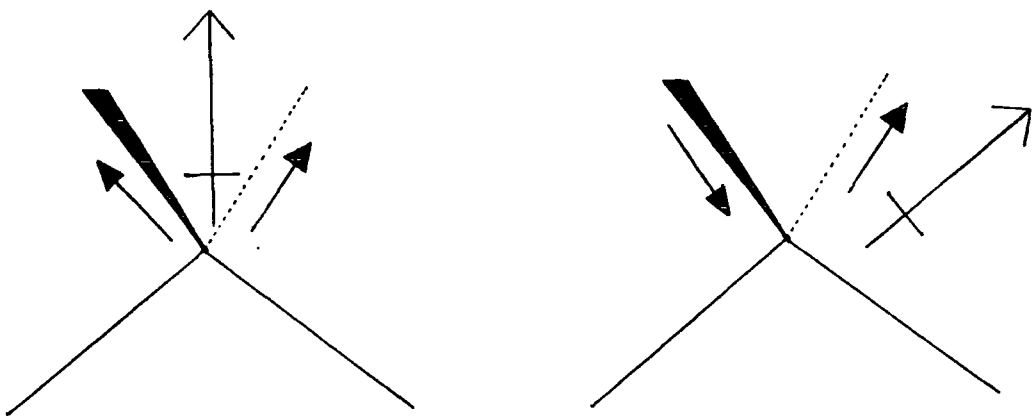

SYMMETRIC ANTI-SYMMETRIC

Figure 2.7 Symmetric and Anti-Symmetric Stretching Modes of CH_2.

High resolution spectra were obtained of the region 3000 to 2800cm^{-1} containing the anti-symmetric CH_2 stretch at 2920cm^{-1} and the symmetric CH_2 stretch at 2850cm^{-1}, depicted in Figure 2.7.[11,17]

On drawing LDPE is observed to undergo a significant

increase in alignment of polymer chains in the outer few hundreds of angstroms, as demonstrated by the increase in the dichroic ratio of the anti-symmetric absorbance, see Table 2.3 and Figure 2.8. This increase in orientation does not appear to be as pronounced as that seen in the bulk polymer, implying that the surface regions are less preferentially aligned by drawing than the bulk material.

Table 2.3 Effect of Drawing on the Surface Orientation of LDPE.

DRAW RATIO	POLARISATION	ABSORBANCE	
		SYMMETRIC	ANTI-SYMMETRIC
0	NONE	10.7	13.0
	H	10.7	13.0
	V	10.2	12.2
	DICHROIC RATIO	1	0.9
8	NONE	6.5	6
	H	7.4	8.1
	V	8.3	13.0
	DICHROIC RATIO	1.1	1.6

The apparent degree of crystallinity of the oriented and the nominally amorphous material was determined by comparing the wholly crystalline absorbance at 2900cm^{-1} with the amorphous and crystalline absorbances at 2920 and 2850cm,$^{-1}$ shown in Table 2.4.

Table 2.4 Effect of Drawing on Surface Crystallinity.

SAMPLE	ABSORBANCE			RATIO	
	2850	2920	2900	2900/2850	2900/2920
LDPE					
0	10.7	13.0	4.5	0.42	0.35
8	6.5	6.0	3.7	0.57	0.62
					±0.03
HDPE					
0	12.5	15.2	5.6	0.45	0.37
8	12.7	12.3	7.9	0.62	0.64

It can be seen that in the top half micron of the HDPE and LDPE films the degree of crystallinity is similar for corresponding orientations. As it has been shown that in the bulk HDPE has a greater degree of crystallinity than LDPE, it is believed that in the outer tens of angstroms sampled using XPS HDPE is probably less crystalline than LDPE. If this were the case it might be expected that the high density polymer would be more susceptible to surface oxidation using plasma methods than the low density material. However, it is not easy to explain why HDPE might be more amorphous in the outermost surface layers, although if this is really the case it might be dependent on the fabrication process, alternatively the more ordered HDPE may limit the possibility of partial reordering of those chains in

the surface region which are excluded from crystals, whereas in the LDPE samples a greater surface mobility may allow a means of local ordering to occur. However, rationalisation of these observations has to be tenuous.

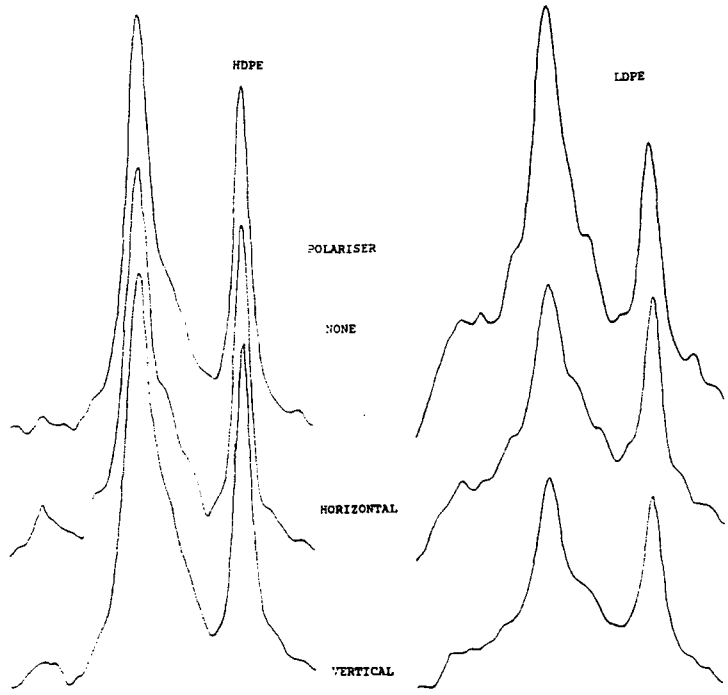

Figure 2.8 ATR Spectra of Oriented HDPE and LDPE

2.3.2 PLASMA MODIFICATION OF DRAWN AND UNDRAWN POLYETHYLENE

LDPE samples of varying orientations were treated with 20W, 30s oxygen plasma: all samples underwent an increase in surface oxidation as shown by the increase in signal intensity in the high binding energy portion of the C1s envelope and the increase in $O_{1s}:C_{1s}$ atomic ratios shown in Figure 2.9 and Table 2.5.

It was observed that orienting LDPE has a dramatic effect on the susceptibility of the polymer to plasma oxidation. Subsequent XPS measurements revealed that the loss of oxidation

at the surface[18] in the two days after treatment was greatly reduced by orientation, see Figure 2.10.

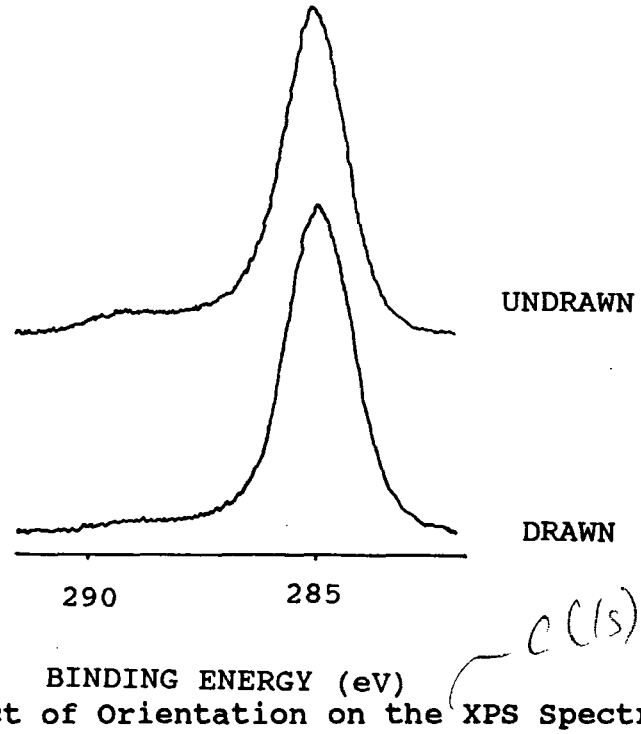

Figure 2.9 Effect of Orientation on the XPS Spectra of LDPE.

Using a 20W, 30s oxygen plasma both low and high density polyethylene were modified, samples were examined using XPS at take off angles of 35 and 70° in order to obtain information about the depth profile of the modification (see Appendix). It was found that both HDPE and LDPE were less susceptible to plasma oxidation after the stretching process, however HDPE showed a tendency to greater oxidation at the surface than LDPE, see Table 2.5. It is thought that this latter observation was due to the apparent lower crystallinity of HDPE at the surface when compared with LDPE, an observation consistent with the somewhat surprising conclusions of the ATR FTIR studies described earlier.

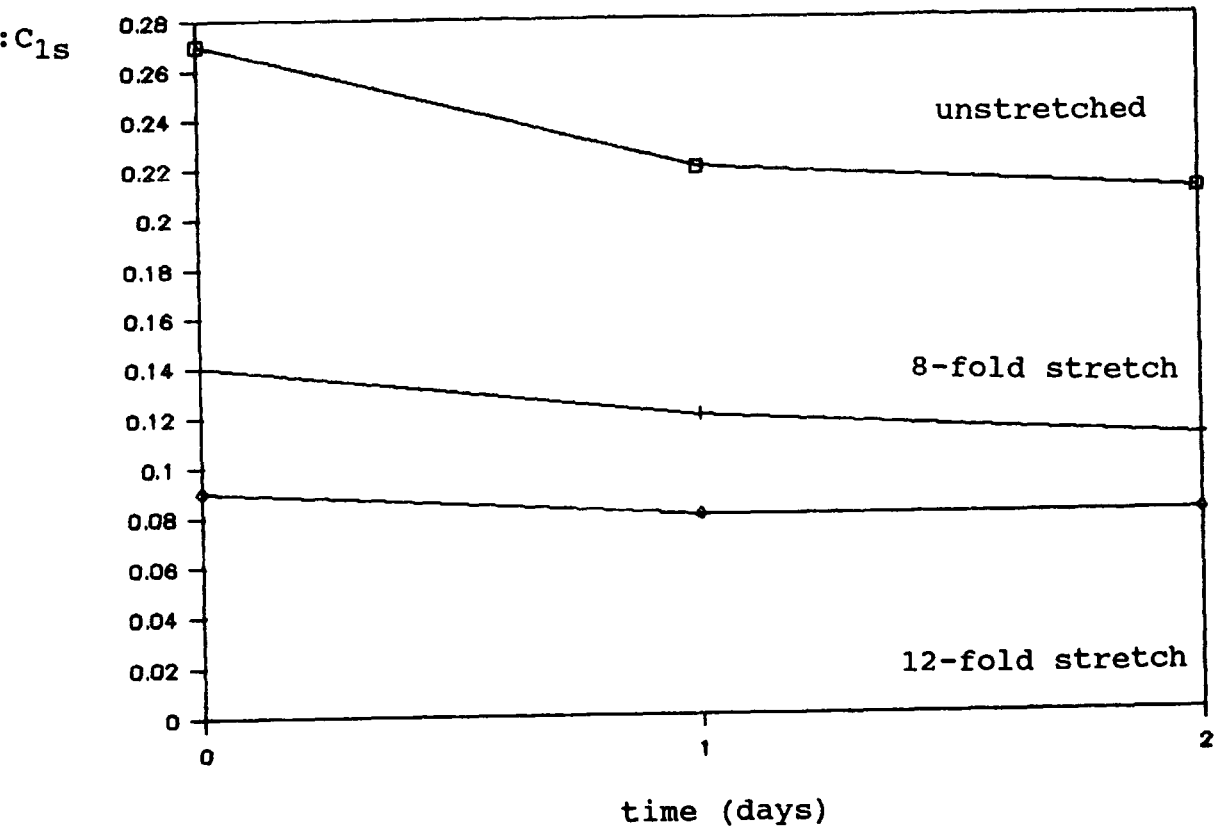

Figure 2.10 Effect of Drawing on the Ageing of Plasma Modified LDPE.

Increasing the duration of treatment of a polymer with an oxygen plasma results initially in an increase in the amount of oxidation at the surface, however, after a time no significant increase in oxidation at the surface occurs, instead further oxidation results in the breakdown and loss from the surface of polymeric fragments.[19] HDPE samples of various draw ratios (0, 8, 12) were treated with a 10W plasma for increasing periods of time. It proved impossible to continue the experiment for more than five samples in the case of the most highly drawn samples because of the difficulty of producing enough sample from one drawing experiment, and it was found that batch to batch

variations were too great for samples from more than one batch to be used for comparison. The XPS O_{1s}:C_{1s} atomic ratios show that the samples have significant differences in oxidation for short treatment times, all samples reach a similar plateau value with the more oriented samples appearing to reach this value less quickly than the more amorphous samples (see Figure 2.11).

Table 2.5 XPS Depth Profiling of Plasma Oxidised PE.

O_{1s}:C_{1s} XPS ATOMIC RATIOS

TAKE OFF ANGLE		35	70
SAMPLE	DRAW RATIO		
LDPE	0	0.27	0.24
	8	0.20	0.18
HDPE	0	0.31	0.35
	8	0.21	0.22

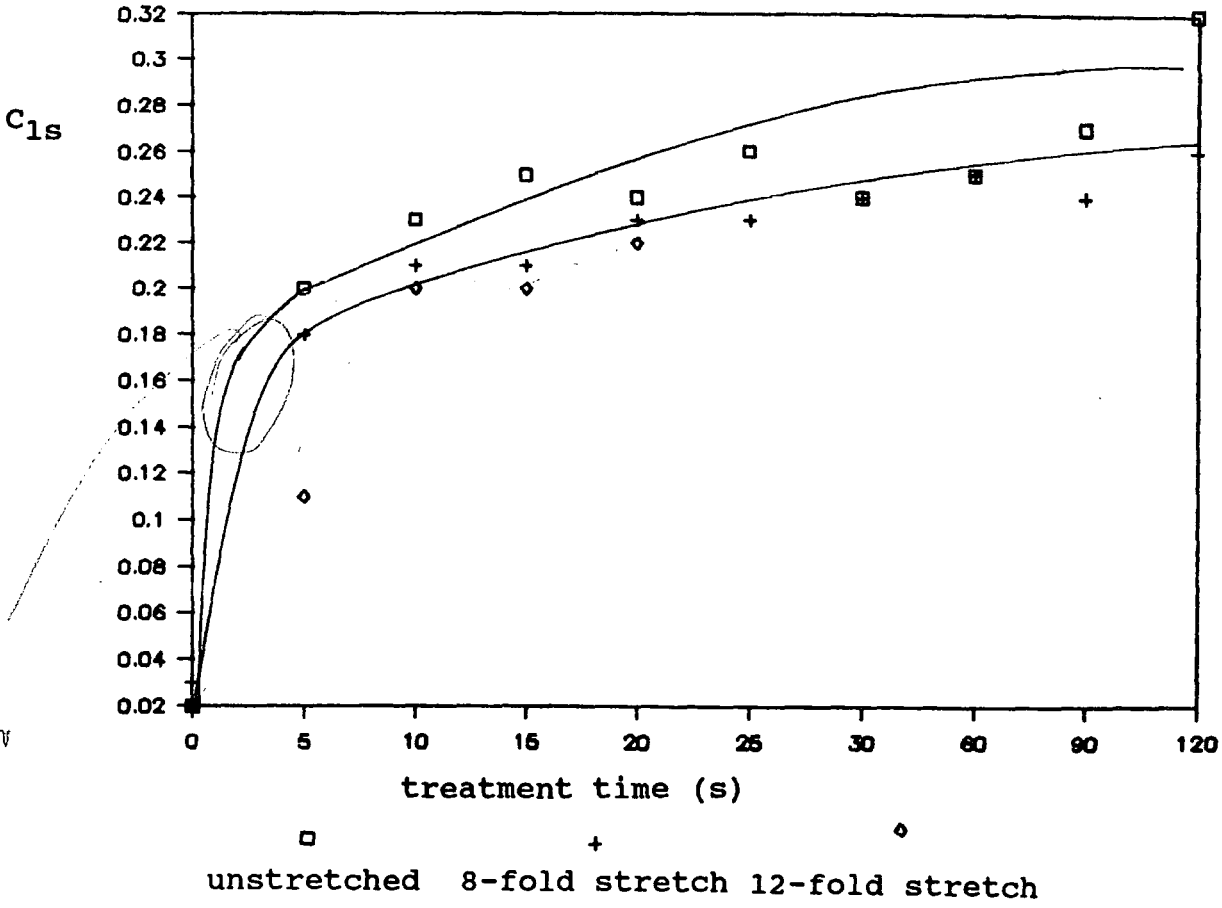

Figure 2.11 Effect of Duration of Plasma on Oxidation of Oriented and Unoriented HDPE Films.

2.3.3 CONCLUSIONS

It has been shown that drawing polyethylene films induces a degree of order in the form of both orientation and crystallinity at the surface. This results in a surface which is less susceptible to plasma oxidation and which once modified, ages less rapidly than the unoriented material.

2.4 EFFECT OF BIAXIAL ORIENTATION ON POLYPROPYLENE

2.4.1 INFRA-RED SPECTROSCOPY OF POLYPROPYLENE

Infra-red spectra of biaxially oriented and unoriented polypropylene were obtained (see Figure 2.12) and the apparent degree of crystallinity measured from various crystalline absorbances[10] in the spectra compared with the amorphous band at 1158 cm^{-1} (see Table 2.6). Only isotactic absorbances were used as only one syndiotactic absorbance was observed at 977cm^{-1}, suggesting that the polymer is predominately isotactic.

Table 2.6 Effect of Biaxial Orientation on the Apparent Degree of Crystallinity of Polypropylene.

	APPARENT DEGREE OF CRYSTALLINITY	
SAMPLE	AMORPHOUS	ORIENTED
ABSORBANCE cm^{-1}		
997	0.9	1.0
842	0.8	0.7
809	0.3	0.3

As can be seen from the above data biaxial orientation does not appear to increase the crystallinity of polypropylene. This is contrary to other work in this area,[20] which suggests that orientation induces crystallinity in polypropylene, however, it is believed that factors such as the atacticity of the sample and

the initial absolute degree of crystallinity will greatly effect orientation induced crystallisation. In this case any effect of stretching the sample on plasma modification will be solely due to the induced orientation of the molecules rather than a loss of mobility caused by the formation of crystallites.

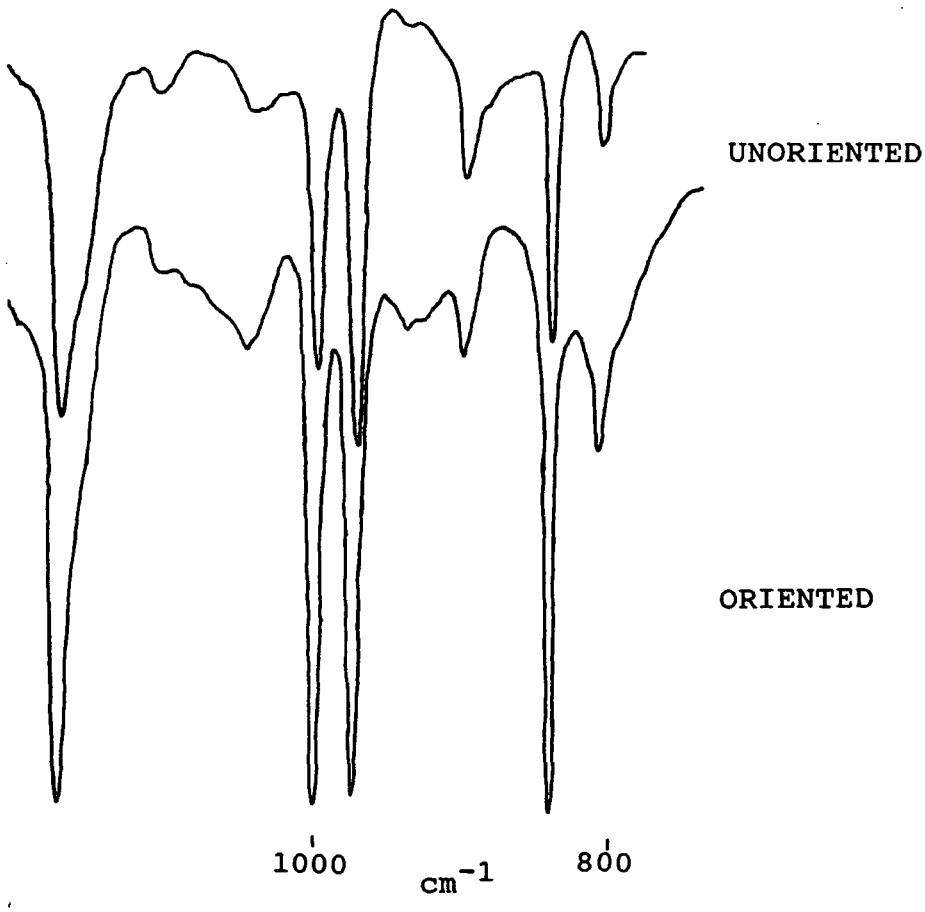

Figure 2.12 Infra-red Spectra of Oriented and Unoriented Polypropylene.

2.4.2 PLASMA MODIFICATION OF POLYPROPYLENE

Unoriented and biaxially drawn polypropylene samples were subjected to two plasma treatments one at 10W for 10s the other at 30W for 30s. On treatment both samples showed a dramatic increase in oxidation as evidenced by the increase in signal intensity in the higher binding energy part of the C_{1s} envelope and the increase in the ratios of O_{1s}:C_{1s} in the XPS spectra, shown in Figure 2.12. It was observed that biaxially oriented polypropylene oxidised to a marginally less than unoriented polypropylene under the influence of a plasma see Table 2.7.

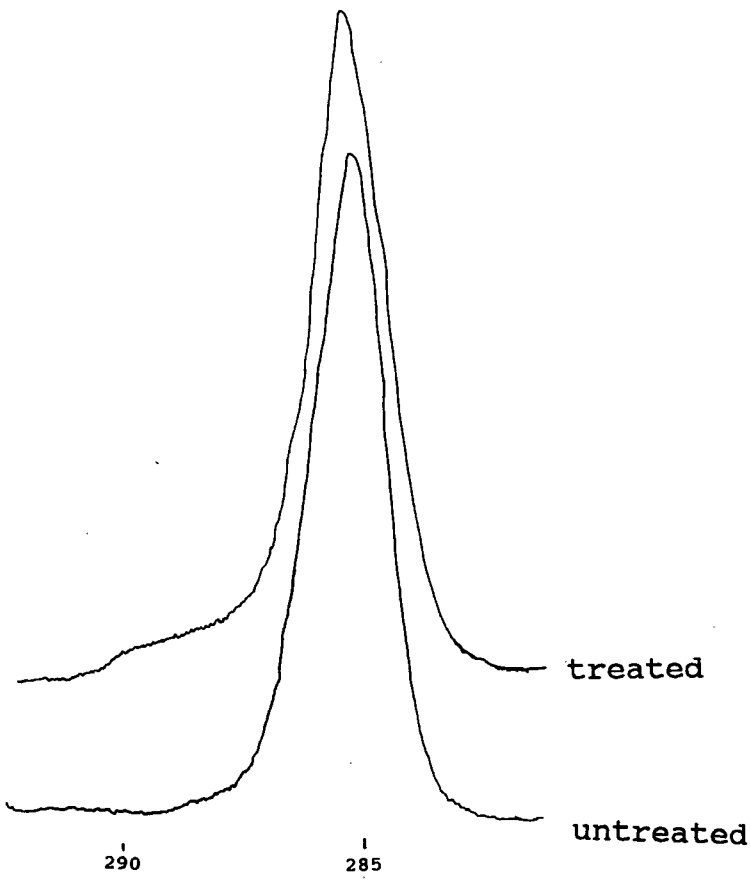

Figure 2.13 C_{1s} Envelope for Treated and Untreated Polypropylene.

Orientation of polypropylene films reduces the susceptibility of samples to plasma oxidation, however this has a relatively small effect on the ageing of the plasma modified surface, see Table 2.8.

Table 2.7 Effect of Plasma Modification on Unstretched and Biaxially Stretched Polypropylene.

TREATMENT	SAMPLE	$O_{1s}:C_{1s}$	
		35	70
30s, 30W	UNSTRETCHED	0.26	0.20
	STRETCHED	0.23	0.19
10s, 10W	UNSTRETCHED	0.31	0.24
	STRETCHED	0.29	0.24

Table 2.8 Ageing of Plasma Modified Polypropylene.

DAY	$O_{1s}:C_{1s}$	
	UNORIENTED	ORIENTED
0	0.26	0.23
1	0.25	0.23
2	0.26	0.23
3	0.23	0.22
4	0.24	0.21
5	0.24	0.22

No significant differences in the contact angles of oriented and unoriented polypropylene were observed, however both samples showed a drop in contact angle with water of 30° on plasma modification. It is thought that the differences observed using XPS were too small to be seen using the contact angle technique.

2.4.3 CONCLUSIONS

It has been shown that the effects of orientation of polypropylene on the extent of plasma modification are similar to those in polyethylene, although not as marked. This inhibitory effect is not apparently due to any increase in crystallinity as infra-red measurements failed to detect this. However, no significant effect was seen in the early stages of the ageing of plasma modified polypropylene.

2.5 PLASMA ETCHING OF POLYMERS

It is known that plasmas of gases such as O_2 and CF_4 will etch or ablate the surface of polymers[6] this technology has been widely investigated with regards to the etching of resist materials in the micro-electronics industry. Plasmas cause fragmentation of the polymer chains, the longer the duration of plasma treatment, the greater the degree of break up of the polymer at the surface. Some of the polymeric fragments generated are small enough to escape from the surface and are lost to the plasma.

2.5.1 XPS ANALYSIS OF PET AND PEEK

Samples of polyethylene terephthalate (PET) and poly (ether ether ketone) (PEEK) were investigated to determine the effect of their crystallinity on their plasma etch rates. Moderate oxygen plasma (30W, 30s) treatment of the samples causes significant changes in the XPS C_{1s} envelope of both polymers, as shown in Figure 2.14. However it should be noted that in the case of PET,

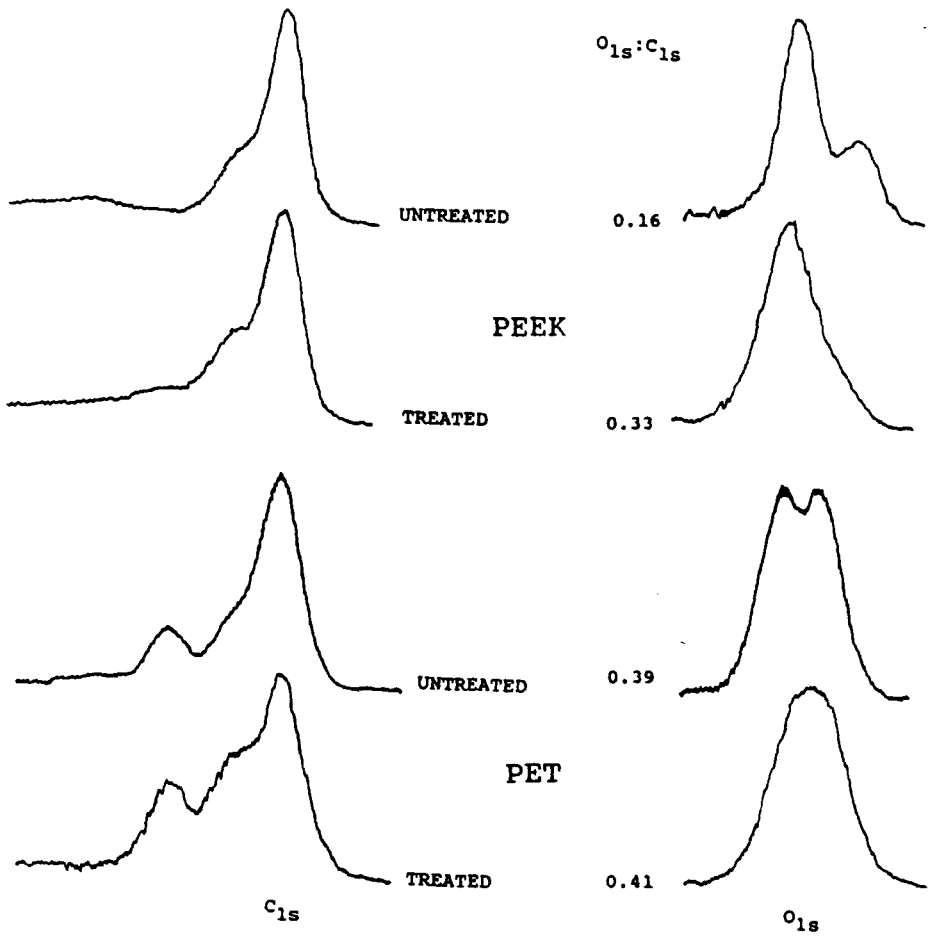

Figure 2.14 XPS Spectra of Plasma Modified PEEK and PET.

plasma treatment did not cause a substantial increase in the $O_{1s}:C_{1s}$ atomic ratios and that a greater degree of crystallinity did not lead to any decrease in surface oxidation. This could be

a result of the samples with a higher bulk crystallinity being less crystalline at the surface, as was thought to be case for polyethylene, however, this is unlikely as the washing in chloroform that these samples received is known to cause surface crystallisation.[9]

2.5.2 PLASMA ETCHING OF PET AND PEEK

Etch rates were measured using weight loss caused by a 50W plasma of 1hr. and 1.5hr. duration, results are outlined in Table 2.9a,b. It was observed that for PEEK the semi-crystalline sample etched to a lesser degree than the amorphous sample, however the reverse was found to be true for PET.

Table 2.9a Effect of Crystallinity on the Etch Rate of PEEK.

CRYSTALLINITY %	SURFACE AREA cm^2	WEIGHT LOSS mg	TIME hr.	ETCH RATE mg $cm^{-2}hr.^{-1}$ ±0.02
0	1.74	0.40	1	0.23
10	1.74	0.35	1	0.20
20-23	1.74	0.34	1	0.19
35	1.74	0.28	1	0.16

SEM micrographs of amorphous and semi-crystalline PEEK are very similar (see Figures 2.15a, b), before treatment the films are very smooth and the pictures had to be obtained by focusing

on scratches and contaminants introduced to the surface. After etching the surface became roughened as some areas etched

Table 2.9b Effect of Crystallinity on the Etch Rate of PET.

CRYSTALLINITY %	SURFACE AREA cm^2	WEIGHT LOSS mg	TIME hr.	ETCH RATE mg $cm^{-2}hr.^{-1}$ ±0.02
0	1.03	0.15	1	0.14
	1.39	0.28	1.5	0.13
22	1.03	0.18	1	0.17
	1.39	0.35	1.5	0.17
51	1.03	0.21	1	0.20
	1.39	0.39	1.5	0.19

preferentially to others but with no abrupt changes from one region to another. Amorphous PET looked very similar to the PEEK samples, however, the 51% crystalline samples were quite different. Before etching the surface was seen to be fairly smooth with some pitting, this was probably caused by the cleaning of the polymer with chloroform causing surface crystallisation. After etching the surface appeared to have lost material in a very selective manner, see Figure 2.16a, b.

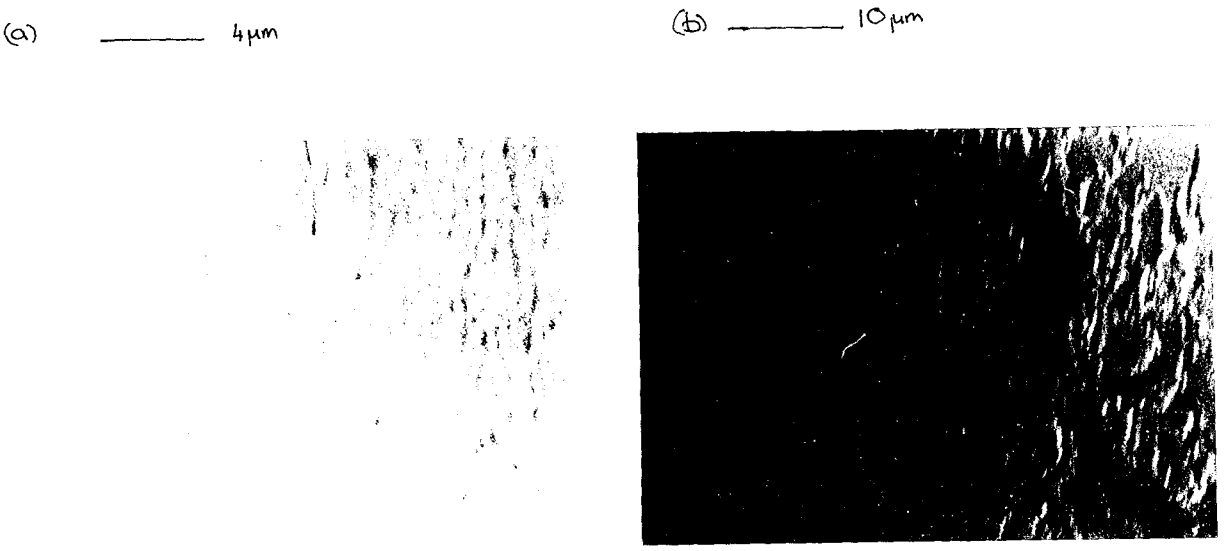

Figure 2.15 SEM Micrographs of Amorphous PEEK a) Unetched b) Etched.

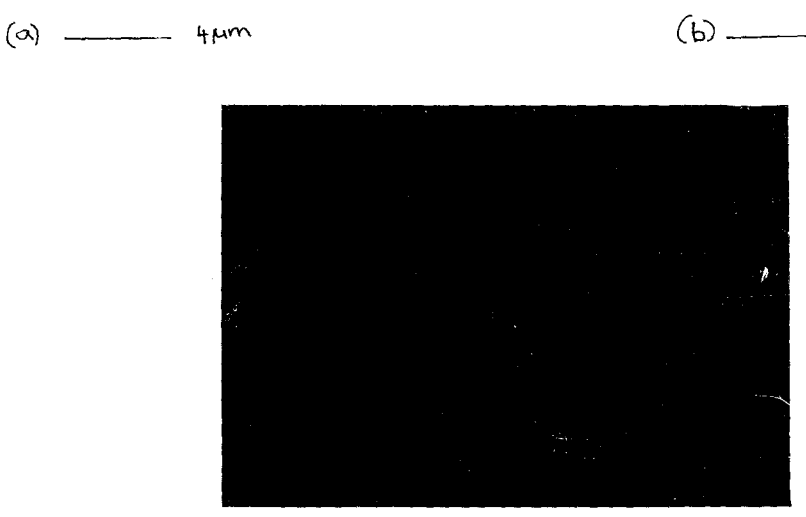

Figure 2.16 SEM Micrographs of 51% Crystalline PET a) Unetched b) Etched.

2.5.3 CONCLUSIONS

The etching of PEEK in an oxygen plasma, as expected, is inhibited by increasing the crystallinity. The unexpected behaviour of PET is thought to be solely due to the method of preparation of the semi-crystalline samples. It is believed that both the method of crystallisation and the solvent washing of PET samples causes the polymer chains at the surface to become highly stressed. These chains can be thought of as being similar to taut pieces of elastic readily relaxing when cut by the plasma. Using this analogy it is apparent that the more highly stressed regions of the PET surface will be more readily etched than the less stressed regions, causing the selective etching observed with SEM. This also provides a basis for a possible explanation of the semi-crystalline PET material etching more readily than the amorphous polymer.

2.6 DISCUSSION

Increasing the ordering of the polymer matrix, by orientation or crystallinity appears to reduce the susceptibility of the polymer surface to plasma oxidation. It is known that increasing the crystallinity of polymers reduces their susceptibility to chemical attack and dye sorption.[2] It has traditionally been assumed that diffusion into the polymer is mainly controlled by chain segmental mobility[20], crystallites in polymers generally inhibit molecular motion, not only in the crystalline regions but also in the directly adjacent amorphous

regions.[21] Rao and Dweltz[22] have observed that the dye uptake of various PET samples was hindered to a greater degree by orientation of the polymer than by increasing the degree of crystallinity. They proposed that the main factors influencing the uptake of dye into the polymer were chain packing, tortuosity, compactness or the size of diffusion channels within the polymer matrix.

These factors could explain why oriented and crystalline samples are less susceptible to plasma oxidation than unoriented and amorphous material. It is believed that the surface morphology of polymers is substantially different from the bulk,[23] probably being more amorphous and less closely entangled than in the bulk. Drawing of polymers increases their nominal surface area, 200-250% in the case of the polyethylene used in this investigation, and reduces film thickness. This will result in the surface region becoming thinner and regions of polymer chains which were previously part of the bulk of the sample could now be regarded as part of the surface region. After the drawing process the excited species from within the plasma will be less able to penetrate into the polymer surface and therefore less oxidation will take place. Increasing the crystallinity of the polymer will have a similar effect, the greater ordering of the polymer simply does not allow any room for the oxidising species to get in and attack.

The relaxation of plasma modified surfaces is believed to depend on the molecular mobility of the substrate,[24] the greater the degree of mobility within the polymer the faster the decay of

surface oxidation. It was observed that in the case of polypropylene, orientation did not introduce any increase in the degree of crystallinity, and that no significant difference was seen in the ageing characteristics of undrawn and biaxially drawn samples. Conversely with polyethylene, where stretching induces a large increase in crystallinity, the oriented samples aged at a slower rate.

REFERENCES

1. Krevelen & Hoftzer, "Properties of Polymers," 2nd Ed., Elsevier, Amsterdam, 1976.
2. R.W. Moncrieff, "Manmade Fibres," Butterworth & Co., London, 1970.
3. I.M. Ward, "Mechanical Properties of Solid Properties," Wiley & Sons, London, 1971.
4. J.M. McKelvey, "Polymer Processing," Wiley & Sons, New York, 1962.
5. F. Beuche, "Physical Properties of Polymers," Wiley & Son, New York, 1962.
6. J. Friedrich, J. Gahda & M. Photil, Acta Polymer., 31(5), p310-315, 1980.
7. T. Liu & I.R. Harrison, Polymer, 28, p1860-62, 1987 and references therein.
8. M.R. Tant & G.R. Wilkes, J. App. Polym. Sci., 26(9), p2813, 1981.
9. S.S. Im & H.S. Lee, J. App. Polym. Sci, 37(7), p1801-14, 1989, and references therein.
10. J.F. Rabek, "Experimental Methods in Polymer Chemistry," J. Wiley & Sons, Chichester, 1980.
11. R.G. Snyder, J. Chem. Phys., 47(4), p1316-60, 1967.
12. S. Krimm, Adv. Polm. Sci., 2, p51, 1960.
13. S.L. Aggerwal, G.P. Tilley & O.J. Sweeting, J. App. Polym. Sci., 1, 19, 1959.
14. J.D Ferry, "Viscoelastic Properties of Polymers," Wiley, New York, 1961, and references therein.

15. C.S.P. Sung & J.P. Hobs, Chem. Eng. Comm., 30, p229-50, 1984.

16. Reference 10 Chapter 15.

17. R.G. Snyder, J. Phys. Chem, 86, p5145-50, 1982.

18. P.M. Triolo & J.D. Andrade, J. Biomed. Mater. Res., 17, p129-147, 1983.

19. A.M, Wrobel, M. Kryszewski, W. Rabowski, M. Oboniewsk & Z. Kubacki, Polymer, 19, p909, 1978.

20. J. Crank & G.S. Park, " Diffusion In Polymers," Academic Press, London, 1968.

21. S. Hu, M. Xu, J. Li, B. Qian, X. Wung, R.W. Lenz & R.S. Stein, Polymer, 29, p789, 1988.

22. M.V.S. Rao & N.E. Dweltz, J. App. Polym. Sci., 33, p835, 1987.

23. F.J.B. Calleja, G. Ortega, & J.M. de Salazar, Polymer, 19, p1094-99, 1978.

24. H.F. Beer, Ph. D. Thesis, Durham, 1980.

CHAPTER THREE

AN INVESTIGATION INTO THE AGEING OF PLASMA MODIFIED PEEK

3.1 INTRODUCTION

The oxygen discharge treatment of polymers has been extensively reported,[1-10] particularly in studies on improving wettability and adhesive properties. Much is known about the immediate changes produced in a variety of substrates, such as polyethylene[1], polydimethylsiloxane[2] and poly(ethylene terephthalate)[3], and by a number of techniques, including corona discharge[4] and both radiofrequency[5] and microwave[6] plasmas. It has been shown that, after treatment there is an initial dramatic decrease in contact angle with water which subsequently increases and levels off to a plateau value after a few days.[7] It has been suggested that this decrease in hydrophilicity is due to a combination of two processes. One involves rotation of surface polar groups into the bulk of the material to reduce the surface energy,[8] the other is due to migration of low molecular weight, polar fragments into the polymer matrix[9]. It has been shown recently[10] that the aged surface becomes transiently hydrophilic before attaining the final plateau value of contact angle. This latter observation suggests that the dynamics of plasma treated surfaces are more complex than originally envisaged.

In the work presented in this chapter, contact angle measurements and XPS have been used to follow changes in the surface chemistry of four oxygen plasma modified samples of poly (ether ether ketone) (PEEK) of different crystallinities and degrees of orientation.

3.2 EXPERIMENTAL

3.2.1 MATERIALS

Samples of PEEK were provided by ICI plc, four different types of film were investigated:

amorphous, A;

10% crystalline and uniaxially oriented, B;

20-23% crystalline and unoriented, C;

35% crystalline and biaxially oriented, D.

Samples were washed in "Micro" detergent as supplied by the International Products Corporation, and thoroughly rinsed in distilled water followed by hot methanol, until XPS showed them to be clean. All samples had an initial contact angle of 87±2° with water.

3.2.2 PLASMA TREATMENT

Samples were treated in a Polaron E2000 Plasma Asher/Etcher, using a 30W oxygen plasma for 30s at a pressure of 0.2mbar. The samples were then stored in air at either -18°C, 2°C, 21°C, or 45°C. All were stored at ambient humidity (R.H. 40-60%) except those at -18°C which were stored in a P_2O_5 desiccator to prevent formation of ice on the surface.

3.2.3 CONTACT ANGLE MEASUREMENTS

Contact angle measurements were performed using the sessile

drop technique using a 1 microlitre drop of distilled water. Averages of at least three measurements were taken, these averages were found to be consistent within ±2° for contact angles greater than 20° and ±3° for contact angles of less than 20°. For contact angles less than ca. 8° a reliable result could not be obtained. In order to determine the surface energy contact angles were also made with 1 microlitre drops of di-iodomethane, the surface energies were calculated according to the method described in Chapter One.

3.2.4 XPS MEASUREMENTS

Core level spectra for C_{1s} and O_{1s} regions were recorded on a Kratos ES200 electron spectrometer using $Mg_{Ka}1,2$ x-rays and an operating pressure of 10^{-7}Torr. Electron take-off angles of 70° and 35° were used to investigate the vertical homogeneity of the sample. A take-off angle of 70° samples a depth of ca. 15Å for carbon and ca. 10Å for oxygen, at 35° the sampling depth is ca. 35Å for carbon and ca. 25Å for oxygen.[11] Atomic ratios were measured to ±1 oxygen per 100 carbon atoms. Peak fitting was performed according to the method of Clark et al.[12] Because of limited spectrometer time XPS spectra were only obtained for amorphous PEEK (sample A) stored at 45°C.

3.2.5 SIMS

SIMS spectra were recorded by Dr. D. Briggs, at ICI

Materials Research Centre, Wilton. Spectra were obtained on a VG Esca Lab #1 Vac System operating at a base pressure of 10^{-9} Torr, using an AG61 Ion Gun, a MM12-12 quadrapole and a LEG 31 electron gun. The ion gun operated using Xenon ions at 4kV with a current density of 1 nano amp/cm^2, the electron gun neutralised the charge on the polymers using electron accelerated by 700eV with similar charge density. Data acquisition rate was 150ms dwell time per channel with 10 channels per a.m.u. Total ion dose was less than 10^{13} ion/cm^2.

3.3 PLASMA MODIFICATION OF PEEK

3.3.1 INITIAL EFFECTS OF TREATMENT

Directly after treatment most samples were completely wetted by water or had contact angles too small to be measured with any degree of accuracy. After approximately five minutes contact angles could be measured and were found to be in the region of 4° to 15°, tending to be lower for the less crystalline samples, however the large relative errors in this region make meaningful comparison difficult if not impossible.

The XPS spectrum of untreated PEEK (see Figure 3.1) shows within experimental error that there are the expected 16 oxygen atoms per 100 carbon atoms. The C_{1s} spectrum shows a shoulder to higher binding energy relative to the main photo-ionisation peak at 285eV indicating carbon singly and doubly bonded to oxygen and a shake-up satellite at a shift of 7eV due to aromaticity.[11] The O_{1s} spectrum of pristine PEEK indicates the presence of two

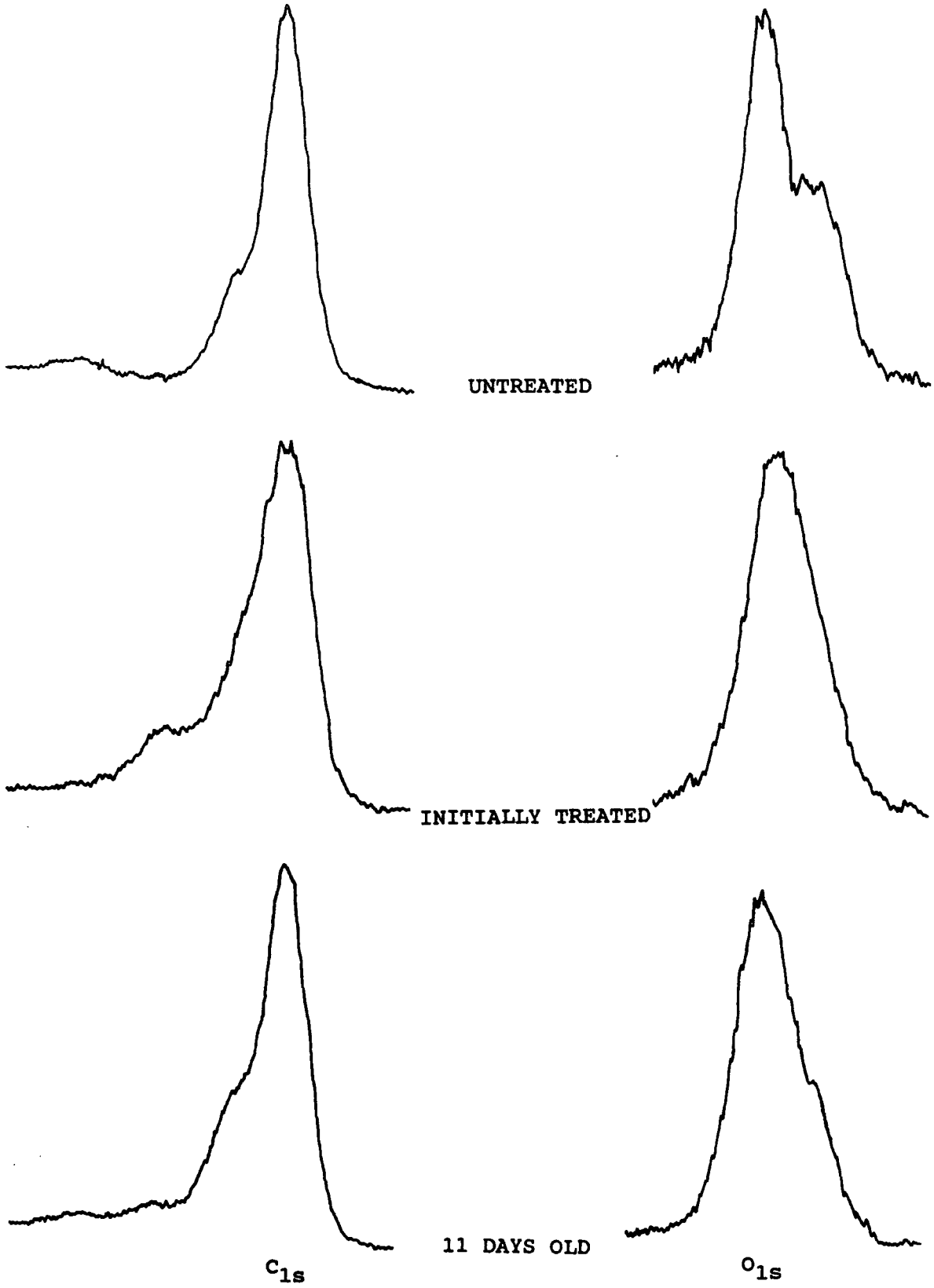

Figure 3.1 XPS Spectra Showing Effect of Plasma Modification on Amorphous PEEK and Subsequent Ageing of the Surface.

oxygen environments namely ether and carbonyl. After plasma treatment the increased complexity of the spectra, (see Figure 3.1), indicates that a variety of new functionalities have been formed. Peak fitting the C1s envelope reveals the presence of C-O, C=O and O=C-O in relatively large quantities and a smaller amount of carbonate as shown in Table 3.2. XPS spectra directly after plasma treatment show an oxygen to carbon ratio of 35 to 100.

3.3.2 CONTACT ANGLE DECAY OF PLASMA MODIFIED PEEK

Most samples show a decay curve as illustrated in Figure 3.2 and in the Appendix 3.1, with the plateau and transient drop in contact angle occurring as recorded in Table 3.1. The semi-crystalline and drawn samples tend to show a slower rate of increase in contact angle and the onset of the sudden transient drop in contact angle is delayed compared to the amorphous polymer. The effect of increasing the temperature is marked. The rate of relaxation of the surface is increased as manifest by: the more rapid attainment of plateau contact angle which is higher at higher temperature; and the earlier occurrence and the brevity of the transient increase in hydrophilicity. The semi-crystalline and biaxially drawn samples (C and D) do not appear to undergo a transient increase in hydrophilicity (see Appendix 3.1), it is possible that the phenomenon does not occur under these conditions or that it occurs between measurements; it is not practically possible to continuously monitor the contact angle.

Table 3.1. Effect of Storage Conditions on Transient Increase in Hydrophilicity and Plateau Contact Angle.

CONDITIONS		PLATEAU VALUE	TIH* TIME	TIH* DURATION DAYS
	°C	°		
AMORPHOUS A	-18	25**	21	3
	2	40	18	2
	21	43	15	2
	45	48	9	1
UNIAXIALLY DRAWN B	-18	31	24	3
	2	40	21	3
	21	45	17	2
	45	49	10	1
SEMI-CRYSTALLINE C	-18	30	23	3
	2	40	20	2
	21	40	17	2
	45	49	--	--
BIAXIALLY DRAWN D	-18	34	25	3
	2	38	22	3
	21	42	--	--
	45	47	--	--

* TIH = transient increase in hydrophilicity.
** samples kept at -18°C did not always reach a plateau value.
-- TIH not experimentally observed.

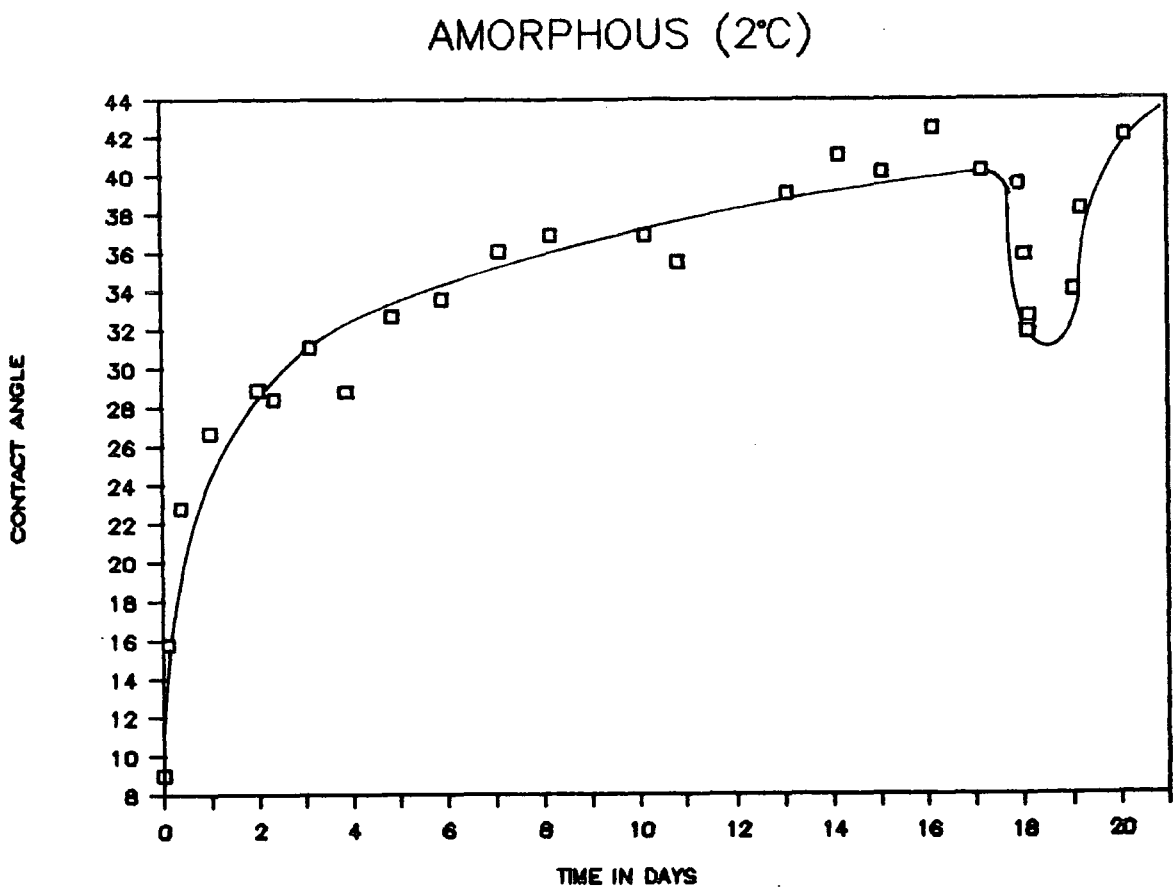

Figure 3.2. Typical Decay of Contact Angle Exhibited by Plasma Modified PEEK

3.3.3 XPS ANALYSIS OF AGEING OF PLASMA MODIFIED PEEK

During the first two days after treatment the level of oxidation at the surface decreases from a value of thirty-five to a steady value of about twenty-eight oxygens per hundred carbons. The shake-up satellite becomes more apparent and the region to the high binding energy end of the C_{1s} envelope decreases in intensity implying that a greater proportion of unmodified material is present at the surface. The general appearance of the O_{1s} envelope also begins to resemble the spectrum obtained for the starting material, in that ether and carbonyl components become more obvious, as shown in Figure 3.1. Initially there were differences in the O_{1s} to C_{1s} ratio obtained

Table 3.2. Relaxation of the Surface of Plasma Modified PEEK as Revealed by XPS.

DAY	TAKE-OFF ANGLE	RELATIVE AREA UNDER C_{1s} ENVELOPE						
		C-C/H	C-O	C=O	O-C=O	CO3	π-π^*	O_{1s}/C_{1s}
0	70°	58	21	9	9	3	0	0.33
1		59	19	9	7	3	2	0.29
8		77	15	3	3	1	2	0.29
8.5		74	15	6	3	2	3	0.28
9		72	16	4	4	2	2	0.29
9.5		66	20	5	4	3	3	0.29
11		74	15	4	3	1	3	0.28
0	35°	64	20	5	5	3	3	0.35
1		64	22	5	4	2	3	0.32
8		64	20	5	3	4	3	0.29
8.5		63	21	5	3	4	4	0.28
9		63	21	5	4	3	3	0.29
9.5		65	22	5	3	3	2	0.28
11		63	21	5	4	3	4	0.28
UNTREATED		70	19	5	0	0	6	0.16

from spectra recorded at take-off angles of 70° and 35°, (see Table 3.2), after about two days both sets of spectra have identical O_{1s} to C_{1s} atomic ratios, although those with take-off angles of 70° show a relatively higher proportion of hydrocarbon carbon compared to oxygen functionalised carbon in the peak fitting of the C_{1s} envelope. The reasons for this initial discrepancy are unclear; hydrocarbon contamination from within the spectrometer could be the cause, however, that would not explain why this effect is only temporary.

During the transient increase in hydrophilicity no increase in O_{1s} to C_{1s} atomic ratio is observed, however, analysis of the C_{1s} envelope implies that a significant increase in the extent of oxidation at the surface occurs at this stage. This is evidenced as an increase in the proportion of carbon associated with various oxygen functionalities especially for the carbon singly bonded to oxygen environment.

3.3.4 SIMS ANALYSIS OF THE AGEING OF PLASMA MODIFIED PEEK.

SIMS spectra were obtained for amorphous (A) and biaxially drawn (D) PEEK, at 1, 5 and 9 days after plasma treatment and during the transient increase in hydrophilicity for the amorphous sample. These spectra are shown in Appendix 3.2 at the end of this chapter.

The spectra of untreated PEEK are typically what would be expected, they are not very intense, suggesting a low level of fragmentation probably due to the aromaticity of the polymer. The

most apparent peaks are those in the negative ion spectrum for fragments associated with C_1 and C_2, which show a typical aromatic pattern.[13] After treatment the observed fragmentation pattern changes dramatically, this is most apparent in the general increase in intensity of the spectra, the very intense mass fragment peaks at 18 and 130 m/e in the positive ion spectrum and the change in fragmentation pattern in the negative ion spectrum. The fragment at 18 m/e is readily explained as water from the environment adsorbed onto the hydrophilic surface. The fragment at 130 m/e has not been assigned, it appears to occur in all plasma oxidised aromatic polymers and is thought to be an aromatic alcohol.[13]

On ageing, the positive ion spectra of amorphous PEEK (A) show a decrease in the amount of water on the surface, also there is a reduction in the intensity of C_2/CO fragments and increases and subsequent decreases in intensity of fragment patterns, firstly with those centred on 55 and followed by those centred on 70 m/e. The fragments at 39, 41 and 43 m/e appear to increase in intensity relative to the other species observed and are probably due to C_3 and C_2O fragments. The negative ion spectra generally show a lessening in intensity of all the mass fragments with time with a slight decrease in the O/OH fragments compared with C/CH fragments and a much larger decrease in the fragments at 41, 43 and 45 m/e when compared to the C/CH fragments.

Spectra recorded during the transient increase in hydrophilicity show differences to the other spectra, viz. in the

positive ion spectrum the counts at higher mass ranges are significantly reduced with the mass fragments at 121 and 129 m/e becoming more apparent and the the 130 m/e ion has becoming less intense. In the negative ion spectrum the intensity of fragments at 41, 43 and 45 m/e has increased along with the ratio of O/OH to C/CH.

As expected the spectra obtained for biaxially drawn samples of PEEK (D) show different ageing characteristics to those seen for amorphous PEEK. In the positive ion spectra the C_2/CO fragmentation pattern is not immediately prominent, however, it is seen in the 5 day old sample and has only decreased marginally compared to the other peaks by the ninth day. Also on the fifth day the fragmentation pattern centred on m/e 55 is apparent and that centred on m/e 70 is beginning to emerge. After 9 days 55 m/e pattern is unchanged and that at 70 m/e has increased in relative intensity. The negative ion spectra generally show a lessening in intensity of all the mass fragments with time, however, there is no decrease in the O/OH or 41, 43 and 45 m/e fragments compared with C/CH fragments. The differences seen between the amorphous and more crystalline samples can be ascribed to the slower decay of surface modification which is thought to occur for the latter sample.

3.3.5 CONCLUSIONS

The data presented here show that the ageing and transient increase in hydrophilicity of plasma treated PEEK is dependent

upon the mobility of the sample as characterised by its relation to crystallinity and temperature. The increase in hydrophilicity suggests that the observed decay in contact angle results from a complex set of interacting processes, which are not yet fully understood. This phenomenon is discussed in greater detail in section 3.5.

3.4 CALCULATION OF YASUDA'S MOBILITY PARAMETER.[14]

3.4.1 INTRODUCTION

Yasuda has investigated the decay of plasma fluorinated surfaces stored in water, defining a mobility parameter, k. In this paper he states:

> "A parameter which describes the surface character for a sample immersed in water for t minutes, A_t, is found to be related to the parameter of the original (unimmersed) film, A_0, by the following equations, which generally describe diffusion controlled chemical reaction in polymer matrices where the extent of reaction is proportional to path length:
>
> $$A_t = A_0 t^{-k} \qquad 3.1$$
>
> or
>
> $$\log A_t = \log A_0 - k \log t." \qquad 3.2$$

It is the authors contention that these equations are not mathematically viable, in the first place they are dimensionally unbalanced. Also, according to the definition given, at t=0, $A_t=A_0$; but, from equation 3.2, as t tends to zero A_t tends to infinity, implying that A_0 is infinite.

The equation used in this work was modified to allow for an increase in contact angle with time and to attempt to overcome some some of the problems already outlined above,

$$A_t = A_1 t^k, \qquad 3.3$$

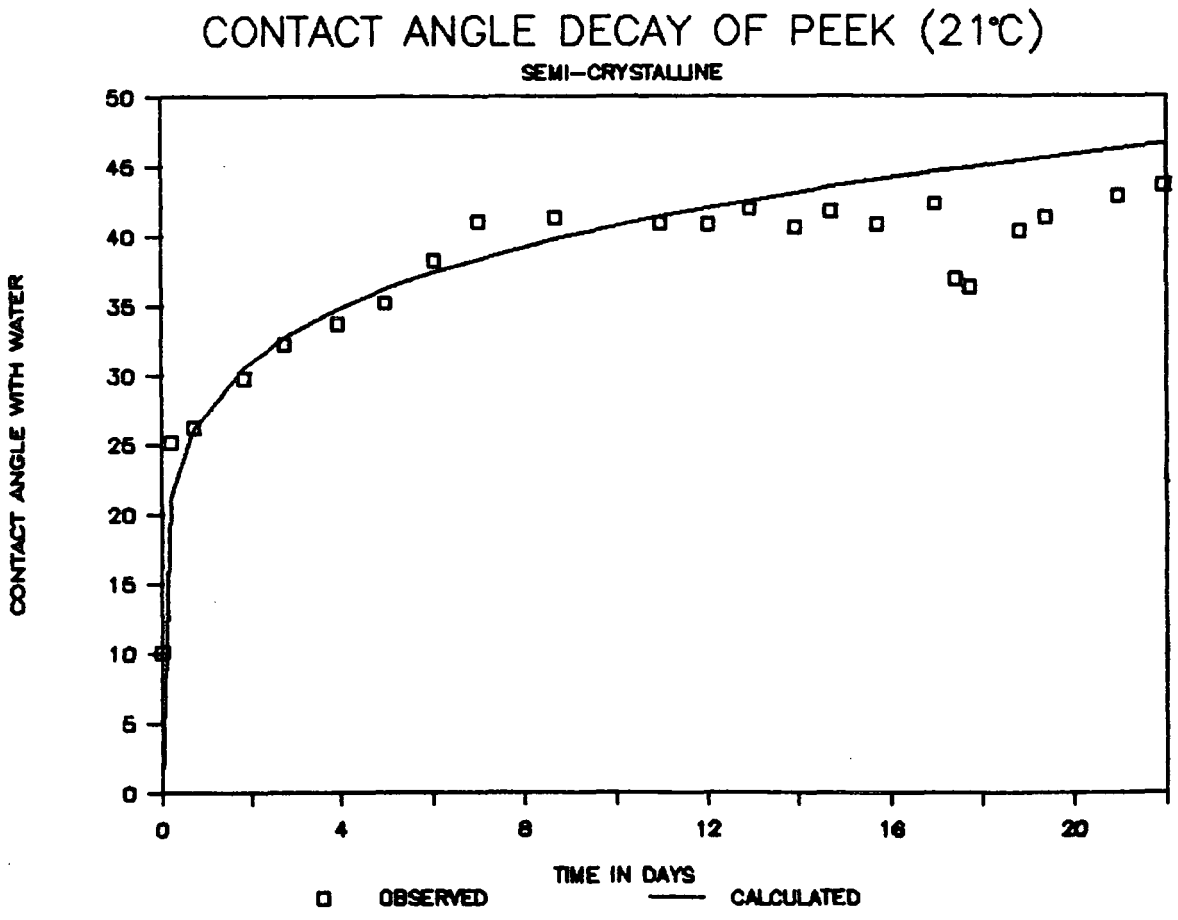

FIGURE 3.3 Comparison of Observed and Calculated Contact Angle.

in effect what has been done is to swap A_0 (i.e. A_t at t=0) for A_1 (i.e. A_t at t=1) in order to obtain a better fit and avoid, the problems described above. It also appears that Yasuda held that the relationship is held was sound because a straight line was obtained for a plot of log contact angle versus log of time, although this appears to be true within the limits of experimental error, it has been found that the modified exponential form of Yasuda's equation i.e. Equation 3.3 only loosely agrees with the data (see Figure 3.3). While there is some correlation between the experimental results and this equation it cannot in any sense be regarded as having any sound scientific validity. In any event in his own publication Yasuda ignored the region below t=1 which is a tacit acknowledgement that the expression used is unsound.

However, the comment was made that this empirical formula was only valid for the initial stages of the ageing process and that the parameter, k, depends on the type of measurement used in the computation, this dependency was attributed to the sensitivity of the measurement to the surface dynamic changes occurring after plasma modification. The value of k was taken as an indication of the surface dynamic mobility of polymers, being related to the ease of rotational and diffusional migrations from the surface into the bulk of a material.

3.4.2 RESULTS AND CONCLUSIONS

Using the modified Yasuda expression, Equation 3.3, plots of

log contact angle versus log time gave fairly straight lines up to the transient increase in hydrophilicity, see Figure 3.4, from these graphs a set of mobility parameters were computed, and are shown in Table 3.3.

It can be seen that k values show the expected trends, increasing with temperature, and decreasing with crystallinity and orientation. From the results shown here and those obtained by Yasuda it would appear that the k parameter does reflect trends in mobility at the polymer surface and it may be related to the ease of various migrations of plasma created species into the bulk.

However, it is unclear how the original equation was derived and what the scientific justifications for it are. It is found experimentally that the equation is not adhered to in the later stages of relaxation (see Figure 3.2) and theoretically it breaks down as t approaches zero, predicting an infinite rate of reaction:

$$A_t = A_1 t^k \qquad 3.3$$

$$\frac{d(A_t)}{dt} = A_1 k t^{k-1} \qquad 3.4$$

$$\frac{d(A_t)}{dt} = A_t k t^{-1}. \qquad 3.5$$

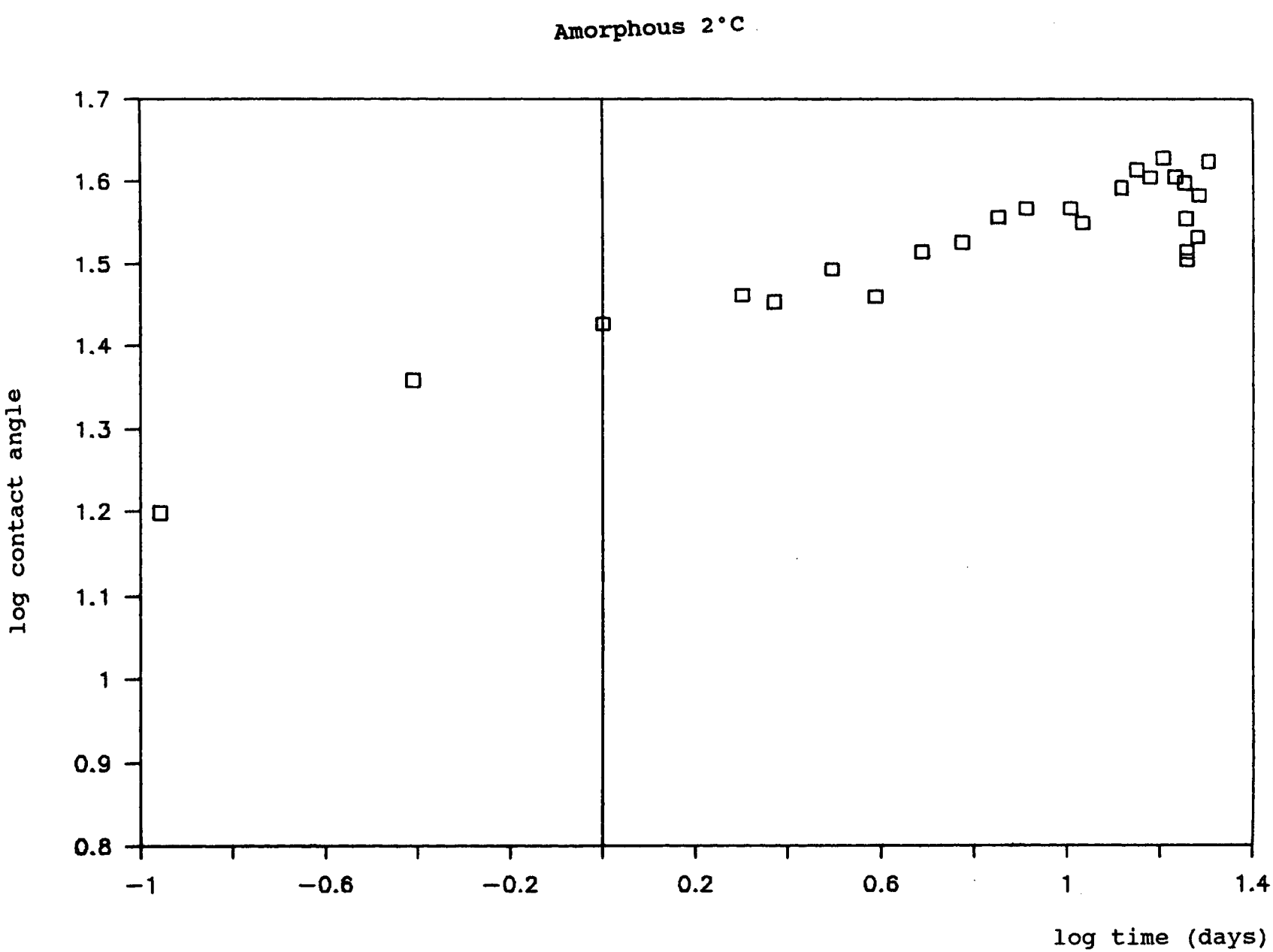

Figure 3.4 Typical Log Contact Angle vs. Log Time plot.

Table 3.3 Effect of Sample and Storage Condition upon k.

		STORAGE CONDITIONS (°C)				
SAMPLE		-18	2	21	45	
AMORPHOUS	A	0.13	0.17	0.19	0.22	
UNIAXIALLY DRAWN	B	0.14	0.15	0.15	0.21	±0.1
SEMI-CRYSTALLINE	C	0.13	0.15	0.17	0.19	
BIAXIALLY DRAWN	D	0.13	0.12	0.12	0.13	

Also despite modification it is still not a dimensionally correct equation so the values of k obtained have no physical meaning.

It is still possible, despite the many reservations that exist with regards to this parameter it may have a use as a "qualitative" indicator of surface behaviour. This number when restricted to depicting trends may shed some light on the relative mobilities at the surfaces of different polymeric materials.

3.5 KINETIC ANALYSIS

3.5.1 THEORY

Consider the highly idealised plasma modified surface depicted in Figure 3.5. Progressing from the unmodified bulk to the outer surface layers one encounters polymer fragments which become increasingly oxidised, smaller in size and less closely packed. It is thought that at the outermost surface the polymeric fragments are highly mobile and will be able to rotate relatively freely when compared to species in the bulk of the material.

Directly after plasma treatment all species will tend towards a more thermodynamically favoured configuration with the more polar regions of the polymeric fragments being directed in towards the bulk. This will have a dramatic effect on the observed contact angle, as the changes are occurring within the sampling depth of this technique. The species will subsequently migrate into the sub-surface layers and possibly into the bulk of the material. This later process will have a less dramatic effect on the contact angle, for two reasons.

Firstly the contact angle technique is highly surface selective[15] and the migrations will be occurring at the limit or beyond the scope of this technique. Thus, the loss from the surface of screened polar groups by migration towards the bulk will be less noticeable than the initial screening of those groups consequent on the initial conformational reorganisation.

Secondly as the smaller species migrate into the material

larger fragments will be uncovered acting in opposition to the general trend of increasing contact angle. However, as these fragments are uncovered they will be subject to the same thermodynamic considerations as the previous fragments, and thus the ageing process continues until equilibrium is reached.

less fragmented and oxidised

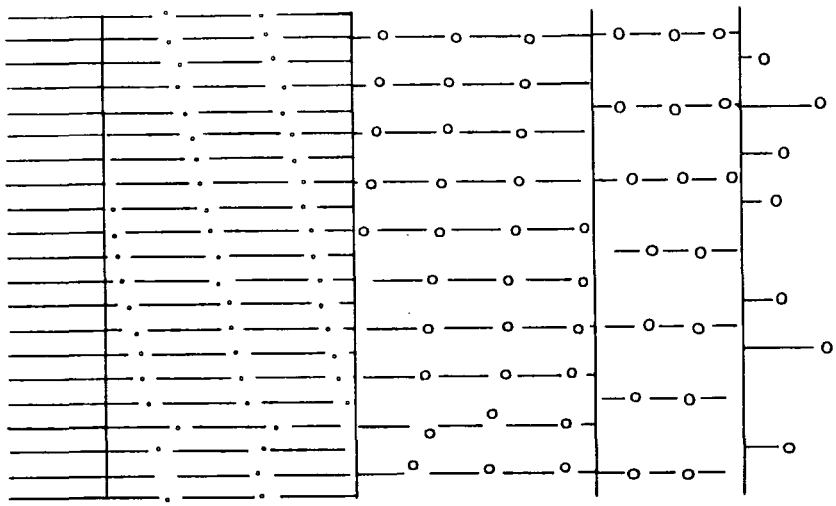

highly fragmented and oxidised

Figure 3.5 Idealised Schematic Representation of a Plasma Modified Polymer Surface.

The rate of decay of the contact angle will be dependent upon the distance from equilibrium relative to the range of contact angles through which the system must progress to acquire an apparently stationary state.[16] Normalising the observed contact angle at time, t, a parameter, A, may be defined:

$$A_t = \frac{\theta_\infty - \theta_t}{\theta_\infty - \theta_0} \cdot \qquad 3.6$$

The normalised contact angle parameter, A, would be expected to decrease with time under the normal course events. The rate of decay of this parameter can be thought of as a summation of interdependent factors, outlined in Figure 3.6 and the equation below:

$$-\frac{dA_t}{dt} = f(\text{rotation of outermost species}) + f(\text{migration of outermost species}) - f(\text{appearance of new species at the surface}) + f(\text{rotation of new outermost species}) \quad 3.7$$

To perform a kinetic analysis on this system several assumptions must be made.

1 The first process is much faster than the others and its effect on the way the contact angle changes will become negligible relatively quickly after plasma modification.

2 Migrations of polymeric fragments will have a negligibly small effect upon contact angle, compared to conformational reordering.

3 Rotations of newly uncovered moieties at the surface will be dependent upon the rate of their appearance and the two terms can be combined.

Having made these assumptions the above equation can be simplified as follows:

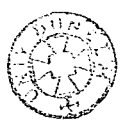

$$-\frac{dA_t}{dt} = f(\text{rotation of outermost species})$$
$$+(a-1)f(\text{appearance of new species at the surface})$$
$$+(b-1)f(\text{appearance of next new species at surface})$$
$$+(c-1)f(\text{appearance of next species at surface}) \ldots \quad 3.8$$

where a, b, c etc. are parameters which reflect the ease with which each species can reorientate towards the bulk.

Although the ageing of the plasma modified surface has been described as a stepwise process involving several surface layers it must be a nearly continuous process, with gradual decrements in the parameters a, b etc., and with one event merging into the next. The appearance of larger less modified fragments at the surface will be dependent upon the migrations of the smaller fragments into the bulk. As the fragments get progressively larger their diffusion into the polymer will be hindered by their size, however, the general permeability of the surface layers of the polymer will be enhanced by the plasticising effect of previous migrations into the polymer by other plasma created moieties.[16] Within the limits of the contact angle technique it can be expected that in the initial stages of surface relaxation only two processes will be seen: the initial rotation of the outer most fragments and the subsequent uncovering and rotation of the next largest family of fragments. Although the parameters governing the later process will change during the relaxation of the surface, these changes would be very gradual and not noticeable for the earlier stages of the reorganisation of the surface within the limits of the experimental technique.

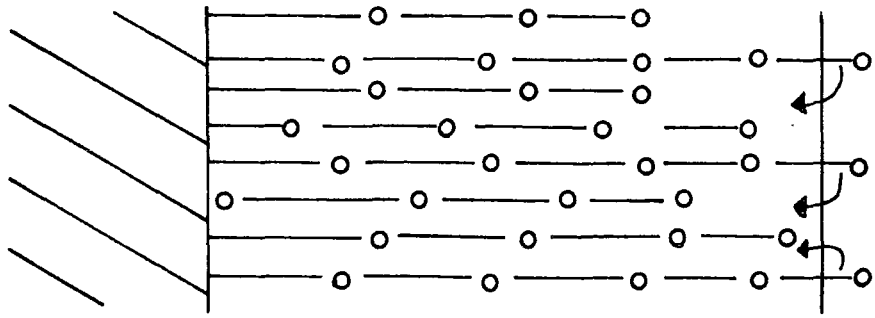

initial rapid rotation of small fragments

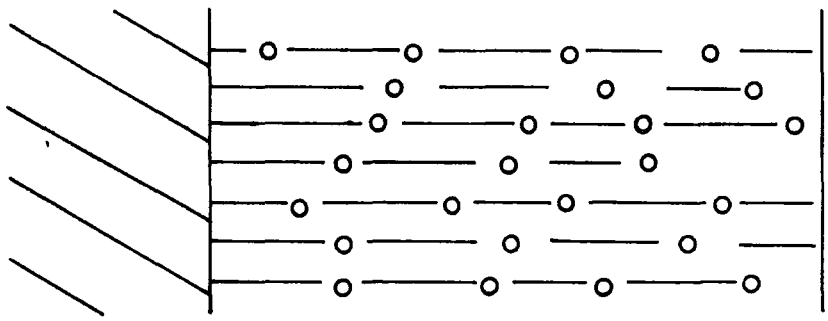

migration into the sub-surface

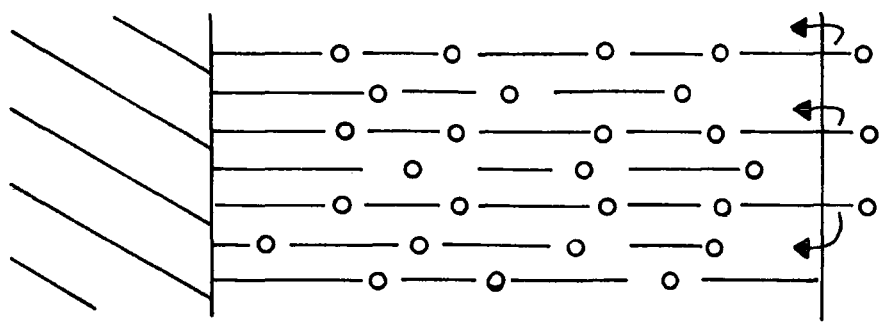

rotation of larger fragments

Figure 3.6 Schematic Representation of the Possible Relaxation Processes After Plasma Modification.

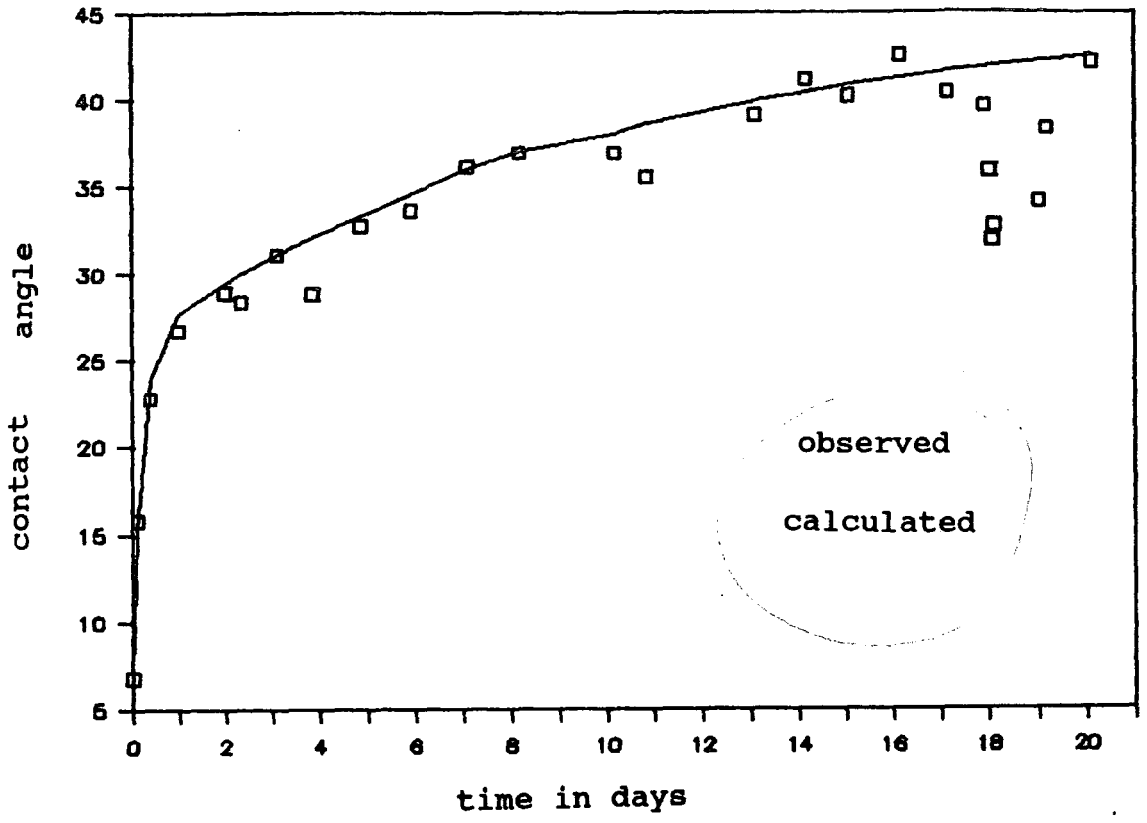

Figure 3.7 Comparison of Theoretical and Observed Contact Angle Decay.

For the initial stages of decay the normalised contact angle would vary according to the following equation:

$$A_t = q_1 e^{-k1t} + q_2 e^{-k2t}, \qquad 3.9$$

and would be expected to give a decay curve as depicted in Figure 3.7. To test this hypothesis equation 3.9 has been applied to the experimental data, a series of first order rate constants have been obtained and these have been used in an Arrhenius analysis equation to give estimates of activation energies which could be and the correlated with the probable processes occurring at the surface.

3.5.2 ANALYSIS OF DATA

Plots of the natural logarithm of the normalised contact angle against time were observed to be typical of that seen in the decay of two first order processes,[18] these analyses are shown in Appendix 3.3 at the end of this chapter. From the first order plots two series of rate constants were obtained, k_1, referring to the initial faster process and, k_2, referring to subsequent reorganisations these are shown in Table 3.4.

As recorded in Table 3.4, the errors involved are very large this will greatly effect the results obtained from an Arrhenius treatment of this data. However, two sets of lnk versus 1/T were obtained, and a linear regression analysis was performed on the points to obtain a best estimate of E_a/R for each system (shown in Figure 3.8). It has to be stressed that the propagation of errors through the procedures outlined above means that the results emerging from this analysis can only give a rough idea of the magnitude of the activation energies.

The activation energies obtained using this method were very low and it was decided to compare those obtained from direct contact angle measurements with those calculated from the surface energies. Contact angles against water and di-iodomethane were monitored in the first hour after the plasma treatment, in this period it was considered that secondary ageing processes would have little impact on the overall rate of surface relaxation. Values of k_1, first order rate constant were calculated from surface energies normalised according to the method described

Table 3.4. First Order Rate Constants for the Decay of Plasma Oxidised PEEK.

SAMPLE	T (K)	1/T (K^{-1}) x10^{-3}	k_1 ($hr.^{-1}$)	k_2	LNk_1	LNk_2
AMORPHOUS	255	3.92	3	0.07	1.10	-2.66
A	275	3.64	6	0.10	1.79	-2.30
	294	3.40	8.5	0.14	2.14	-1.97
	318	3.14	10	0.20	2.30	-1.61
UNIAXIALLY	255	3.92	2	0.04	0.69	-3.22
DRAWN	275	3.64	4	0.05	1.39	-3.00
B	294	3.40	4.5	0.11	1.50	-2.21
	318	3.14	6	0.18	1.79	-1.72
SEMI-	255	3.92	1.5	0.03	0.41	-3.51
CRYSTALLINE	275	3.64	2	0.07	0.69	-2.66
C	294	3.40	3.5	0.12	1.25	-2.12
	318	3.14	5	0.11	1.61	-2.21
BIAXIALLY	255	3.92	1	0.05	0.00	-3.00
DRAW	275	3.64	1	0.05	0.00	-3.00
D	294	3.4	2	0.06	0.69	-2.81
	318	3.14	5	0.12	1.61	-2.12
ERRORS			±0.5	±0.02		

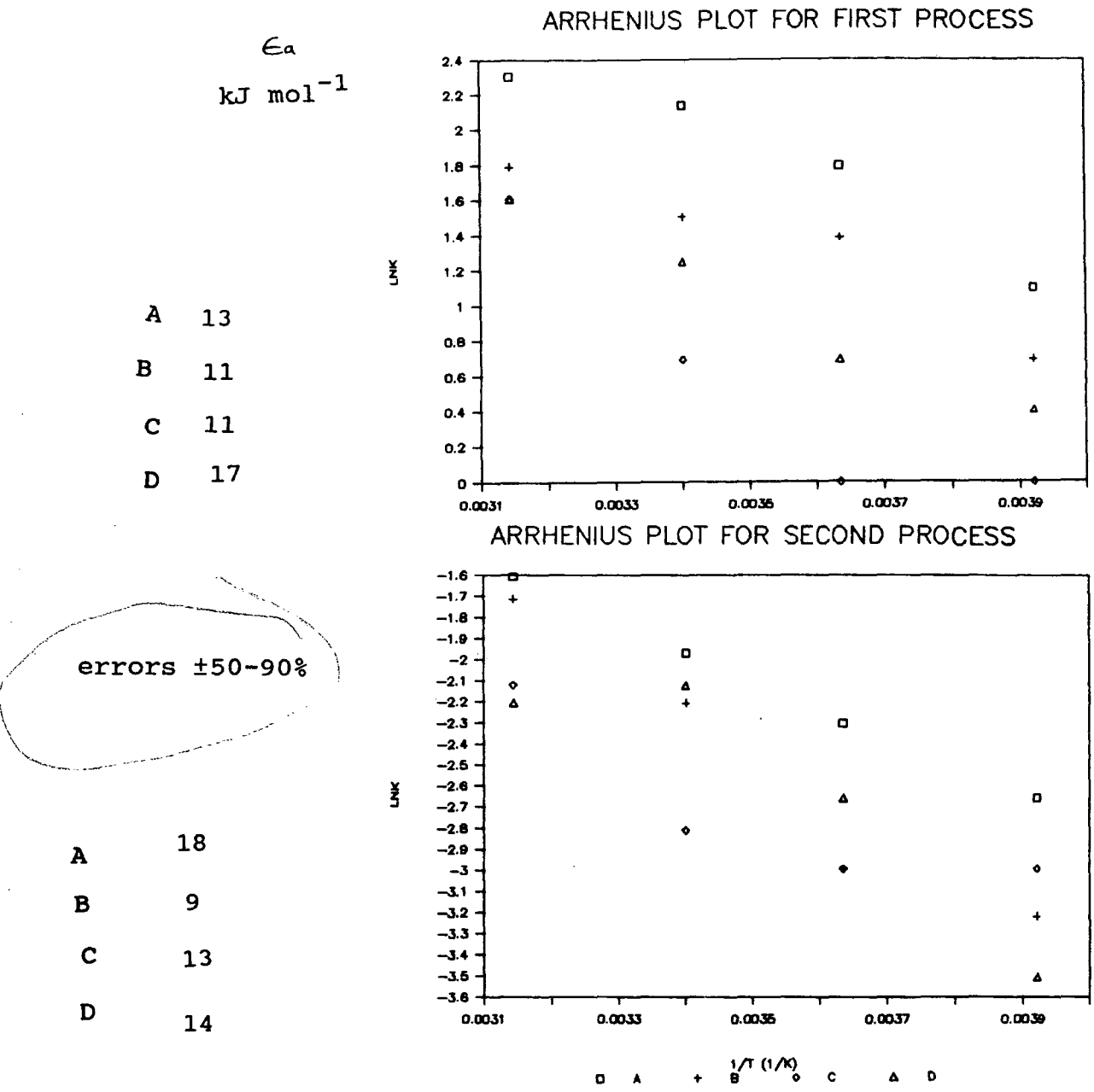

Figure 3.8 Arrhenius Plots for the Decay of Plasma Modified PEEK.

in Chapter One. However, it emerged that this method gave errors at least as large as those obtained from contact angles against water alone, also, the activation energies calculated from these measurements were similar to those obtained previously (see Table 3.5).

Table 3.5. Activation Energies Obtained from Normalised Surface Energies.

SAMPLE	A	B	C	D
E_a(kJ mol^{-1})	12±21	14±10	8±22	12±12

3.5.3 CONCLUSIONS

It should be noted that even allowing for the enormous errors on the activation energies obtained, the values are too low to be compared with any bulk motions in the PEEK. The lowest energy relaxation of PEEK found in the literature was the sub Tg ß-transition at 40 kJ mol^{-1} as determined by Starkweather and Avakian.[19]

3.6 DISCUSSION

From the contact angle data it is apparent that reorganisation of the surface is taking place within the region sampled by the contact angle experiment, said to be ca. 5Å,[20] the initial very rapid change in contact angle observed in the first few minutes after plasma modification is probably due to the reorientation of highly mobile fragments created by the treatment. The changes in the surface over the next few days were observed with XPS, SIMS and contact angle measurements

suggesting that at least some of these changes are due to migration of fragments from the surface into the bulk. Subsequently a further slight decrease in the amount of oxidation at the surface and a similar increase in the contact angle with water is observed. At the transient increase in hydrophilicity a discrepancy in the XPS and contact angle data is seen. The XPS data obtained during this work consistently shows no significant increase in the amount of oxygen at take off angles of either 70° or 35°, however, previous work using more vigorous plasma oxidation and storage at 20°C[10] does show a significant increase in oxidation for a sampling depth of 25Å during the transient increase in hydrophilicity. Although in this work no increase in the total amount of oxygen present was observed, the C_{1s} envelope does show an apparent increase in the proportion of oxygen functionalised carbon relative to hydrocarbon.

The results of the SIMS analysis indicate that the nature of polymeric fragments at the surface changes during the ageing process. At the transient increase in hydrophilicity the peak at m/e 130 in the positive ion spectrum is greatly reduced, this suggests that the surface has lost a proportion of the species which give rise to this fragment. Whether these species have been lost by migration into the sub-surface or by some other means is unclear. It is not known if the decrease in number of these polymeric fragments at the surface leads to the transient increase in hydrophilicity, however, it is consistent with the hypothesis set out in section 3.5.1.

The estimates of the activation energies are very low the true values probably lying somewhere between 10 and 20 kJ mol^{-1} for both stages of surface relaxation. Values in this region are comparable to rotations around the carbon carbon bond in ethane, butane[21] and polymethylene,[22] (12 kJ mol^{-1}) and are also similar to those for diffusion limited reactions in solution,[23] but somewhat less than typical values for the permeation of gases and solvents into polymers,[17,24] (25-100 kJ mol^{-1}) and certainly less than the activation energies for self-diffusion into polymers[17] (45-85 kJ mol^{-1}).

There are certain reservations in applying the Arrhenius equation to this system, the original approach was based on the kinetic theory of ideal gases and as such it cannot meaningfully be applied to all dynamic processes.[25] Although it is known that polymers below their glass transition temperature do not approximate to this model and that many polymeric relaxations show some deviations from linearity on Arrhenius plots, it is believed that in highly mobile systems such as plasma modified surfaces this approach will be applicable. Although both the activation energies are apparently low and of similar magnitude, the rate constants observed for the secondary process are one or two orders of magnitude less than those calculated for the primary process. This difference is probably related to the pre-exponential term in the Arrhenius equation according to the transition state theory as applied to gases[26] this factor is proportional to the term, $e^{sS0/R}$. In any gaseous process involving special geometrical arrangements or conformations for

reactions, the formation of the activated complex will involve a decrease in entropy and will thus lower the rate constant. Applying a similar premise to the reorganisations at the polymer surface it can be seen that entropic or steric considerations play a much greater role in the secondary relaxation processes.

It is probable that plasma modification produces highly fragmented species at the surface, and further into the bulk fragmentation becomes progressively less. The mobility of the species created at the surface is high and the larger fragments in the sub-surface have a correspondingly lower mobility. Directly after treatment the species at the surface reorientate very quickly and begin to migrate into the bulk. As these smaller species migrate into the bulk, larger species will replace them at the surface, reorienting as they are exposed. The reasonable hypothesis that the larger fragments of polymer chains reorientate at a slower rate than migration of the smaller species,[9] provides a basis for a possible explanation for the transient increase in hydrophilicity. Thus, the low contact angle observed at this point results from the presence of oxidised species in the surface. These species reorientate or migrate into the bulk at different rates and also have different extents of oxidation.

McBriar suggested[10] that migration of small polar fragments could result in an incompatibility between these fragments and the less polar sub-surface layers, thus providing a driving force for a reorganisation via a transient higher surface energy intermediate.

An effect that has not been considered so far is that of atmospheric interactions. The newly modified material is likely to contain free radicals, radical ions and other reactive species at the surface, it is possible that these will undergo reaction with moisture and oxygen in the air which could lead to a classical auto-oxidative degradation process[27] which will compete with the reorientation and migration processes. It is possible that this could lead to the observed temporary increase in the polarity of the surface. It is also possible that during the ageing process free radicals initially within the sub-surface are uncovered and then react with atmospheric water and oxygen, further complicating the observed surface characteristics. This concept receives some support from the analysis of ageing in CF_4 and NH_3 plasma treated polymers in Chapter Four.

From the above discussion it is clear that the dynamics of the ageing of plasma modified polymer surfaces are very complex and governed by many parameters including; the nature of the treatment, the polymer, and the storage conditions. The processes occurring at the transient increase in hydrophilicity are not fully understood. The hypotheses outlined above are all reasonable yet do not completely explain all the complexities seen in this or previous work. It is possible that the anomaly between the O_{1s}:C_{1s} atomic ratios and the changes in the C_{1s} envelope at the time of the transient increase in hydrophilicity (see Table 3.2) are due to the greater sensitivity of the O_{1s} peak to hydrocarbon contamination within the spectrometer, thus

causing the measured O_{1s}:C_{1s} atomic ratios to be apparently less than the true values. No explanation has been advanced for the apparent disappearance of the transient increase in hydrophilicity at higher temperatures for the more crystalline samples. The trends suggest that if the decrease in contact angle occurs at lower temperatures it should occur sooner at higher temperatures, and it may be of such short duration that it escapes observation.

Increasing the crystallinity and orientation of the samples increases the degree of order and reduces the free volume in a significant proportion of the polymer matrix. This hinders the movement of the polymer chains and therefore slows the ageing processes of migration and reorientation. This in turn causes the delaying of the conditions which lead to the onset of the increase in hydrophilicity. Conversely, raising the temperature of the PEEK increases the mobility of the polymer chains, thus causing the ageing processes to occur at a faster rate.

REFERENCES

1. D. Briggs, & C.R. Kendall, Intern. J. Adhesion and Adhesives. 2(1), p13, 1982.
2. J.R. Hollahan, & G.L. Carlson, G.L. J. Appl. Polymer Sci., 14, p2499, 1970.
3. D. Briggs, D.G. Rance, C.R. Kendal, & A.R. Blythe, Polymer, 21, p895, 1981.
4. L.J. Gerrenser, J.F Elman, M.G. Mason, & J.M. Pochan, Polymer, 26, p1162, 1980.
5. R.G. Nuzzo, & G. Smolinsky, Macromolecules, 17, p1013, 1987.
6. A.J. Dilks, Polymer Sci., Polymer Chem Ed., 19, p1319, 1981.
7. P.M. Triolo, & J.D. Andrade, J. Biomedical Materials Research, 17, p1013, 1987.
8. H. Yasuda, "Plasma Polymerisation," Academic Press Inc., London, 1985.
9. D. Briggs, & M.P. Seah, "Practical Surface Analysis," John Wiley and Sons, Chichester, pp359-392, 1983.
10. H.S. Munro, & D.I. McBriar, J. Coatings Technology, 60(766), p41, 1988.
11. D.T. Clark, & D. Shuttleworth, J. Polymer. Sci., Polymer Chemistry Ed., 16, p1093, 1978.
12. D.T. Clark, & A. Dilks, J. Polymer Sci., Polymer Chemistry Ed., 17, p957, 1979.
13. Private communications with D. Briggs and W.J. Brennan, ICI, Wilton.

14. T. Yasuda, K. Yoshida, T. Okuno, & H. Yasuda, J. Polym. Sci.: B Polym. Phys, 26, p1781, 1988.

15. Cherry, B.W., "Polymer Surfaces," Cambridge University Press, Cambridge, 1981.

16. D. Margerison in, "Comprehensive Chemical Kinetics," eds. C.H. Bamford & C.F.H. Tipper, Vol. 1, chapt. 5, Elsevier, Amsterdam, 1969.

17. J. Comyn, "Polymer Permeability," Elsevier, Amsterdam, 1985.

18. A. Dilks, Ph. D. Thesis, Durham, 1977.

19. H.W. Starkweather Jr. & P. Avakian, Macromolecules, 22(10), p4040-2, 1989.

20. F. Garbassi, M. Morra, E. Occhiello, & L. Pozzi, 9th International Symposium on Plasma Chemistry. Symposium Proceedings: Vol3. P1595, 1989.

21. W.J. Orville-Thomas, "Internal Rotations in Molecules," J. Wiley & Sons, London, 1974.

22. A. Abe in "Comprehensive Polymer Science," Vol. 2, Eds. G. Allen & J.C. Bevington, Chapter 2, Pergamon Press, Oxford, 1989.

23. C.H. Bamford, C.F.H. Tipper & R.G. Compton, "Comprehensive Chemical Kinetics," Vol. 25, Elsevier, Amsterdam, 1969.

24. J.H. Flynn, Polymer, 23, p1325, 1982.

25. D. Dollimore, Analytical Proceedings, 25, p10, 1988.

26. R. P. Wayne in "Comprehensive Chemical Kinetics," Eds. C.H. Banford & C.F.H. Tipper, Chap. 3, Vol. 2, Elsevier, Amsterdam, 1969.

27. Photodegradation, Photo-oxidation and Photostabalization of Polymers. John Wiley and Sons, London (1975).

APPENDIX 3.1 CONTACT ANGLE DECAY OF PEEK

AMORPHOUS (−18°C)

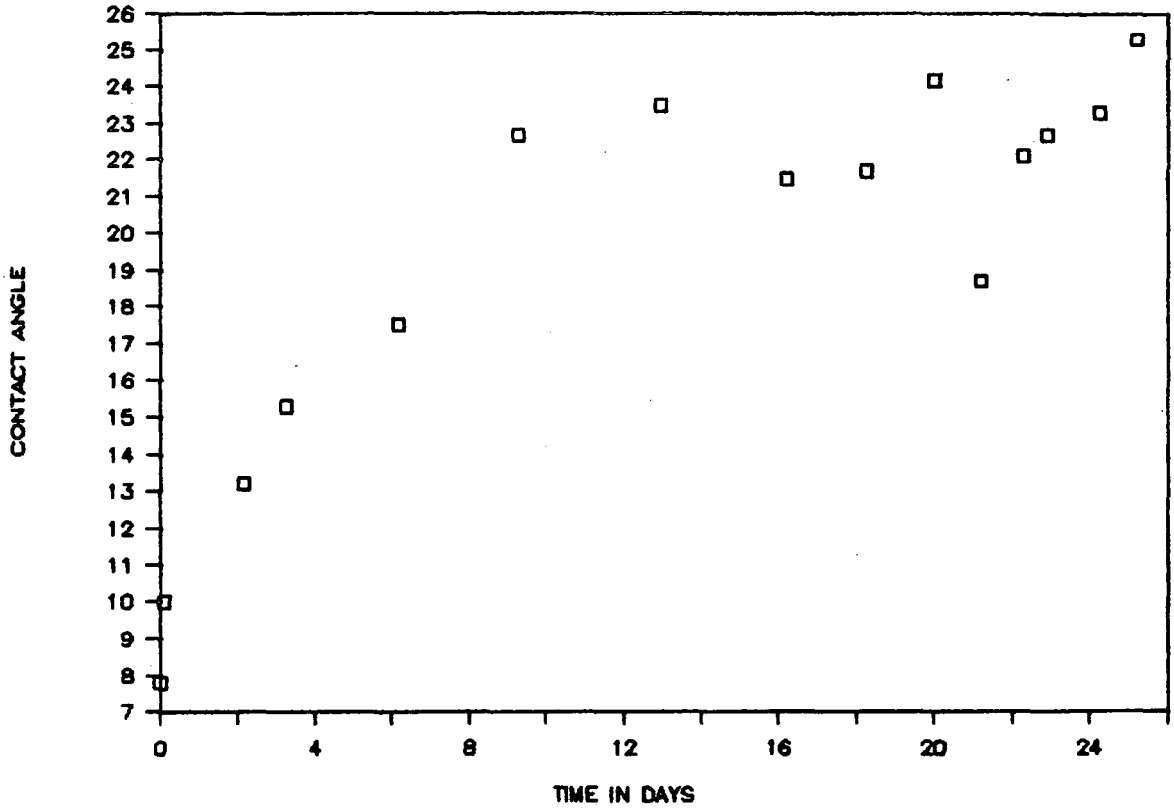

AMORPHOUS (2°C)

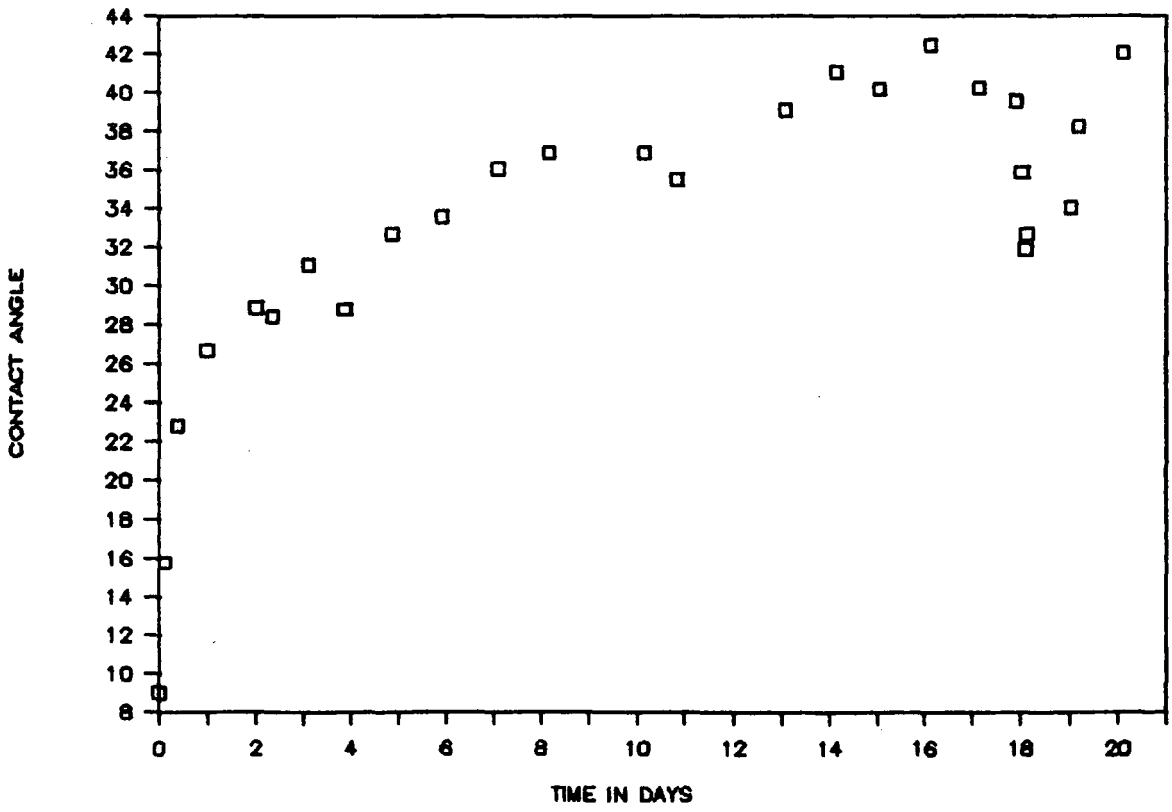

AMORPHOUS (45°C)

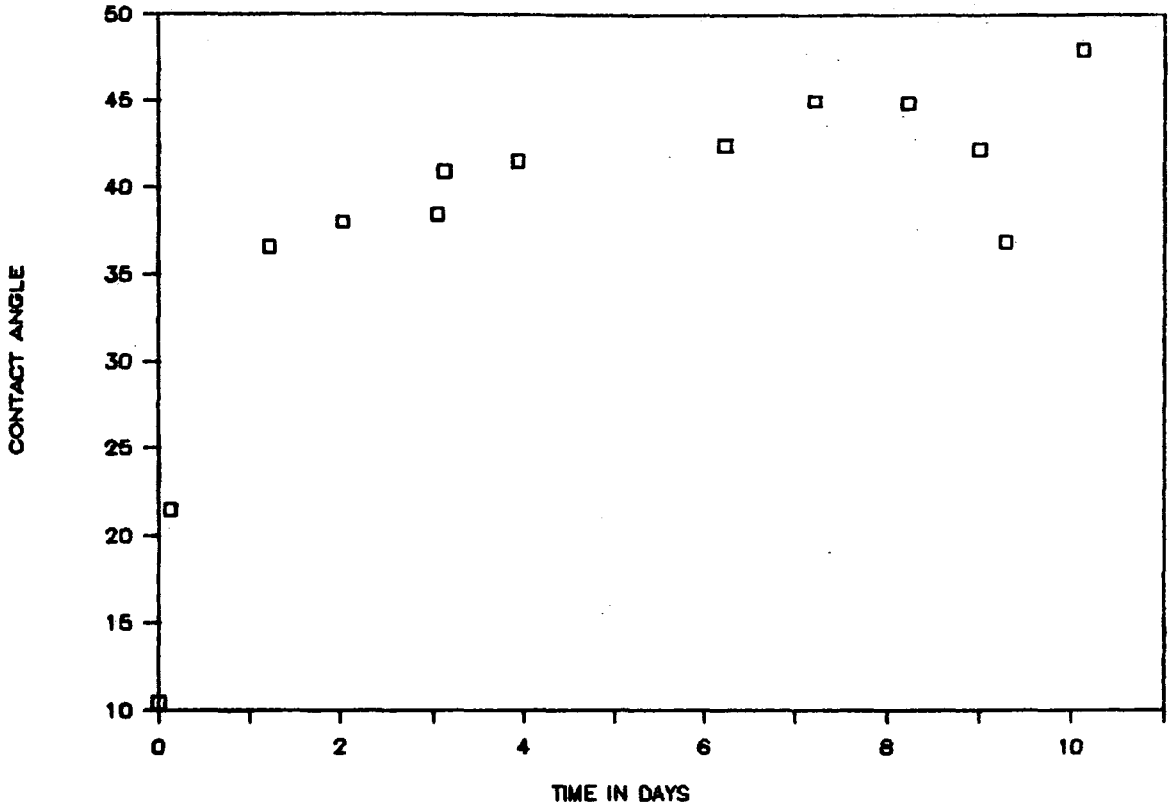

UNIAXIALLY DRAWN (−18°C)

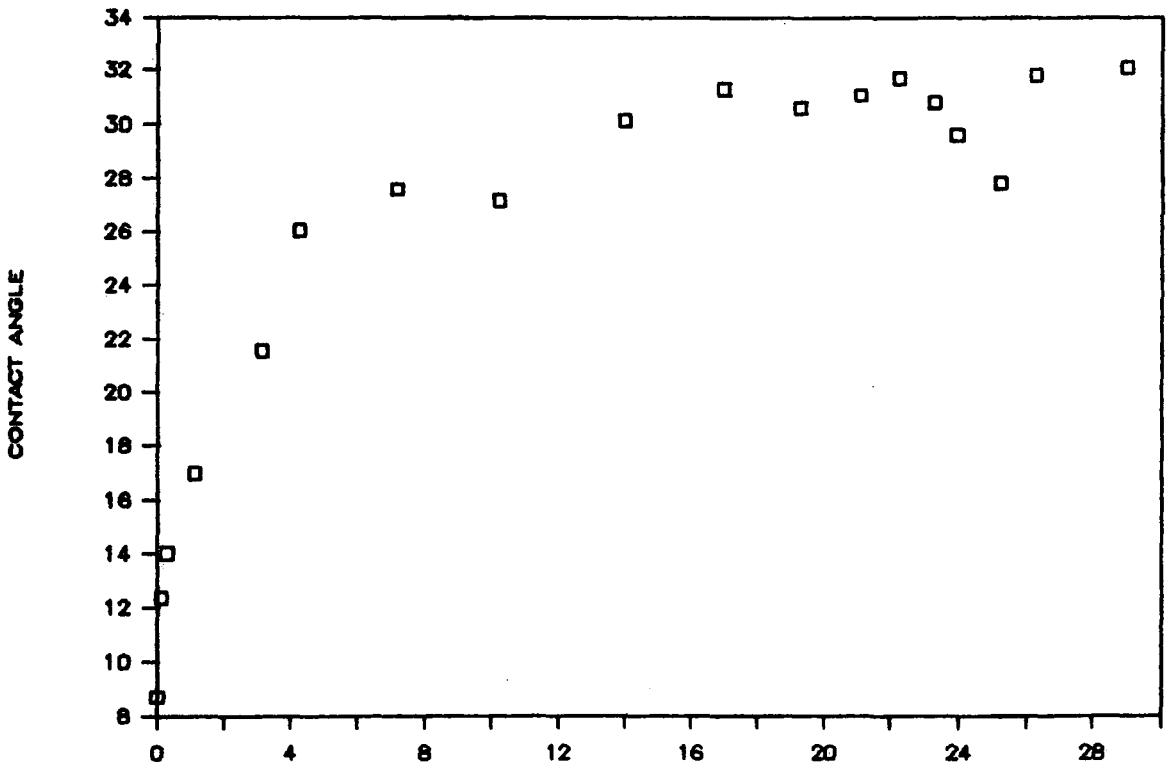

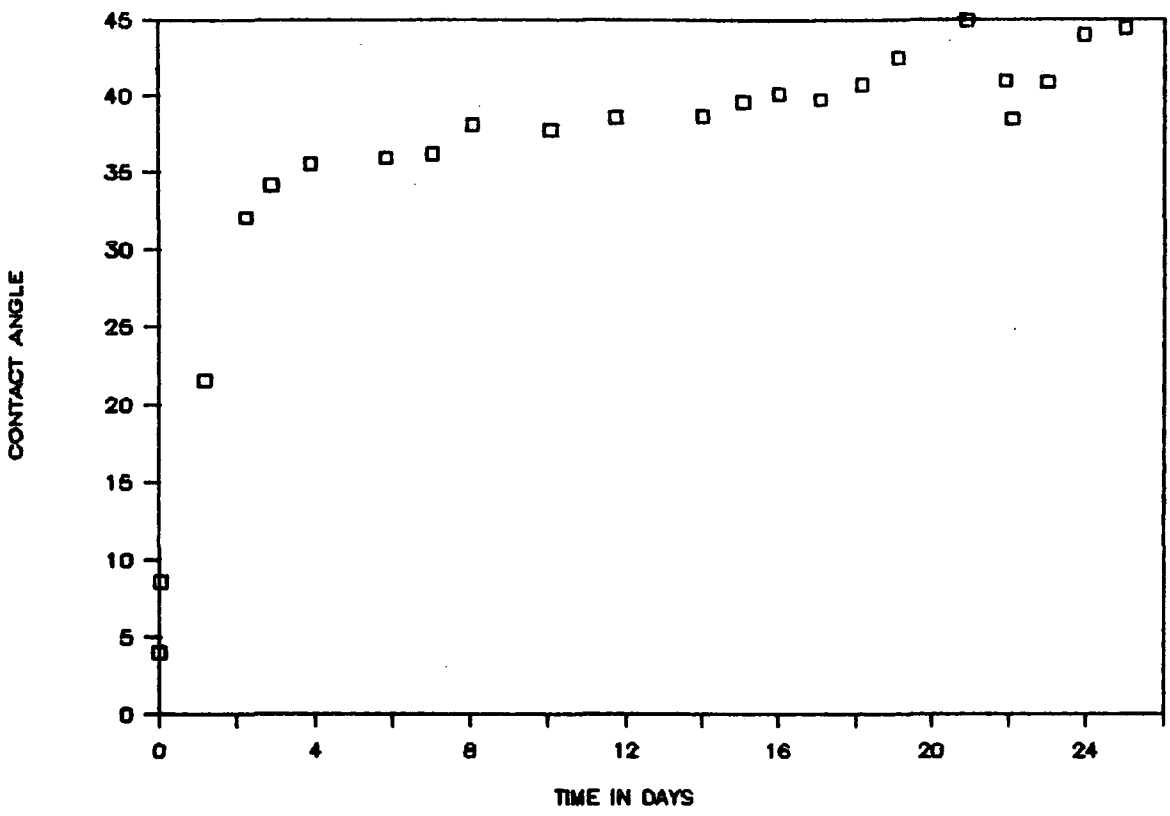
UNIAXIALLY DRAWN (2°C)
CONTACT ANGLE
45
40
35
30
25
20
15
10
5
0
0
4
8
12
16
20
24
TIME IN DAYS

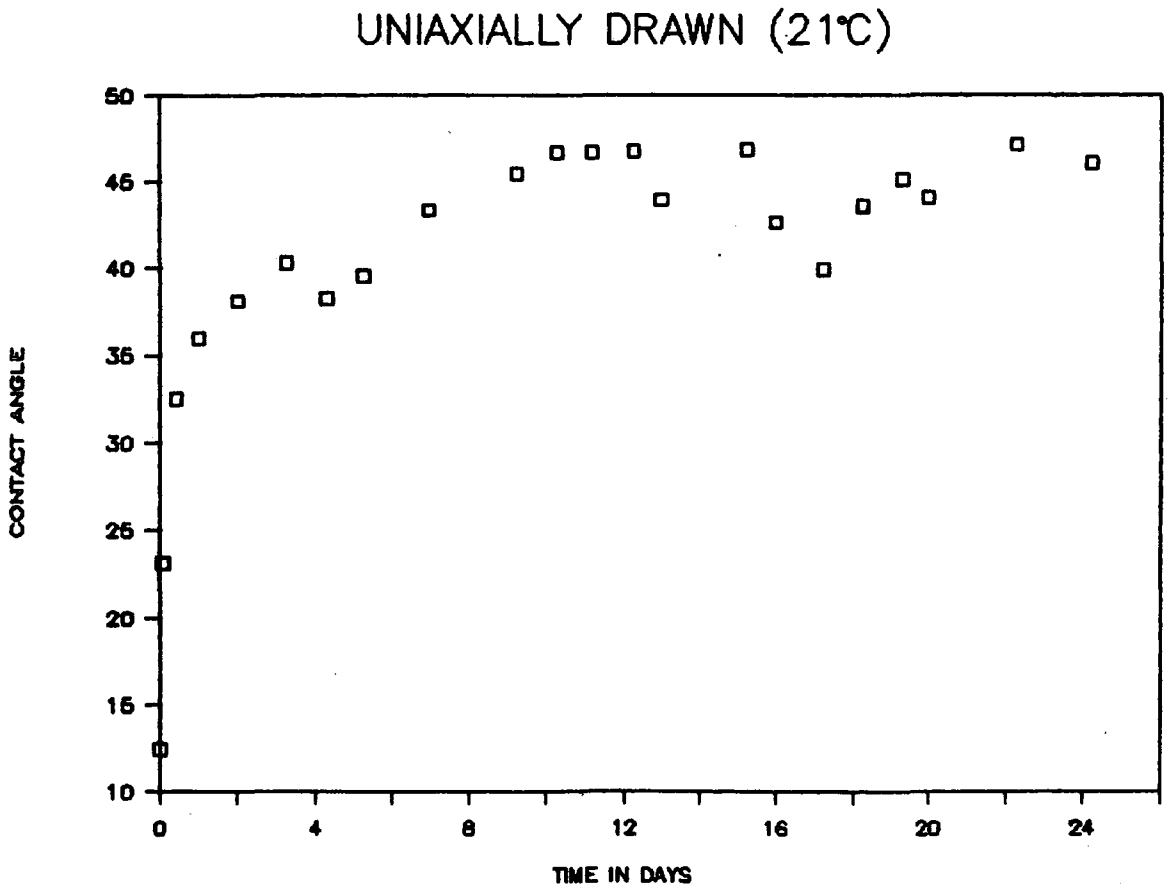
UNIAXIALLY DRAWN (21°C)
CONTACT ANGLE
50
45
40
35
30
25
20
15
10
0
4
8
12
16
20
24
TIME IN DAYS

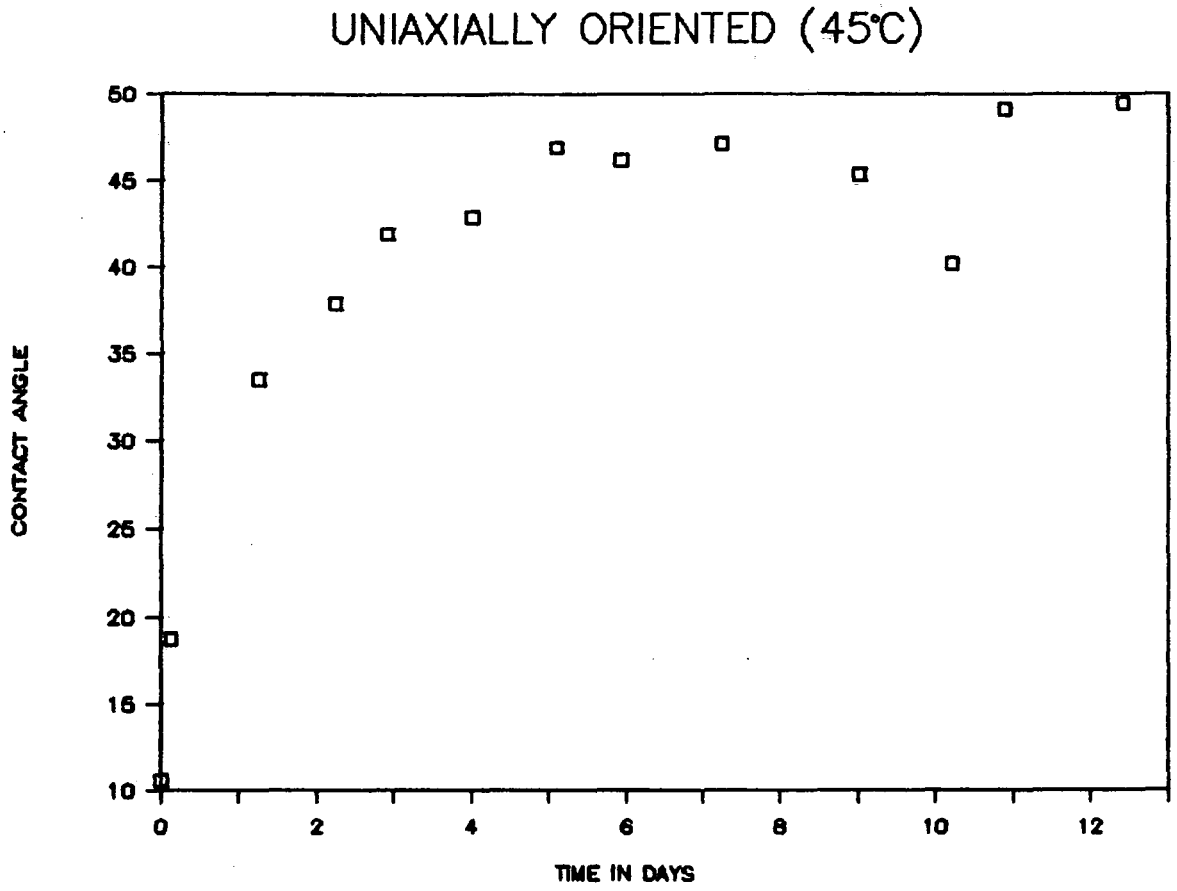
UNIAXIALLY ORIENTED (45°C)
CONTACT ANGLE
50
45
40
35
30
25
20
15
10
0
2
4
6
8
10
12
TIME IN DAYS

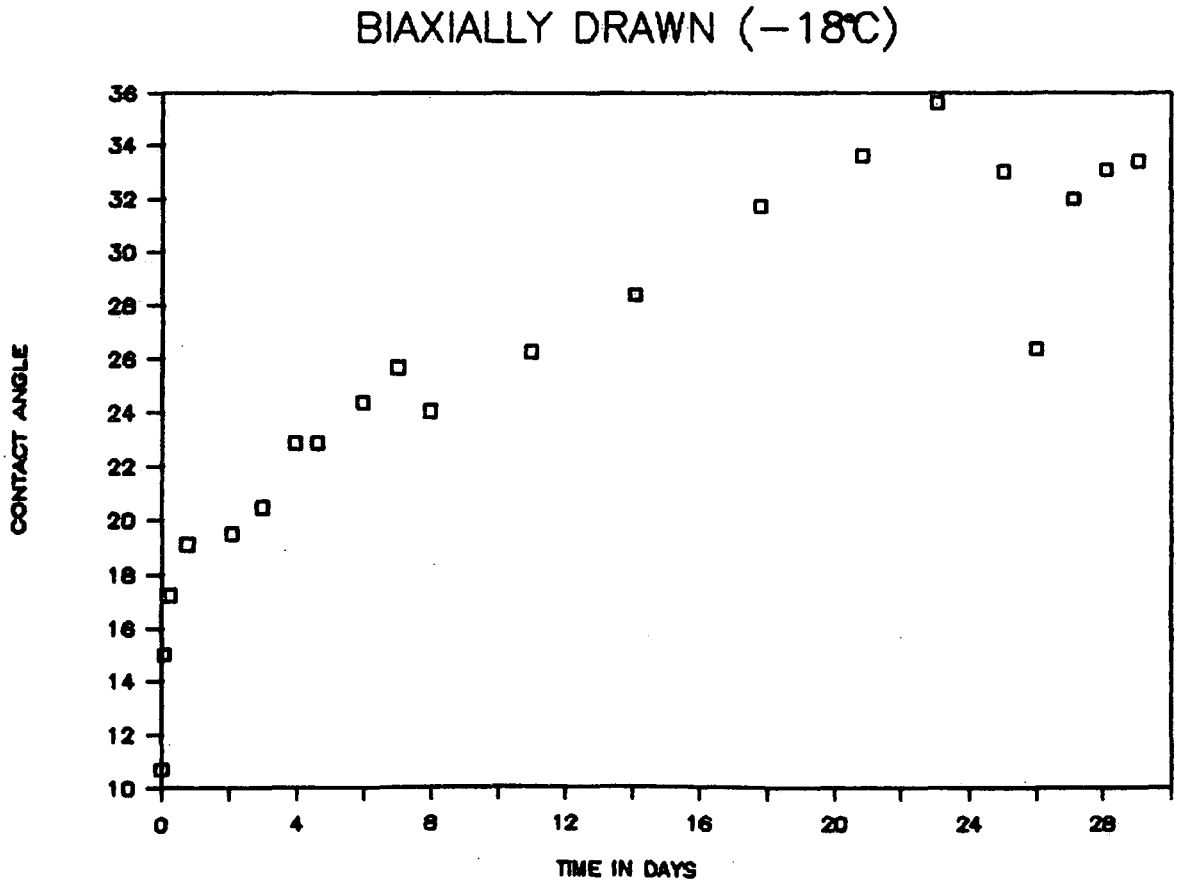
BIAXIALLY DRAWN (−18°C)
CONTACT ANGLE
36
34
32
30
28
26
24
22
20
18
16
14
12
10
0
4
8
12
16
20
24
28
TIME IN DAYS

BIAXIALLY DRAWN (21°C)

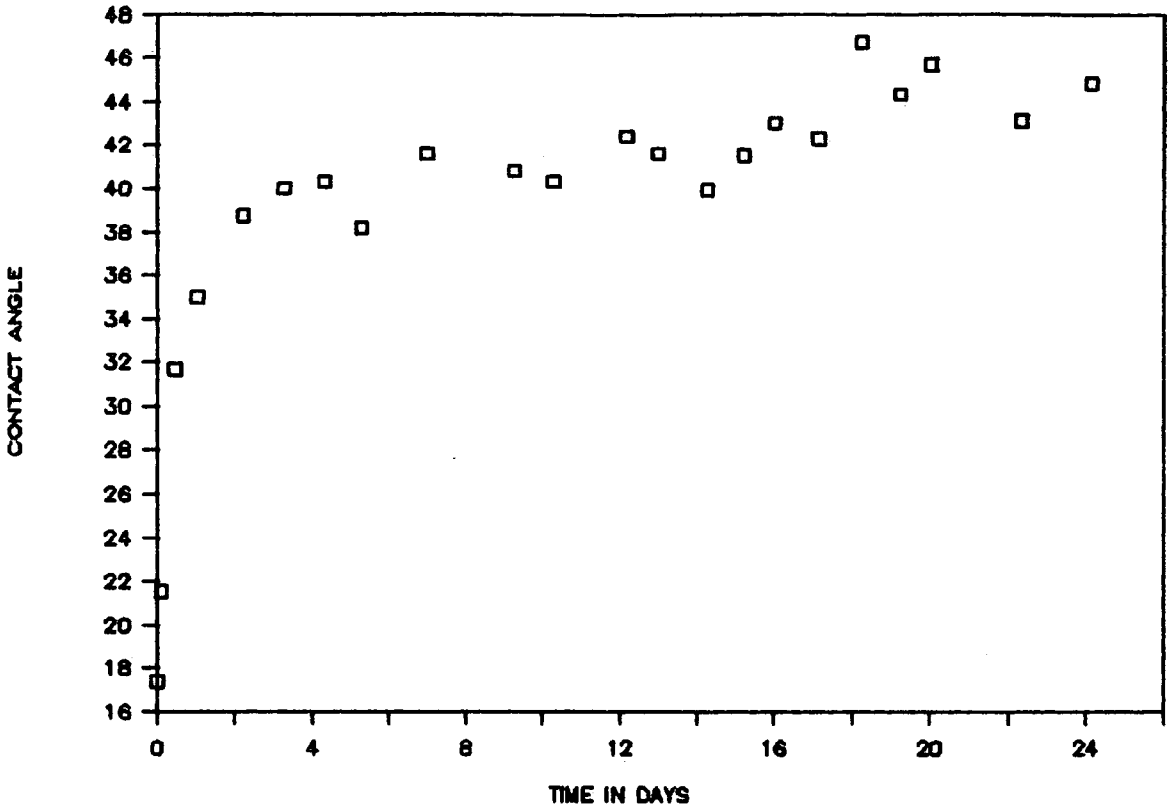

BIAXIALLY DRAWN (45°C)

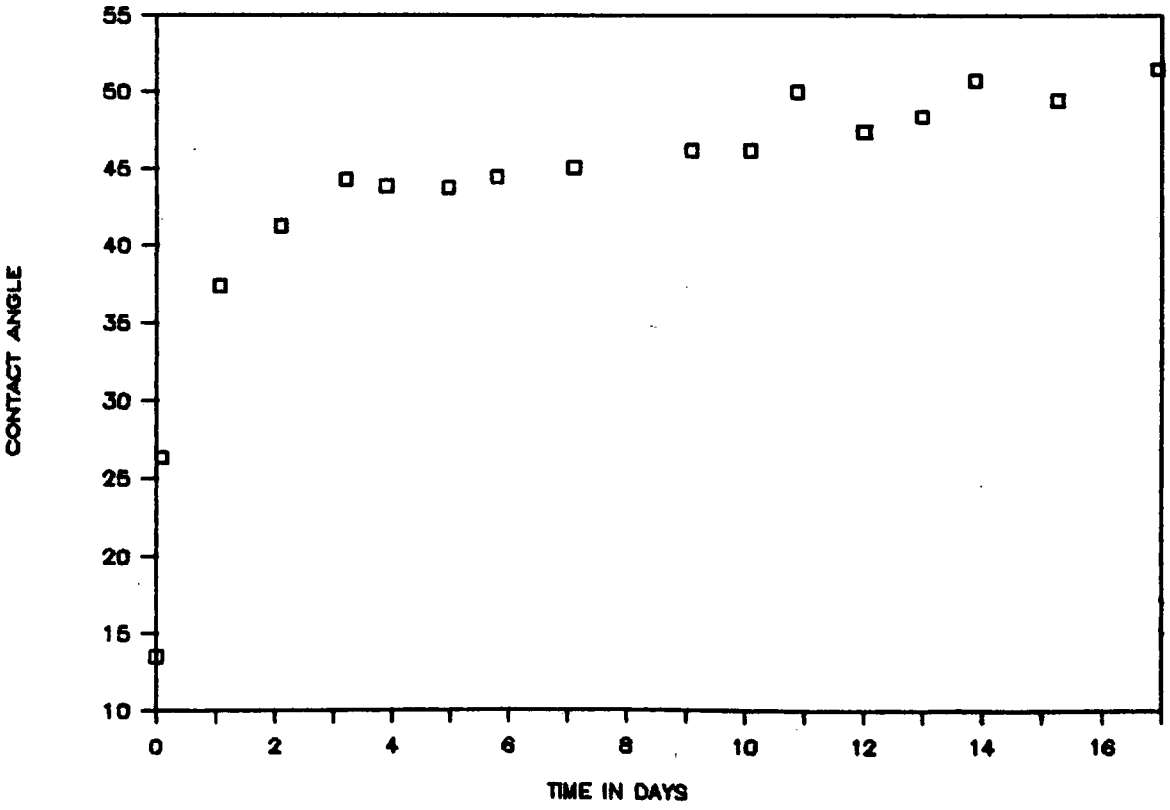

SEMI–CRYSTALLINE (–18)

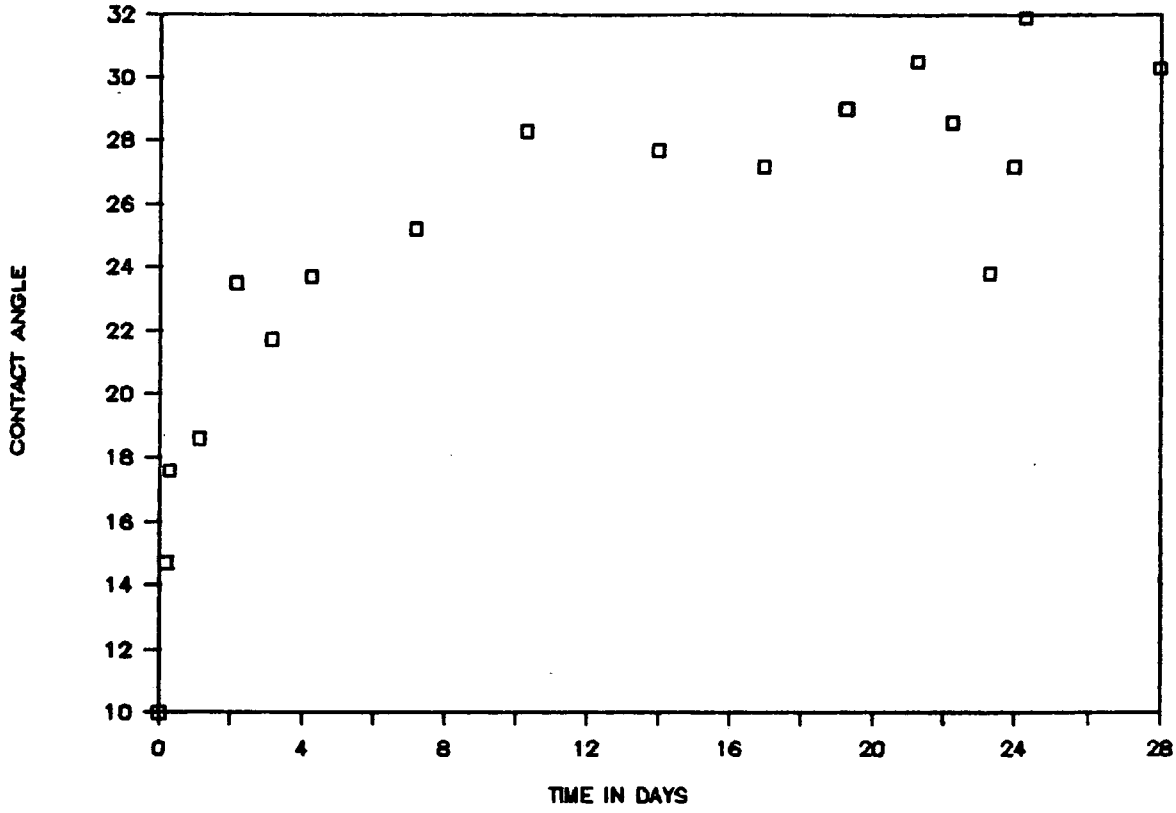

SEMI–CRYSTALLINE (2)

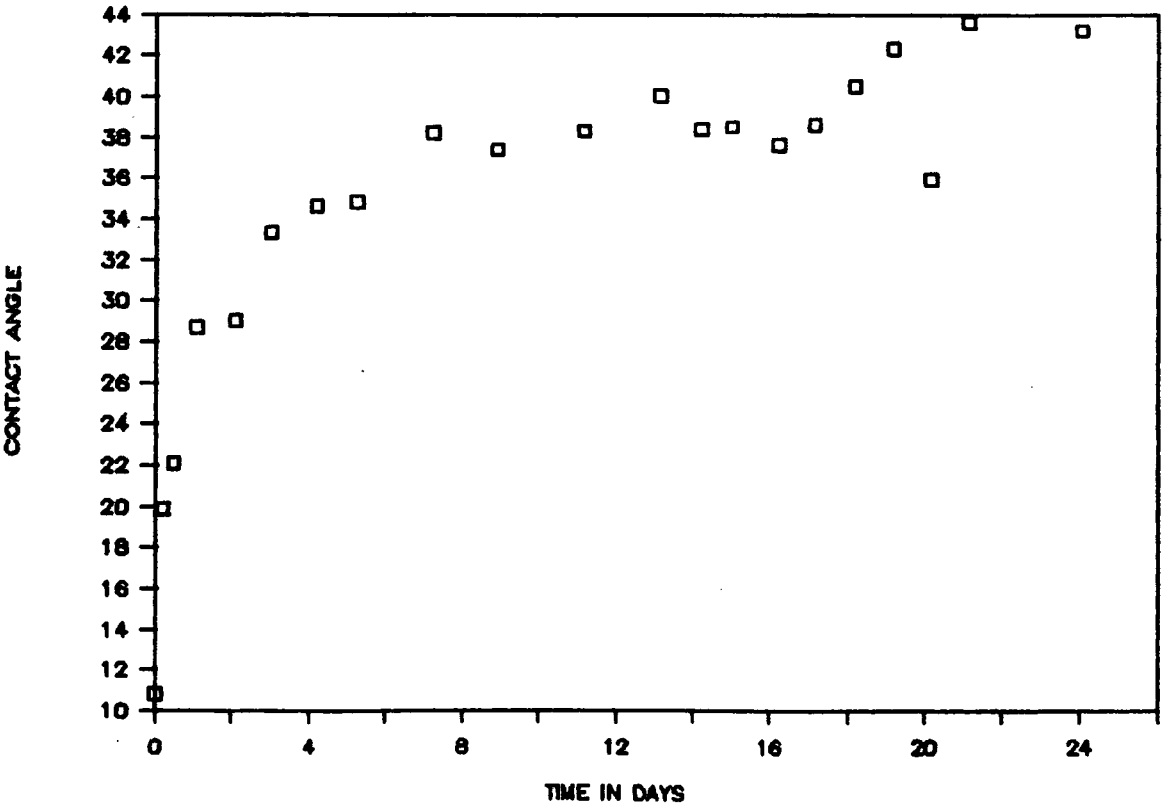

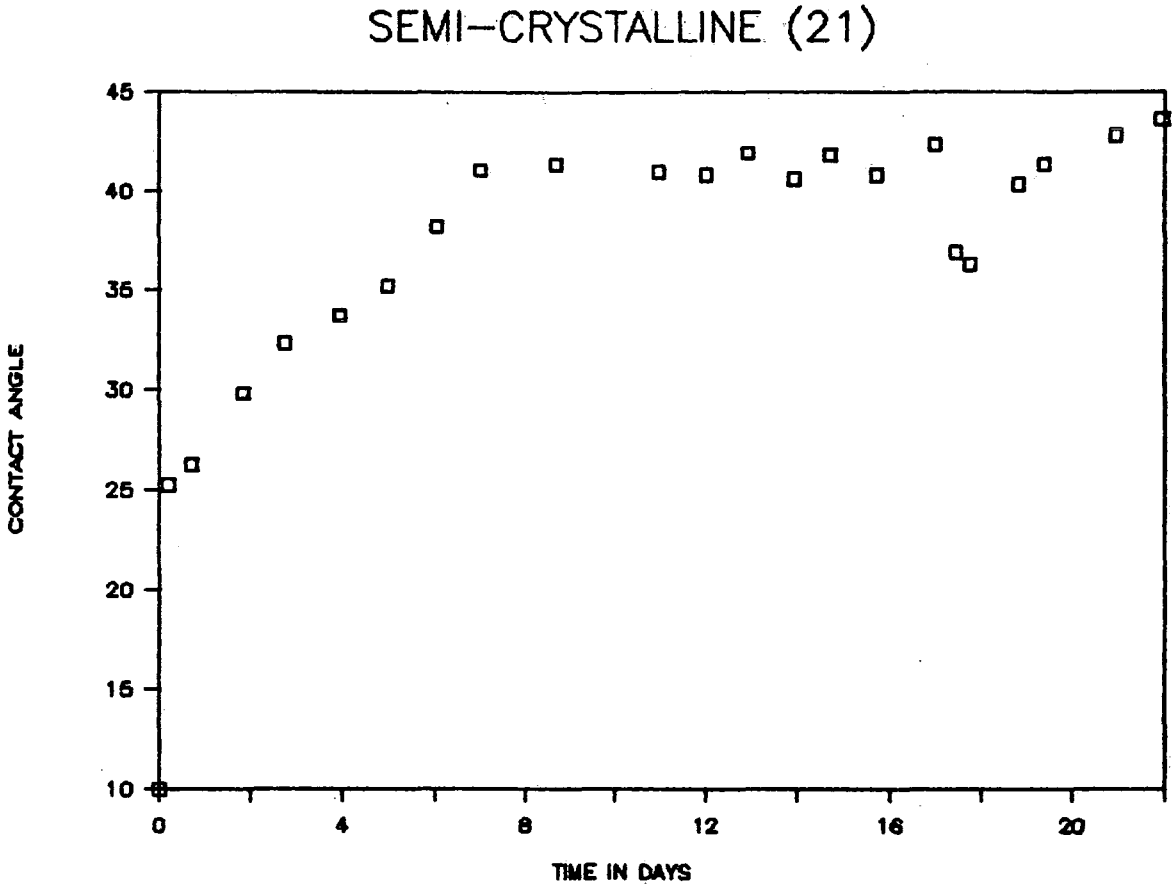
SEMI–CRYSTALLINE (21)
CONTACT ANGLE
45
40
35
30
25
20
15
10
0
4
8
12
16
20
TIME IN DAYS

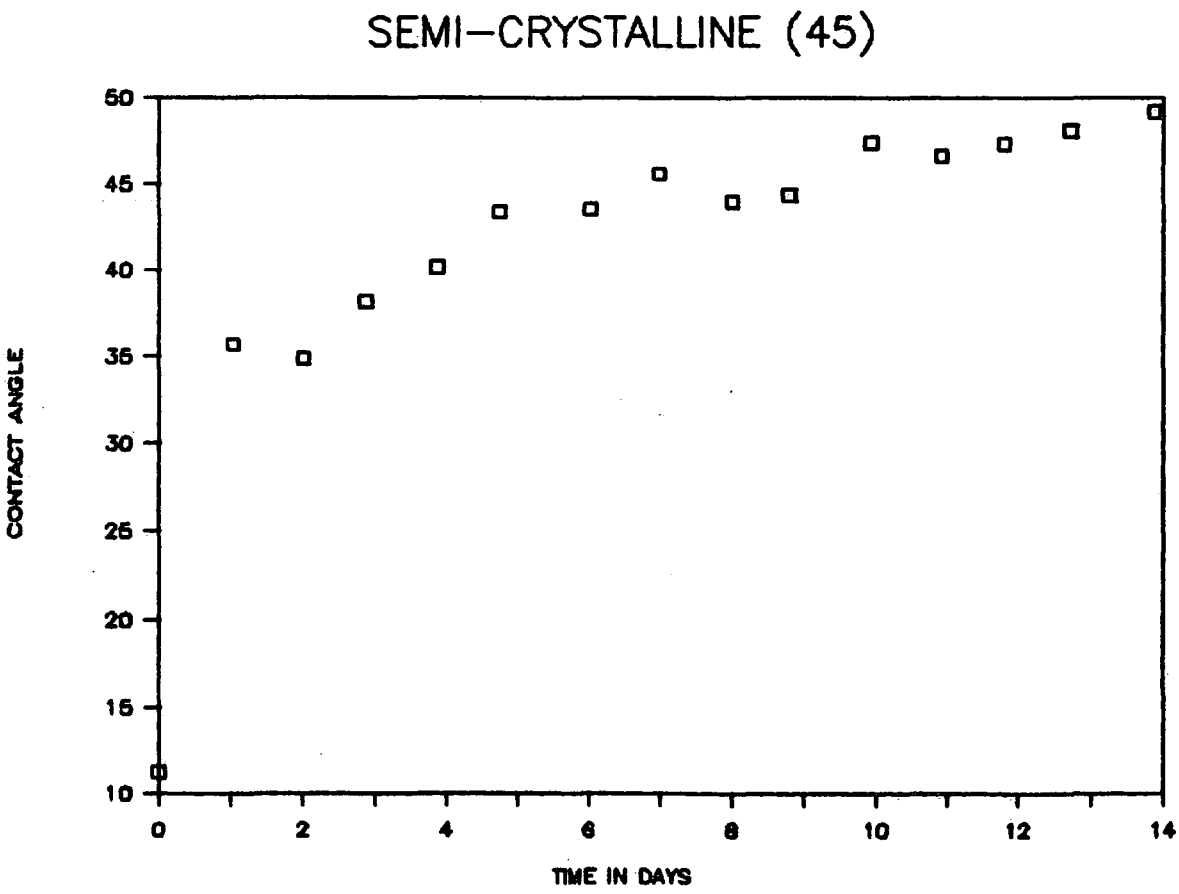
SEMI–CRYSTALLINE (45)
CONTACT ANGLE
50
45
40
35
30
25
20
15
10
0
2
4
6
8
10
12
14
TIME IN DAYS

AMORPHOUS (21°C)

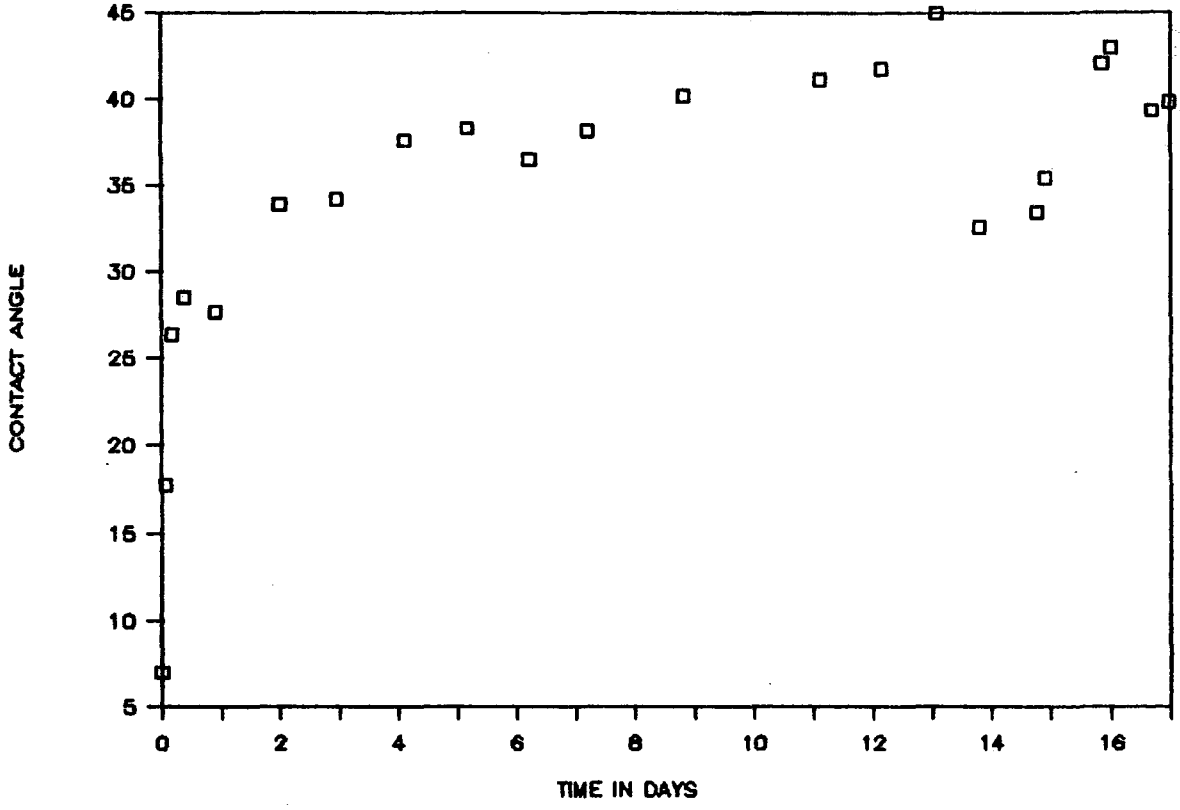

BIAXIALLY DRAWN (2°C)

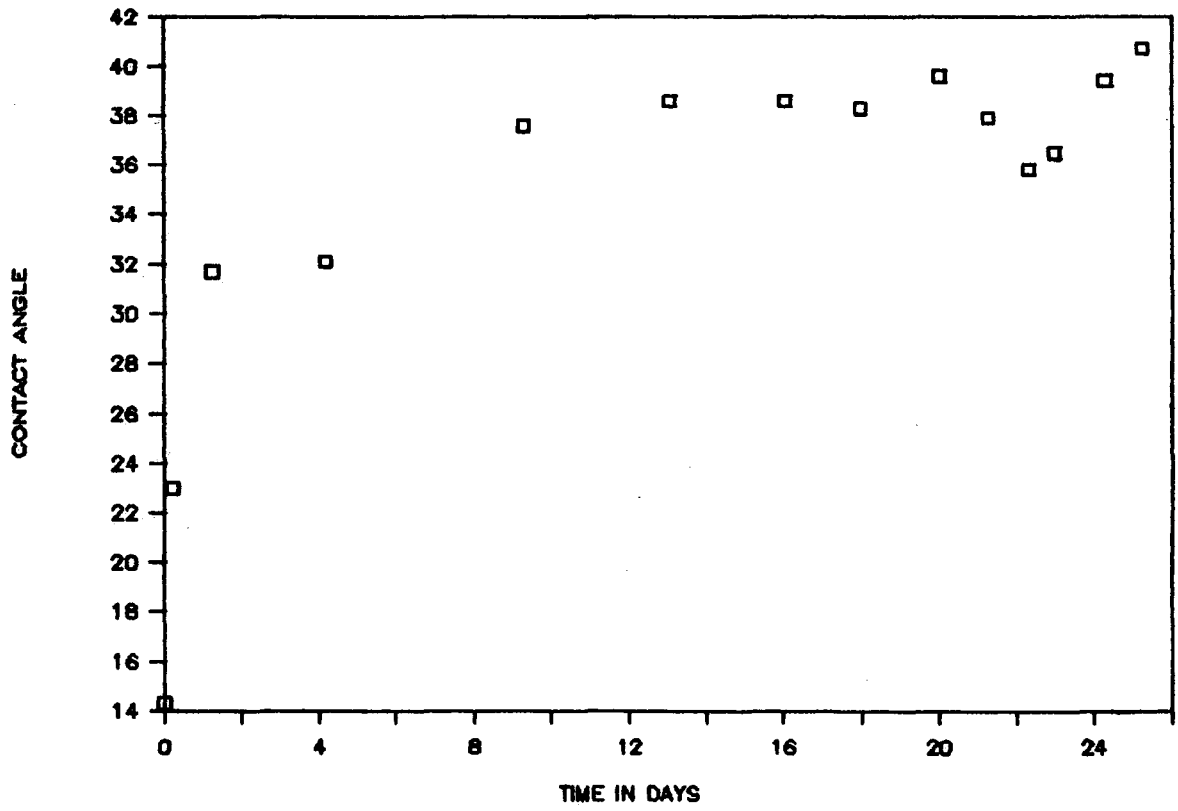

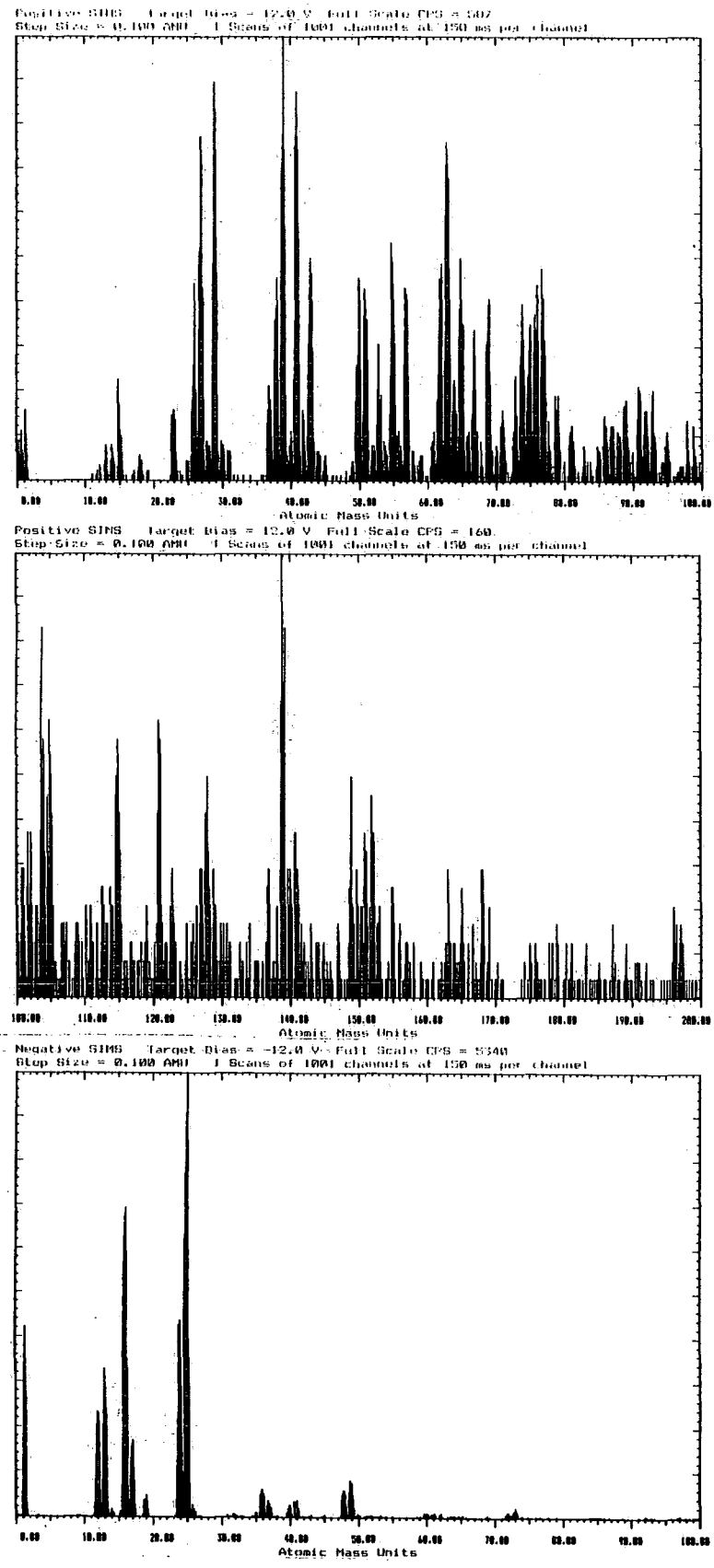

UNTREATED AMORPHOUS PEEK

AMORPHOUS PEEK 1 DAY OLD

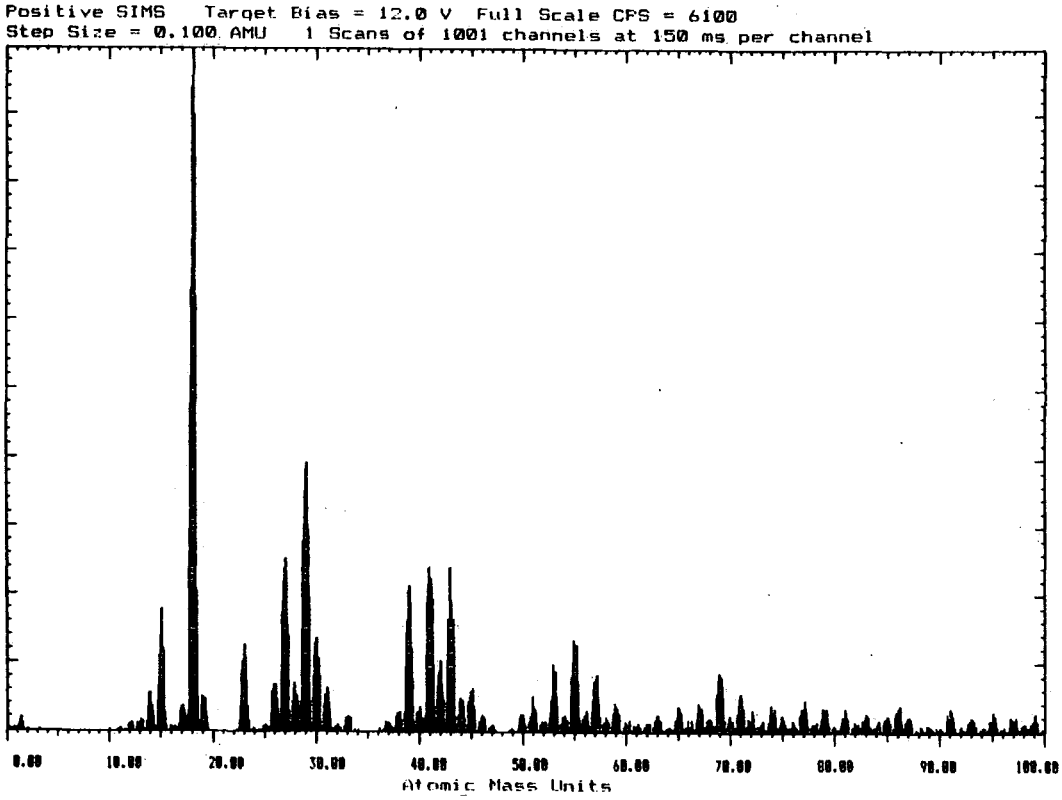

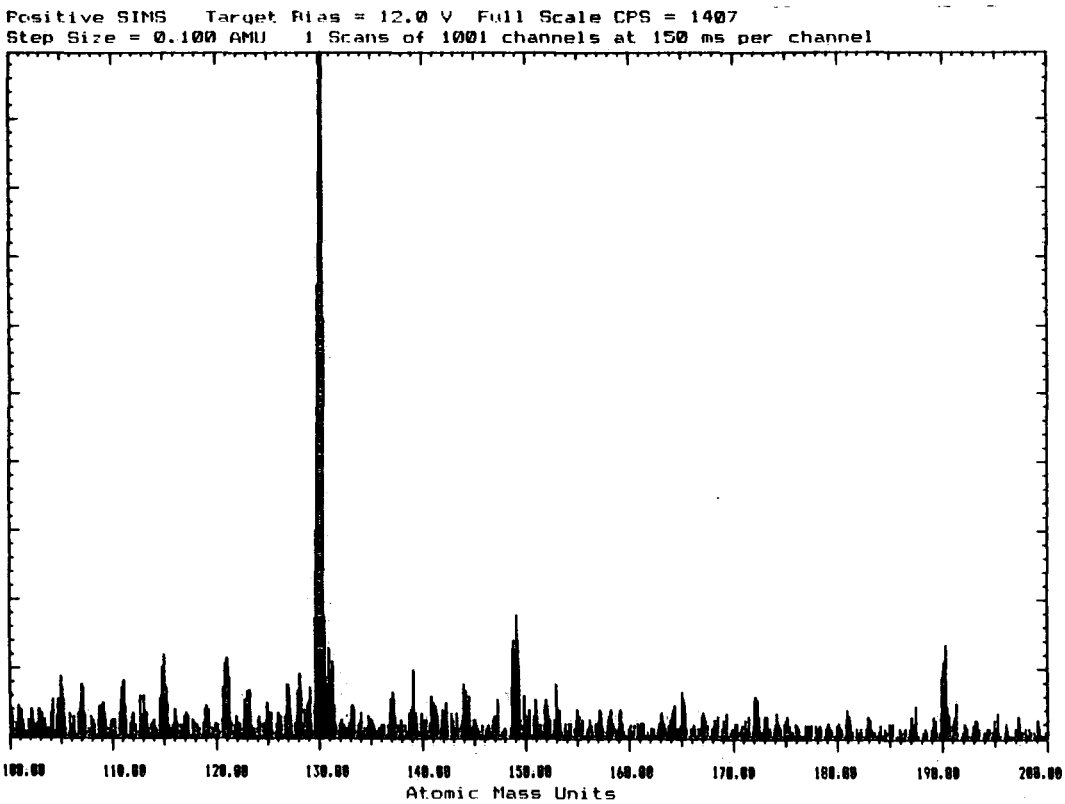

AMORPHOUS PEEK 1 DAY OLD

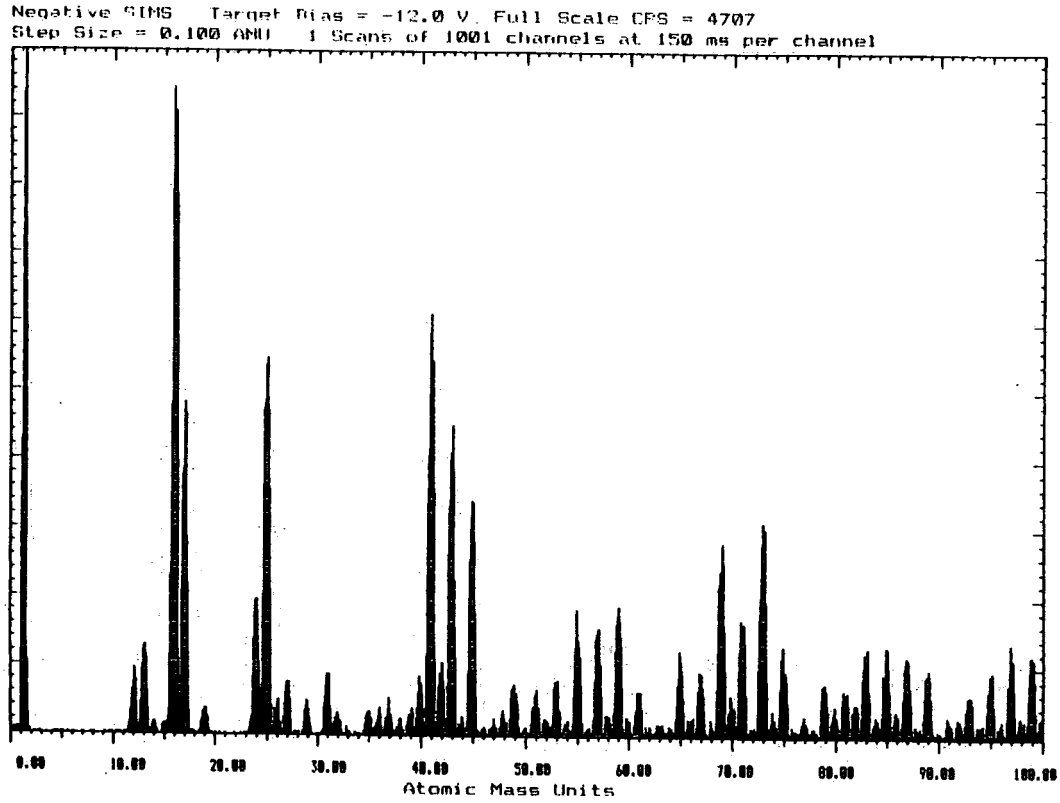

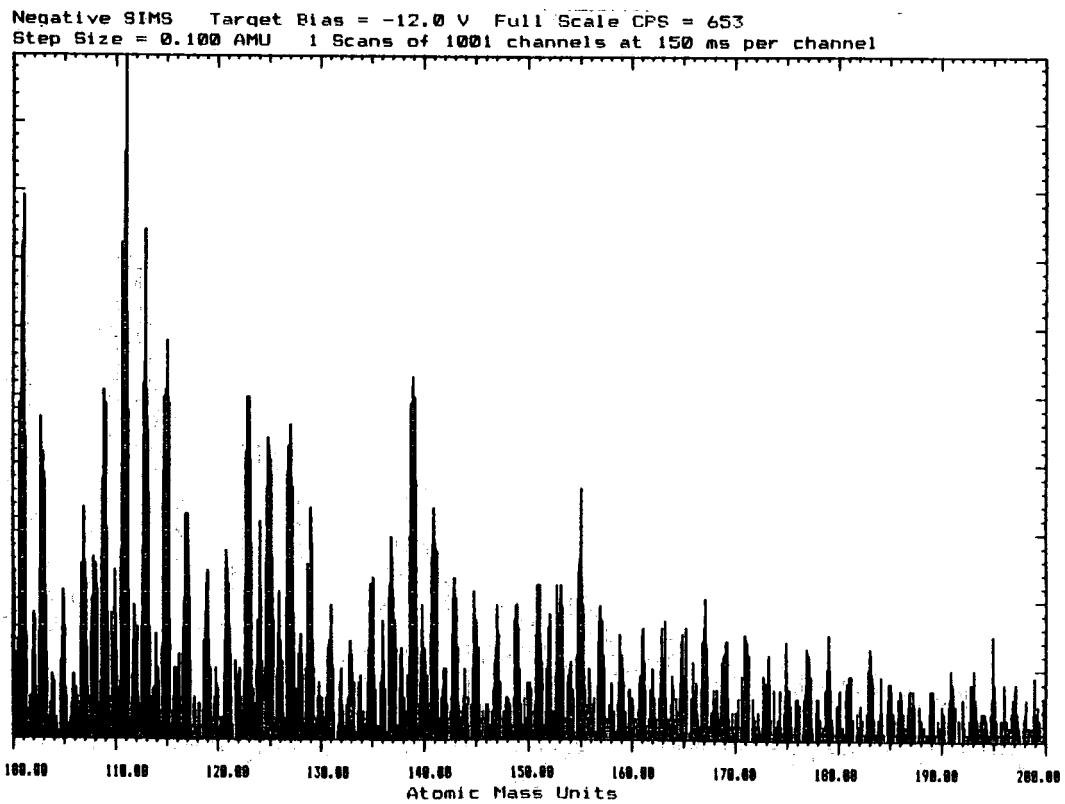

AMORPHOUS PEEK 5 DAYS OLD

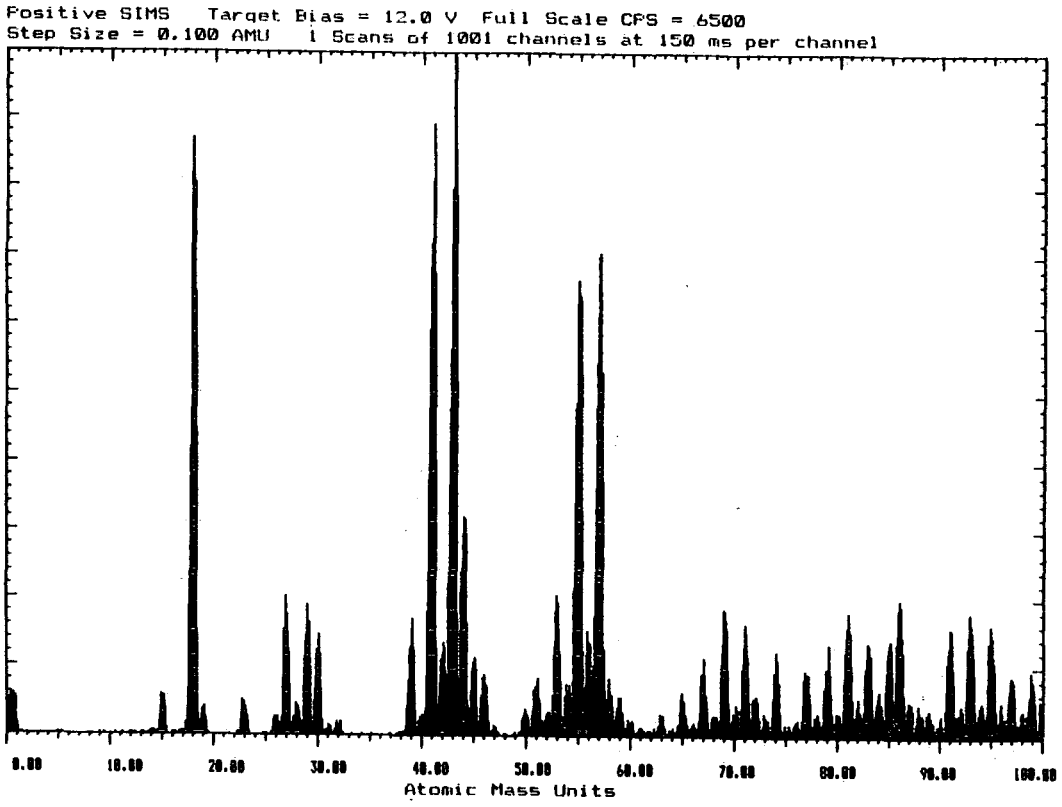

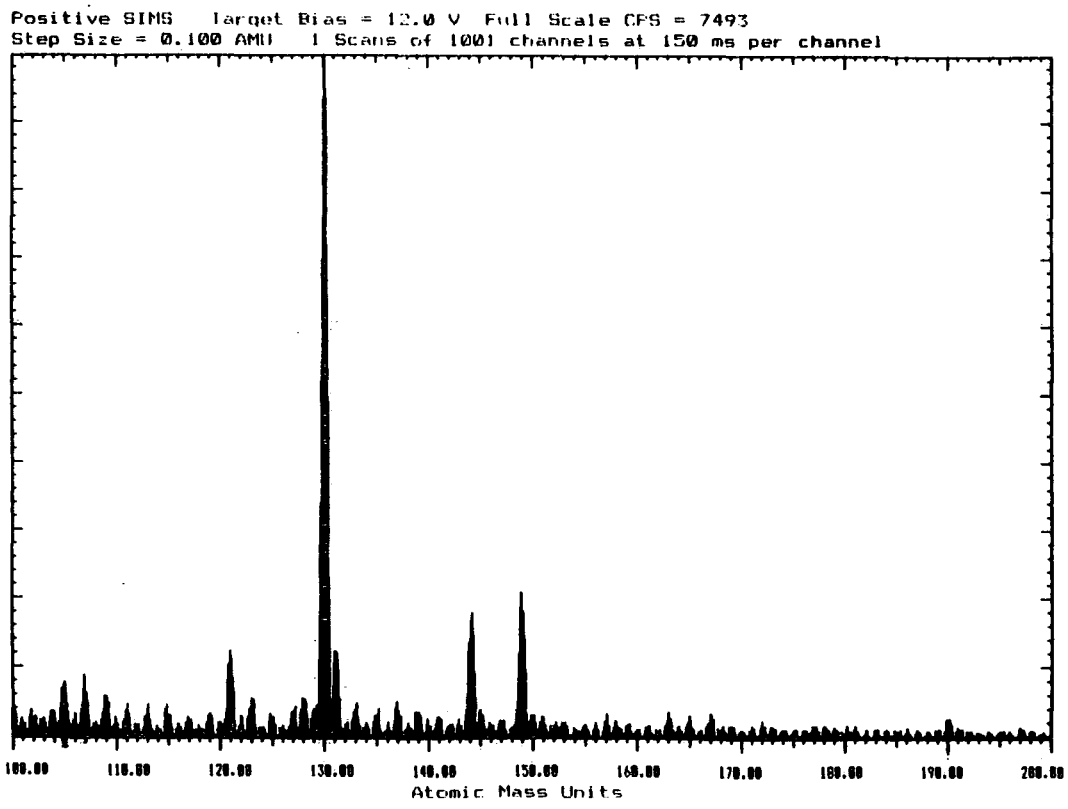

AMORPHOUS PEEK 5 DAYS OLD

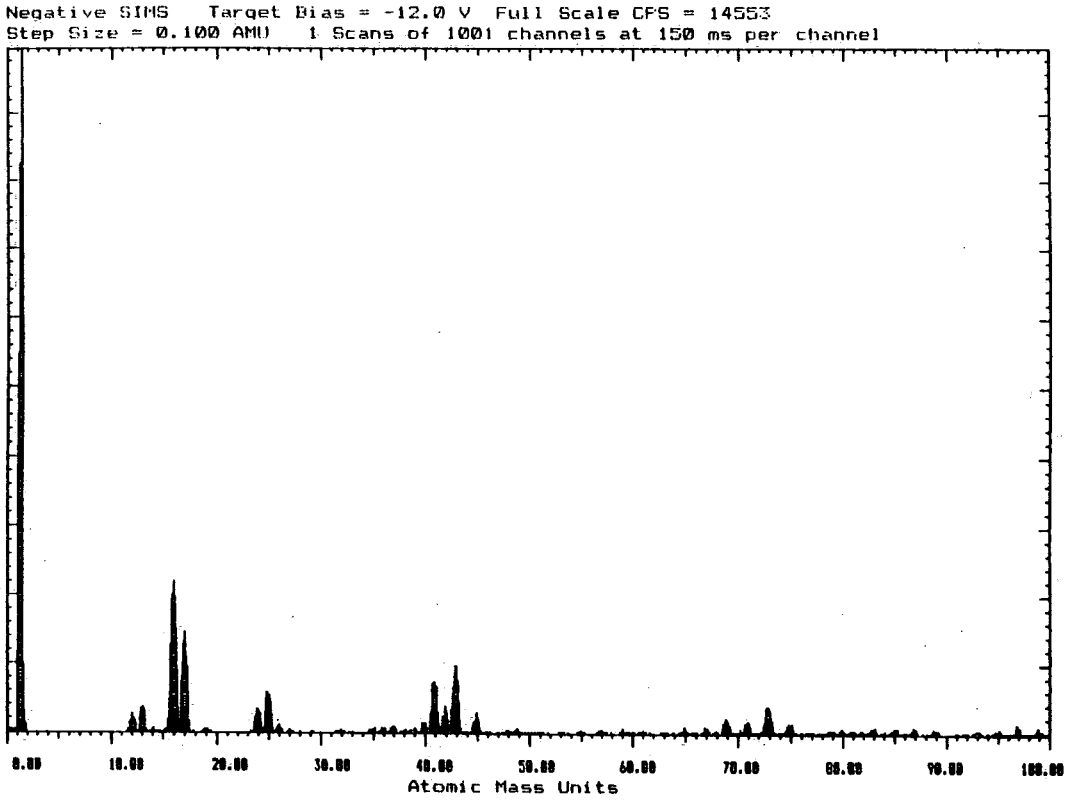

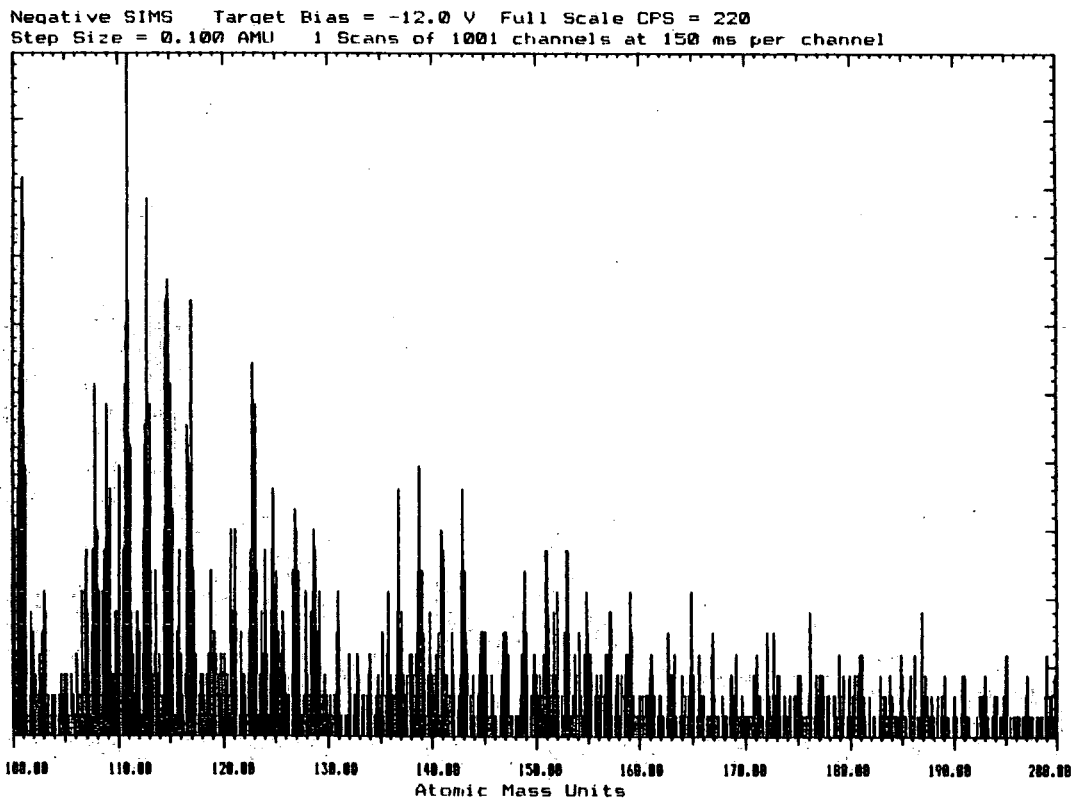

AMORPHOUS PEEK 9 DAYS OLD

Positive SIMS Target Bias = 12.0 V Full Scale CPS = 21300
Step Size = 0.100 AMU 1 Scans of 1001 channels at 150 ms per channel

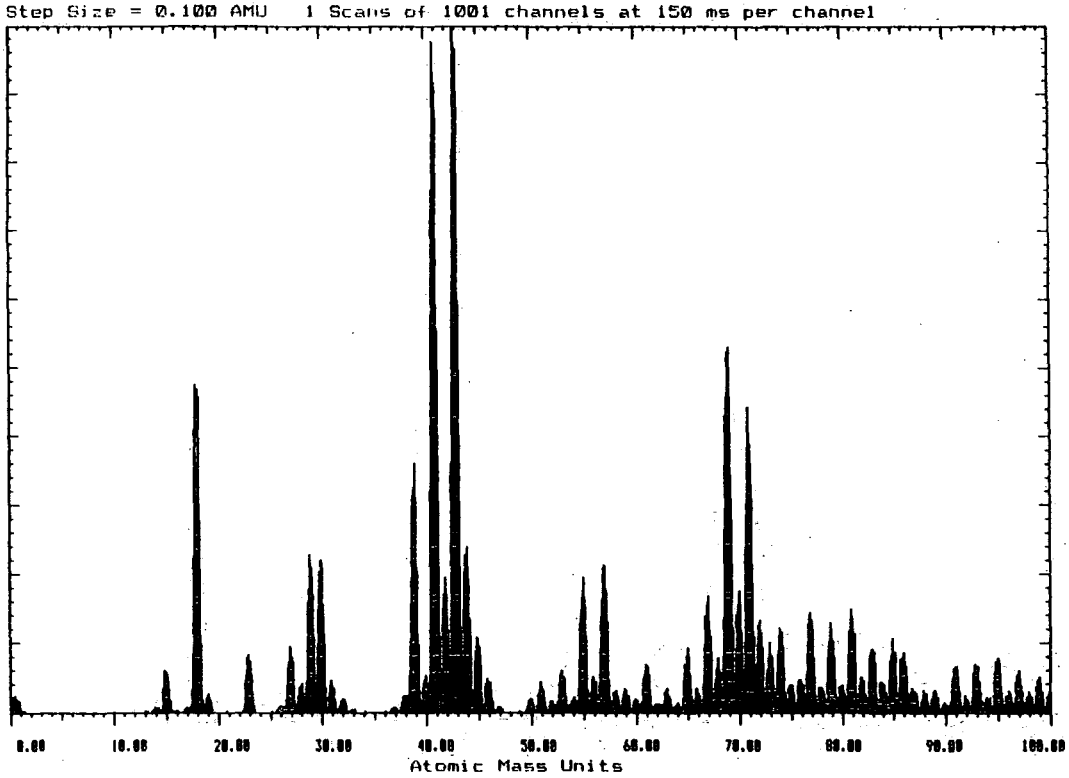

Positive SIMS Target Bias = 12.0 V Full Scale CPS = 6533
Step Size = 0.100 AMU 1 Scans of 1001 channels at 150 ms per channel

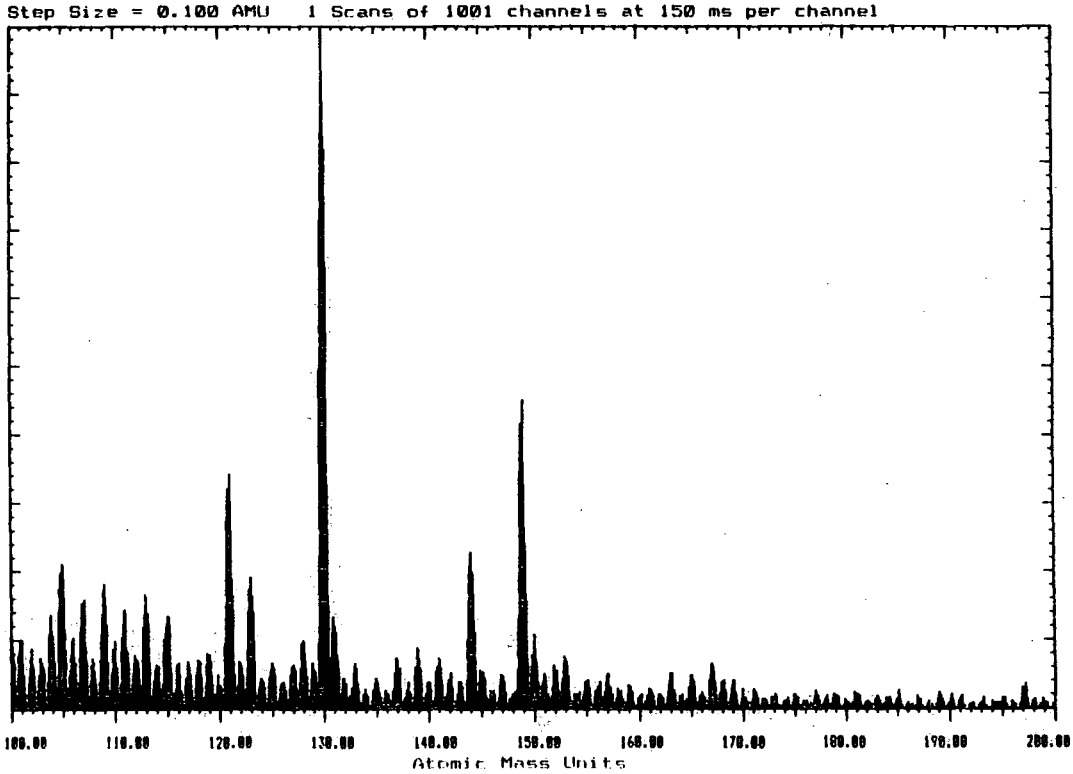

AMORPHOUS PEEK 9 DAYS OLD

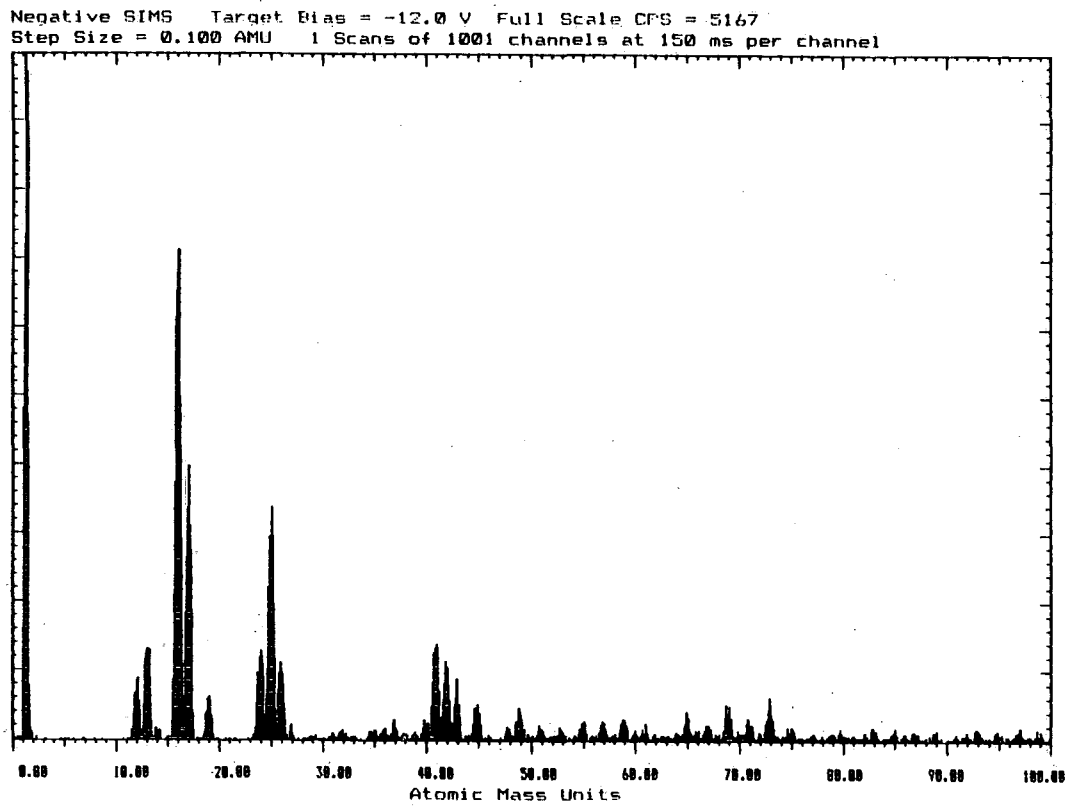

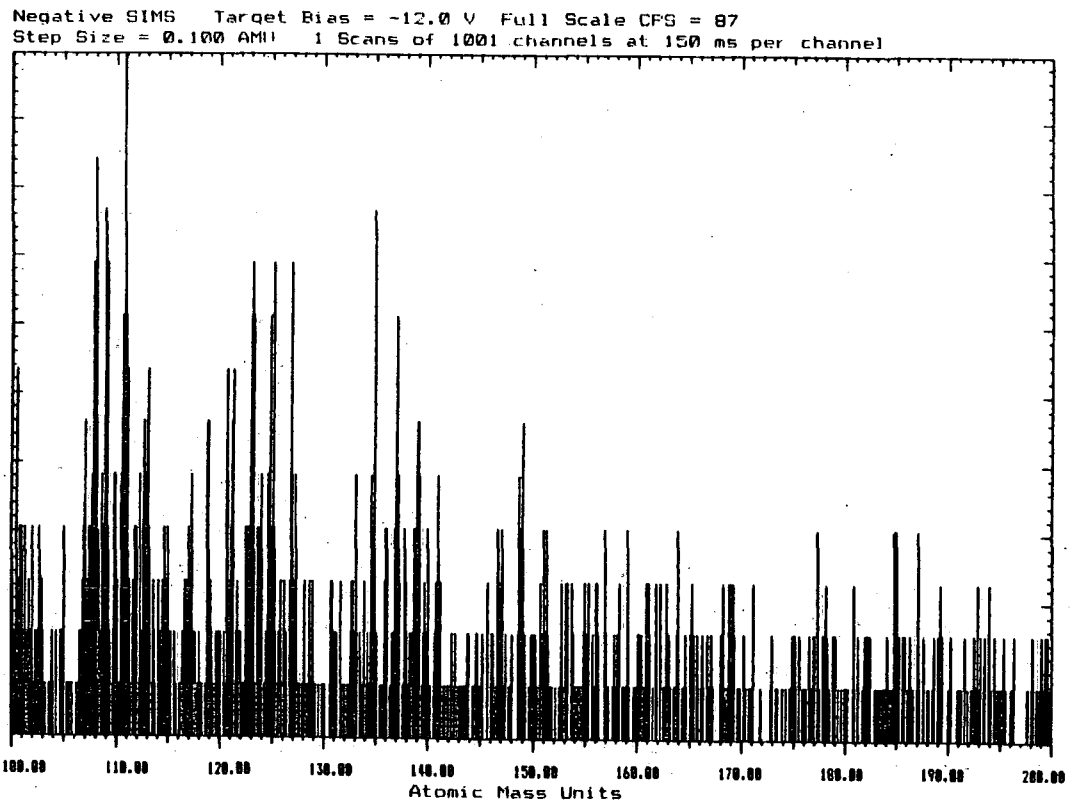

AMORPHOUS PEEK AT TRANSIENT INCREASE IN HYDROPHILICITY

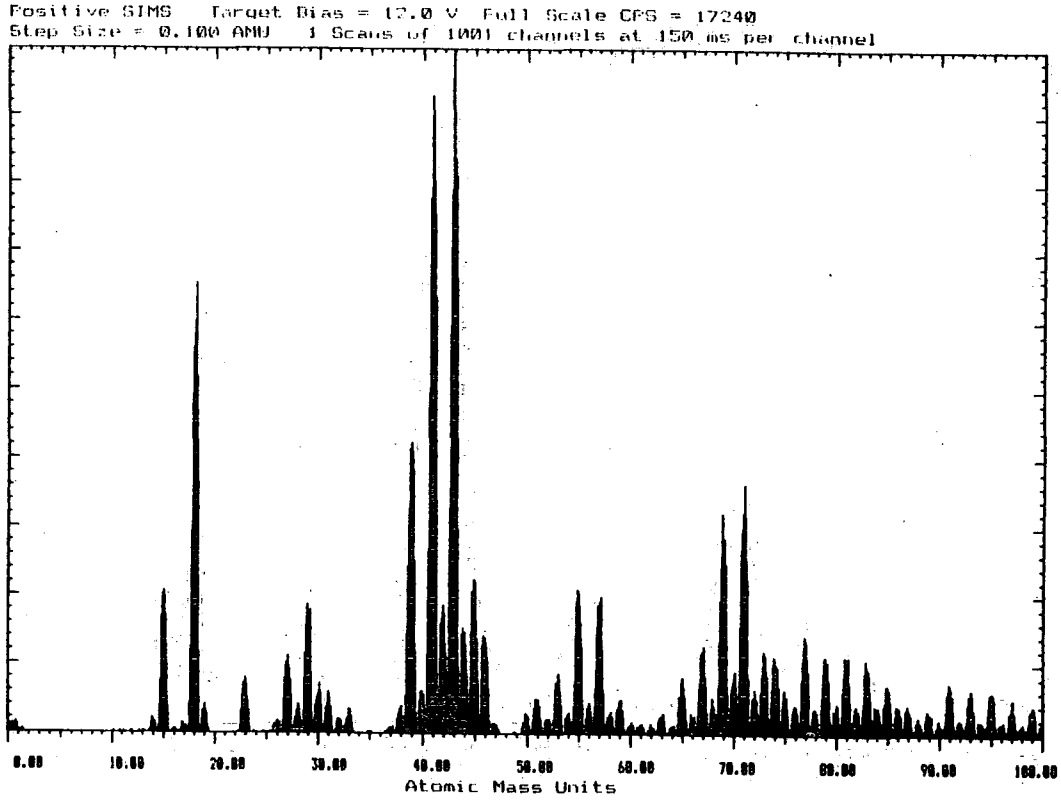

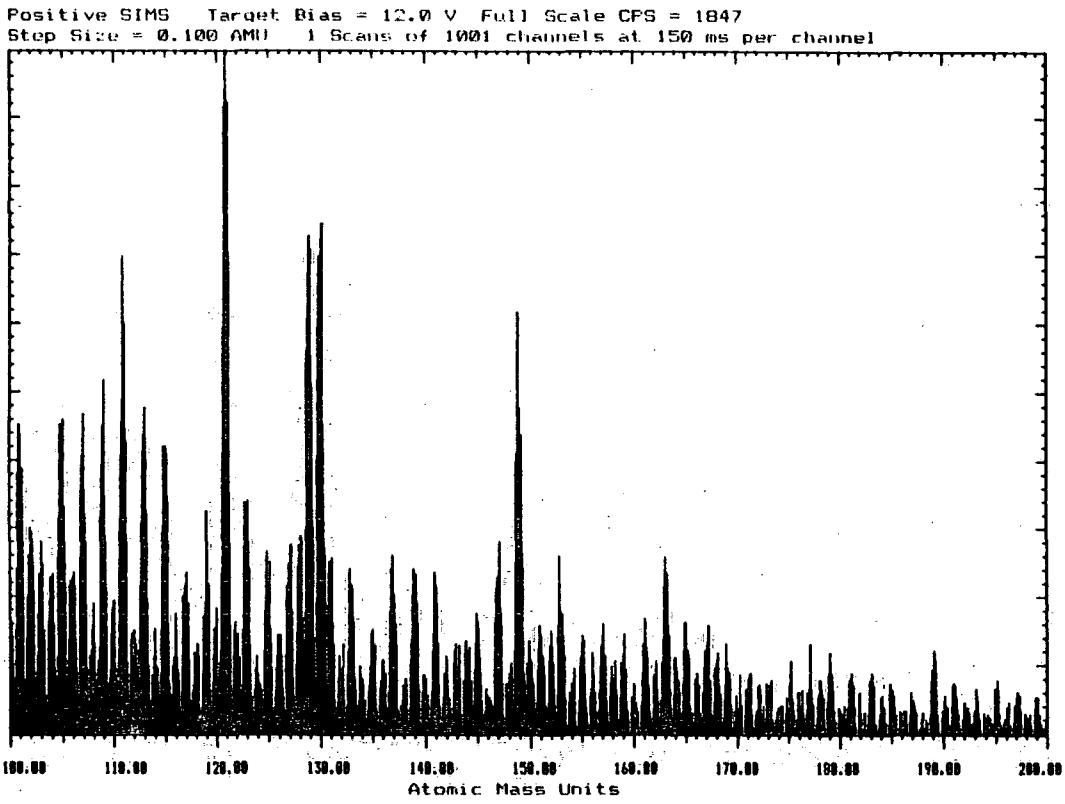

AMORPHOUS PEEK AT TRANSIENT INCREASE IN HYDROPHILICITY

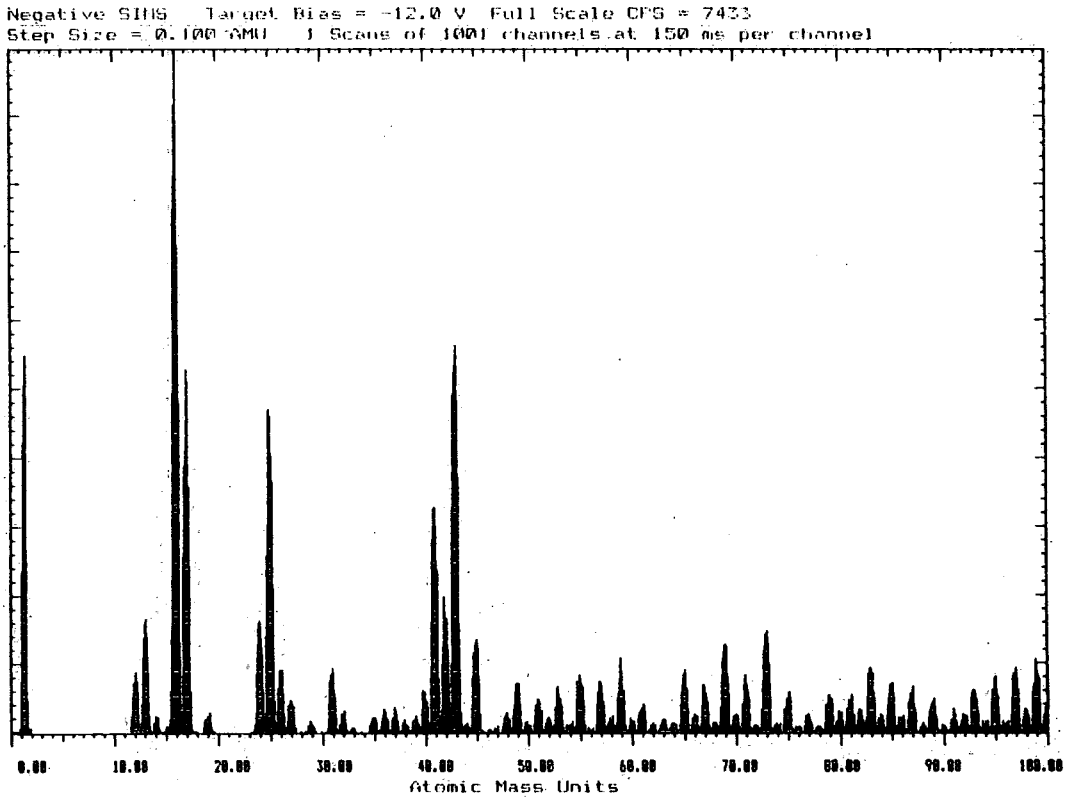

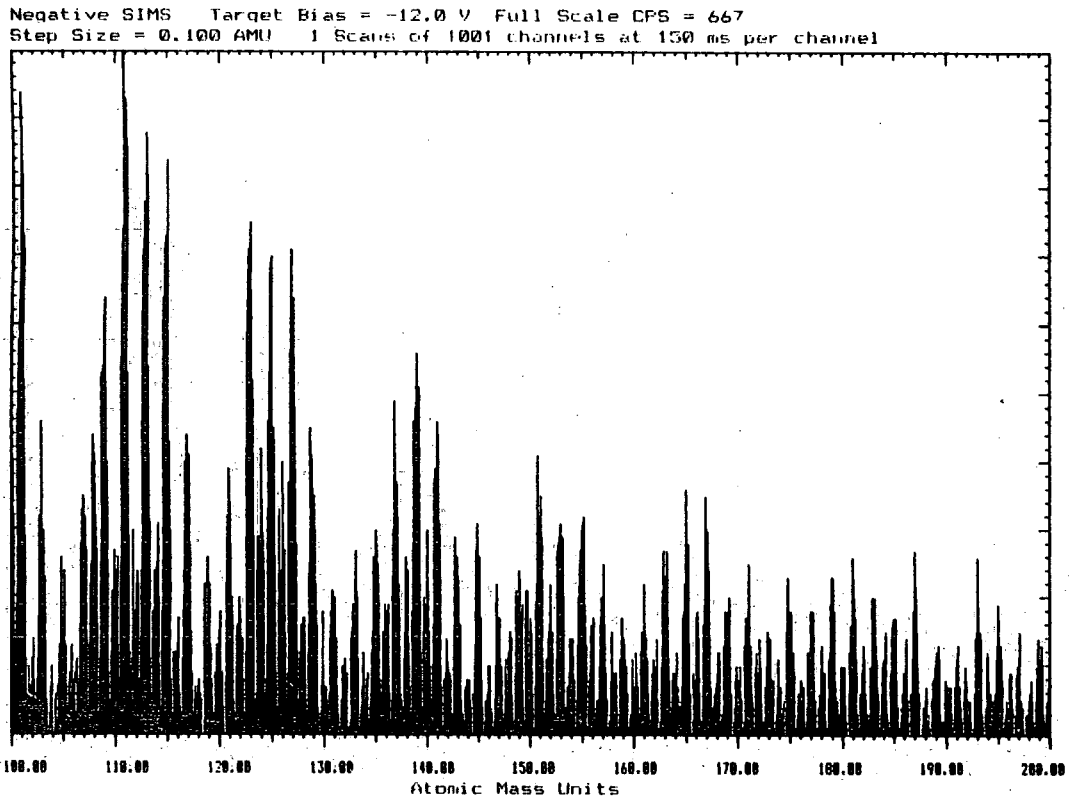

BIAXIALLY DRAWN PEEK 1 DAY OLD

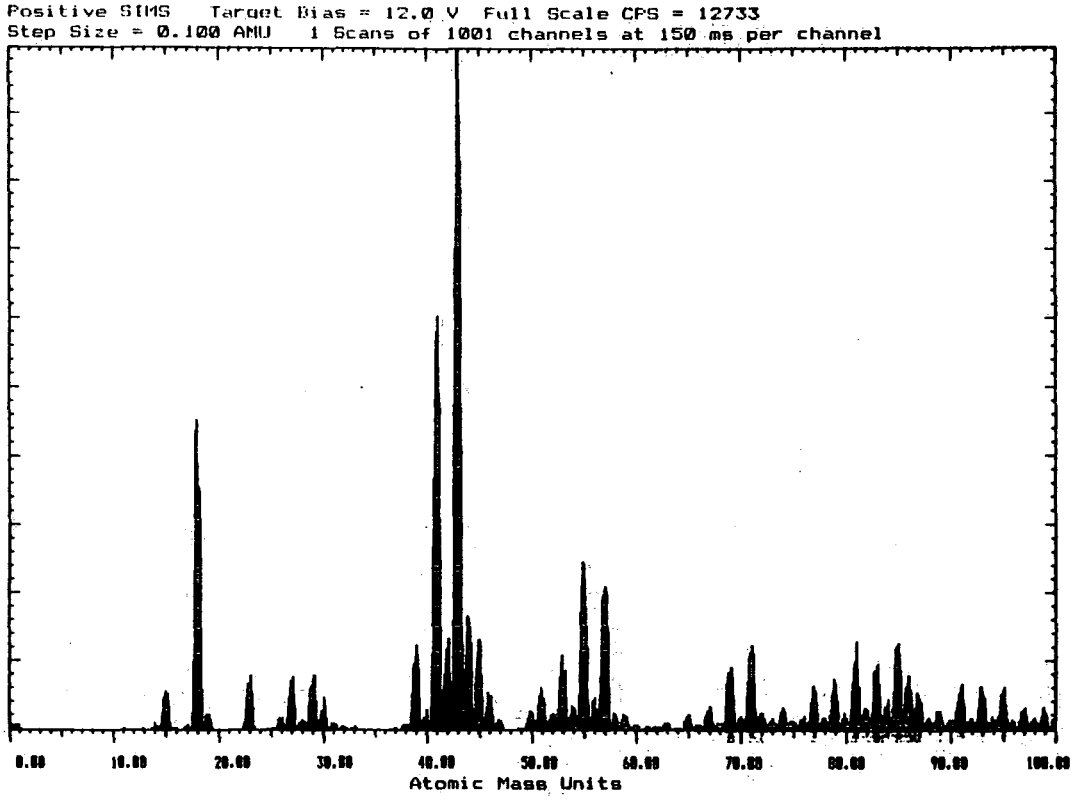

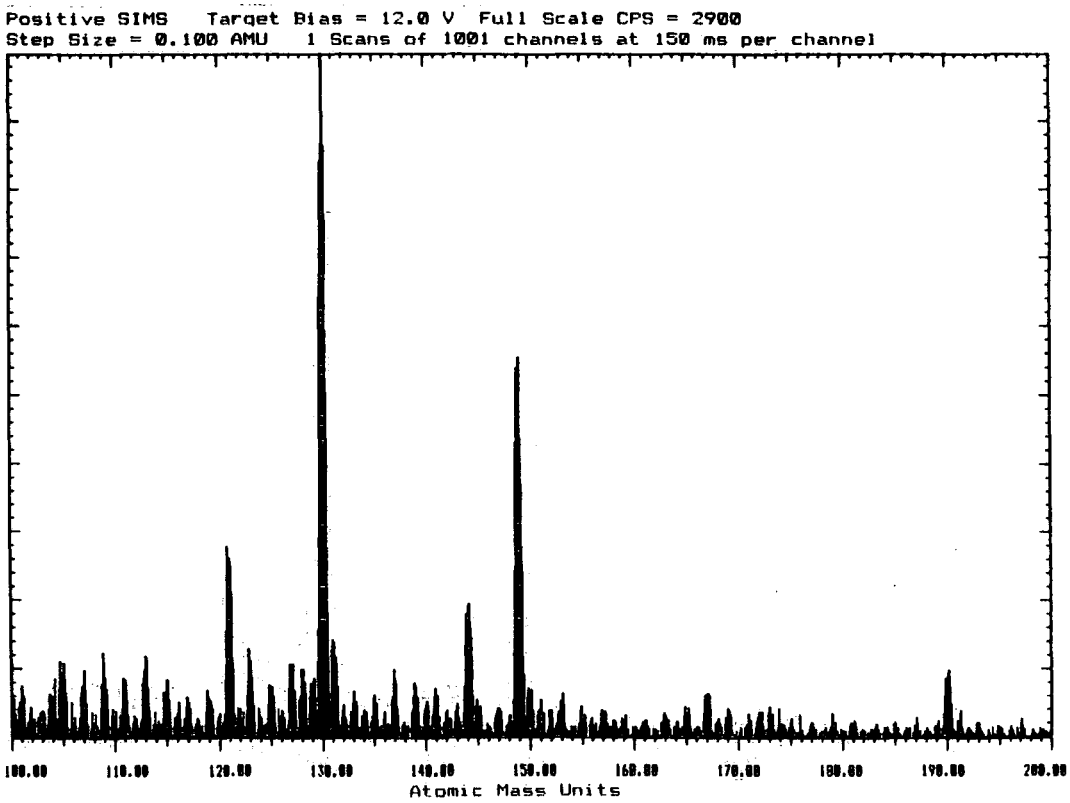

BIAXIALLY DRAWN PEEK 1 DAY OLD

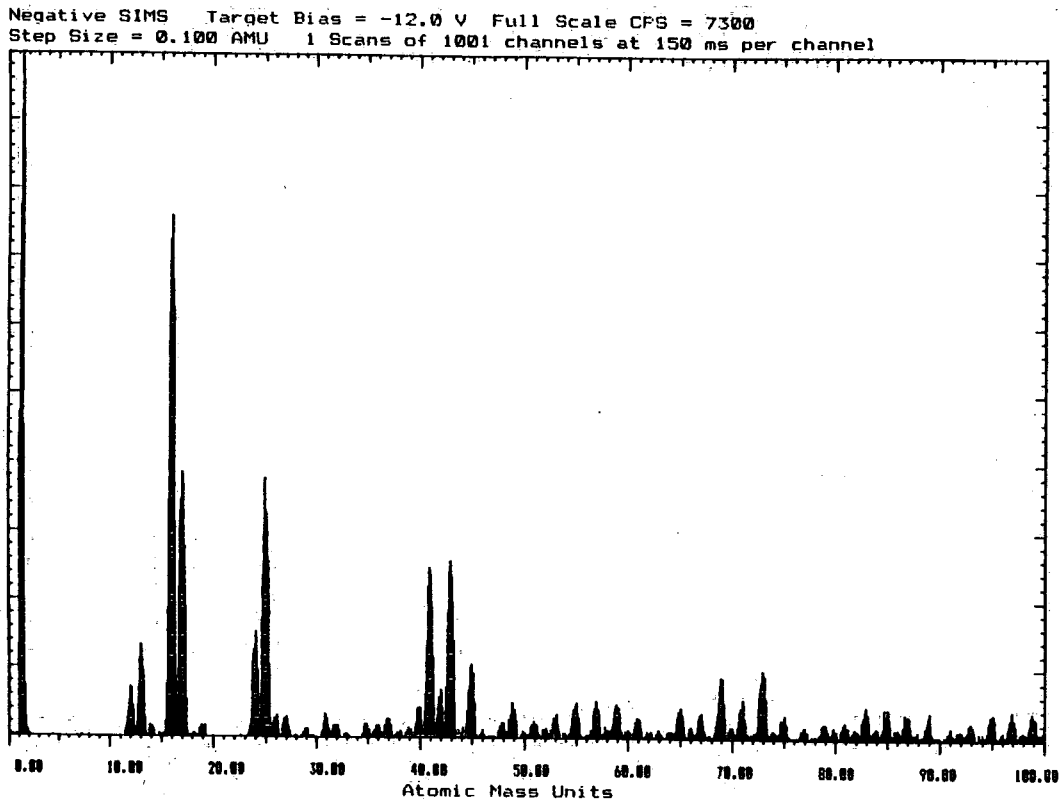

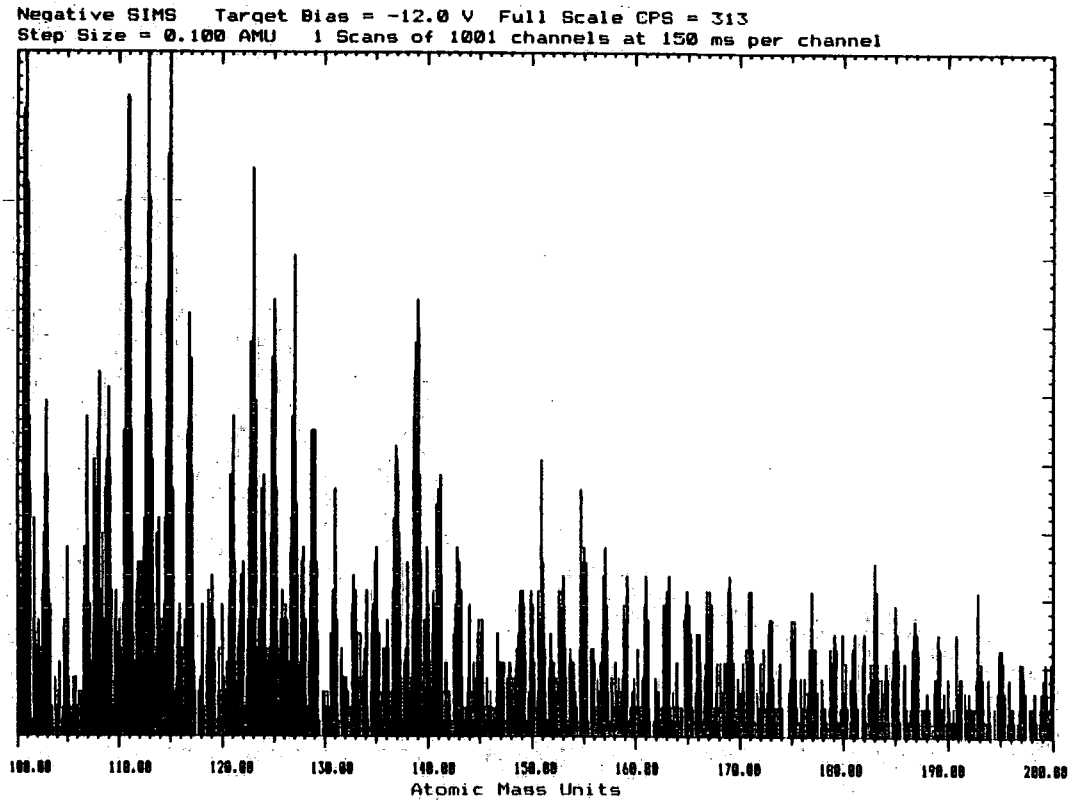

BIAXIALLY DRAWN PEEK 5 DAYS OLD

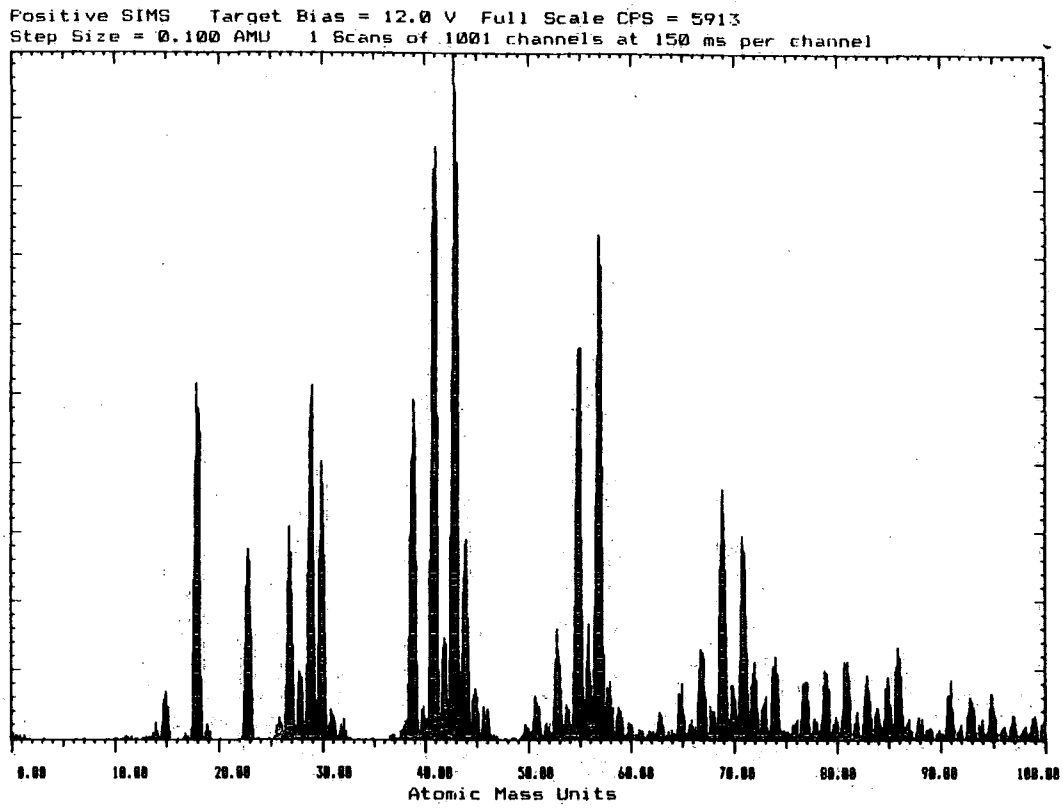

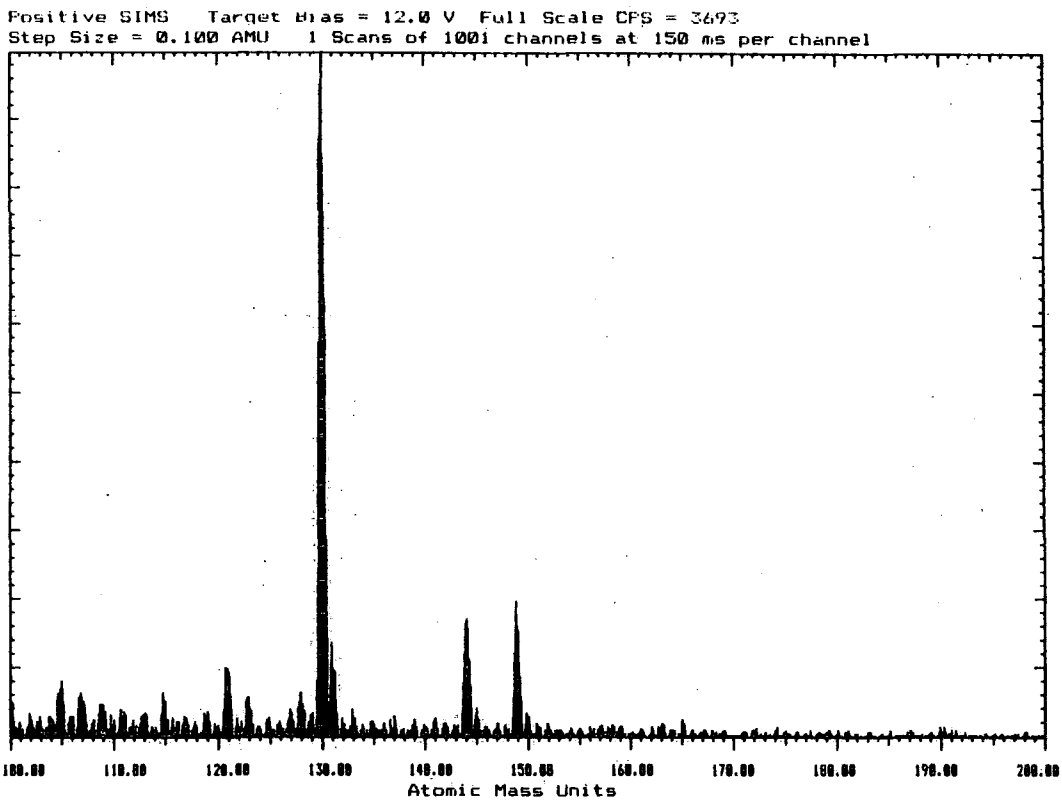

BIAXIALLY DRAWN PEEK 5 DAYS OLD

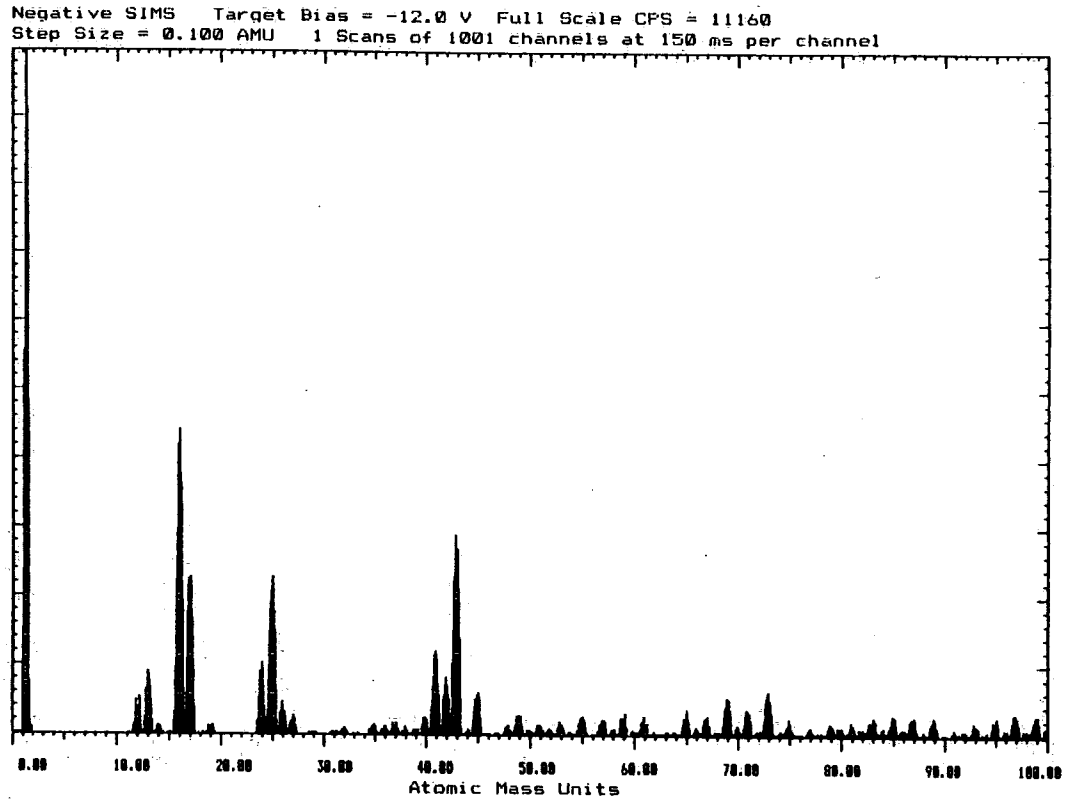

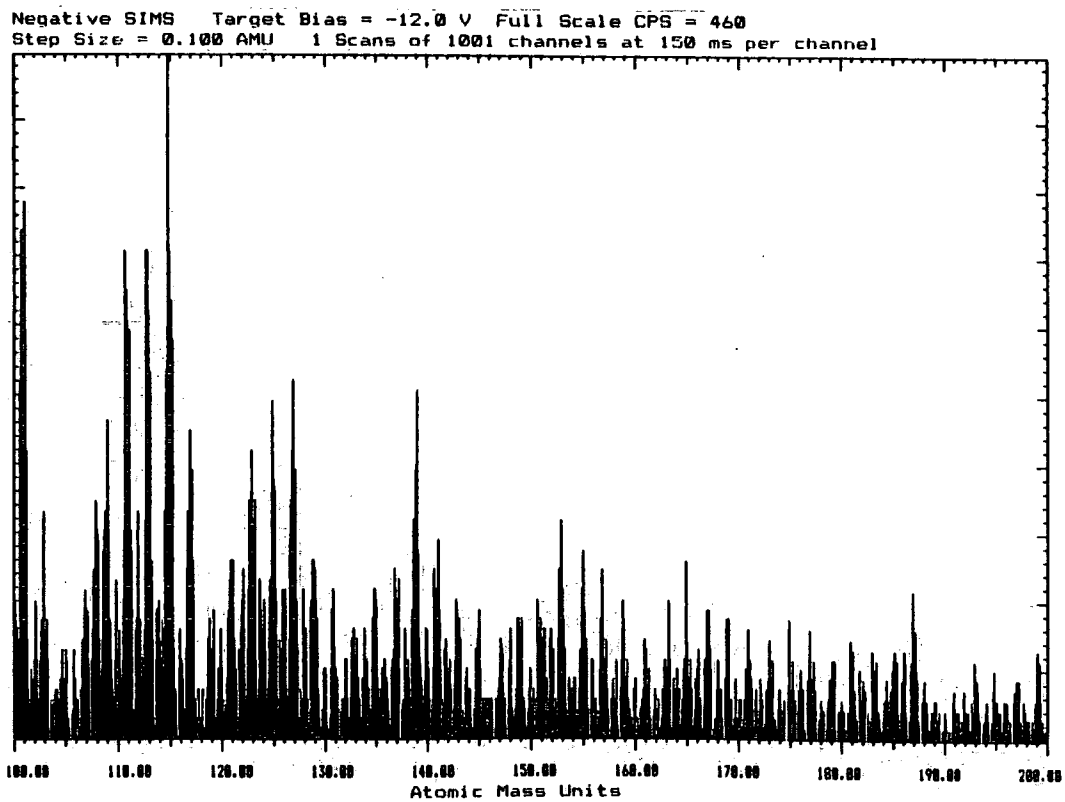

BIAXIALLY DRAWN PEEK 9 DAYS OLD

Positive SIMS Target Bias = 12.0 V Full Scale CPS = 10240
Step Size = 0.100 AMU 1 Scans of 1001 channels at 150 ms per channel

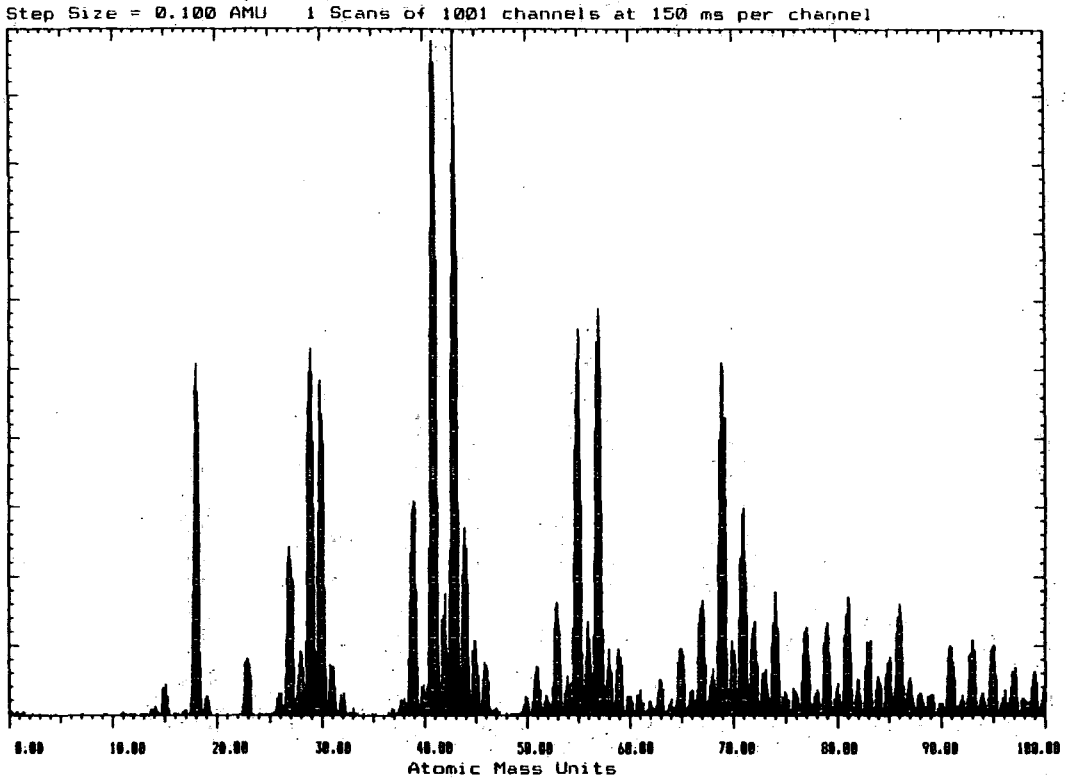

Positive SIMS Target Bias = 12.0 V Full Scale CPS = 8607
Step Size = 0.100 AMU 1 Scans of 1001 channels at 150 ms per channel

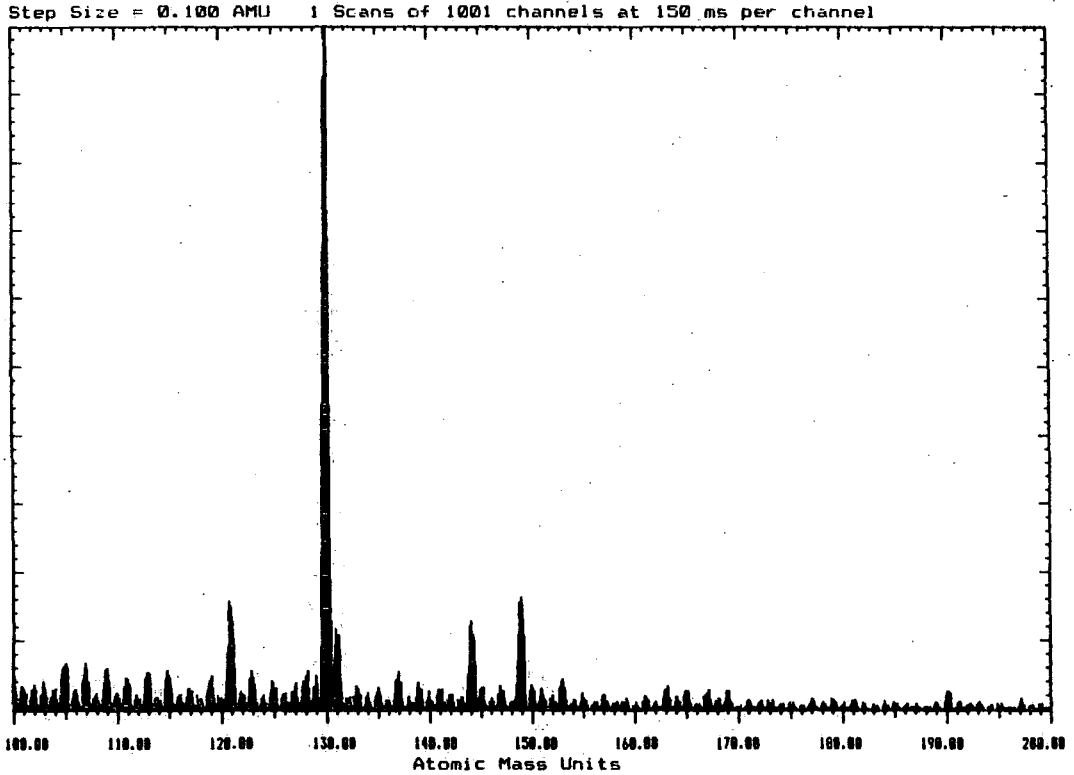

BIAXIALLY DRAWN PEEK 9 DAYS OLD

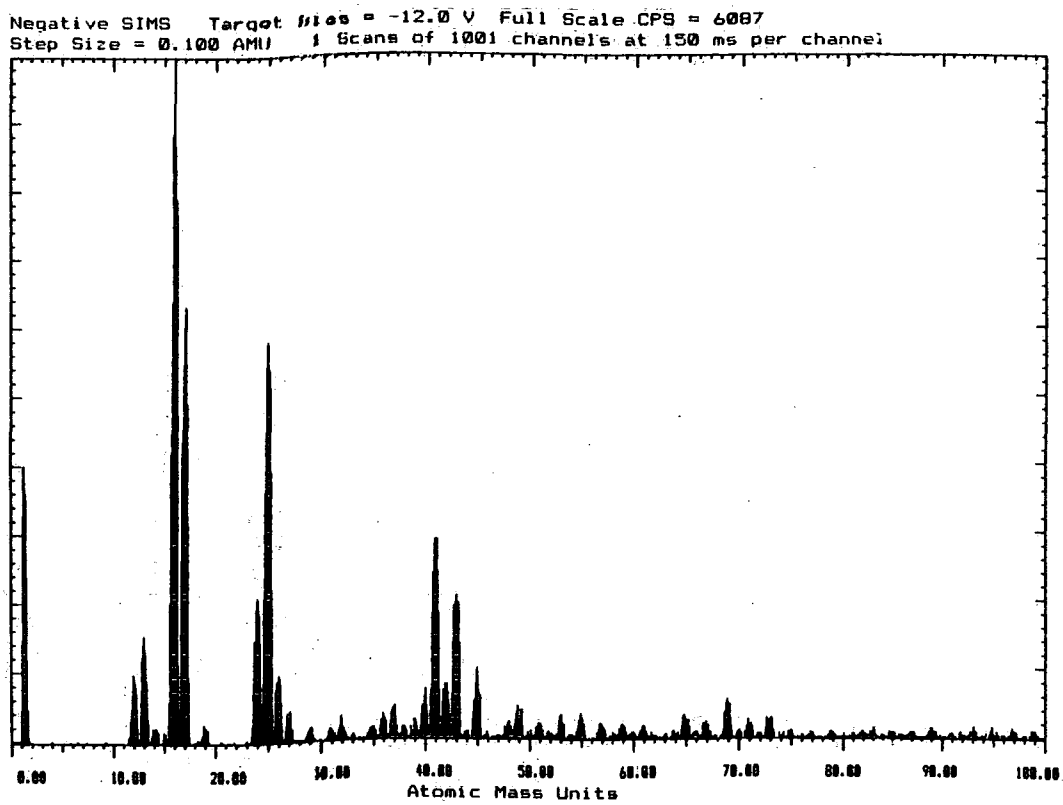

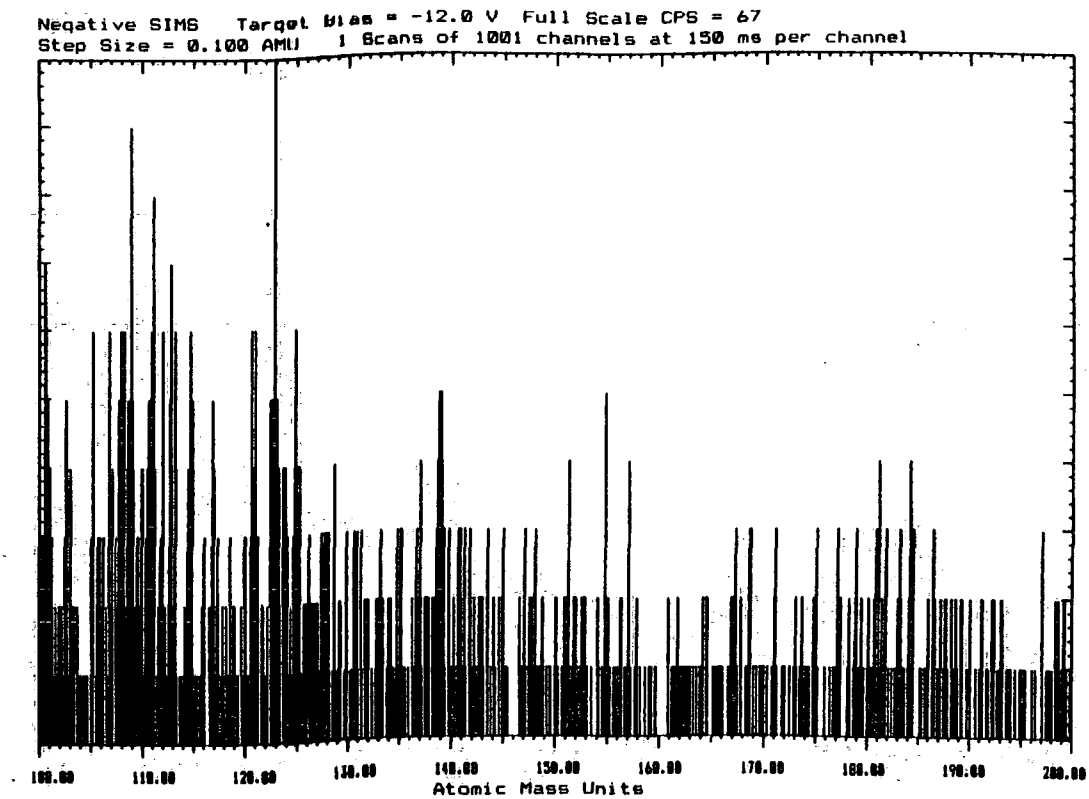

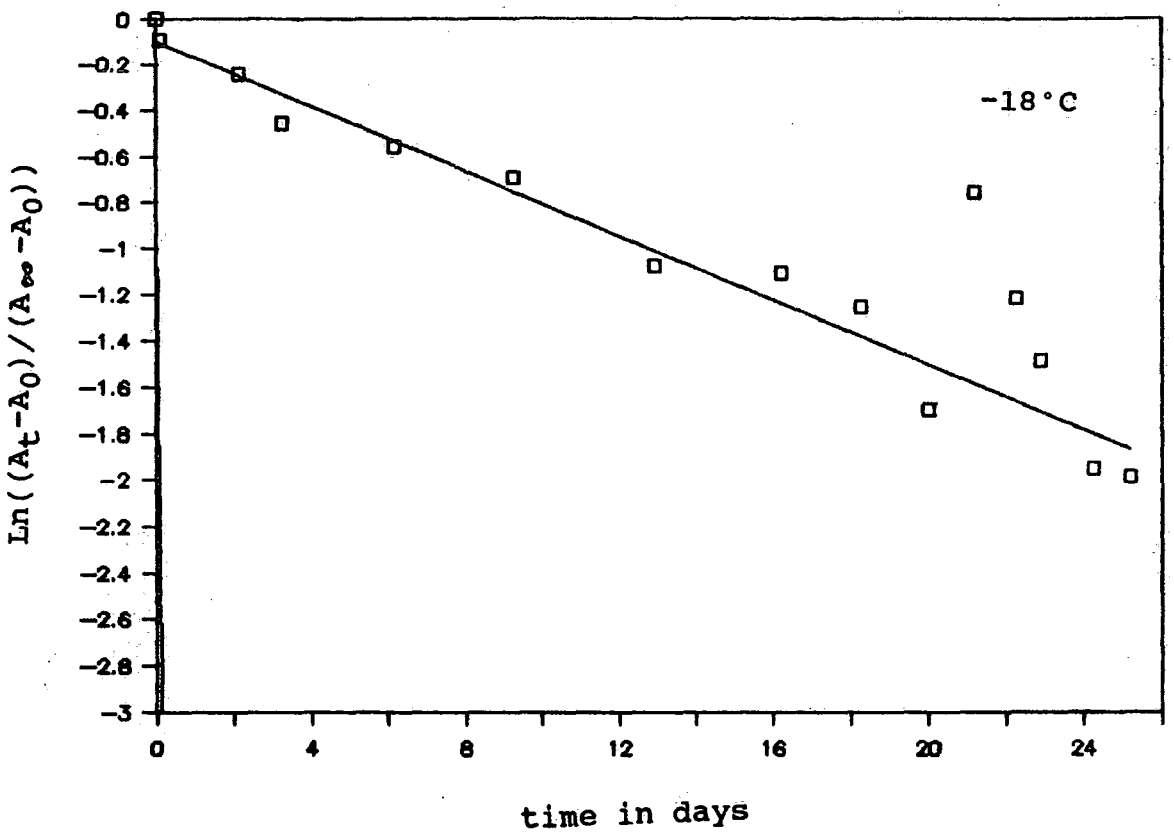
-18°C
Ln((At-A0)/(A∞-A0))
time in days

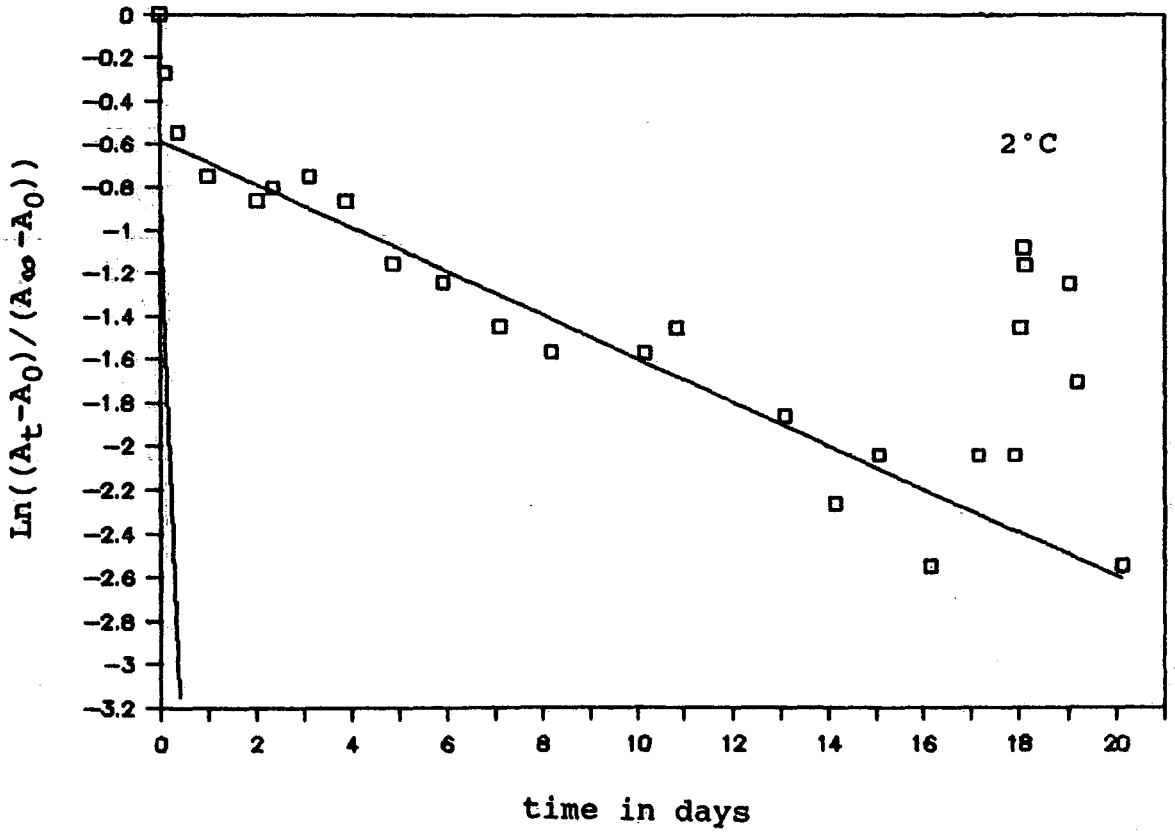
2°C
Ln((At-A0)/(A∞-A0))
time in days

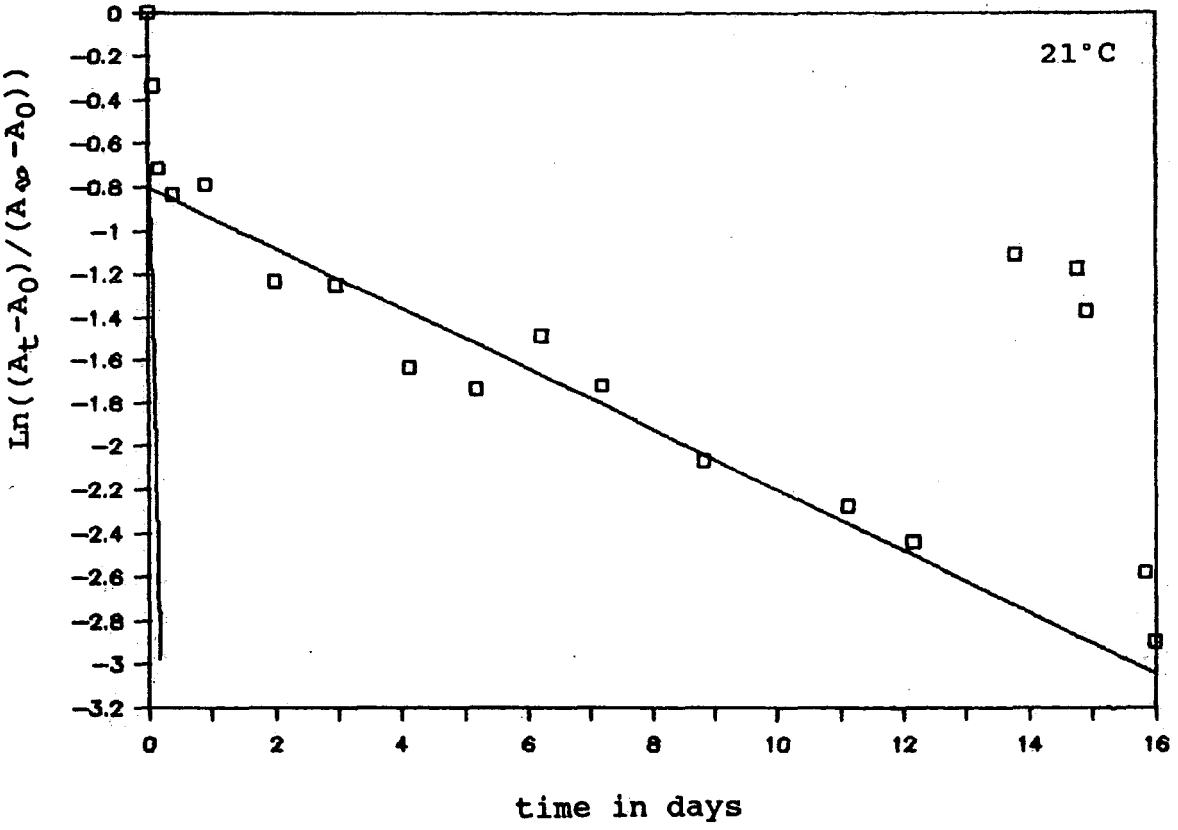
21°C
Ln((At-A0)/(A∞-A0))
0
-0.2
-0.4
-0.6
-0.8
-1
-1.2
-1.4
-1.6
-1.8
-2
-2.2
-2.4
-2.6
-2.8
-3
-3.2
0
2
4
6
8
10
12
14
16
time in days

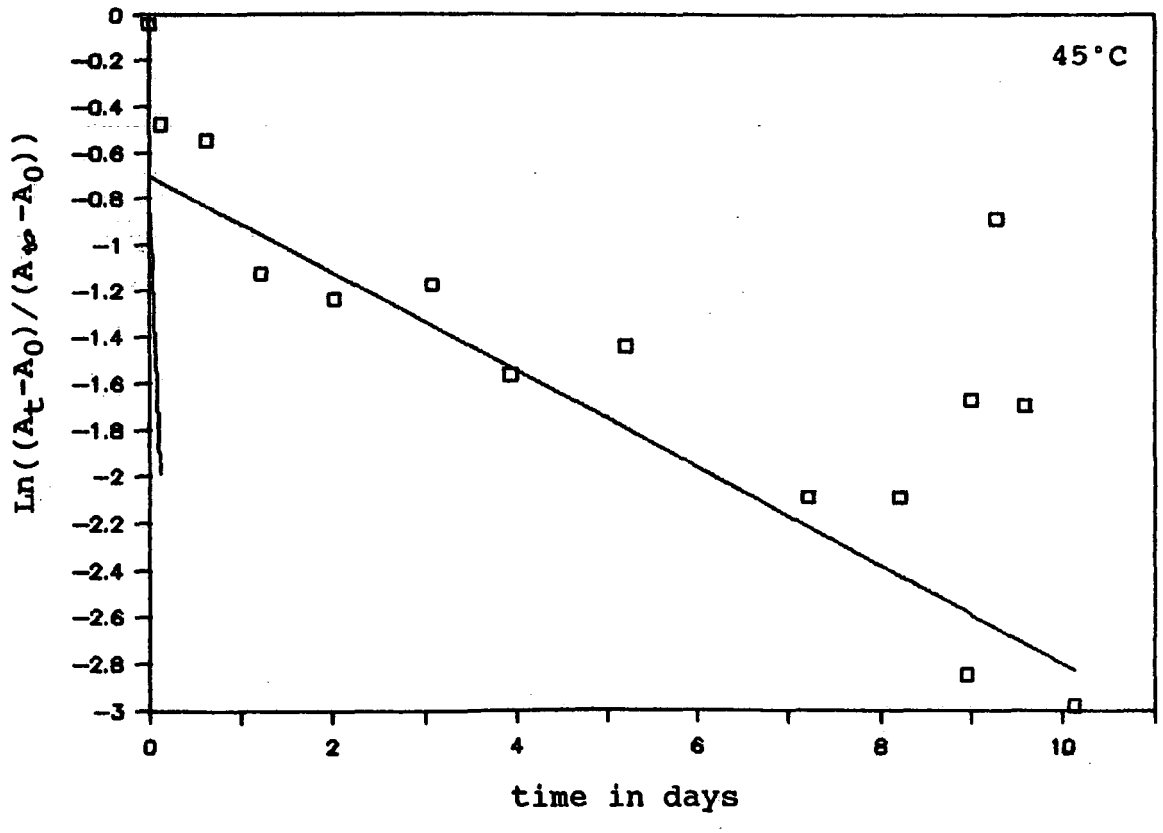
45°C
Ln((At-A0)/(A∞-A0))
0
-0.2
-0.4
-0.6
-0.8
-1
-1.2
-1.4
-1.6
-1.8
-2
-2.2
-2.4
-2.6
-2.8
-3
0
2
4
6
8
10
time in days

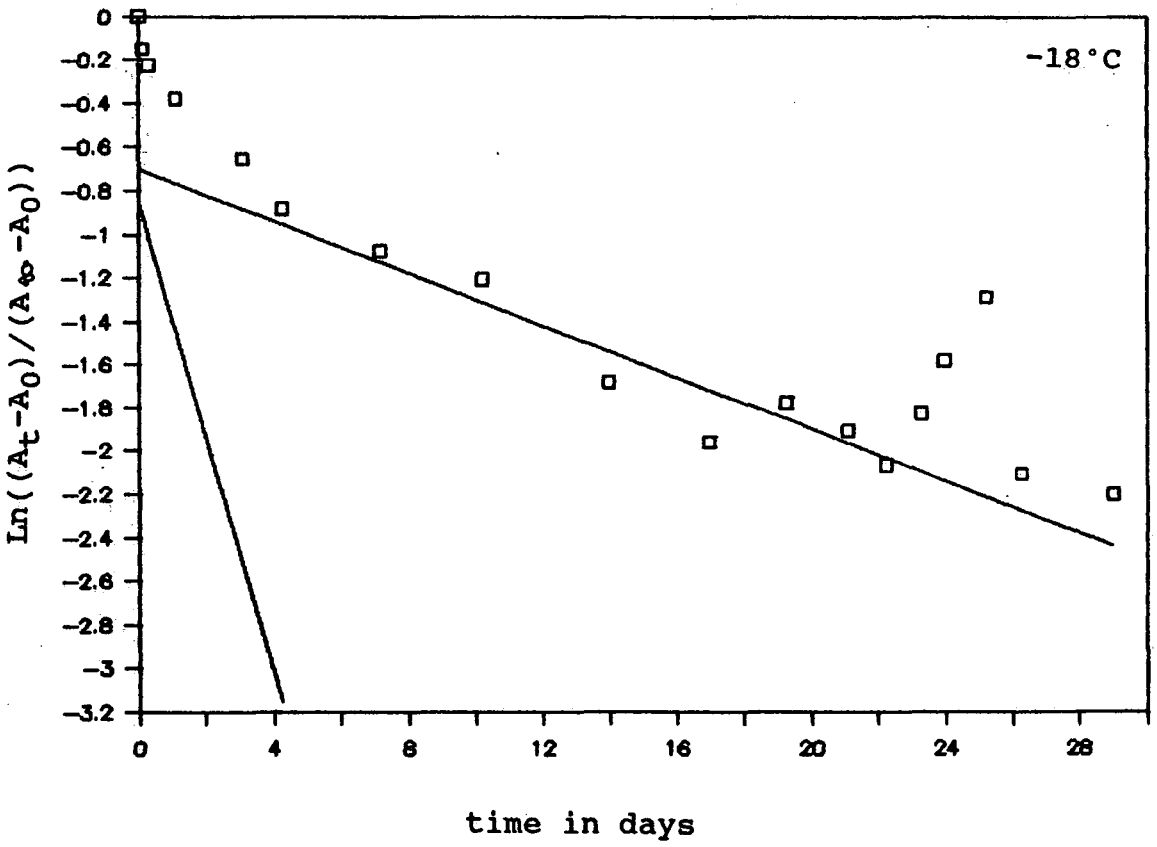
-18°C
Ln((At-A0)/(A∞-A0))
0
-0.2
-0.4
-0.6
-0.8
-1
-1.2
-1.4
-1.6
-1.8
-2
-2.2
-2.4
-2.6
-2.8
-3
-3.2
0
4
8
12
16
20
24
28
time in days

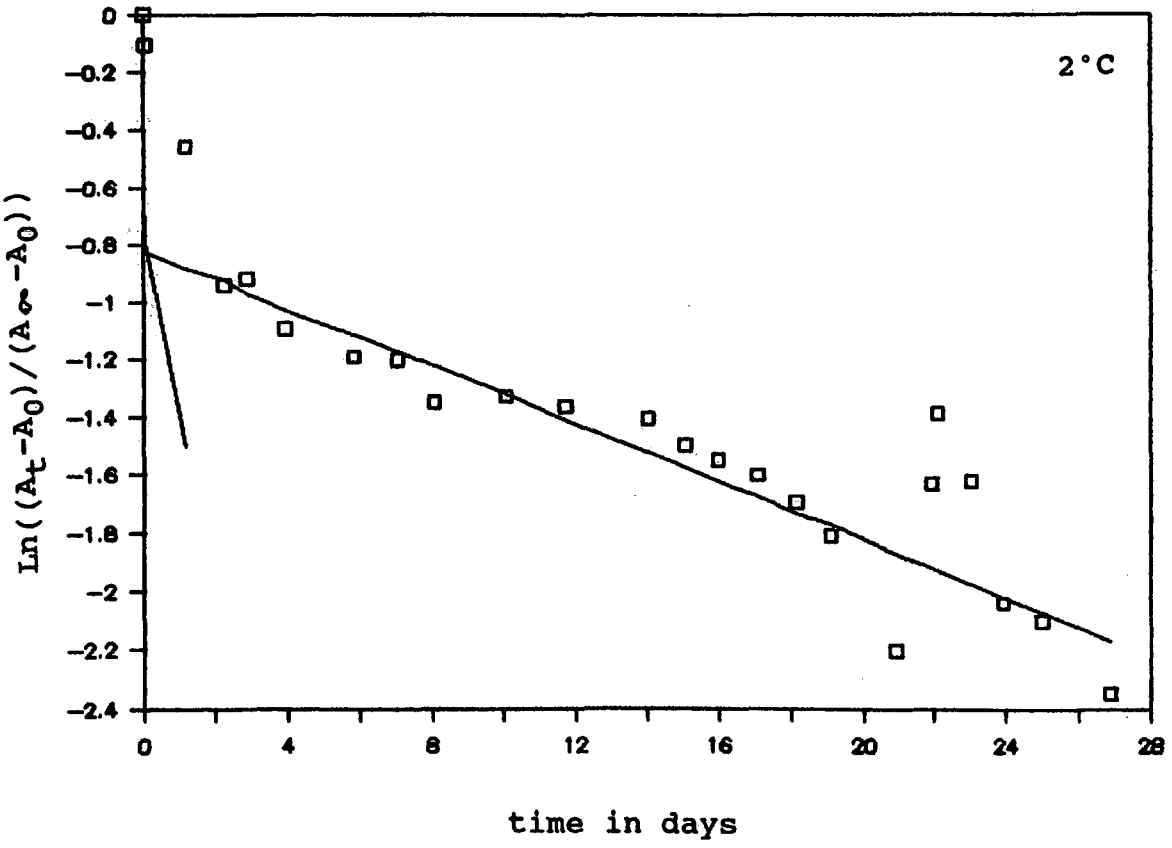
2°C
Ln((At-A0)/(A∞-A0))
0
-0.2
-0.4
-0.6
-0.8
-1
-1.2
-1.4
-1.6
-1.8
-2
-2.2
-2.4
0
4
8
12
16
20
24
28
time in days

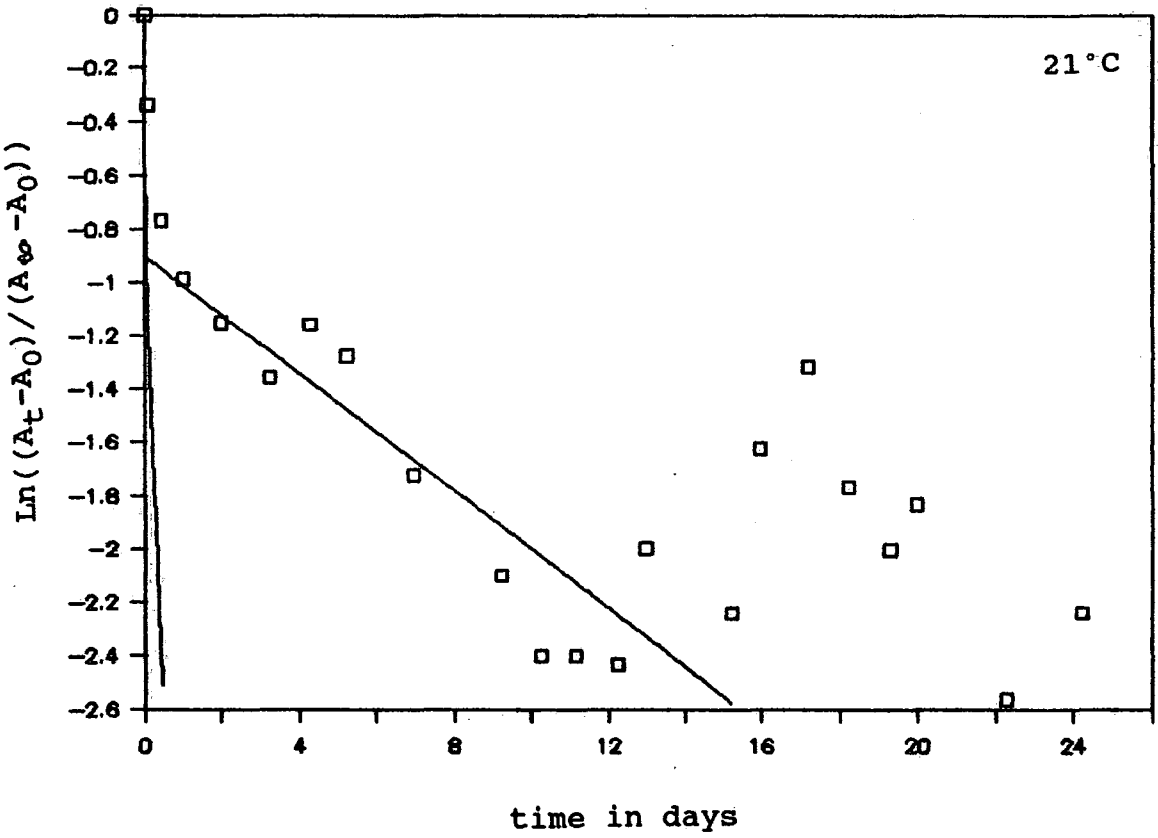
21°C
Ln((At-A0)/(A∞-A0))
0
-0.2
-0.4
-0.6
-0.8
-1
-1.2
-1.4
-1.6
-1.8
-2
-2.2
-2.4
-2.6
0
4
8
12
16
20
24
time in days

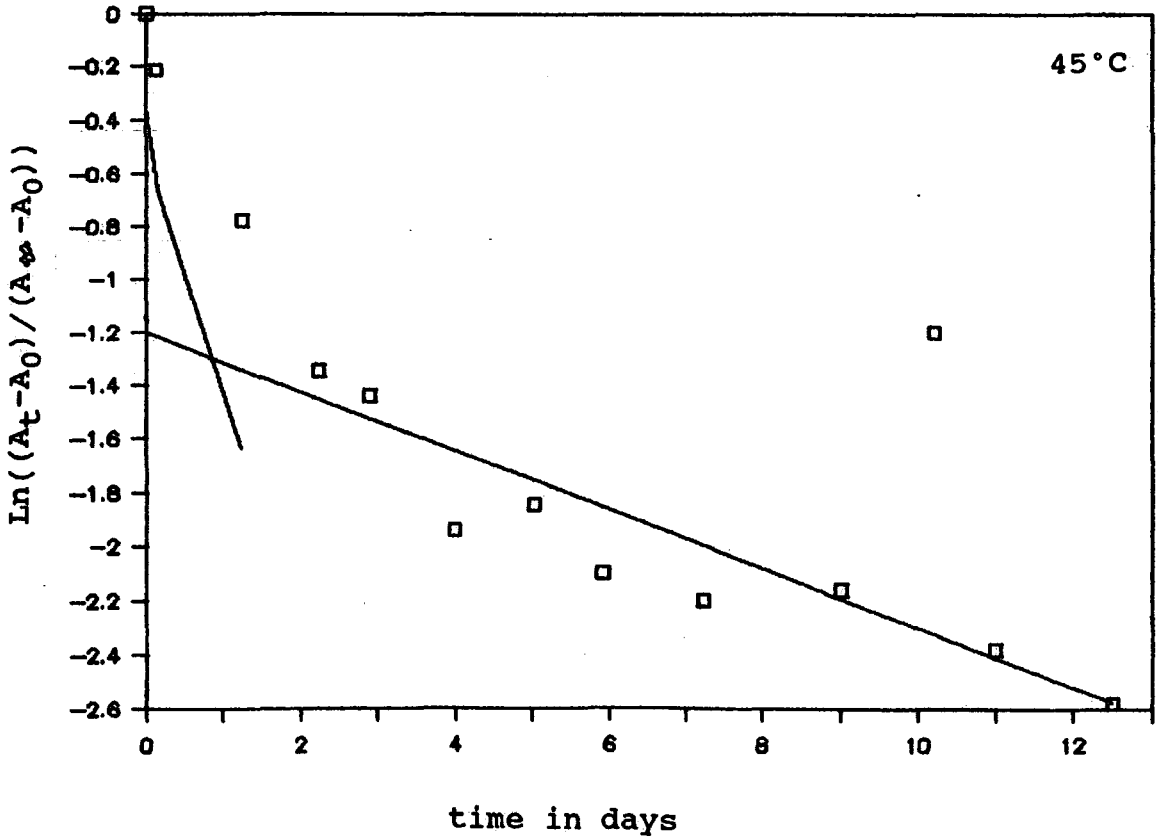
45°C
Ln((At-A0)/(A∞-A0))
0
-0.2
-0.4
-0.6
-0.8
-1
-1.2
-1.4
-1.6
-1.8
-2
-2.2
-2.4
-2.6
0
2
4
6
8
10
12
time in days

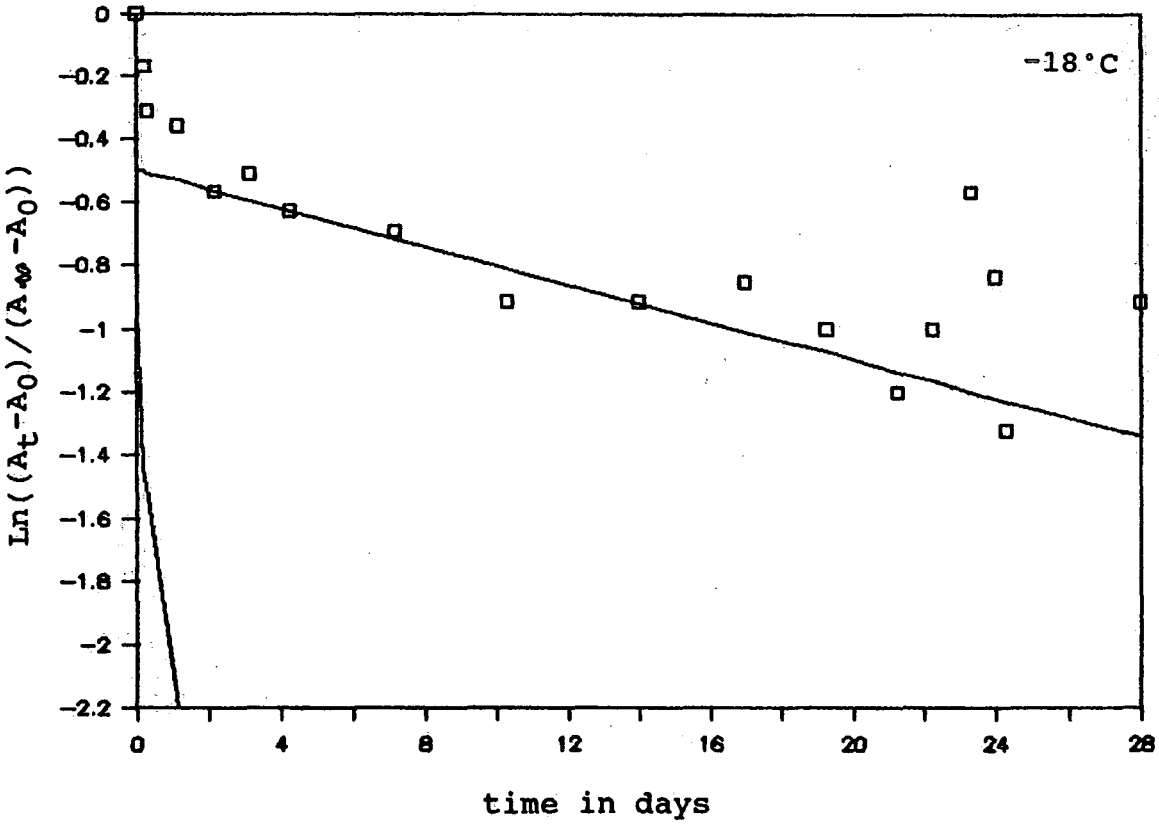
-18°C
Ln((At-A0)/(A∞-A0))
0
-0.2
-0.4
-0.6
-0.8
-1
-1.2
-1.4
-1.6
-1.8
-2
-2.2
0
4
8
12
16
20
24
28
time in days

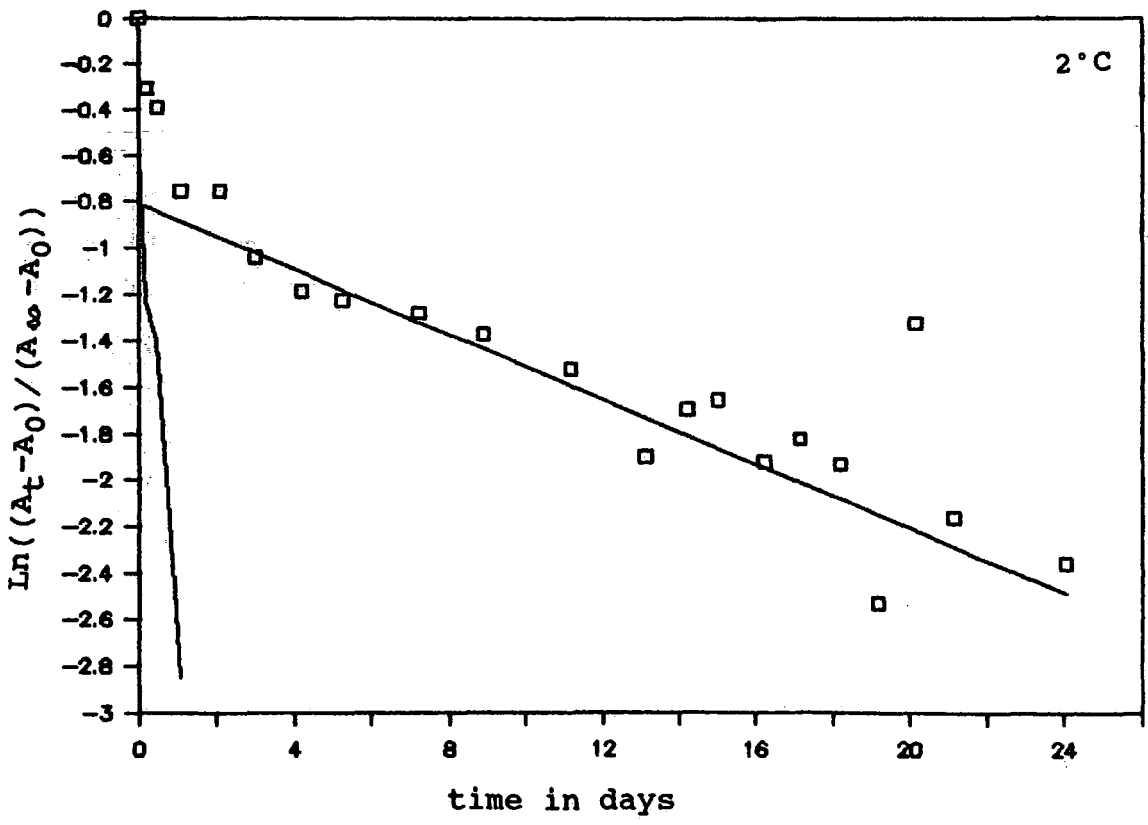
2°C
Ln((At-A0)/(A∞-A0))
0
-0.2
-0.4
-0.6
-0.8
-1
-1.2
-1.4
-1.6
-1.8
-2
-2.2
-2.4
-2.6
-2.8
-3
0
4
8
12
16
20
24
time in days

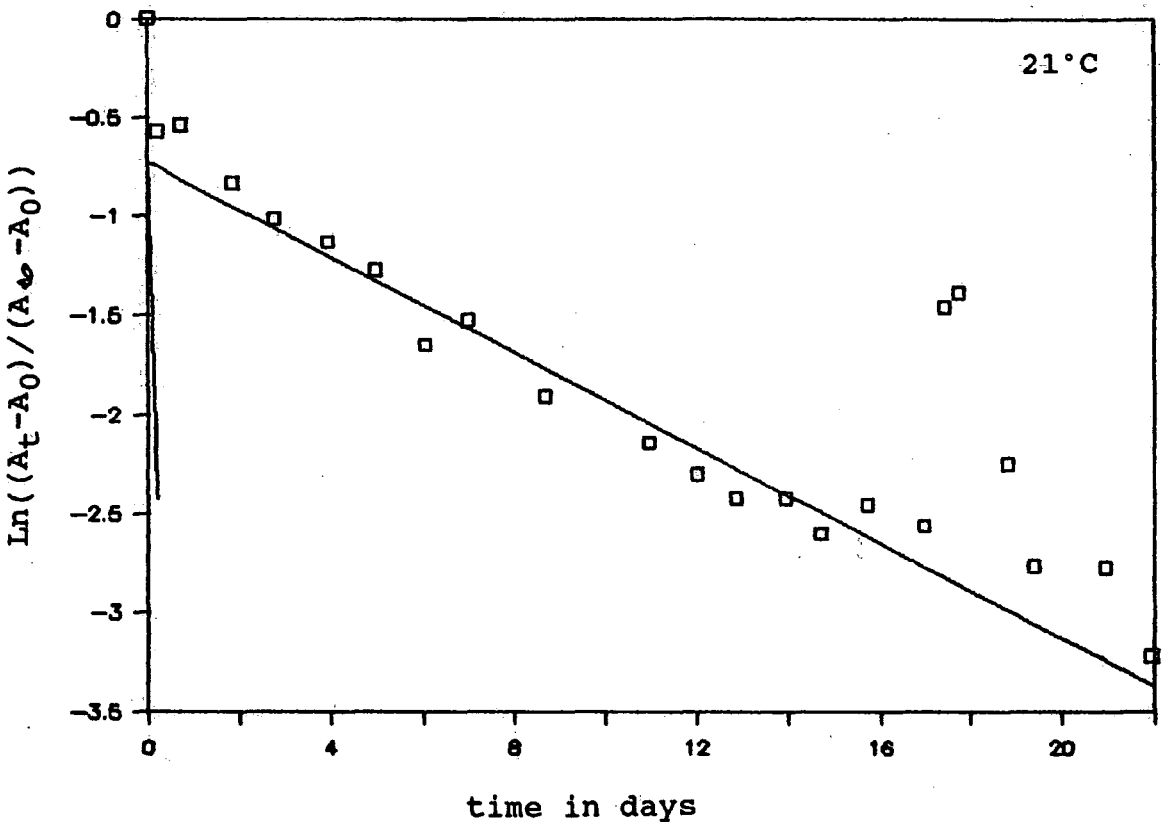
21°C
Ln((At-A0)/(A∞-A0))
0
-0.5
-1
-1.5
-2
-2.5
-3
-3.5
0
4
8
12
16
20
time in days

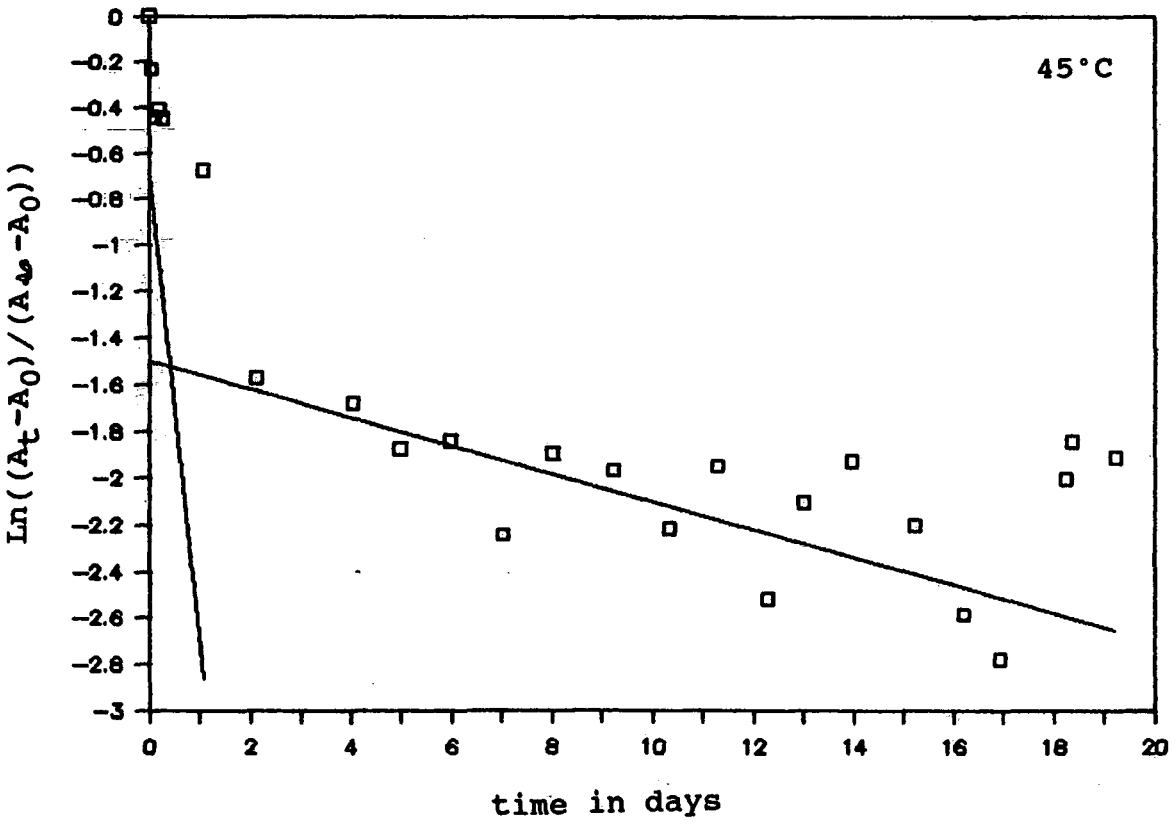
45°C
Ln((At-A0)/(A∞-A0))
0
-0.2
-0.4
-0.6
-0.8
-1
-1.2
-1.4
-1.6
-1.8
-2
-2.2
-2.4
-2.6
-2.8
-3
0
2
4
6
8
10
12
14
16
18
20
time in days

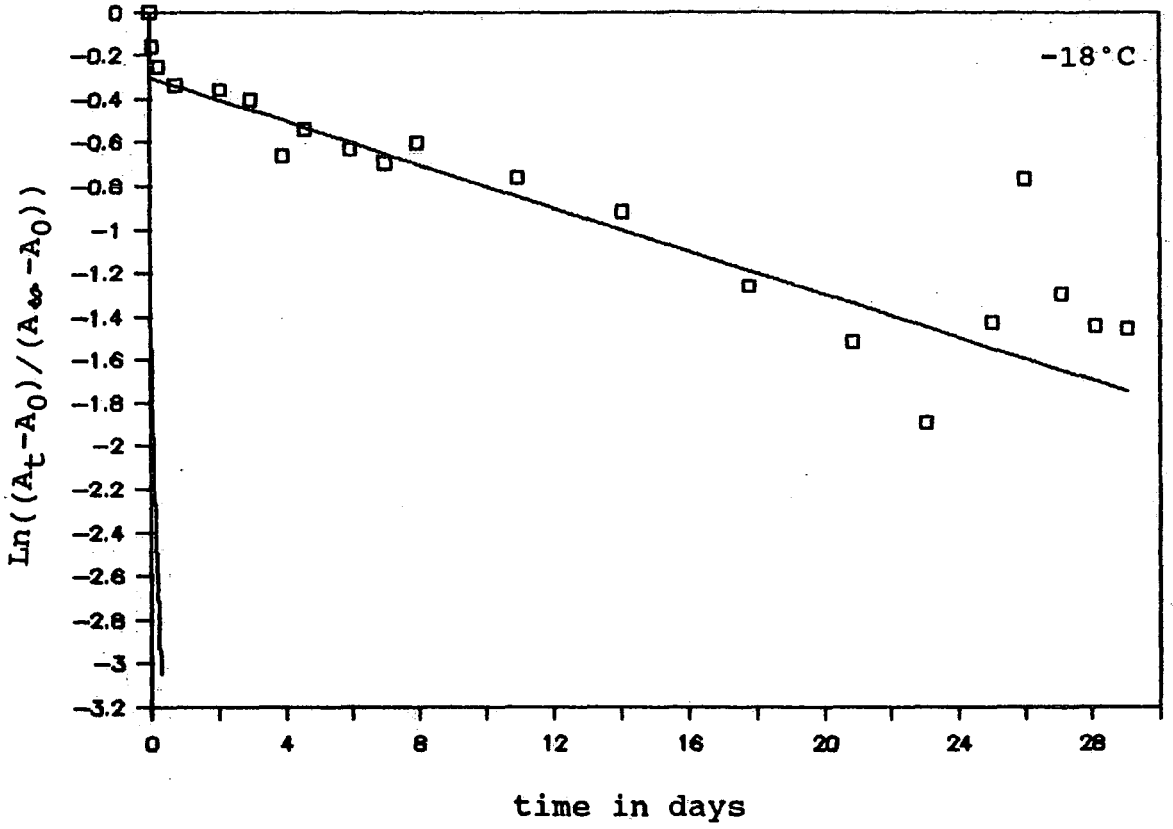
-18°C
Ln((At-A0)/(A∞-A0))
time in days

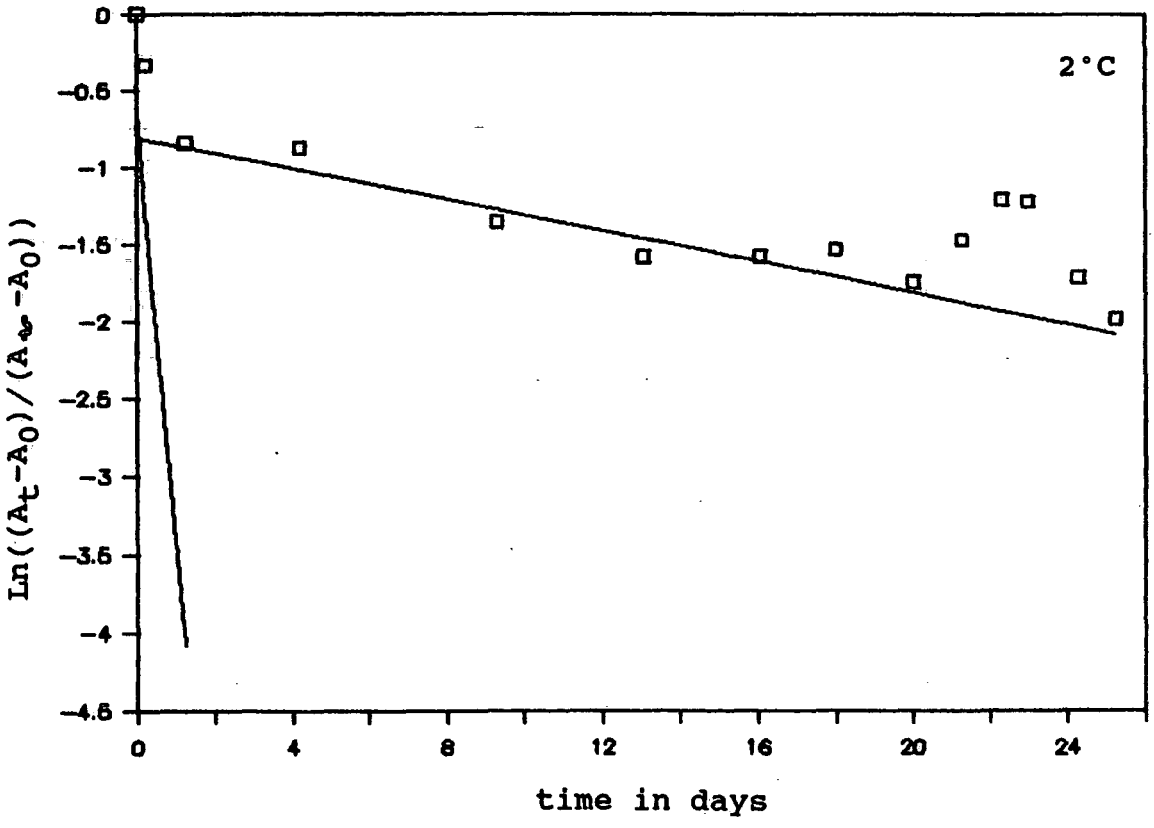
2°C
Ln((At-A0)/(A∞-A0))
time in days

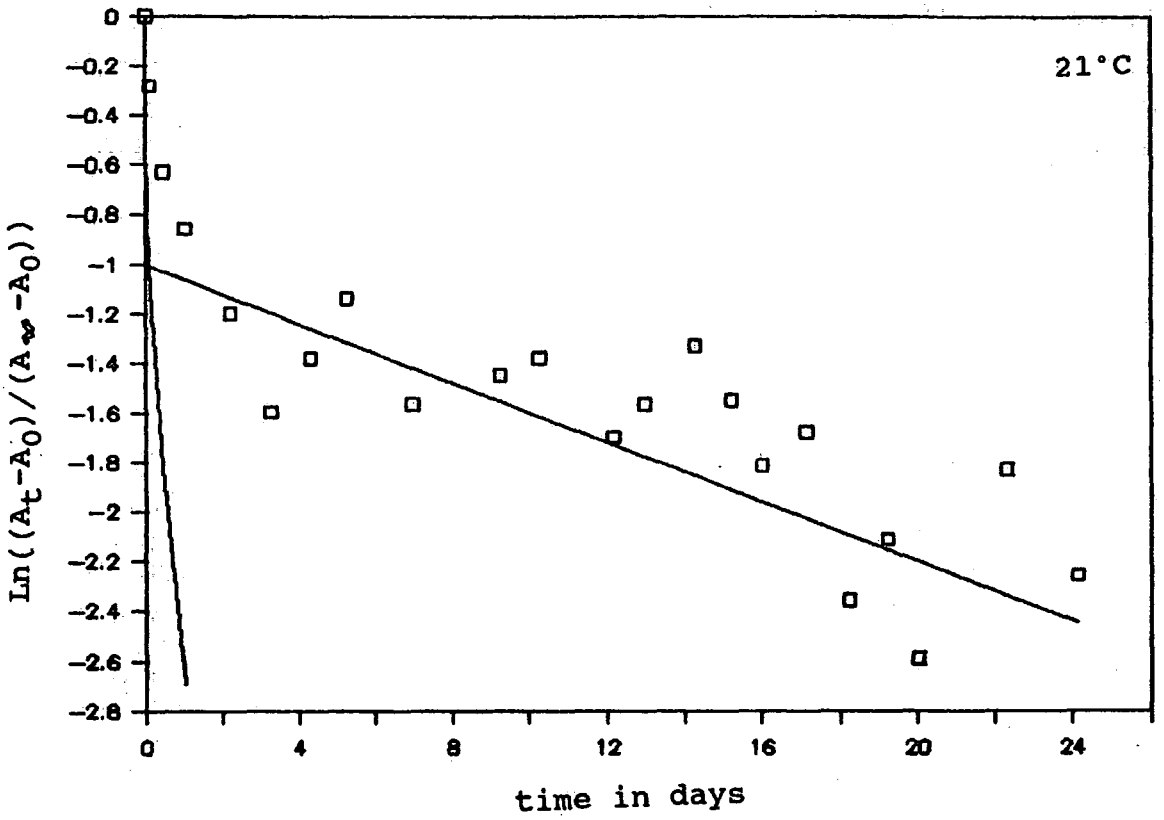
21°C
Ln((At-A0)/(A∞-A0))
0
-0.2
-0.4
-0.6
-0.8
-1
-1.2
-1.4
-1.6
-1.8
-2
-2.2
-2.4
-2.6
-2.8
0
4
8
12
16
20
24
time in days

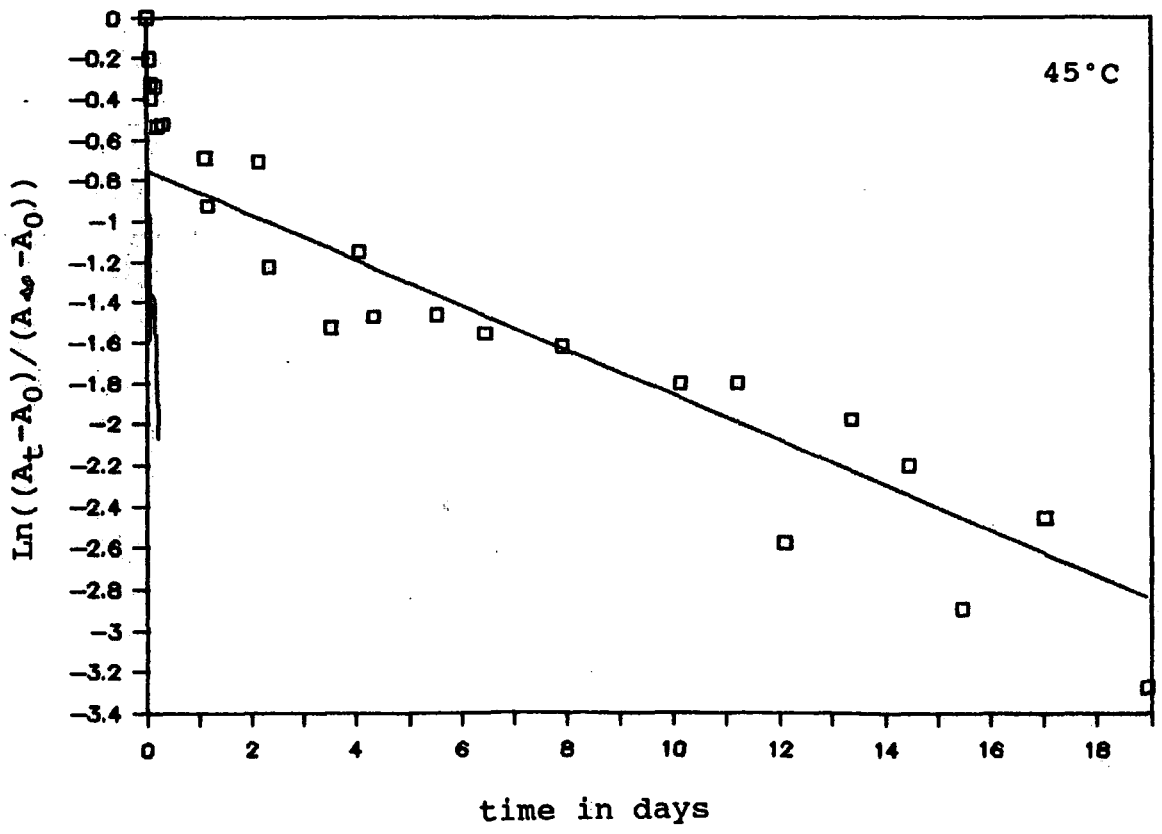
45°C
Ln((At-A0)/(A∞-A0))
0
-0.2
-0.4
-0.6
-0.8
-1
-1.2
-1.4
-1.6
-1.8
-2
-2.2
-2.4
-2.6
-2.8
-3
-3.2
-3.4
0
2
4
6
8
10
12
14
16
18
time in days

CHAPTER 4

FURTHER STUDIES ON THE AGEING OF PLASMA MODIFIED SURFACES.

4.1 INTRODUCTION

Although the transient increase in hydrophilicity has been previously reported,[1] this phenomenon is not widely known and its true nature not fully understood. It is not known whether the transient increase in hydrophilicity is a feature of decay of all plasma oxidised polymers or only a few special cases. It has been previously observed in polymethyl methacrylate and PEEK[1]. Lawson[2] has reported data on the decay of the surface modification effect on corona treated elastomers as measured by the change in contact angle with glycerine. His results show evidence for a transient increase for hydrophilicity although the author does not comment on the deviation from the idealised decay curve, the data are shown in Figure 4.1.

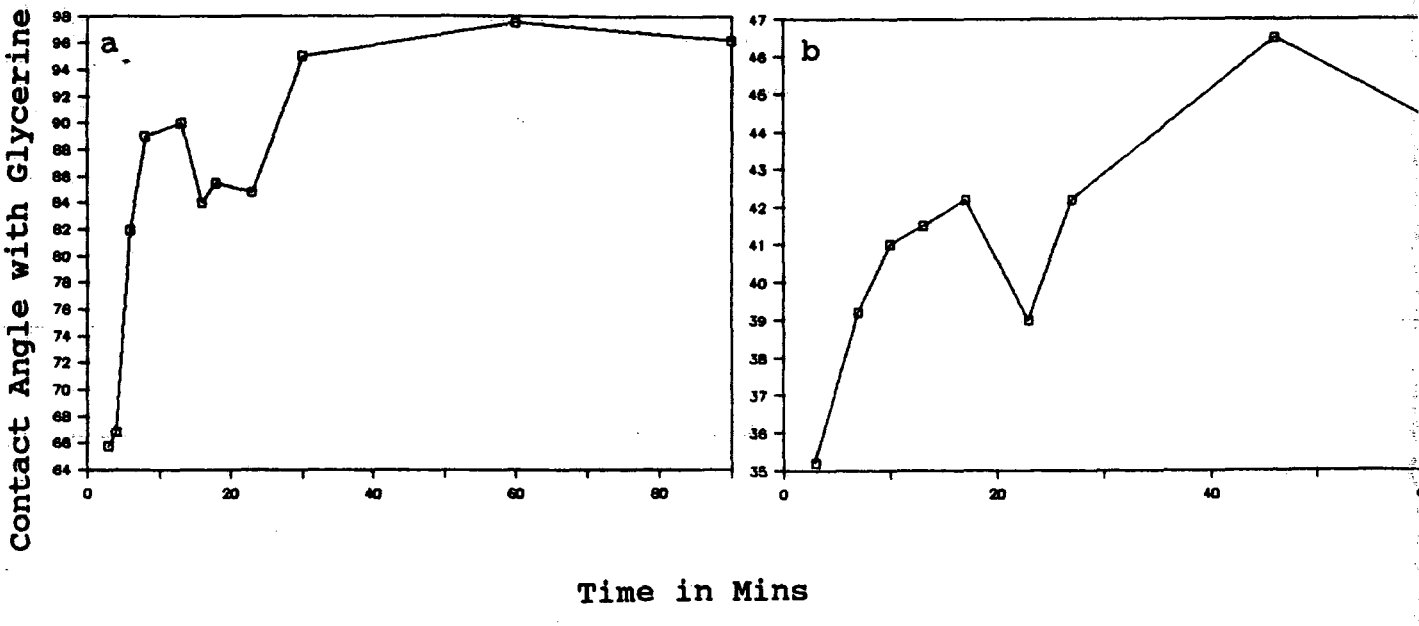

Figure 4.1 Contact Angle Decay of a) 70% Chlorobutyl-30% Natural Rubber and b) Ethylene-propylene-diene Monomer Rubber,[2] after corona discharge treatment.

In this chapter the ageing of plasma oxidised polyethylene terephthalate (PET) and plasma modification of PEEK with tetrafluoromethane and ammonia are reported and discussed with respect to the transient increase in hydrophilicity observed with plasma oxidised PEEK.

4.2 EXPERIMENTAL

4.2.1 MATERIALS

PET and PEEK samples were prepared as described in Chapter Two. Oxygen was supplied by BOC, tetrafluoromethane was supplied by Fluoro Chem Ltd. and anhydrous ammonia was supplied by Aldrich Chemical Co., all these gases were used without further purification.

4.2.2 PLASMA MODIFICATION

Plasma oxidation was carried out as described in Chapter Three, other plasma modifications were carried out in a tubular Pyrex reactor, illustrated in Figure 4.2, connected to a grease and mercury free vacuum line. Flanged joints and the cold trap were sealed with Viton O rings whilst all other connections were made with Cajon Ultra Torr couplings. Vacuum taps were sealed with PTFE stoppers. The apparatus was pumped down to a base pressure of about 3×10^{-2} torr using Edwards ED2M2 mechanical rotary pumps. Pressure measurements were made using a Pirani gauge.

At the start of each experiment the leak rate of the vacuum line was tested by isolating the pump and measuring the rise in pressure over a period of time. When the leak rate was less, than 0.03 cc/min reactant gas or vapour was let into the reactor through an Edwards needle valve to fill the reactor with plasma gas at the desired pressure. All plasma modification experiments were carried out with a flow of reactant through the apparatus, i.e. the reactor was open to the pumping system during the experiment.

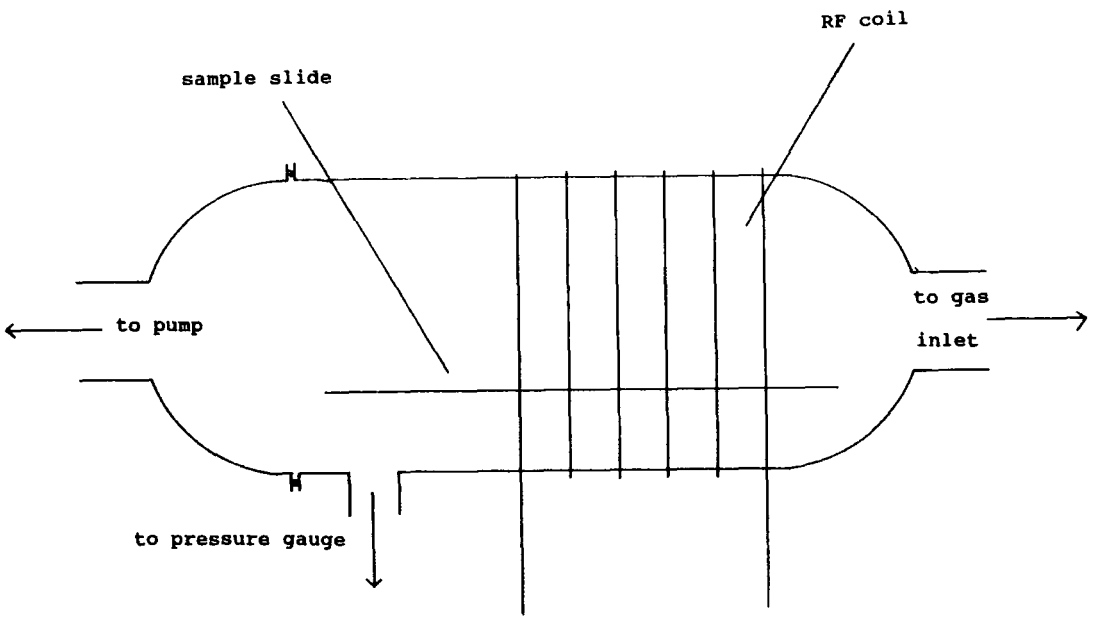

Figure 4.2 Plasma Reaction Vessel.

The radiofrequency (RF) power supplied by a 13.56 MHz RF generator was inductively coupled to the reactor through an externally wound copper coil via an inductance-capacitance matching network. A DIAWA SW110A meter was used to measure the RF power and standing wave ratio defined as the ratio of total power generated to power going into the plasma.

4.2.3 XPS MEASUREMENTS

XPS spectra were obtained as described in Chapter 3. Electron take-off angles of 70° and 35° were used to investigate the vertical homogeneity of the sample. A take-off angle of 70° samples a depth of ca. 15Å for carbon, ca. 10Å for oxygen and 10Å for fluorine, at 35° the sampling depth is ca. 35Å for carbon, ca. 25Å for oxygen and ca. 20Å for fluorine.[3]

4.2.4 CONTACT ANGLE MEASUREMENTS

Contact angles were measured with one microlitre drops of distilled water according to the sessile drop method described in Chapter One.[4]

4.2.5 SIMS MEASUREMENTS

SIMS spectra were recorded by Dr. D. Briggs, on samples treated on the previous day in the manner described in Chapter Two.

4.3 PLASMA OXIDATION OF PET

PET was treated in a 0.2mbar, 50W oxygen plasma for 30 minutes and then stored at 45°C. It was hoped that the more vigorous treatment would overcome some of the effects of sample preparation described in Chapter Two, viz. the formation of highly stressed regions and extensive crystallisation at the surface. The decay of the plasma modified surface was monitored using contact angles, the results are shown in Figures 4.3 a, b and c. Both amorphous and 22% crystalline materials show a transient increase in hydrophilicity that of the amorphous sample occurring before that observed for the semi-crystalline. No transient decrease in contact angle was seen for the 51% crystalline material, this is consistent with the results for PEEK described earlier in Chapter Three.

Both the 22% and 51% PET show a decreased rate of decay of contact angle compared to the amorphous material, reflecting the decreased mobility at the surface. The transient decrease in contact angle occurred sooner in PET than in PEEK at similar temperatures (9-days). This could be due to both the greater mobility of PET when compared to PEEK or the much harsher treatment which would lead to the surface being broken up to a larger extent causing the decay to occur more rapidly if is predominately dependent on the mobility of small fragments.

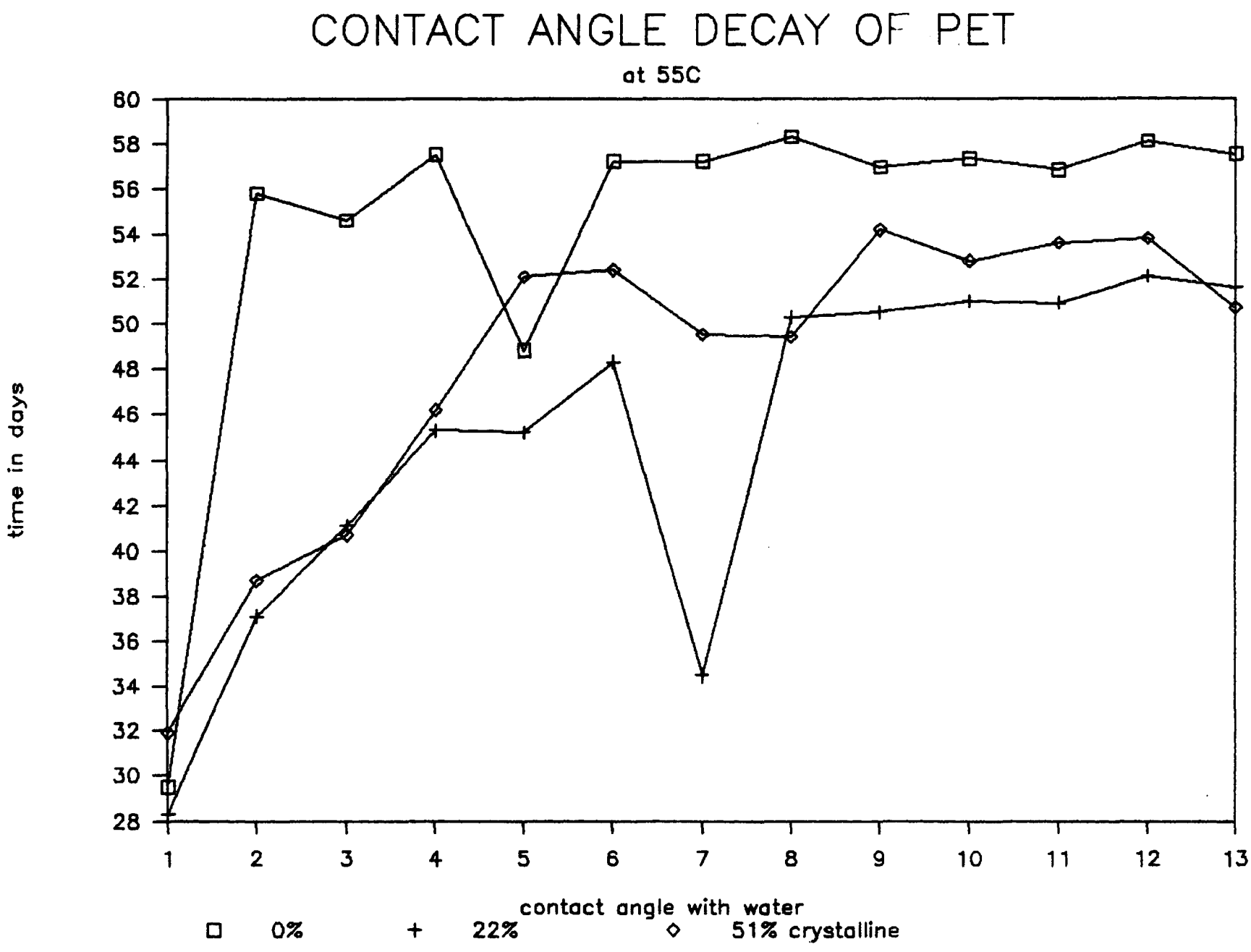

FIGURE 4.3. Contact Angle Decay of Plasma Oxidised PET

4.4 PLASMA FLUORINATION OF PEEK

Plasma fluorination of polymers with tetrafluoromethane has been widely studied,[5,6,7] it has been generally noted that the modified surface is initially hydrophobic and relatively mobile, subsequently undergoing a decay of hydrophobicity when stored in water. However, one group have described the use of tetrafluoromethane to induce a hydrophilic surface with a resistance to ageing.[7] It was thought that their results might be explained by the high level of oxygen incorporated during their plasma modification process. In this work PEEK was fluorinated using 0.2mbar 30s, 30W tetrafluoromethane RF plasma, and stored in distilled water at room temperature. The change in the composition of the surface with time was monitored using XPS, prior to insertion in the spectrometer samples were dried in a stream of dry air for about one minute. Spectra were acquired immediately to minimise the reorganisation that occurred before the collection of data, however the limiting factor on this source of error was the time taken to accumulate a complete spectrum, about one hour.

Plasma fluorination of PEEK puts a wide range of fluorine environments at the surface, as shown in Figure 4.4, with most of the carbon in the surface region being attached in some manner to fluorine. SIMS spectra show, as expected, no trace of water and large fluoride ion peak in the negative ion spectrum (see Figure 4.6a and b). It is also apparent that the extent of fragmentation at the surface is quite considerable, larger than that seen for

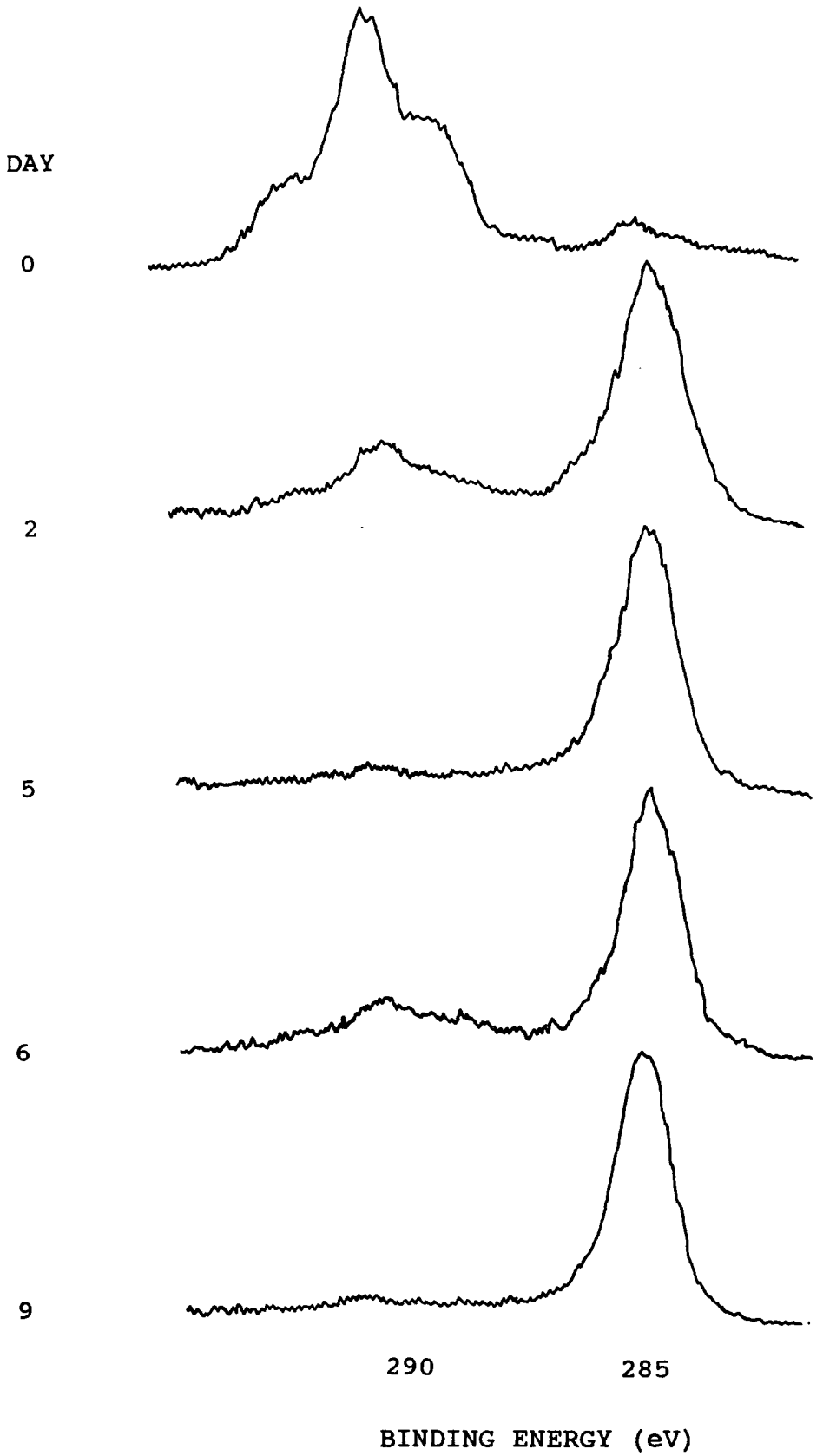

Figure 4.4 Changes in the XPS C_{1s} Envelope of PLasma Fluorinated PEEK with Time.

plasma oxidised PEEK in the previous chapter, this high level of fragmentation suggests that the tetrafluoromethane plasma treatment disrupts the surface to a greater extent than an oxygen plasma treatment.

Figure 4.5 illustrates the dramatic change in the elemental composition of the surface which occurs on storage in water. The amount of oxygen increases initially and then remains fairly constant with the outermost surface region tending to be less oxidised than the sub-surface region. The fluorine concentration decreases dramatically with a transient increase occurring after six days storage in the water.

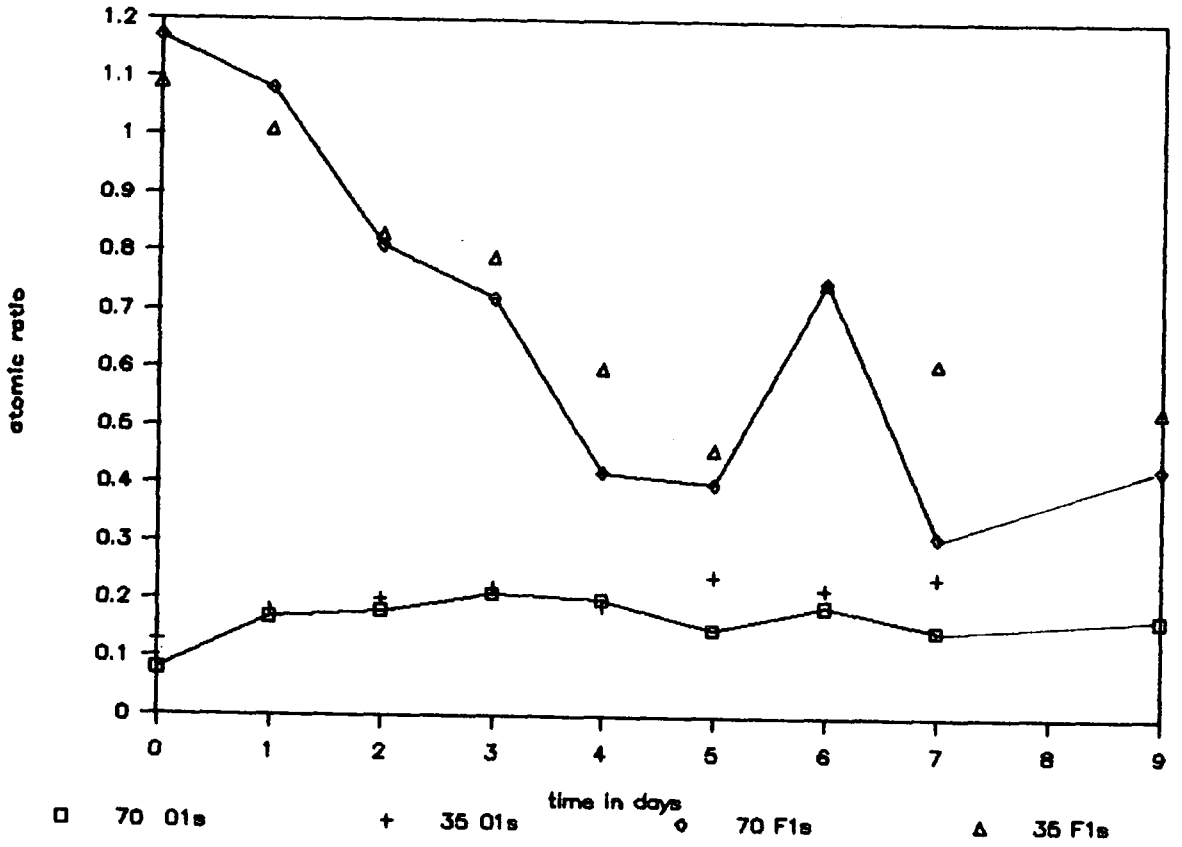

Figure 4.5 Change in Fluorine and Oxygen to Carbon Ratios With Time of Plasma Fluorinated PEEK Stored in Water.

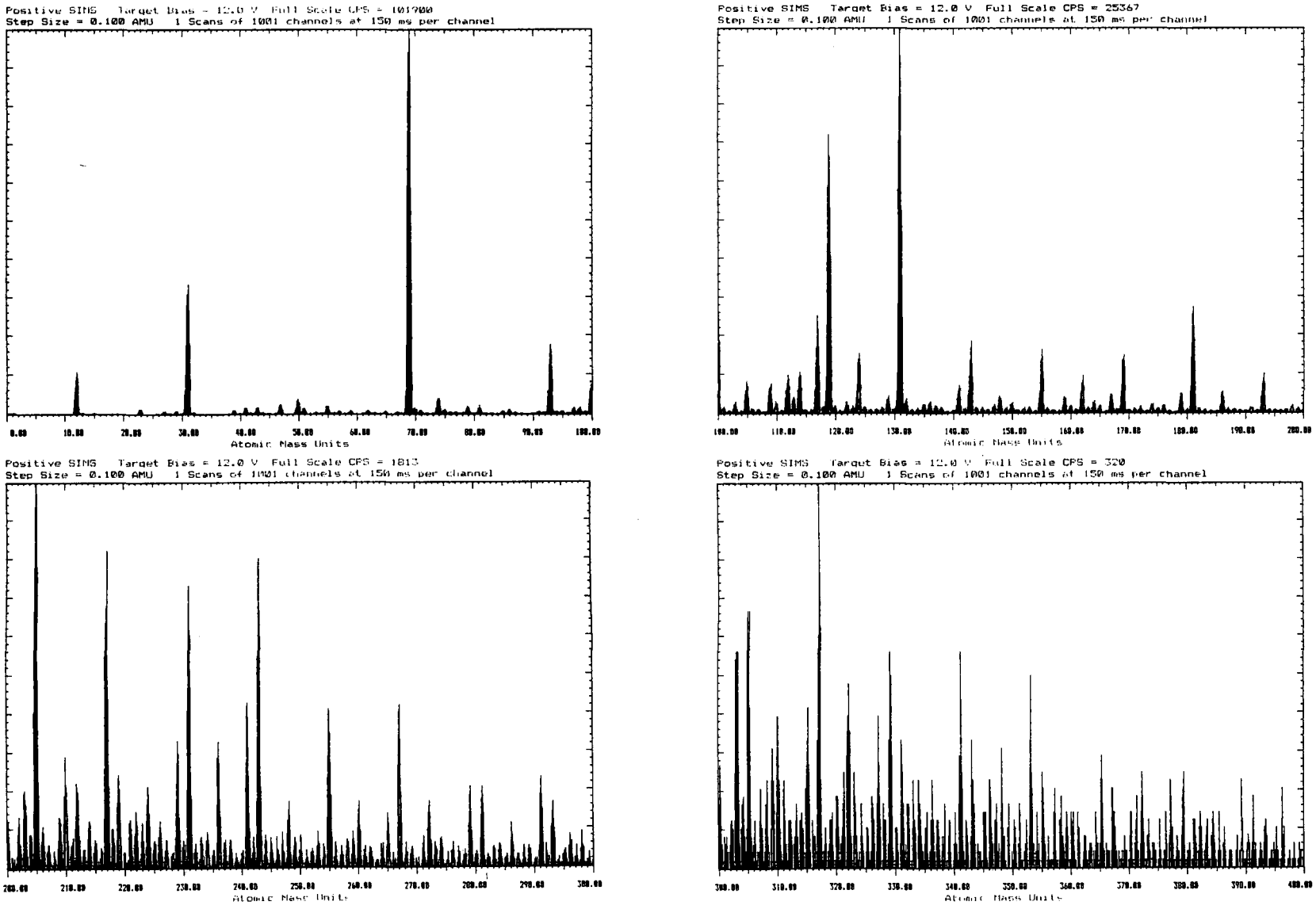

Figure 4.6a. Positive SIMS of Plasma Fluorinated PEEK.

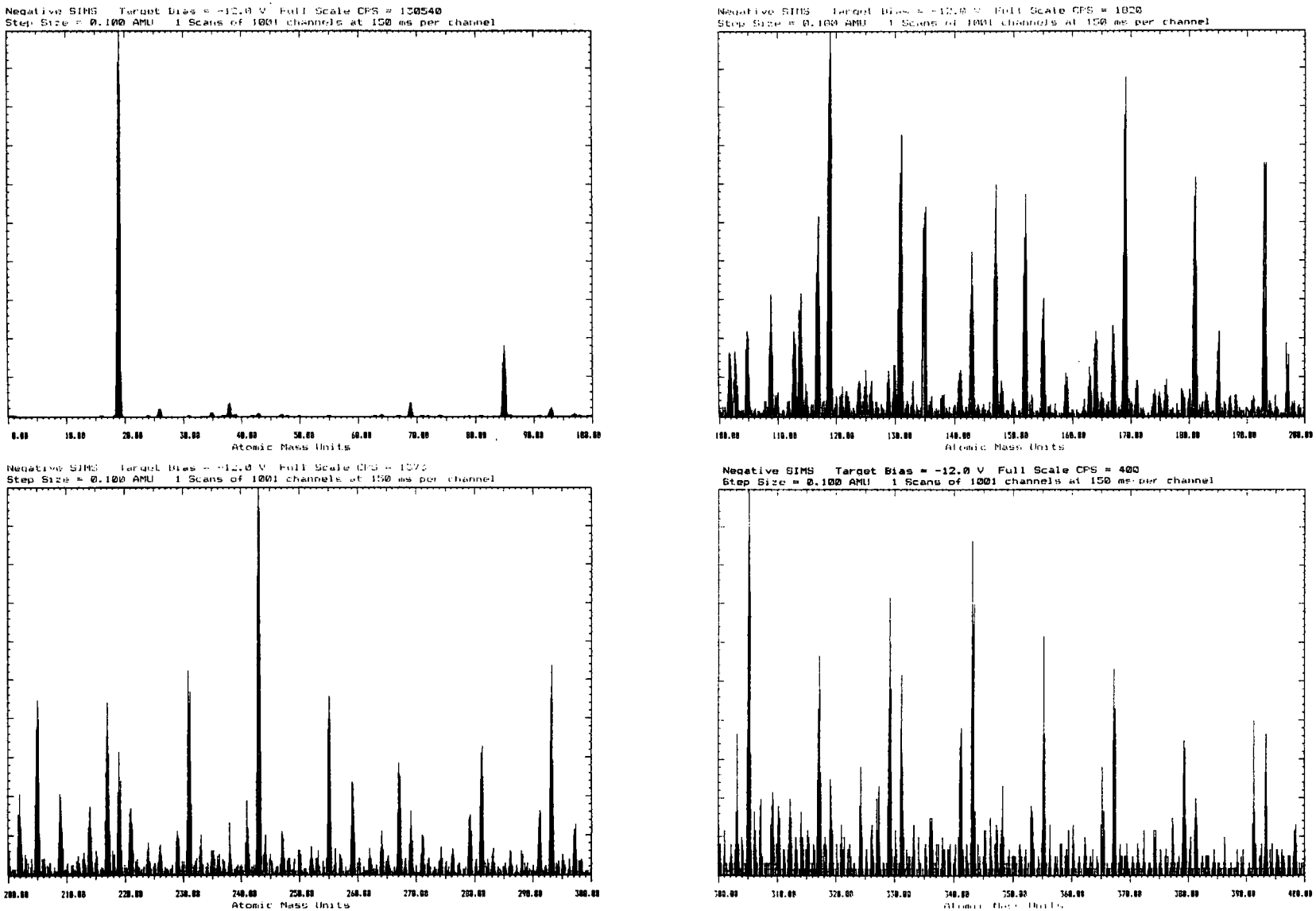

Figure 4.6b. Negative SIMS of Plasma Fluorinated PEEK.

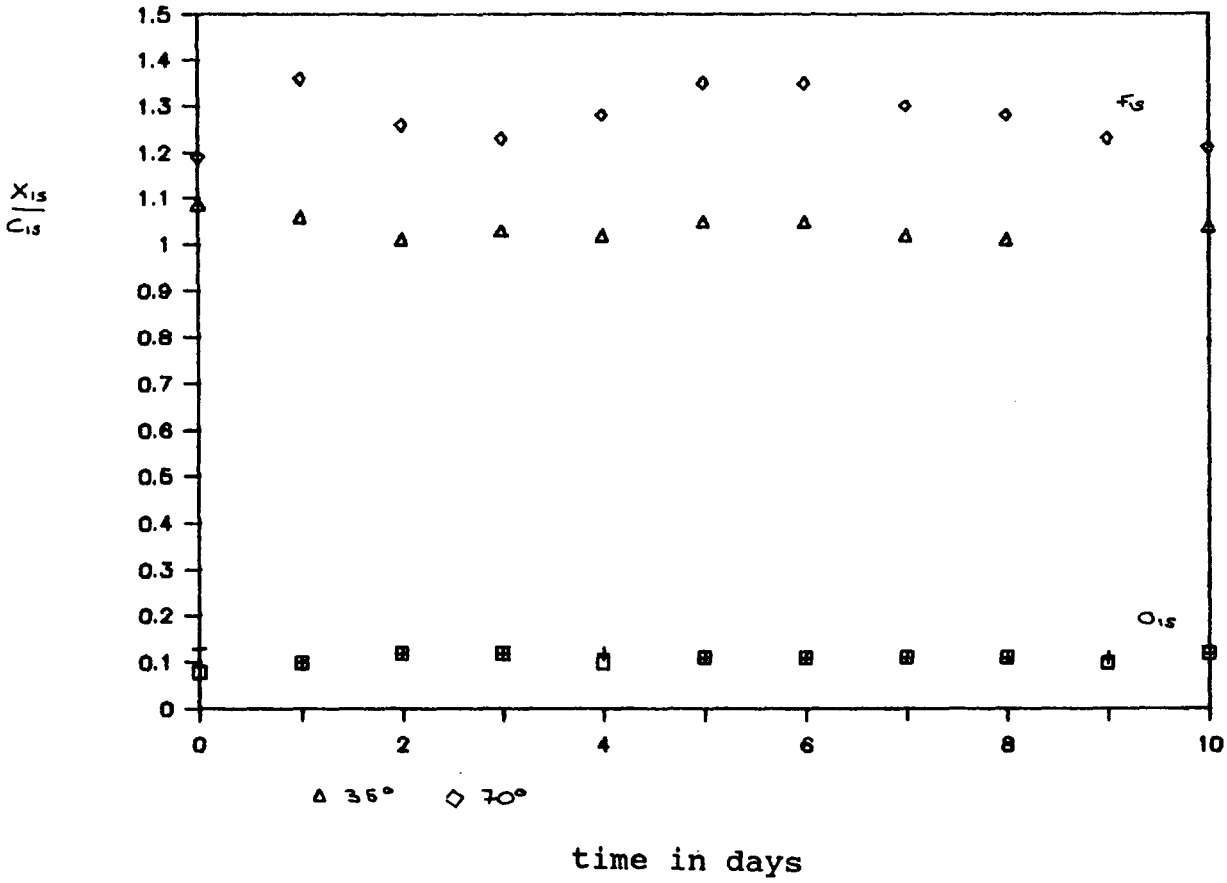

Figure 4.7 Changes in the Composition of Plasma Fluorinated PEEK Stored in Air.

Plasma fluorinated PEEK stored in air showed a small increase in oxidation of the outermost surface layers and a similar smaller decrease in oxidation of the general surface region, both staying at a constant value of eleven to twelve oxygens per hundred carbons. The fluorine concentration at the surface increased initially and then remained fairly steady appearing to fluctuate about a mean value, shown in Figure 4.7. This fluctuation is probably due to changes in humidity in the laboratory as variations from the mean value were not dependent on the time elapsed since treatment, however, samples of different age showed similar deviations on the same date.

4.5 PLASMA MODIFICATION OF PEEK USING AMMONIA PLASMA.

PEEK was treated with an ammonia plasma using the same treatment conditions as used with the tetrafluoromethane plasma modification. XPS measurements show that after treatment nitrogen has been incorporated into the surface of the PEEK without substantial oxidation, see Figure 4.7. The SIMS spectra show that the surface has been disrupted by the plasma treatment, with a much narrower range of mass fragments being produced than was observed with the tetrafluoromethane treatment and very few fragments observed with mass greater than 100 a.m.u., as illustrated in Figure 4.8.

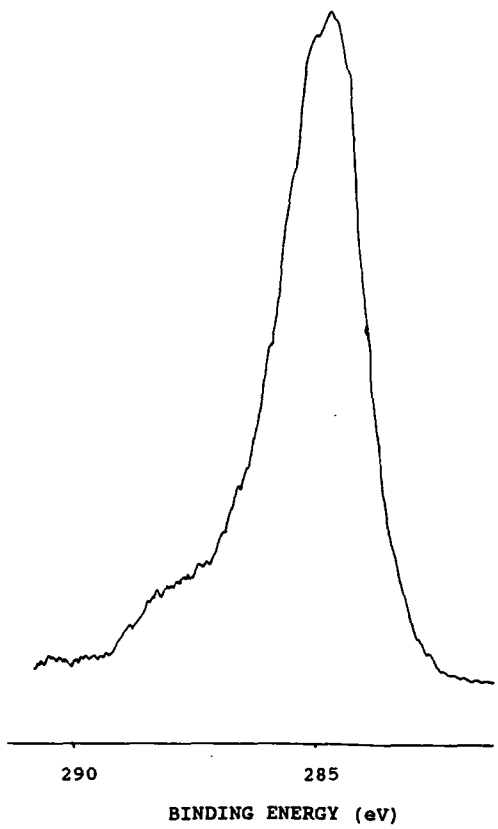

Figure 4.7 XPS Spectra of NH_3 Plasma Modified PEEK.

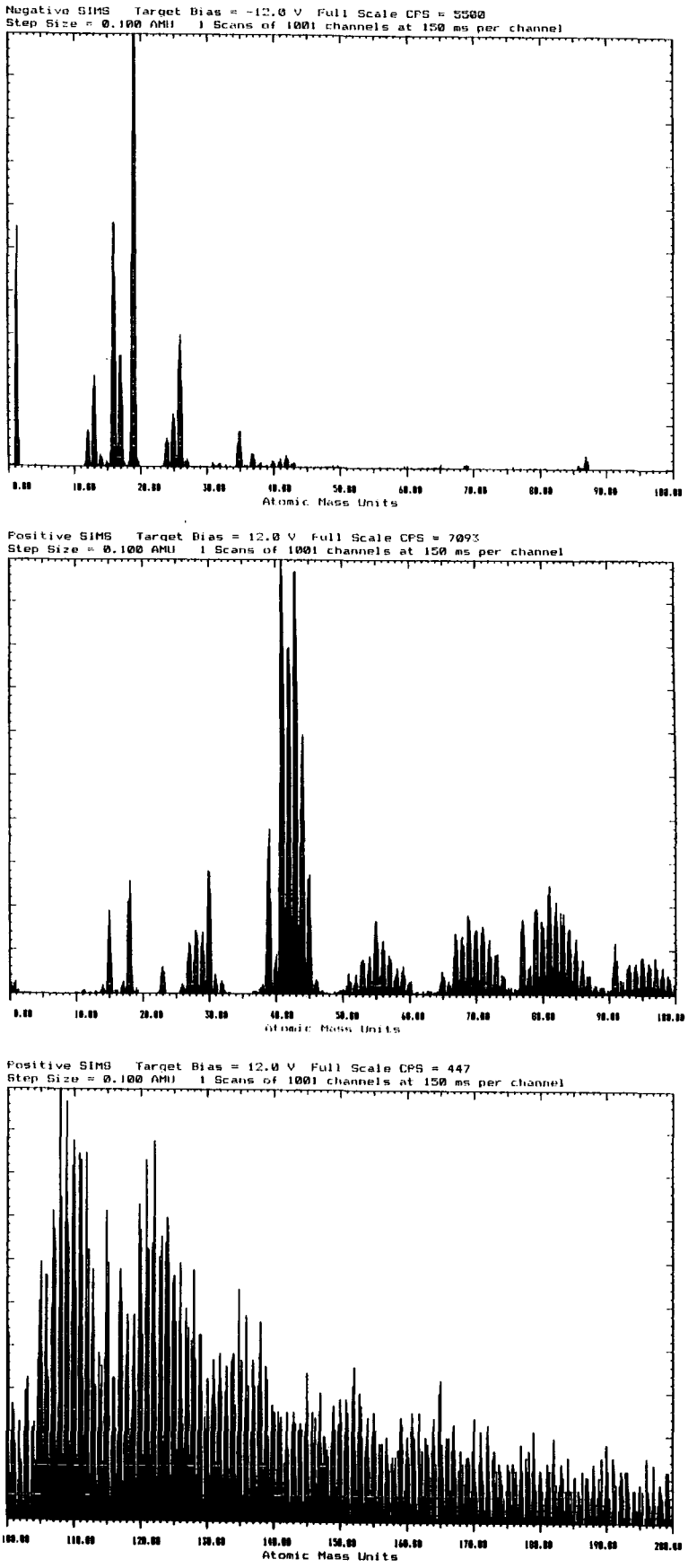

Figure 4.8 SIMS of NH_3 Plasma Modified PEEK.

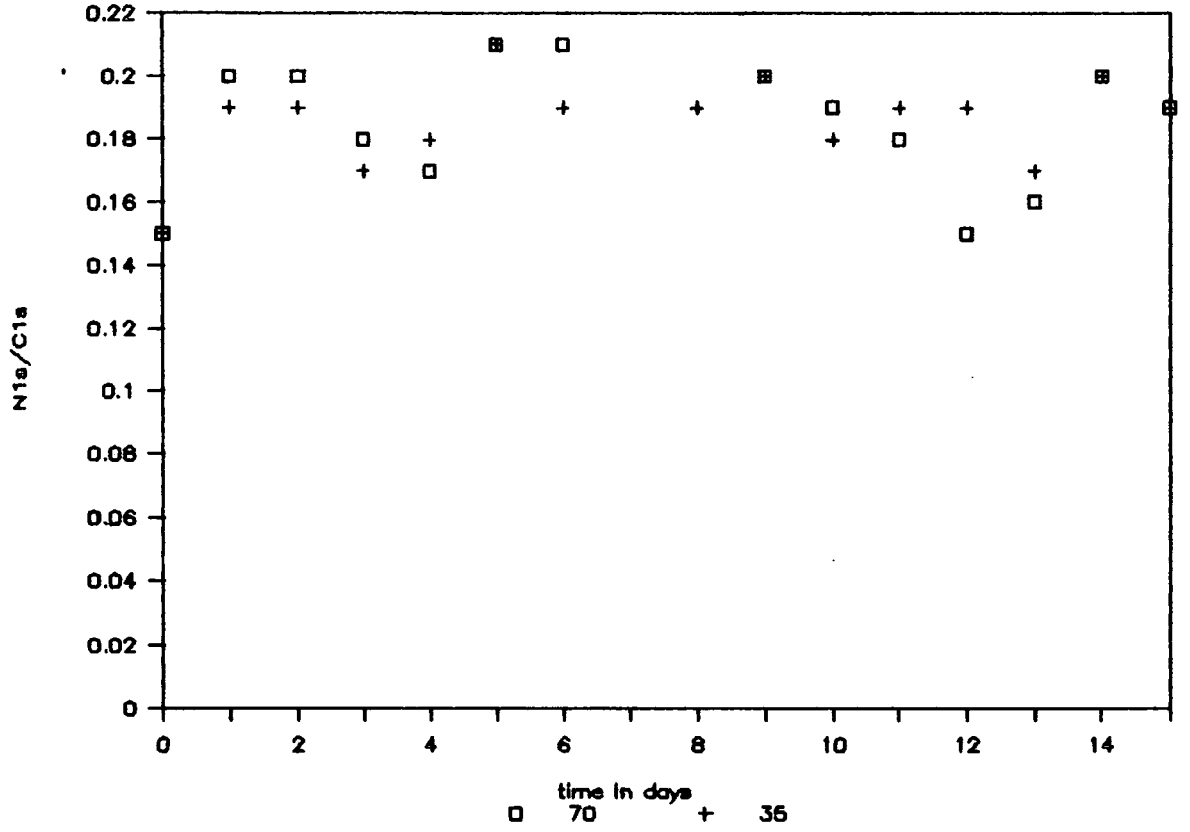

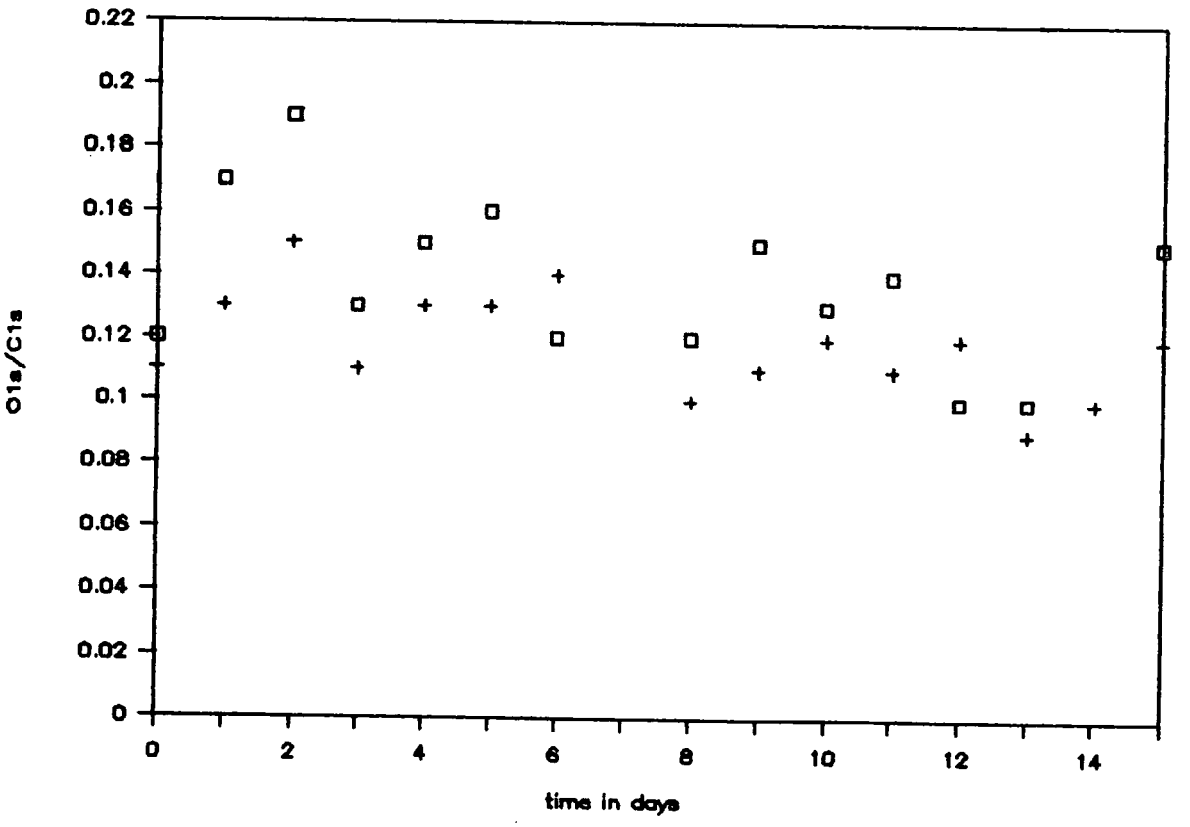

Figure 4.9 Effect of Storage on Atomic Ratios of NH_3 Plasma Modified PEEK.

After treatment the modified films were stored in air and their XPS spectra were monitored, Figure 4.9 shows the changes observed in the O_{1s} and N_{1s} atomic ratios, the reason for the large degree of scatter on the results is unclear, however, it was not thought to be due changes in humidity in the laboratory. The O_{1s} spectra reveal an increase in oxidation occurring in the first day, subsequently there was no perceptible change in the amount of oxidation at the surface. No reproducible changes were seen in the N_{1s} spectra, however, it is possible that changes do occur in this system, either within the limits of experimental error or at times longer than the duration of this experiment.

4.6 DISCUSSION

The transient increase in hydrophilicity was observed in the plasma oxidised PET, and a similar transient increase in hydrophobicity also occurred with the plasma fluorinated PEEK. These observations encourage the belief that the transient change in the ageing characteristics of plasma modified polymers is a fairly general phenomenon, which probably occurs in any plasma modified polymer system where the polymer surface is or becomes sufficiently mobile. It is also probable that the interfacial tension between the sample surface and storage medium needs to be larger than a certain critical level. The fact that no change was seen for the ammonia plasma treated samples shows that the ammonia plasma does not disrupt the surface to such a large extent as the oxygen and fluorine plasmas. Also the surface

polarity is not sufficiently altered to promote the typical decay of surface modification with time. However, it must be stressed that failure to observe the phenomenon does not prove that it does not occur. Plasma fluorinated PEEK stored in air also apparently does not undergo a transient increase in hydrophobicity unlike similarly treated PEEK stored in water. In this case the difference in interfacial tension is the predominant cause of the different ageing characteristics.

All the non oxygen treated systems showed an increase in oxidation at the surface after initial treatment, this can be explained by the interaction between reactive sites formed during the plasma modification process and the storage media, similar to the classical auto-oxidative degradation process discussed in the previous chapter. No apparent increase in oxidation was seen for the oxygen plasma treated samples, however, any effect would be masked by the decrease in oxidation levels at the surface caused by the ageing process.

REFERENCES

1. H.S. Munro and D.I. McBriar, J. Coatings Technology, 60(766), p41, 1988.
2. D.F. Lawson, Rubber Chemistry and Technology, 60, p102, 1986.
3. D.T. Clark and D. Shuttleworth, J. Polymer Sci., Polymer Chem Ed., 16, p1093, 1979.
4. B.W. Cherry, "Polymer Surfaces," Cambridge University Press, Cambridge, 1981.
5. T. Yasuda, K. Yoshida, T. Okuno, and H. Yasuda, J. Polym. Sci.: B Polym. Phys, 26, p1781, 1988.
6. T. Yasuda, K. Yoshida, T. Okuno and H. Yasuda, J. Polym. Sci.: B Polym. Phys., 26, p2061, 1988.
7. P. Montazer Rahmati, F.Arefi, J. Amouroux and A. Ricard, in proceedings of 9th International Symposium on Plasma Chemistry, vol.2, p1195, 1989.

CHAPTER 5

PLASMA MODIFICATION OF CARBON FIBRES

5.1 INTRODUCTION

5.1.1 COMPOSITES[1,2]

Modern materials are frequently required to meet many different and often conflicting needs; for example, stiffness and load bearing capacity may be required but weight limitations implicit in the intended use, may demand low density. In applications such as aeronautical, automotive and leisure equipment these requirements are sometimes met using high performance plastics or composite materials. Composites are commonly constructed using fibres such as glass, carbon or aramids embedded in a polymeric or ceramic matrix.

The properties of the fibre-matrix interface, or interfacial region, play an important role in determining the mechanical properties of the final composite[3]. The toughness that composites characteristically exhibit is dependent to a great extent on the many fibre matrix interfaces which exist and their ability to inhibit crack propagation perpendicular to the fibre. A strongly bound interfacial region will give a rigid material with high strength but low impact toughness conversely a weak fibre-matrix bond will be tough but unable to support loads in shear or compression. Often the fibres to be used in the formation of composites do not bond readily to the matrix material and surface modification is used to improve the properties of the end product.

5.1.2 CARBON FIBRES[4]

Carbon fibres for composite manufacture are usually made from polyacrylonitrile (PAN)[5]. The polarity of the nitrile groups in the PAN produces relatively strong intermolecular forces

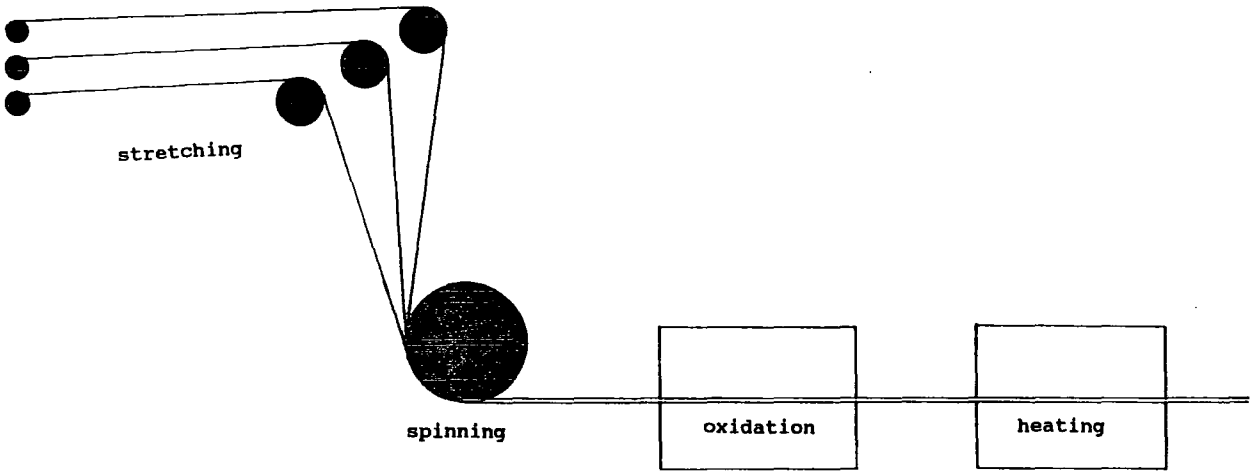

FIGURE 5.1 Manufacture of Carbon Fibres.

but the as made fibres are essentially amorphous. However, during the production process, illustrated schematically in Figure 5.1, the PAN fibre is stretched many times its original length, resulting in a fibre with a highly oriented structure. The PAN fibres are spun into tows of several thousand filaments, these tows are oxidised under tension at about 220^{o}C, and subsequently heated in an inert atmosphere at higher temperature when "graphitization" with loss of hydrogen, nitrogen and oxygen occurs. The structure of carbon fibres has been shown to consist of graphitic layers, forming crystallites several nanometres

across, with preferred orientation along the fibre axis. Across the fibre the crystallites are arranged randomly giving the fibre an overall structure resembling a Flake chocolate log as shown in Figure 5.2.

To obtain efficient bonding between carbon fibres and the matrix it is essential that the fibres are completely wetted by

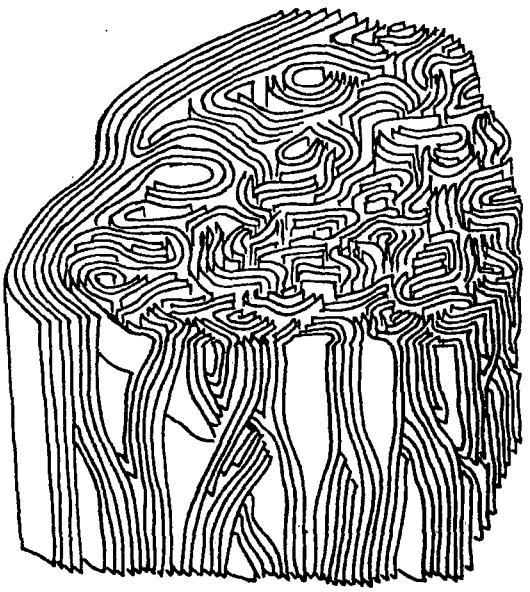

Figure 5.2 Schematic Representation of a Typical Carbon Fibre Structure.[4]

the matrix resin. If this occurs, intermolecular forces can result in strong fibre-matrix adhesion; by contrast, if wetting is incomplete adhesion will be poor, even for strong interaction between the material and the fibres. Untreated carbon fibres are not readily wetted by matrix resins, for an adequate interface between the materials it is generally necessary to treat the surface of the fibres. There are two types of treatment that can

be applied to the fibres, chemical modification and physical roughening. The latter can work in two ways, an interface is formed, into which the matrix medium may mechanically key, also the surface will have a greater area and hence an improved adhesion. Chemical modification increases the surface energy of the fibres and hence their wettability by polar matrices. The various moieties introduced at the surface may also allow chemical bonds to be formed between matrix and fibre. Most proprietary treatments involve oxidation, several different methods of treatment are used, anodisation, acid etching and high temperature oxidation are amongst the most common.

5.1.3 COMPOSITE TESTING[2,6]

The range of properties of composite materials that can be, and often are, tested is enormous: they encompass mechanical, thermal, chemical, electrical and optical properties. The greatest emphasis is usually placed on mechanical properties, and tensile, compressive, impact and sheer strength, and surface hardness are frequently reported.

When choosing a testing method it must be remembered that strength is normally gained at the expense of toughness. The nature of the composite, for example its anisotropy and expected mode of failure, and its final application must be considered when choosing which test to apply.

Many techniques have been developed for the mechanical testing of fibre reinforced composites, they typically suffer

from problems of irreproducibility with errors in the range of ±10%. The errors are thought to arise from the problems of forming flaw free, spatially homogeneous composites; any resin rich area will allow cracks to propagate readily, other imperfections can act as centres of high stress at which fracturing can occur. Results of different tests for similar properties are not well correlated and thus cannot be used for direct comparison. In this work the transverse tensile strength was measured using the disc compression test, described in section 5.2.5, and the numbers obtained were used to compare one sample with another.

5.1.4 XPS STUDIES OF CARBON FIBRES

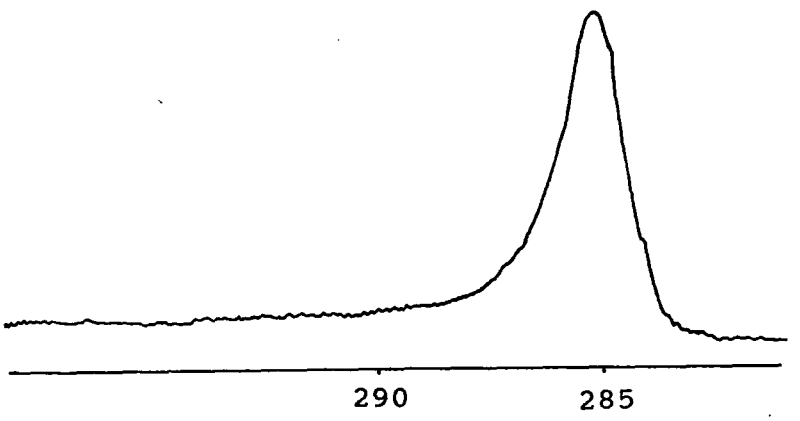

FIGURE 5.3 XPS Spectrum of Untreated Carbon Fibres.

The XPS spectra of carbon fibres are complicated by the shape of the C1s peak[7] (see Figure 5.3). This exhibits an asymmetric tailing to high binding energy, a phenomenon similar to the tailing seen in the spectra of simple metals and is due to shake up processes. To the valence electrons associated with an atom the loss of a core electron by photo-emission appears to increase the nuclear charge. This major perturbation gives rise to substantial reorganisation of the valence electrons, which may involve excitation of one of the electrons to a higher, unfilled energy level. This "shake up" uses energy which is not then available to the primary photoelectron and thus the two electron process leads to discrete structure on the low energy side of the main peak. In solid metal there exists a distribution of unfilled one electron levels above the Fermi energy level which are available for shake up type processes following core electron emission. In this case, instead of discrete satellites to low kinetic energy side of the peak, the main peak is accompanied by a tailing. The greater the density of states at the Fermi level the more significant this tailing becomes[8].

The asymmetry of the C1s envelope leads to difficulty in peak fitting the spectra obtained from carbon fibres. There are several methods which have been reported to overcome this.[9] Firstly a non-linear background subtraction can be performed, this method does not take account of the area of the C1s envelope under the tail function and leads to erroneously high oxygen to carbon ratios. An alternative method is that of difference spectra,[10] the spectrum of the untreated fibre is subtracted from

the spectrum of the treated fibre so that the degree of oxidation can be determined.

In the difference method it is essential to have a good signal to noise ratio otherwise the difference spectra are too distorted by noise to interpret, it is also important to have spectra of the same widths at half height otherwise incomplete or excessive subtraction will occur. Another difficulty with this method is that it is extremely likely that upon oxidation the

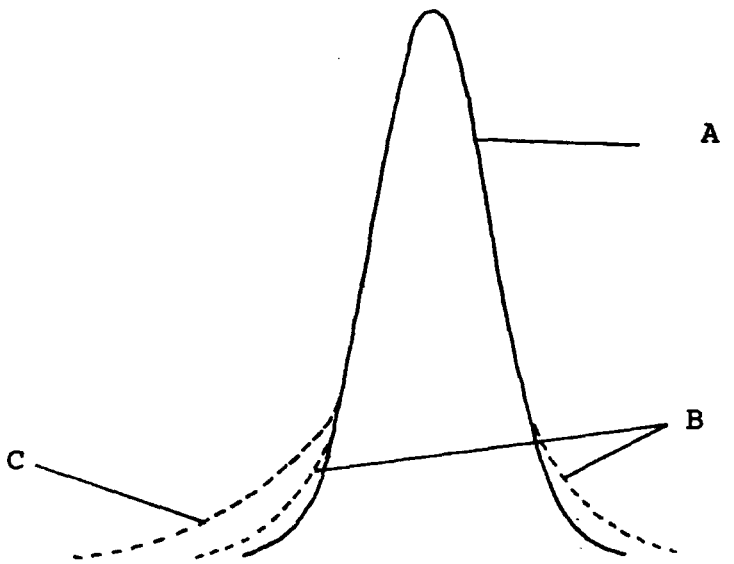

Figure 5.4 A) Gaussian B) Gaussian/Lorentzian C) Gaussian with Tail Peak Fitting Curves.

degree of tailing will decrease as the conductivity of the surface decreases, if this does occur excessive subtraction leads to an apparently reduced degree of oxidation.

Sherwood et al.[7,8] have attempted peak fitting of carbon fibre spectra using a tailing function which was developed for the curve fitting of simple metal systems. The curve generating function frequently used to fit XPS spectra creates a Gaussian curve (see Figure 5.4), and is governed by the relatively simple expression:

$$F(x)=H\exp-[(\ln 16)(x-x_0)^2/W^2] \qquad 5.1$$

where;

H is the maximum peak height,

x_0 is the peak centre,

W is the full width at half height.

Another commonly used expression is the more accurate mixed Gaussian/Lorentzian function (see Figure 5.4) which is somewhat more complex:

$$F(x)=H[1+4M(x-x_0)^2/W^2]^{-1}\exp-\{(1-M)[(\ln 16)(x-x_0)^2]/W^2\} \qquad 5.2$$

where,

M is the mixing ratio (0 for a pure Gaussian peak).

When the tailing function is introduced the equations become fairly complicated e.g. for the Gaussian only (Figure 5.4):

$$F(x)=H\{\exp-[(\ln 16)(x-x_0)^2/W^2]+[1+\exp-[(\ln 16)(x-x_0)^2/W^2]](1-T)\exp-[(x-x_0)E]\} \quad 5.3$$

where;

T is the tail mixing ratio,

E is the exponential tail ratio.

An inherent fault in the use of the tailing function is that it is not known by how much surface treatment effects the tailing ratios. Sherwood's calculations[10] for oxidised functionalities on hypothetical fragments of graphitic surfaces suggest that the chemical shifts on carbon fibres are significantly different to those obtained for polymers by Clark et al.[11,12] These results imply that any attempt at peak fitting the XPS spectra of carbon fibres may be somewhat arbitrary.

In this work it was decided that atomic ratios and surface labelling might prove to be more useful methods for determining the extent of carbon fibre surface modification, as these techniques are more direct and do not suffer from the complications outlined above.

Surface labelling is a useful technique to determine which functionalities are present after plasma treatment. It is preferable to perform gas phase labelling to solution phase

labelling because the solvent medium may dissolve the surface modification, or cause reorientation of surface groups. It is known[13] that trifluoroacetic anhydride (TFAA) is a good labelling reagent for hydroxyl groups, amides and primary and secondary amines. Similarly, trimethylsilylimidazole (TMSI) is known to be a labelling agent[9] for carboxylic acid groups. It has also been suggested[14] that nitric oxide is a suitable labelling agent for alcohol and hydroperoxide groups.

5.2 EXPERIMENTAL

5.2.1 MATERIALS

Carbon fibres were supplied by ICI plc, Material Research Centre, Wilton. Those used for plasma modification were untreated unsized hysol-grafil x/a-s, those used for comparison similar fibres with a standard commercial treatment known as 100% treatment and a similar treatment in excess known as 400% treatment. Carbon foils of 99.8% purity were obtained from Goodfellow, and used without subsequent purification. Oriented graphite for X-ray and neutron analysis was obtained from Union Carbide, fresh surfaces were prepared by cleaving the sample prior to modification or analysis.

5.2.2 PLASMA MODIFICATION

Plasma modifications were carried out in two tubular Pyrex reactors, illustrated in Figures 5.5 and 5.6, connected to grease

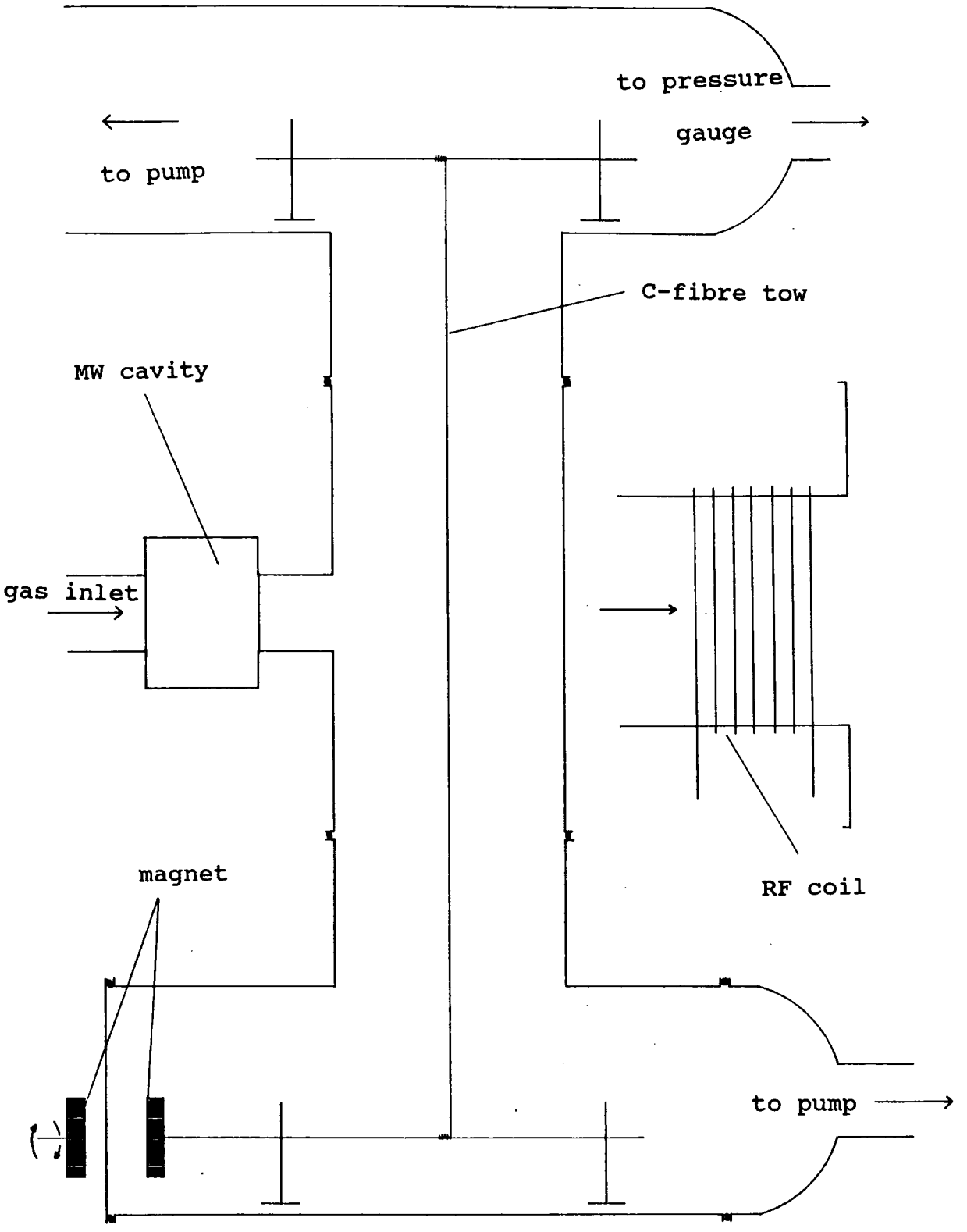

Figure 5.5 Semi-continuous Plasma Modification Rig.

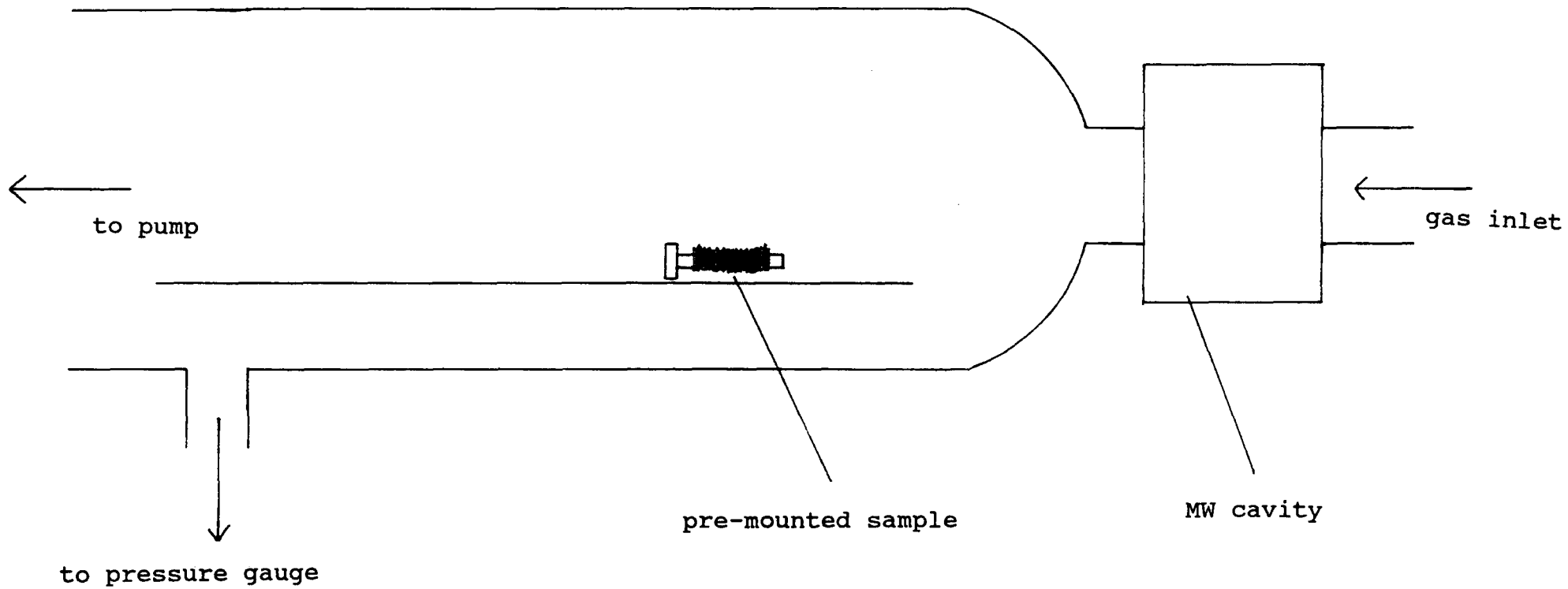

Figure 5.6 Batch Plasma Modification Rig.

and mercury free vacuum lines. Flanged joints and the cold trap were sealed with Viton O rings whilst all other connections were made via Cajon Ultra Torr couplings. Vacuum taps were sealed with PTFE stoppers. The apparatus was pumped down to a base pressure of about $3x10^{-2}$ torr using Edwards ED2M2 mechanical rotary pumps. Pressure measurements were made using a Pirani thermocouple gauge.

The semi-continuous rig was used to modify up to 4 metres of carbon fibre tow in one batch for the purpose of composite manufacture. The batch reactor was used for modification of graphite foils and premounted samples.

At the start of each experiment the leak rate of the vacuum line was tested by isolating the pump from the line and measuring the rise in pressure over a period of time. When the leak rate was sufficiently low (0.05 cm^3min^{-1} or less), reactant gas or vapour was let into the reactor through an Edwards needle valve to the desired pressure. All plasma modification experiments were carried out with a flow of gas or vapour through the apparatus.

Previous work[15] indicated that more extensive fibre treatment was obtained using a microwave power source rather than a radiofrequency generator. Most of the fibres were treated using a plasma generated in an EMS Microtron 200 microwave cavity operated at a frequency of 2450 MHz.

Treatments with allyl alcohol were performed using a radiofrequency (RF) power source in the adapted semi continuous

rig (Figure 5.5b). The RF power supplied by a 13.56 MHz RF generator was inductively coupled to the reactor through an externally wound copper coil via an inductance-capacitance matching network. A DIAWA SW110A meter was used to measure the RF power and standing wave ratio defined as the ratio of total power generated to power going into the plasma.

Allyl alcohol with 99+% purity was supplied by Aldrich and oxygen by BOC. Allyl alcohol and distilled water were degassed using alternate freeze thaw cycles before use.

5.2.3 XPS ANALYSIS

Core level spectra for C_{1s} and O_{1s} regions were recorded on an Kratos ES200 electron spectrometer using $Mg_{Ka}1,2$ x-rays and an operating pressure of 10^{-7}Torr. Electron take-off angles of 70° and 35° were used to investigate the vertical homogeneity of the sample.

All samples were labelled in the plasma rigs at the saturated vapour pressure of the labelling agent for thirty minutes unless otherwise stated. Tri-fluoroacetic anhydride (TFAA) was the surface labelling agent used predominantly in this work. Tri-methylsilylimidizole (TMSI) was found to be very sensitive to any traces of water, because of the difficulty in completely removing all of the water adsorbed onto the fibres after a water plasma treatment this method was found to be too slow and unreliable.

The use of nitric oxide as a labelling agent was tested to determine its usefulness in this work. Model films of polyacrylic acid (PAC) and polyvinyl alcohol (PVA) were cast from a 10% solution in water. The films were exposed to one atmosphere

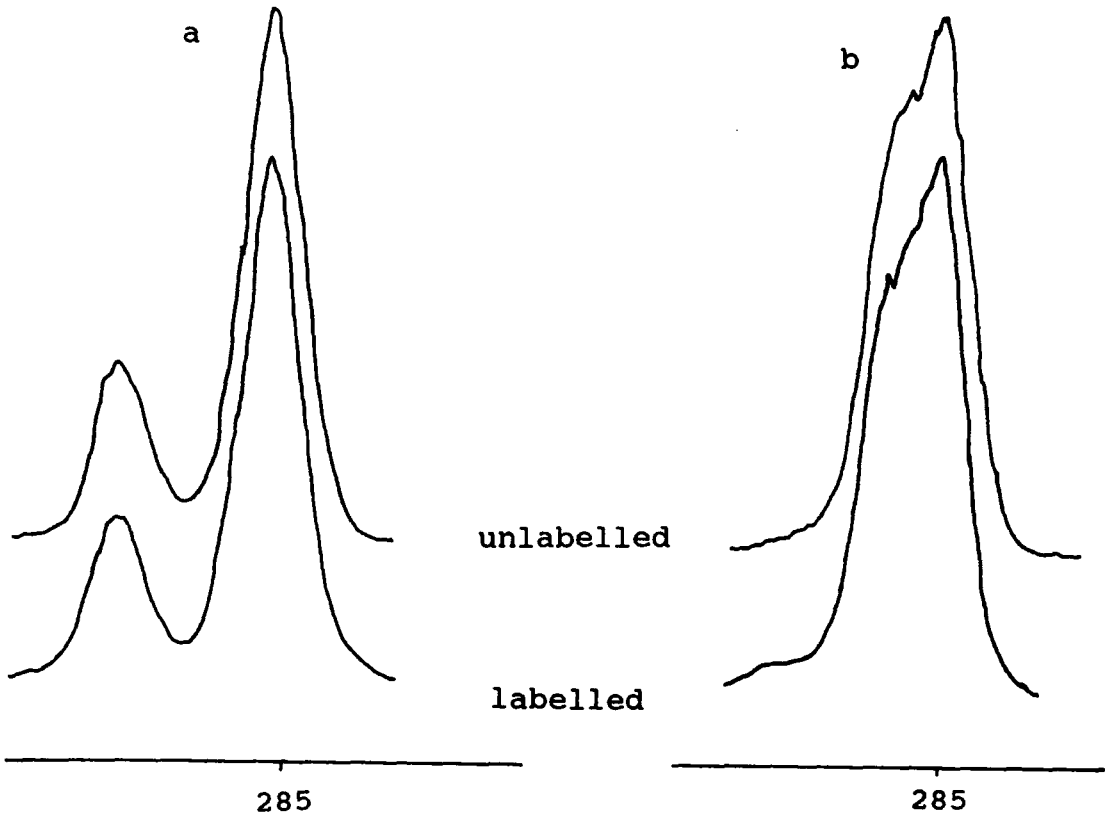

Figure 5.7 XPS Spectra of Unlabelled and NO Labelled a) PAC b) PVA

of nitric oxide for 12hrs. The XPS spectra were run before and after treatment (see Figure 5.7), and no appreciable labelling was observed. The claims which were made for nitric oxide as a labelling agent for alcohol and hydroperoxide[14] groups were based

on oxidation of various polyethenes using gamma-irradiation. It is thought that the irradiation of the polymers introduces free radicals which could react with the nitric oxide, this may account for the apparent discrepancy between the authors experience and that of earlier workers.

5.2.4 CONTACT ANGLE MEASUREMENTS

Contact angle measurements were performed on graphite using the sessile drop technique using 1 microlitre drops of distilled water or di-iodomethane. Averages of at least three measurements were taken, these averages were found to be consistent within ±2°. The surface energy was calculated according to the method described in Chapter One.

Contact angles on single fibres were measured against water and di-iodomethane using the Wilhelmy plate technique described in Chapter One with a Cahn dynamic contact angle analyser. Using water as the wetting medium each sample was cycled (lowered and raised within the liquid) up to 5 times, a trace was obtained of force versus stage height. Di-iodomethane was strongly adsorbed onto the tape used to fix the fibre to the balance, leading to an apparent increase in the weight of the fibre. However, the use of "Super-Glue" to fix the fibres to the balance alleviated the problem to a some extent. Only one measurement cycle was used with di-iodomethane as there was still an apparent decrease of contact angle with cycling. The errors obtained in this technique were large (±5°) but are thought to arise mainly from

the real fibre to fibre variations rather than from random errors generated in the technique.

5.2.5 COMPOSITE MANUFACTURE AND TESTING

The matrix medium was formed from a commercial epoxy novalac resin, D.E.N. 431 (see Figure 5.8) and hardened with methylene dianiline (MDA) used in proportion 2:0.7 resin to hardener.

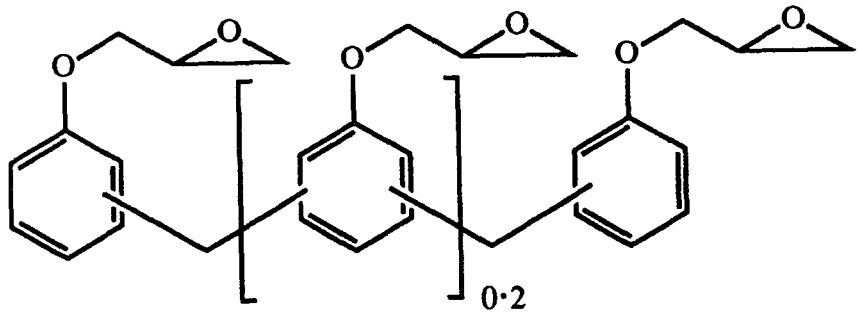

Figure 5.8. D.E.N. 431

The cure procedure was that recommended by the suppliers (Dow Corning); 16hrs at 55°C followed by 2hrs at 125°C and then another 2hrs at 175°C.

A carbon fibre tow was wound round two glass rods, approximately 10cm apart. Twenty lengths of fibre were used, these were attached, at the centre, to some nylon fishing line, so that the final bundle consisted of 40 lengths of ca. 6cm lengths as shown in Figure 5.9. The bundles were soaked in resin,

then drawn into the moulds and cured as described previously. The resin was formed by heating both chemicals separately to 90°C, and mixing them together over a 55°C water bath, this temperature was maintained whilst the fibres were immersed.

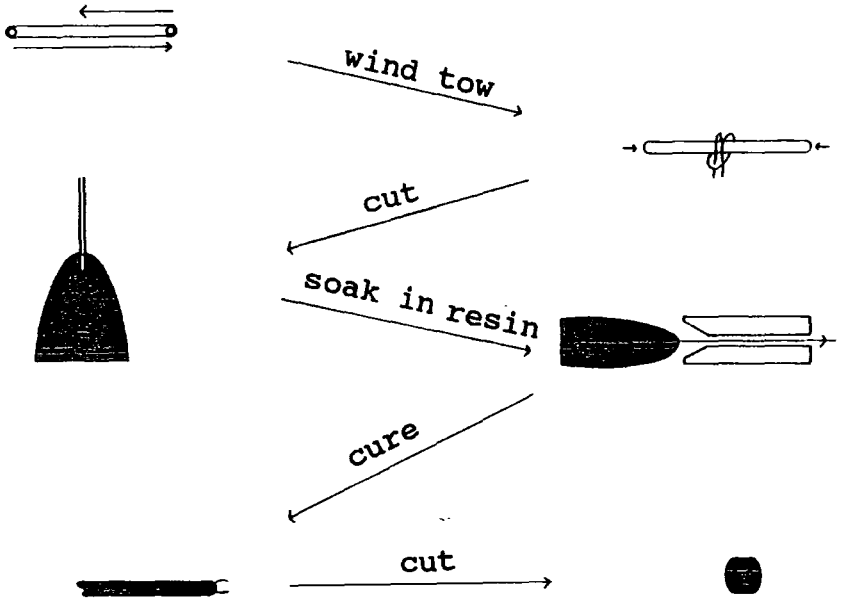

Figure 5.9. Preparation of Composite Discs.

In previous work[15] the composites were formed in glass moulds, however, the resin adhered exceptionally well to the glass, making it difficult to draw the fibres into the moulds, and impossible to remove the composite after curing. In this work it was decided to use teflon moulds, which do not suffer these disadvantages and are also reusable. The composites were removed from the moulds after the 55°C cure stage, the remainder of the remainder of the cure cycle being carried out with

unconstrained samples. A disadvantage of this method is that the composite rods could expand freely after removal from the moulds also, it was occasionally noted that the rods formed did not have a perfectly circular cross section probably due to sagging during the mould free cure cycle. After curing the rods were cut into disks and tested by Dr. T. Parry from the School of Engineering and Applied Science at the University of Durham, using an Instron Tensile Tester.

The test chosen was a diametric compression test,[16,17] disks of composite (6mm diameter by 2.5mm thickness) were formed and placed between two plates as depicted in Figure 5.10, the top plate was capable of increasing the load applied to the composite. In this test protocol failure occurs in the central region of the sample and propagates outwards and thus giving a better indication of the strength of the interfacial region than a test which initiates failure at the surface. The transverse tensile strength is given by:

$$r_t = \frac{2P}{\pi dt} \qquad 5.5$$

where,

r_t is the transverse tensile strength,

P is the force to induce failure,

d is the diameter,

t is the thickness.

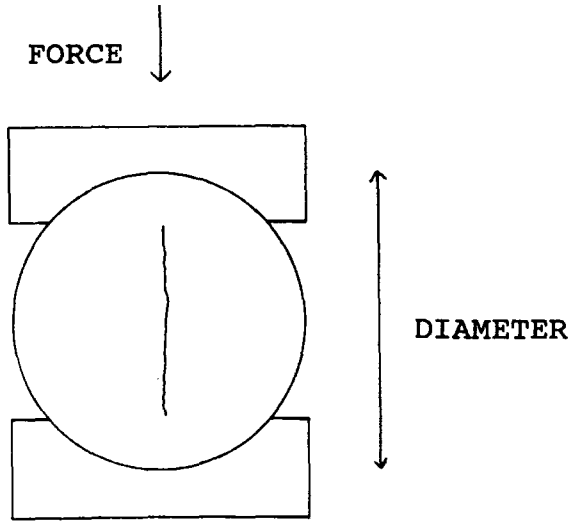

Figure 5.10 Schematic Representation of the Disc Compression Test

There are certain draw backs to this method of testing, the state of stress where the failure is initiated is complex and the correlation between values measured by this and other tensile tests is generally poor. However, when used as a simple comparative test, these reservations are relatively unimportant. Stress concentrating effects at the loading and contact points can cause premature failure initiation sites due to high local shear stresses, concave loading anvils were found to alleviate this problem.[15]

5.3 PLASMA MODIFICATION OF CARBON FIBRES

5.3.1 INTRODUCTION

It was thought that plasma modification of the carbon fibres would produce high surface energy fibres, with many reactive polar groups which could chemically interact with the resin. The treatments used were various oxygen and water microwave and radio

frequency plasmas. It was hoped to optimise these treatments with respect to composite performance, and to determine the importance of any differences in surface functionality that may exist after oxygen or water treatment.

When treating a tow of fibres with a microwave plasma the fibres are passed through the post glow region, however, when using a radio frequency plasma the tow passes through the glow region. It has been previously noted that increased oxidation was seen in the batch reactor when using RF plasmas rather than MW plasmas[15]. However, the power density of the MW plasma is much greater than the RF plasma due to the different dimensions of the microwave cavity (i.d.=2cm) compared to the RF coil (i.d.=5cm).

In a further attempt to determine how hydroxyl functionality may promote or inhibit adhesion, allyl alcohol plasma polymers were deposited on the carbon fibre surface, it is known that this polymer can be formed with a high density of hydroxyl groups at the surface.[18] It was envisaged that if this method of treatment was successful, the hydroxyl rich surface could then react with other species, e.g. acetic anhydride, to form other functionally specific surfaces.

5.3.2 RESULTS

5.3.2.1 MICROWAVE TREATMENT

Fibres for composite manufacture were treated in the semi-continuous reactor in 3m batches. Both water and oxygen plasma

modification were carried out under the same conditions: leak rates of ca. 0.05$cm^3min.^{-1}$ or less; flow rates of ca. 6$cm^3min.^{-1}$; gas pressure of 0.1mbar; microwave power of 40W; the time in plasma effluent was varied. The O1s:C1s atomic ratios obtained are shown in Table 5.1 and typical spectra are shown in Figure 5.11.

It was noted that although both methods of treatment show substantial increase in oxidation, there was no real correlation between time and extent of oxidation. This could be primarily due to the spatial heterogeneity of the plasma treatment, less

Table 5.1 Time Dependence of Microwave Treatment in the Semi-continuous Rig.

PLASMA	TREATMENT TIME (s)	$O_{1s}:C_{1s}$
WATER	60	0.14
	40	0.13
	25	0.16
OXYGEN	60	0.27
	40	0.30
	25	0.29

modification occurs in the centre regions of the tow, and the random nature of the uncovering of the less treated regions

before XPS analysis. Also as the treatment progresses fibres build up on the lower spindle, this causes the rate at which the fibres travel through the treatment area to increase. However, water modified fibres consistently showed less oxidation than oxygen modified fibres, as shown in Figure 5.11.

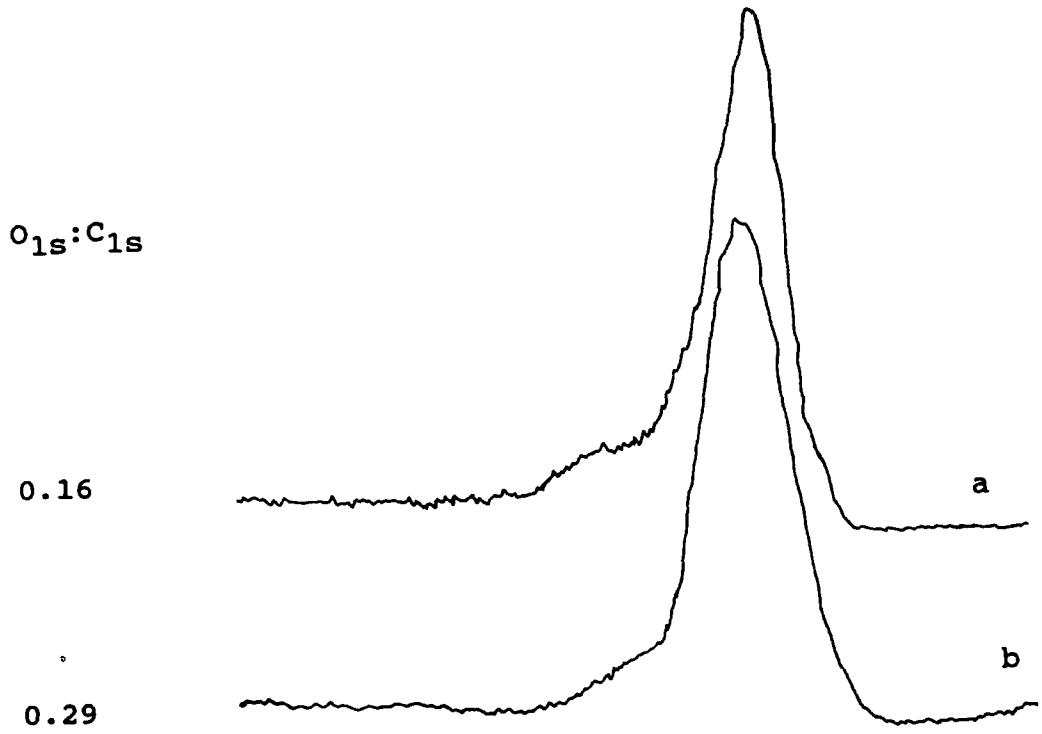

Figure 5.11 a) Water and b) Oxygen 25s Treated Carbon Fibres.

5.3.2.2 LABELLING

Fibres for labelling were treated in the batch reactor, which is known to give rise to a higher degree of oxidation. The fibres were premounted on a gold backed probe tip, before labelling they were treated with a 30W, 0.2mbar, 30s oxygen or water microwave plasma,leak rates of ca. 0.05 $cm^3min.^{-1}$ or less and flow rates of ca. $2cm^3min.^{-1}$. Samples to be labelled were exposed to a

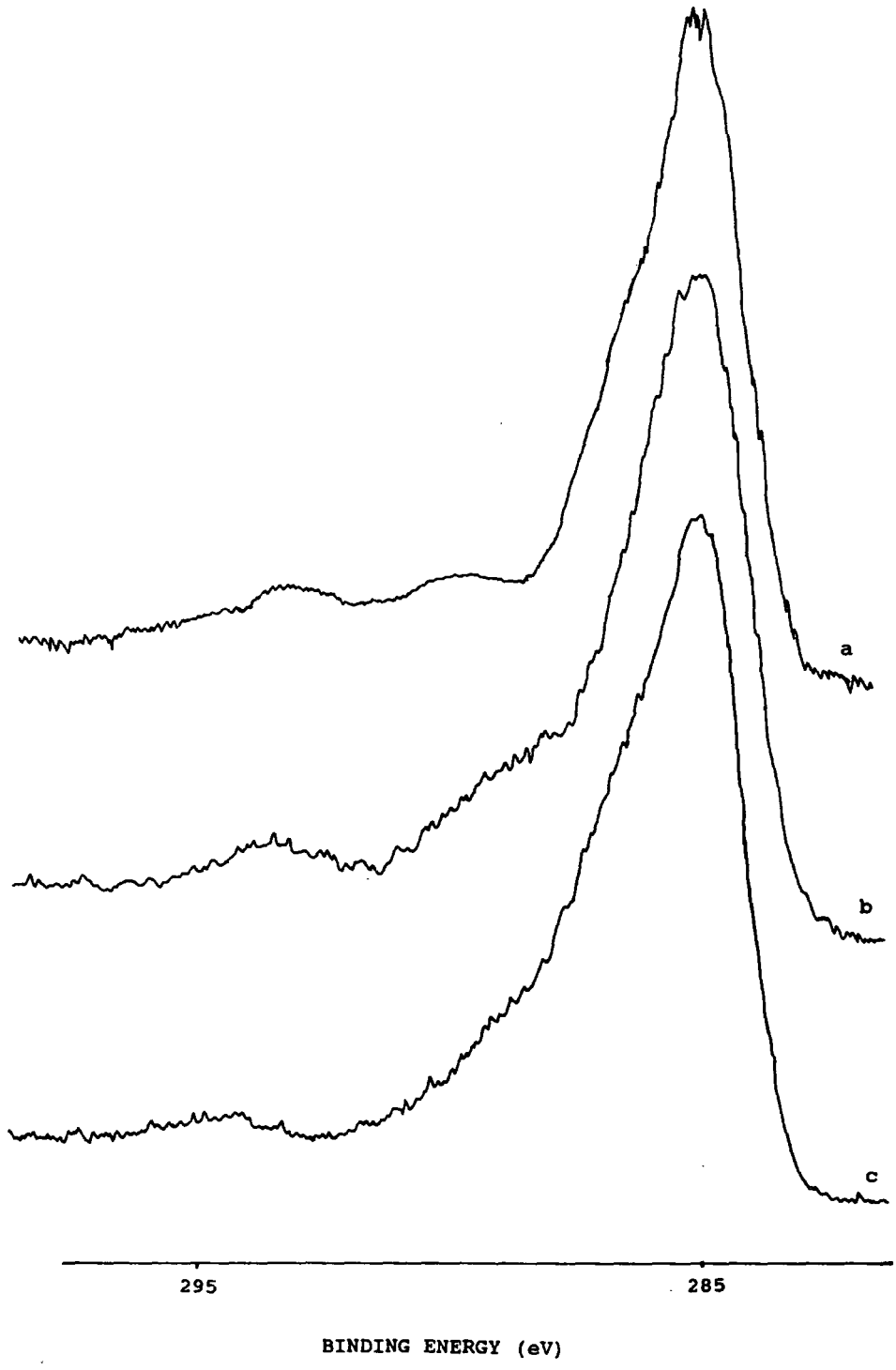

Figure 5.12 TFAA Labelled Fibres a) Untreated b) Water Treated and c) Oxygen Treated.

saturated vapour pressure of TFAA for 30 min. All spectra displayed a CF_3 peak at approximately 293eV as shown in Figure 5.12, atomic ratios obtained are shown in Table 5.2.

It can be seen that the untreated fibre has a high level of oxygen functionality with a relatively high proportion of hydroxyl groups; it must remembered, however, that TFAA will also label the surface contaminants, which will probably be removed during the surface treatment. The water treatment appears to cause less oxidation although more hydroxyl groups are present. For the oxygen treatment, however, the reverse is true with a significantly lower degree of hydroxylation at the surface.

Table 5.2. XPS Atomic Ratios of Labelled Carbon Fibres.

	ATOMIC RATIOS		[OH]/[O]
	O_{1s}/C_{1s}	F_{1s}/C_{1s}	
untreated	0.10	0.06	0.25
water treated	0.25	0.11	0.17
oxygen treated	0.27	0.08	0.11

5.3.2.3 RF PLASMA TREATMENT

Allyl alcohol plasma polymer deposition was attempted to produce a hydroxyl functionally specific surface. Depositing allyl alcohol using microwave plasmas failed to retain the

Table 5.3 Allyl Alcohol Deposition on Carbon Fibres and Aluminium

TREATMENT	ATOMIC RATIO		[OH]/[O]
	$O_{1s}:C_{1s}$	$F_{1s}:C_{1s}$	
WITHOUT LABELLING			
ALUMINIUM	0.27	----	
CARBON FIBRES	0.25	----	
WITH LABELLING			
ALUMINIUM	0.30	0.32	0.52
CARBON FIBRES	0.29	0.33	0.53

hydroxyl functionality. By contrast, low power high flow rate RF plasma treatments in a rig similar to that used for microwave treatments but having a wider bore side arm (see Figure 5.5) with deposition times of 2-5 min. succeeded in depositing allyl alcohol plasma polymer with a high degree of hydroxyl functionality on both aluminium foil and carbon fibres. These results were confirmed by labelling with TFAA (see Figure 5.13).

The fibres were also treated using 30W, 0.1mbar RF oxygen and water plasmas in the same rig used for the allyl alcohol deposition. There seemed to be no significant increase in the amount of oxidation that had occurred after 30s in the plasma, hence, it was decided to draw the tow slowly through the glow region to prevent snagging (about 2min.). The resultant fibres

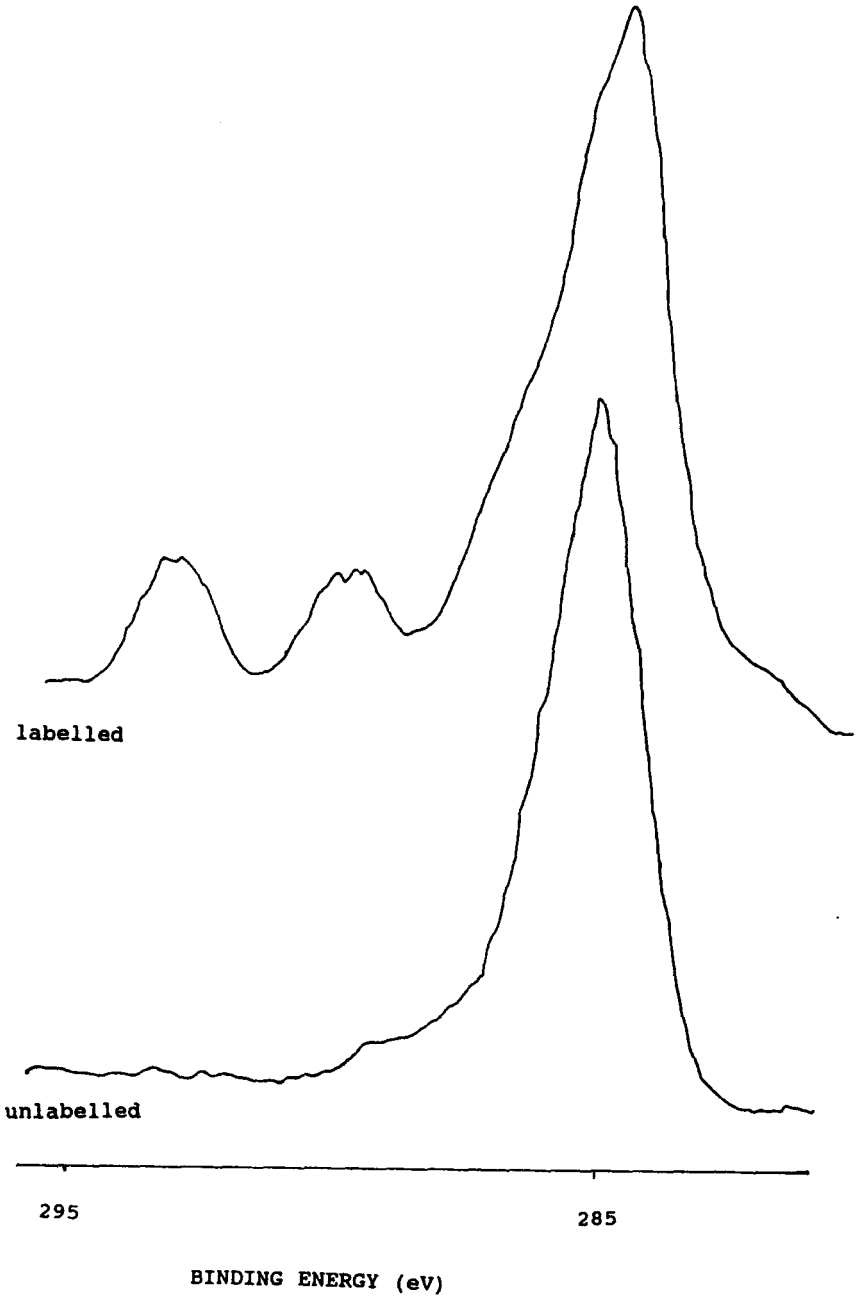

Figure 5.13 XPS Spectra of Labelled and Unlabelled Plasma Polymerised Allyl Alcohol.

were examined using XPS and found to have oxygen to carbon atomic ratios of 0.14 for the oxygen plasma treated and 0.13 for the water plasma treated samples.

5.4 COMPOSITE TESTING

5.4.1 MICROWAVE PLASMA TREATED FIBRES

The results of the disk compression test show a good correlation between disks taken from the same composite sample, however, the sample to sample variation is rather large. These errors are mainly due to, not being able to keep all the variable factors constant, such as: resin/hardener ratio, rate of heating, exact temperature of cure and the number of flaws in the final composite.

The treated fibres all show a marked improvement over the untreated ones but within the limitations of this test, all treatments appear to result in similar transverse tensile strengths. It was decided that the test could only reliably be used to determine whether a treatment was successful, rather than to what extent the treatment had affected composite performance. A treatment was considered to have improved composite performance when the transverse tensile strength of the treated sample was at least 100% better than that of an untreated sample prepared at the same time.

Table 5.3. Results of the Disc Compression Test.

Treatment	d(mm)	t(mm)	P(N)	r_t(MPa)	Average	O:C
untreated						
i)						
	6.50	2.35	650	27.1		
	6.55	2.33	610	25.4	26.1±0.7	0.11
	6.54	2.35	620	25.7		
ii)						
	6.35	1.31	600	45.9	47.2±1.3	
	6.36	1.32	640	48.5		
commercially surface treated fibres						
	6.55	1.97	1280	63.2		
	6.50	1.95	1550	77.8	69.5±6.1	0.17
	6.54	1.96	1360	67.5		
water						
	6.45	1.95	1530	77.4		
	6.43	1.92	1359	68.3	69.0±6.6	0.16
	6.44	1.85	1160	61.2		
oxygen						
	6.50	1.98	1540	76.2		
	6.00	1.95	1300	70.7	74.3±2.5	0.29
	6.50	1.98	1530	75.7		

5.4.2 COMPOSITE TESTING OF RF TREATED FIBRES.

RF plasma oxygen and water modified fibres were tested along side the fibres treated with allyl alcohol so that the effects of adaptation of the plasma rig and the different methods of excitation could be considered.

The only RF plasma modified sample which shows any improvement in tensile strength is that made with oxygen treated fibres, however this improvement is within the limits of sample to sample variation.

Table 5.4. Results of the Disc Compression Test on RF Modified Fibres.

	TRANSVERSE TENSILE STRENGTH (MPa)
PLASMA TREATMENT	
UNTREATED	23
WATER	28
OXYGEN	43
ALLYL ALCOHOL	19

5.4.3 EFFECT OF HUMIDITY

Composites made from both RF and MW plasma oxidised fibres were subjected to storage at 55°C, 100% R.H. for two weeks prior

to testing and compared to samples from the same batch stored under normal laboratory conditions during the same period. The effect of these different post formation storages are outlined in Table 5.5.

Table 5.5. Effect of Storage Environment on Transverse Tensile Strength.

TRANSVERSE TENSILE STRENGTH (MPa)

	STORAGE CONDITIONS	
PLASMA TREATMENT	AMBIENT	HUMID
MW		
UNTREATED	30	31
OXYGEN	80	65
WATER	74	52
RF		
UNTREATED	23	23
WATER	28	24
OXYGEN	43	38

The transverse tensile strength of composites formed from plasma modified fibres appears to be reduced by about 15-20% on storing in a humid environment. The usual errors seen across one composite sample are about 10% so this is a significant reduction in strength.

5.5 CONTACT ANGLE MEASUREMENTS ON CARBON FIBRES

The traces obtained using water as a wetting medium were very noisy (see Figure 5.14) and large fibre to fibre variations were noted, several factors cause this, non-uniform fibre perimeter, inhomogeneities of treatment, and in the case of the untreated fibres where a large effect was noted, impurities at the surface. The errors due to differences between individual fibres were far greater than those induced by the random variations along the length of an individual fibre. Using di-iodomethane much smoother traces were obtained, but these were thought to be distorted by the adsorption of the solvent, see Figure 5.15.

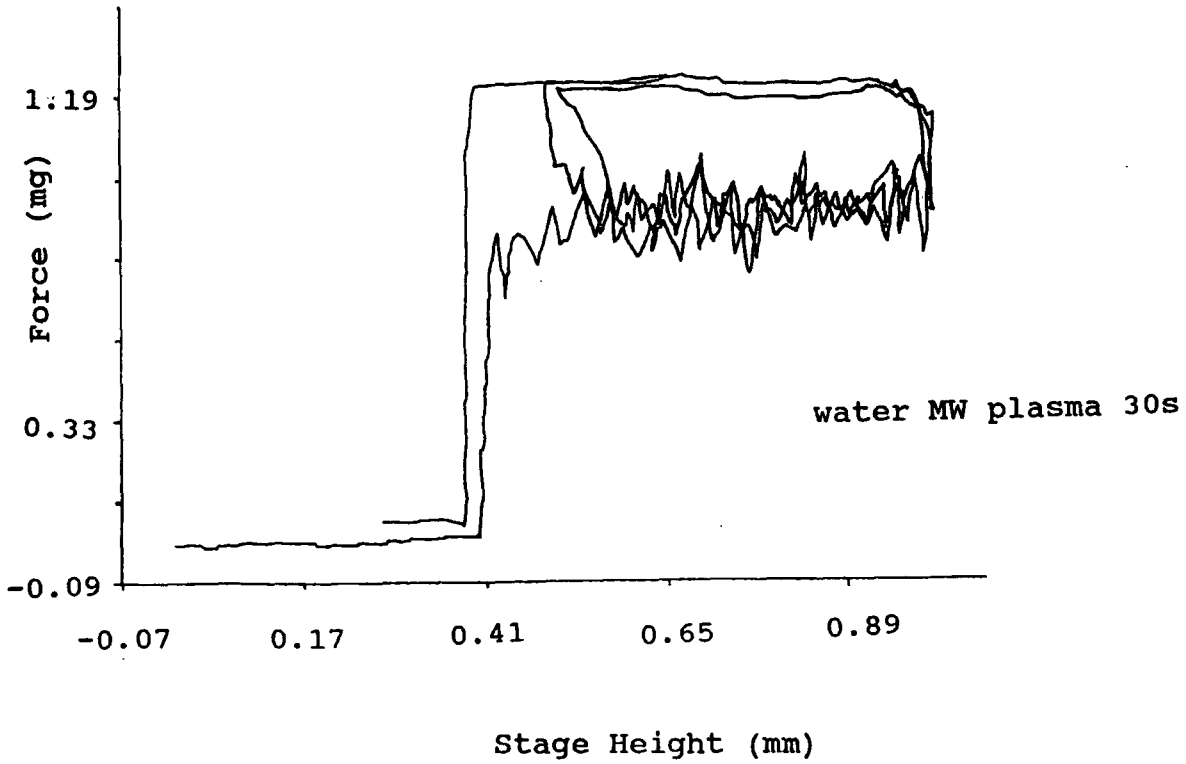

Figure 5.14 A Typical Graph Showing Contact Angle Hysteresis for a Single Fibre.

Both oxygen and water plasma treatments greatly increase the polarity of the carbon fibre surfaces, values are given in Table 5.6. The decrease in the dispersive contributions to surface energy are much less than values obtained for plasma treated polymers, but similar to those obtained for plasma treated graphite foils, see section 5.6.

Table 5.6. Effect of Plasma Treatment on Surface Energy.

TREATMENT	CONTACT ANGLE		SURFACE ENERGY (mNm^{-1}	
RF	CH_2I_2	H_2O	γ^d	γ^p
O_2				
5s	46	40	27	31
30s	52	34	23	37
H_2O				
5s	52	43	24	31
30s	53	35	23	38
MW				
O_2				
5s	47	38	26	33
30s	53	22	22	46
H2O				
5s	53	43	23	32
30s	54	42	23	33
untreated	47	75	32	7

Table 5.7. Effect of Ageing on Carbon Fibre Surface Energy.

TREATMENT	RECENTLY TREATED		AGED	
MW	γ^d	γ^p	γ^d	γ^p
O_2				
5s	26	33	29	16
30s	22	46	29	18
H_2O				
5s	23	32	27	26
30s	23	33	28	21

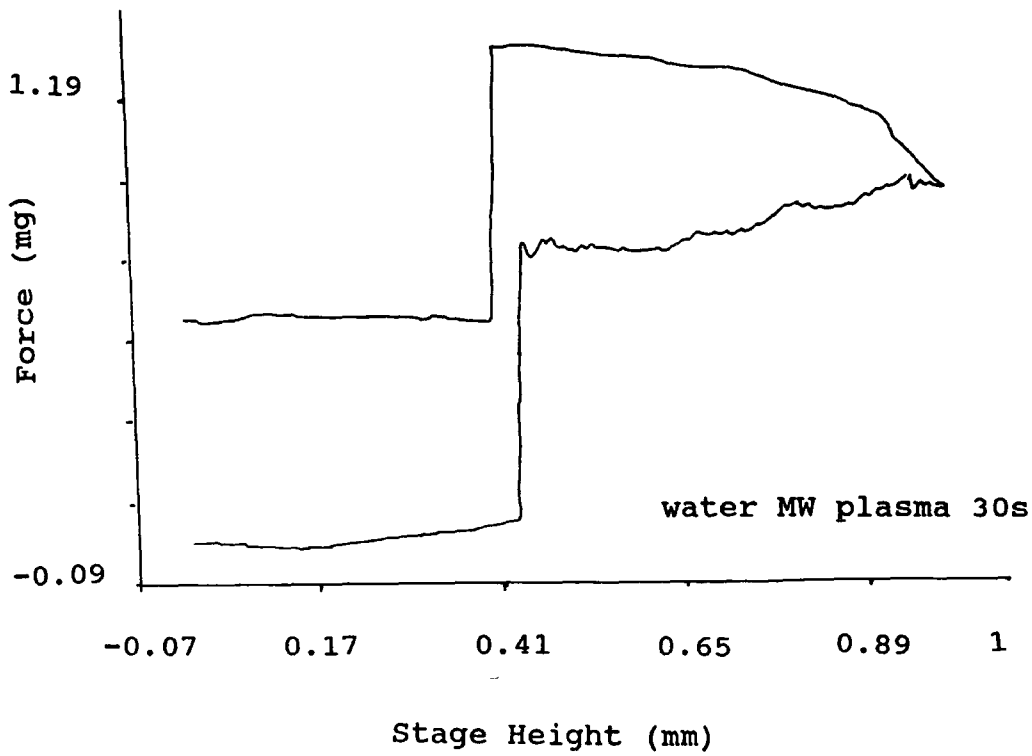

Figure 5.15. The Apparent Increase of Fibre Weight with Di-iodomethane.

On leaving the samples for three months prior to measuring their contact angles, the results show a significant decrease of the polar and slight increase of the dispersive contributions to the surface energy shown in Table 5.7. This is what would be expected if surface oxidised species were migrating into the bulk. It is unlikely that oxidised species are lost to the atmosphere as they are seen with XPS at 10^{-8} torr. It must also be noted that no significant changes were seen in the first five days after treatment, the ageing process is relatively slow reflecting the rigid structure of the carbon fibres.

5.6 PLASMA MODIFICATION OF GRAPHITE

5.6.1 INTRODUCTION

There are many problems incurred when analysing carbon fibres using XPS. It is impossible to depth profile the spectra as the incident X-rays impinge on the fibres at various angles. It is not possible to accurately determine the extent of oxidation after modification because of the incomplete penetration of the plasma into the carbon fibre tow. Also the fibres are electrically conducting and stray fibres tend to earth the plasma and can short circuit electrical equipment. Amorphous carbon foils are relatively safe, cheap and easy to work with. It was hoped that it would be possible to use these along with the more expensive oriented graphite foil as model systems for carbon fibres, so that depth profiling, extent of treatment, labelling and contact angles could be studied.

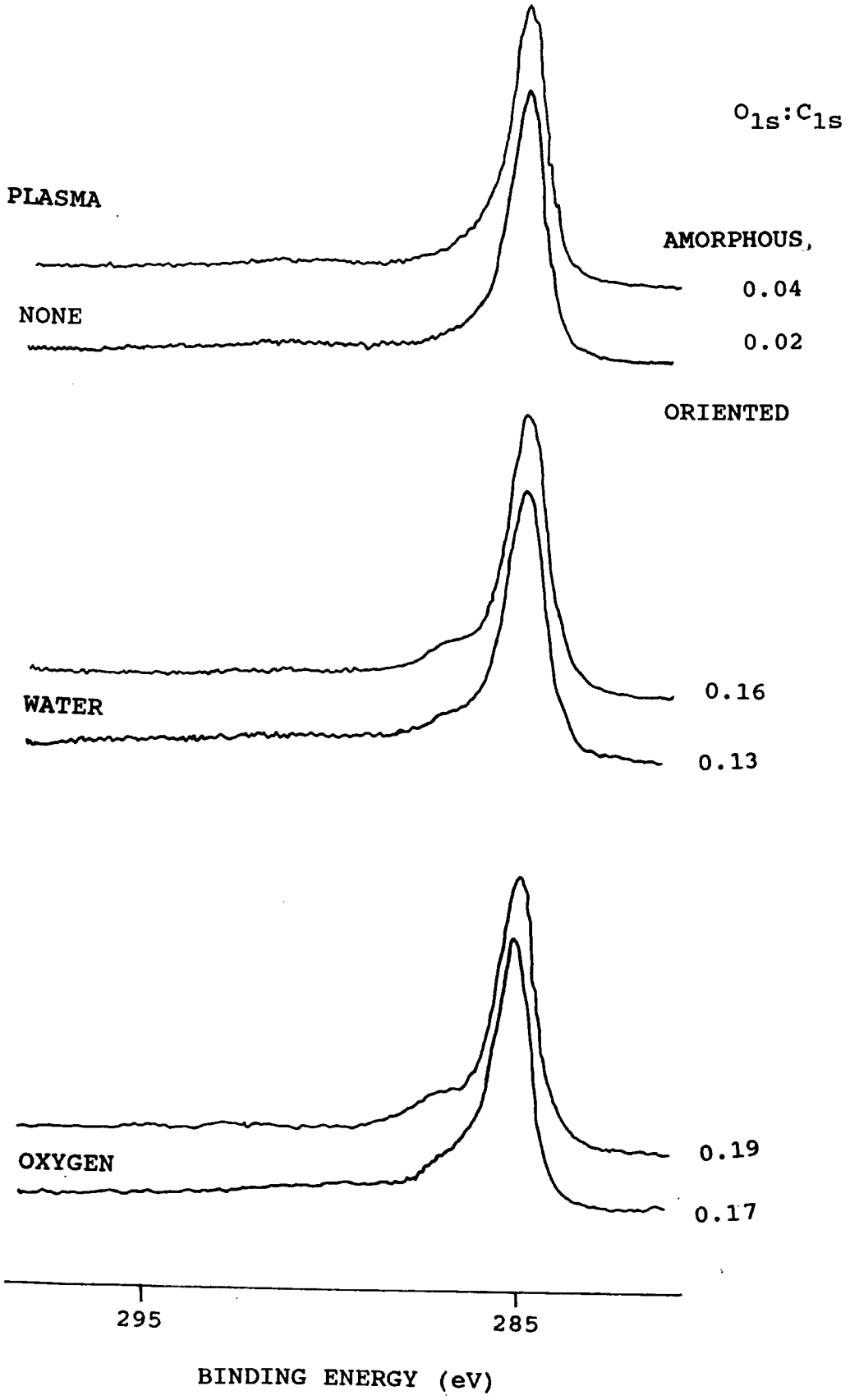

Figure 5.16. Plasma Modification of Graphite.

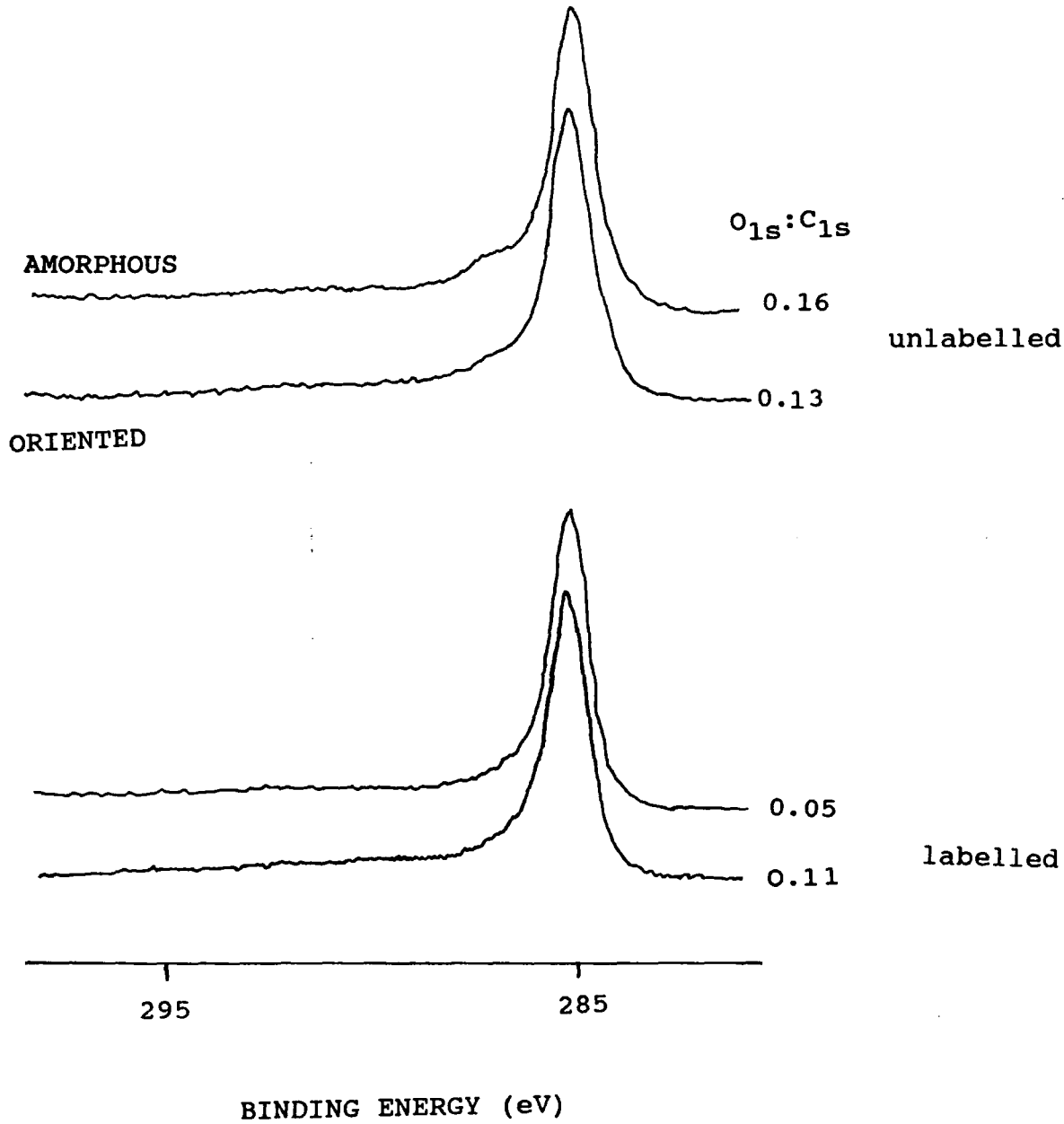

Figure 5.17. TFAA Labelling of Water Treated Graphite.

5.6 PLASMA MODIFICATION

The plasma treatments used were water, and oxygen microwave 40W, 30s, 0.1mbar, with leak rates of ca. $0.02cm^3min.^{-1}$ and flow rates of ca. $3cm^3min.^{-1}$. XPS spectra were obtained with take off angles of 35^o and 75^o, no significant difference was observed. All data presented is for spectra obtained at a take off angle of 35°. Figure 5.16 shows the effects of water and oxygen plasma treatments on oriented and amorphous graphite. As with the carbon fibres, water plasmas cause less oxidation than oxygen plasmas.

Oriented graphite is consistently but only marginally less

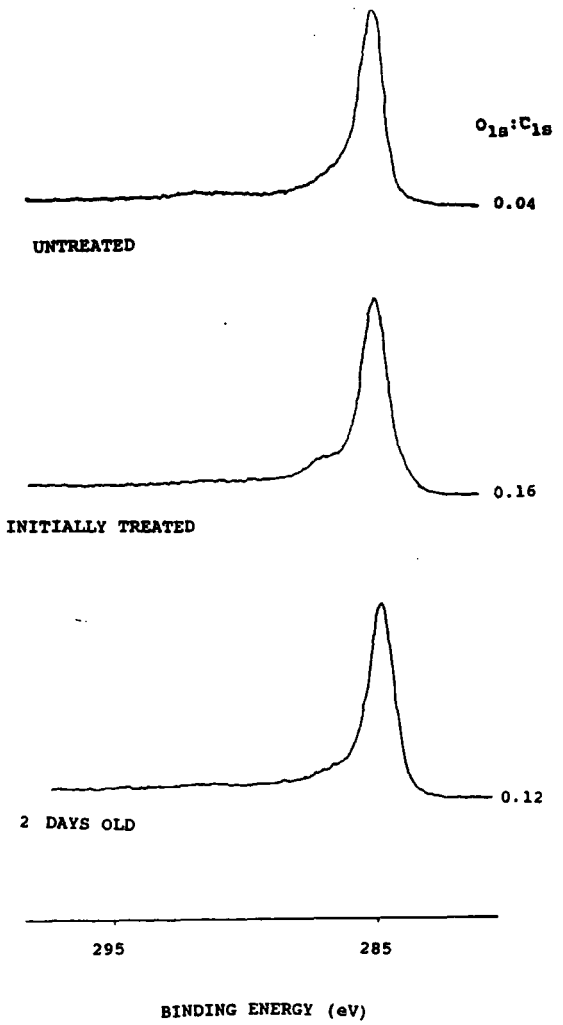

Figure 5.18. Ageing of Plasma Treated Amorphous Graphite.

oxidised than the amorphous material. All samples were oxidised to a lesser extent than the treated carbon fibres, however this may be due to the different initial extents of oxidation of the two materials. The most significant differences between the carbon fibres and graphite foils when the materials were labelled with TFAA. Figure 5.17 shows how TFAA labelling appears to remove all surface modification from the amorphous graphite, whereas with oriented samples some modification is lost and some labelling does occur. The greater instability of the plasma modified amorphous graphite surface was also reflected in its ease of removal with distilled water and its rapid surface decay, shown in Figure 5.18. In the case of oriented graphite some surface modification remained after washing and no significant changes were seen in the XPS spectra after ageing for two days.

Table 5.8. Contact Angle Measurements on Plasma Treated Graphite.

Sample	θ_w^o	θ_{CH2I2}^o	$\gamma^p(mNm^{-1})$	$\gamma^d(mNm^{-1})$
untreated graphite foils	54±1	21±1	17±0.5	39±3
untreated oriented graphite	51±3	48±3	26±1	50±3
oxidised graphite foils	31±1	38±6	38±1	27±3
oxidised oriented graphite	40±4	41±1	33±1	27±3

A similar water treatment was performed on amorphous graphite and oriented graphite. The contact angles with water and di-iodomethane were then measured, using the sessile drop method.[19] The polar and dispersive components of the surface tension in mNm^{-1} were calculated using the method outlined in Chapter One. The results are given in Table 5.8.

The oriented graphite initially has a much higher surface energy than the amorphous material this is most readily seen in the difference in the dispersion component of the surface energy, reflecting the more ordered surface structure of the oriented sample. After treatment both materials had similar dispersive components of surface energy indicating that in both samples the plasma had disrupted the surface to the same level. However, the polar component of the surface energy increased to the greatest extent in the amorphous graphite material.

5.7 DISCUSSION

It has been shown that all forms of plasma oxidation result in an increase in the amount of oxygen observed with XPS and a decrease in the surface energy of the carbon fibres, thus promoting the wetting of fibres with resin during composite manufacture. The untreated fibres show a high level of contamination at the surface, this will lead to what is known as a weak boundary layer,[20] which will inhibit adhesion of the fibres to the matrix material to the detriment of composite

strength. Plasma treatment cleans the carbon fibres resulting in a stronger interfacial region. Workers in China have ascribed the improvement in interlaminar shear strength observed upon plasma oxidation to an improvement in the carbon fibre surface strength[21] caused by the removal of this weak boundary layer. Other workers have concentrated on the increase in the polar component of the surface energy which occurs on plasma modification.[22,23] It is probable though that a combination of the cleaning and increase in polarity of the surface lead to the enhancement of transverse tensile strength.

RF plasma modification although increasing the degree of oxidation and the polar component of the surface energy, does not do so to the same extent as MW modification. This difference can be accounted for by the lower power density of the RF plasma compared to the MW plasma, although both plasmas were generated with the same amount of power the microwave plasma was generated in a much smaller volume leading to more vigorous oxidising conditions. The lower degree of oxidation and polarity does not entirely explain the low value of the transverse tensile strengths which are not significantly different to those for untreated fibres when the normal sample to sample variations are considered. It is possible that RF plasmas are not efficient at removing the weak boundary layer causing a weak interfacial region, however, the exposure times for the RF plasma modification were significantly longer than those used for the MW treatment. It is possible that the microwave plasmas induce different forms of modification compared to the radio frequency

plasmas, in the former case treatment occurs in the post glow region of the plasma whereas the RF plasma glow region completely filled the reaction vessel, thus the excited species reaching the fibres will be different in each case. The differences could be explained if MW treatment induced more crosslinking at the surface than RF oxidation, however the dispersive components of the surface energy after treatment show little evidence for this.

After allyl alcohol deposition, it appears that a hydroxyl rich surface has been formed on the carbon fibres, however it does not appear to have any great effect on the compressive strength of the composites formed. It is probable that incomplete coverage of the surface has occurred since the plasma is unlikely to flow extensively into the tow of fibres due to the limited volume[24] and the conductivity of the fibres causing the plasma to earth. It is also possible that the allyl alcohol plasma polymer itself is not adhering well to the carbon fibres, this is not of immediate relevance due to the incomplete coverage of the surface. The former problem could perhaps be overcome by treating small batches of fibres loosely spread in the batch reactor, this is somewhat impractical when considering the large amounts which need to be treated for subsequent testing. Adhesion of the plasma polymer could be improved by pretreating the fibre to clean the surface prior to plasma deposition.

The effect of humidity on composite strength has been documented before, and is thought to be due to the plasticising effect of water on the epoxy matrix.[25] It was observed that the humid environment had no detectable effect on the untreated

fibres, only a slight effect on the RF oxidised fibres and a more noticeable effect on the MW oxidised fibres. The increase in this effect with increasing composite strength is probably due to the change being more detectable, although it is possible that the different treatments render the fibre matrix interface more susceptible to penetration by water vapour.

Plasma modification of the graphitic foils showed initially similar results as those seen for carbon fibres, in that oxygen plasmas oxidise the graphite surface more than water plasmas.

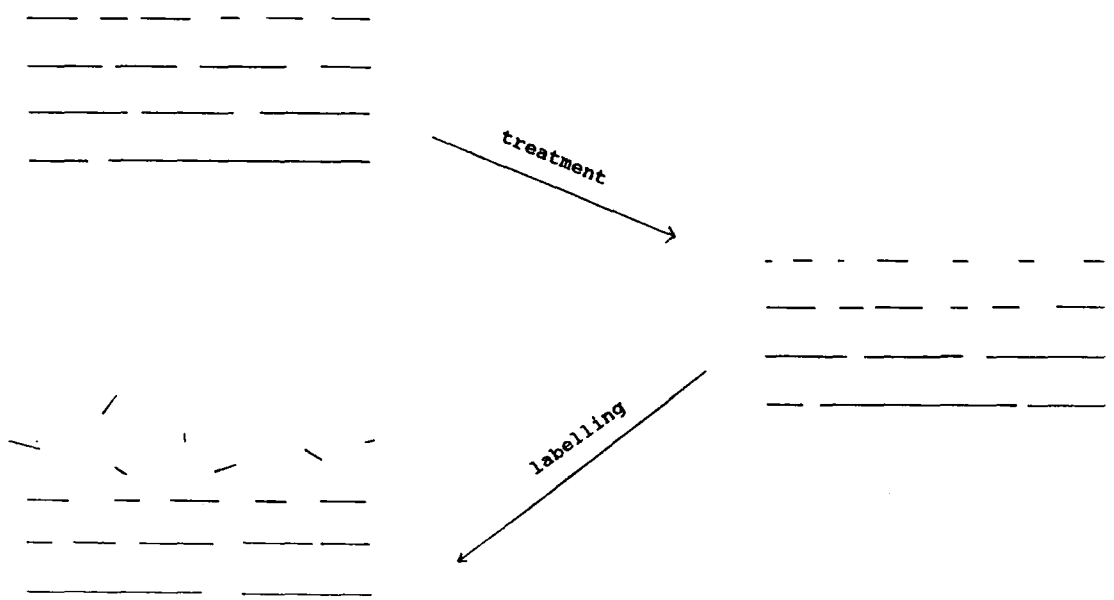

Figure 5.19 Schematic Representation of TFAA labelling of Graphite.

However, graphite had a very weakly bound surface, this resulted in the plasma modified surface having a great mobility. The ageing phenomenon seen after plasma modification is normally ascribed to the formation of a high energy surface which becomes more stable as a consequence of some of the oxidised species reorienting or migrating into the bulk. The results of the labelling experiment suggest that the surface formed after plasma oxidation of graphite may be more labile than has been observed previously in polymeric systems. Figure 5.19 shows schematically how volatilisation of the surface may occur.

The disappearance of the modified surface does not occur to such a great extent with oriented graphite suggesting that the more regular structure inhibits the removal of the modified layer.

The work described here amounts to a preliminary investigation into plasma modification of carbon fibres to enhance composite strength. Plasma treatment has been shown to be as good as current commercial treatments at improving composite performance in the disc compression test. This is despite the limited treatment of fibres in the centre of the tow. It can be envisaged that a more thorough treatment of the fibres on a production line before they are closely packed in a tow or formed into prepregs may further enhance composite properties. One of the main disadvantages of any commercial plasma treatment is the reduction of oxidation with time after modification and the tendency of newly modified surfaces to take up water from the

atmosphere and thus weaken the final composite. It is possible to overcome both of these problems by immediate formation of prepregs and the use of a controlled environment in the production, although this may not always be a reasonable alternative to current procedure.

REFERENCES

1. J.L. Kardos in "Molecular Characterisation of Composite Interfaces," Eds. H. Ishida & G. Kumar, Plenum Press, New York, 1985.
2. G. Lubin, "Handbook of Fibreglass and Advanced Plastic Composites," R.E. Kreiger, New York, 1969.
3. L.B. Greszczuk, Interfaces in Composites ASTM STP 452, 42, p58, 1969.
4. G. Dorey, J. Phys. D. Appl. Phys., 20, p245-256, 1987.
5. T. Takahagi et al., J. Polymer Sci. A, 244, p3101-3107, 1986.
6. Broutman, Interfaces in Composites ASTM STP 452, 42, p27-42, 1969.
7. A. Proctor & P.M.A. Sherwood, J. Electron Spec., 27, p39-56, 1982.
8. D. Briggs & M.P. Seah, "Practical Surface Analysis," John Wiley & Sons, Chichester, 1983.
9. C. Davis, Unpublished data.
10. A. Proctor and P.M.A. Sherwood, Carbon, 21, p53-59, 1983.
11. D.T. Clark and D. Shuttleworth, J. Polymer Sci., Polymer Chem. Ed.,16, p1093, 1978.
12. D.T. Clark, and A. Dilks, J. Polymer Sci., Polymer Chemistry Ed., 17, p957, 1979.
13. C. Davies and H.S. Munro, Polymer Communications, 29, p47, 1988.
14. D.J. Carlsson, R. Brousseau, Z. Can and D.M. Wiles, Polym. Degr. and Stability, 17, p305-38, 1987.

15. C. Till, unpublished data.

16. A. Rudnick, A.K. Hunter, F.C. Holden, Materials Research And Standards, April 1963.

17. J.C. Jaeger and E.R. Hoskins, J. Geophysical Research, 71, p2651, 1966.

18. W.R. Gombotz and A.S. Hoffman, Polym. Mater. Sci. Eng., 56, p720, 1987.

19. B.W. Cherry, "Polymer Surfaces," Cambridge University Press, Cambridge, 1981.

20. J.J. Bikerman, Ind and Eng. Chem, p40, September 1967.

21. T. Xiaoqiu, Y. Wei, Z. Zeng, Fuhe Cailiao Xuebao, 3(3), p1-7, 1986.

22. J.B. Donnet, M. Brendle, T.L. Dhami and O.P. Bahl, Carbon, 24(6), p757-70, 1986.

23. J.B. Donnet, T.L. Dhami, S. Dong and M. Brendle, J. Phys. D. Appl. Phys., 24(6), p757-70, 1986.

24. A.T. Bell in "Techniques and Applications of Plasma Chemistry", Eds. J.R. Hollahan And A.T. Bell, Wiley, New York, 1974.

25. J.M. Augl and A.E. Berger, Natl. SAMPE Tech. Conf., 8(Bicenten. Mater.), p383-427, 1976.

APPENDIX 1

DEPTH PROFILING WITH XPS

In the depth profiling experiment the angle of the sample surface to the incident X-rays is altered so that electrons at a depth, x, have to travel further to escape from the sample. However there is only a certain distance that the electrons can travel within the sample without undergoing inelastic collisions and forming part of the background noise detected by the analyser. Thus, the effective sampling depth is decreased (see figure).

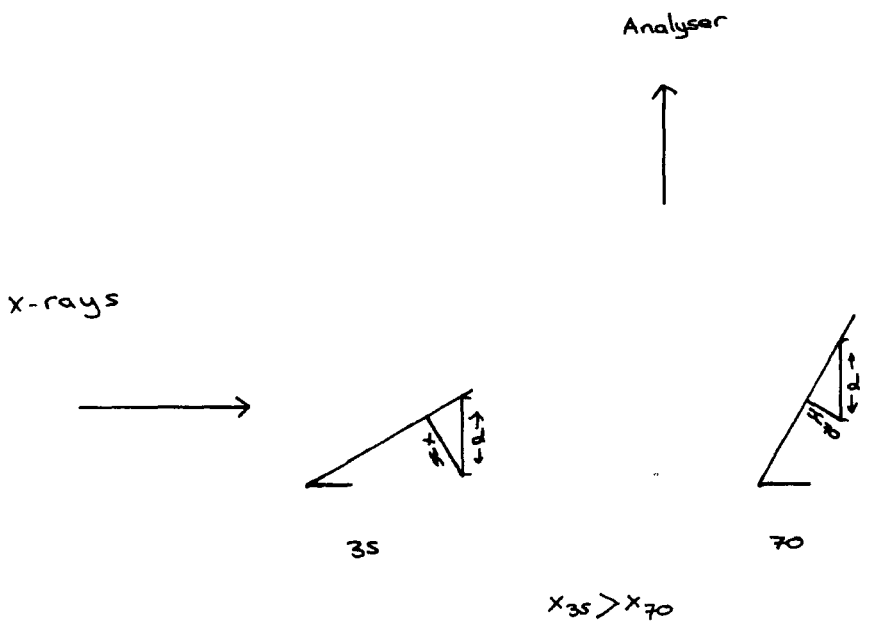

APPENDIX 2

COLLOQUIA, LECTURES AND SEMINARS GIVEN BY INVITED SPEAKERS IN DURHAM UNIVERSITY CHEMISTRY DEPARTMENT,

OCTOBER 1987 - APRIL 1990.

(Lectures attended are marked with an asterisk)

OCTOBER 1987 - JULY 1988

* BIRCHALL, PROF. D. (ICI ADVANCED MATERIALS) 25 APR 1988
ENVIRONMENTAL CHEMISTRY OF ALUMINIUM

* BORER, DR. K. (UNIVERSITY OF DURHAM INDUSTRIAL RESEARCH LABS.) 18 FEB 1988
THE BRIGHTON BOMB - A FORENSIC SCIENCE VIEW

BOSSONS, L. (DURHAM CHEMISTRY TEACHERS' CENTRE) 16 MAR 1988
GCSE PRACTICAL ASSEMENT

* BUTLER, DR. A.R. (UNIVERSITY OF ST. ANDREWS) 5 NOV 1988
CHINESE ALCHEMY

CAIRNS-SMITH, DR. A. (GLASGOW UNIVERSITY) 28 JAN 1988
CLAY MINERALS AND THE ORIGINS OF LIFE

DAVIDSON, DR. J. (HERRIOT-WATT UNIVERSITY) NOV 1987
METAL PROMOTED OLIGOMERISATION REACTIONS OF ALKYNES

* GRAHAM, PROF. W.A.G. (UNIVERSITY OF ALBERTA, CANADA) 3 MAR 1988
RHODIUM AND IRIDIUM COMPPLEXES IN THE ACTIVATION OF CARBON HYDROGEN BONDS

* GRAY, PROF. G.W. (UNIVERSITY OF HULL) 22 OCT 1987
LIQUID CRYSTALS AND THEIR APPLICATIONS

HARTSHORN, PROF M.P. (UNIVERSITY OF CANTERBURY, NEW ZEALAND) 7 APR 1988

* HOWARD, DR. J. (ICI, WILTON) 3 DEC 1987
CHEMISTRY OF NON-EQUILIBRIUM PROCESSES

* LUDMAN, DR C.J. (DURHAM UNIVERSITY) 10 DEC 1987
EXPLOSIVES

* MC DONALD, DR. W.A. (ICI, WILTON) 11 MAY 1988
LIQUID CRYSTAL POLYMERS

MAJORAL, PROF. J.-P. (UNIVERSITE PAUL SABATIER) 8 JUN 1988
STABILISATION BY COMPLEXATION OF SHORT LIVED PHOSPHORUS SPECIES

MAPLETOFT, MRS. M. (DURHAM CHEMISTRY TEACHERS' CENTRE) 4 NOV 1987
SALTERS' CHEMISTRY

NIETO DE CASTRO, PROF. C.A. (UNIVERSITY OF LISBON AND IMPERIAL COLLEGE) 18 APR 1988
TRANSPORT PROPERTIES OF NON-POLAR FLUIDS

* OLAH, PROF G.A. (UNIVERSITY OF SOUTHERN CALIFORNIA) 29 JUN 1988
NEW ASPECTS OF HYDROCARBON CHEMISTRY

* PALMER, DR. F. (UNIVERSITY OF NOTTINGHAM) 21 JAN 1988
LUMINESCENCE

PINES, PROF. A. (UNIVERSITY OF CALIFORNIA, BERKELEY, USA) 28 APR 1988
SOME MAGNETIC MOMENTS

RICHARDSON, DR. R. (UNIVERSITY OF BRISTOL) 27 APR 1988
X-RAY DIFFRACTION FROM SPREAD MONOLAYERS

* ROSE VAN MRS. S. (GEOLOGICAL MUSEUM) 29 OCT 1987
CHEMISTRY OF VOLCANOES

SAMMES, PROF P.G. (SMITH, KLINE AND FRENCH) 19 DEC 1987
CHEMICAL ASPECTS OF DRUG DEVELOPMENT

* SEEBACH, PROF. D. (ETH ZURICH) 12 NOV 1987
FROM SYNTHETIC METHODS TO MECHANISTIC INSIGHT

SODEAU, DR. J. (UEA) 11 MAY 1988
DURHAM CHEMISTRY TEACHERS' CENTRE LECTURE: "SPRAY CANS SMOG AND SOCIETY"

SWART, MR. R.M. (ICI) 16 DEC 1988
THE INTERACTION OF CHEMICALS WITH BILIPID LAYERS

TURNER, PROF. J.J. (UNIVERSITY OF NOTTINGHAM) 11 FEB 1988
CATCHING ORGANOMETALLIC INTERMEDIATES

* UNDERHILL, PROF. A. (UNIVERSITY OF BANGOR) 25 FEB 1988
MOLECULAR ELECTRONICS

WILLIAMS, DR. D.H. (UNIVERSITY OF CAMBRIDGE) 26 NOV 1987
MOLECULAR RECOGNITION

* WINTER, DR. M.J. (UNIVERSITY OF SHEFFIELD) 15 OCT 1987
PYROTECHNICS

AUGUST 1988 - JULY 1989

* AVEYARD, DR. R. (UNIVERSITY OF HULL) 15 MAR 1989
SURFACTANTS AT YOUR SURFACE

AYLETT, PROF. B.J. (QUEEN MARY COLLEGE, LONDON) 16 FEB 1989
SILICON BASED CHIPS THE CHEMISTS CONTRIBUTION

* BALDWIN, PROF. J.E. (OXFORD UNIVERSITY) 9 FEB 1989
RECENT ADVANCES IIN THE BIOORGANIC CHEMISTRY OF PENICILLIN BIOSYNTHESIS

* BALDWIN AND WALKER, DRS. R.R. AND R.W. (HULL UNIVERSITY) 24 NOV 1988
COMBUSTION: SOME BURNING PROBLEMS

BUTLER, DR. A.R. (ST. ANDREWS UNIVERSITY) 15 FEB 1989
CANCER IN LIXIAM

* CADOGAN, PROF. J.I.G. (BP) 10 NOV 1988
FROM PURE SCIENCE TO PROFIT

CASEY, DR. M. (UNIVERSITY OF SALFORD) 20 APR 1989
SULPHOXIDES IN STEREOSELECTIVE SYNTHESIS

CRICH, DR. D. (UNIVERSITY COLLEGE LONDON) 27 APR 1989
SOME NOVEL USES OF FREE RADICALS IN ORGANIC SYNTHESIS

DINGWALL, DR. J. (CIBA GEIGY) 19 OCT 1988
PHOSPHORUS CONTAINING AMINO ACIDS

FREY, DR. J. (SOUTHAMPTON UNIVERSITY) 11 MAY 1989
SPECTROSCOPY OF THE REACTION PATH

* HALL, PROF. L.D. (ADDENBROOKES HOSPITAL) 2 FEB 1989
NMR - A WINDOW TO THE HUMAN BODY

HARGROVE, DR. G. (ST. OLAF COLLEGE USA) DEC 1988
POLYMERS IN THE PHYSICAL CHEMISTRY LABORATORY

JENNINGS, PROF. R.R. (WARWICK UNIVERSITY) 26 FEB 1989
CHEMISTRY OF THE MASSES

JOHNSON, DR. B.F.G. (CAMBRIDGE UNIVERSITY) 23 FEB 1989
BINARY CARBONYLS

* LUDMAN, DR. C.J. (DURHAM UNIVERSITY) 18 OCT 1989
THE ENERGETICS OF EXPLOSIVES

MACDOUGALL, DR. G, (EDINBURGH UNIVERSITY) 22 FEB 1989
VIBRATIONAL SPECTROSCOPY OF MODEDL CATALYTIC SYSTEMS

* MCLAUCHLAN, DR. K.A. (UNIVERSITY OF OXFORD) 16 NOV 1988
THE EFFECT OF MAGNETIC FIELDS ON CHEMICAL REACTIONS

MOODY, DR. C.J. (IMPERIAL COLLEGE) 17 MAY 1989
REACTIVE INTERMEDIATES IN HETEROCYCLIC SYNTHESIS

PAETZOLD, PROF. P. (AACHEN) 23 MAY 1989
IMINOBORANES XB=NR

POLA, PROF J. (CZECHOSLOVAK ACADEMY OF SCIENCES) 15 JUN 1989
CARBON DIOXIDE LASEER INDUCED CHEMICAL REACTIONS

REES. PROF. C.W. (IMPERIAL COLLEGE) 27 OCT 1988
SOME VERY HETROCYCLIC COMPOUNDS

SCHMUTZLER, PROF. R. (TECHNISCHE UNIVERITAT BRAUNSCHWEIG) 6 OCT 1988
FLUOROPHOSPHINES REVISITED

* SCHROCK, PROF. R.R. (MIT) 13 FEB 1989
RECENT ADVANCES IN LIVING METATHESIS

SINGH, DR. G. (TEESSIDE POLYTECHNIC) 9 NOV 1988
TOWARDS THIRD GENERATION ANTI-LEUKAEMICS

* SNAITH, DR. R. (CAMBRIDGE UNIVERSITY) 1 DEC 1988
EGYPTION MUMMIES

STIBR, DR. R. (CZECHOSLOVAK ACADEMY OF SCIENCE) 16 MAY 1989
RECENT DEVELOPMENTS IN SITED CARBORANES

AUGUST 1989 -APRIL 1990

* BADYAL, DR. J.P.S (DURHAM UNIVERSITY) 1 NOV 1989
BREAKTHROUGHS IN HETEROGENEOUS CATALYSIS

BECHER, DR. J. (ODENSE UNIVERSITY) 13 NOV 1989
SYNTHESIS OF NEW MACROCYCLIC SYSTEMS USING HEREOCYCLIC BUILDING BLOCKS

BERCAW, PROF. J.E. (CALAFORNIA INSTITUTE OF TECHNOLOGY) 10 NOV 1989
SYNTHETIC AND MECHANISTIC APPROACHES TO ZIEGLER-NATTA POLYMERISATION OF OLEFINS

BLEASDALE, DR. C. (NEWCASTLE UNIVERSITY) 21 FEB 1990
THE MODE OF ACTION OF SOME ANT-TUMOUR AGENTS

BOWMAN, PROF. J.M. (EMORY UNIVERSITY) 23 MAR 1990
FITTHNG EXPERIMENT WITH THEORY IN AROH

CHADWICK, DR. P. (UNIVERSITY OF DURHAM) 24 JAN 1990
RECENT THEORIES OF THE UNIVERSE

* CHEETHAM, DR. A.K. (OXFORD UNIVERSITY) 8 MAR 1990
CHEMISTRY OF ZEOLITE CAGES

* CLARK, PROF. D.T. (ICI, WILTON) 22 FEB 1990
USING NATURE'S PARADIGM IN THE ADVANCED MATERIALS ARENA

COLE-HAMILTON, PROF. D.J. (ST. ANDREW'S UNIVERSITY) 29 NOV 1989
NEW POLYMERS FROM HOMOGENEOUS CATALYSIS

* CROMBIE, PROF. L. (NOTTINGHAM UNIVERSITY) 15 FEB 1990
THE CHEMISTRY OF CANNABIS AND KHAT

DYER, DR. U. (GLAXO) 31 JAN 1990
SYNTHESIS AND COONFORMATION OF C- GLYCOSIDES

* FLORIANI, PROF. C. (UNIVERITY OF LAUSANNE, SWITZERLAND) 25 OCT 1989
MOLECULAR AGGREGATE - A BRIDGE BETWEEN HOMOGENEOUS AND HETEROGENEOUS SYSTEMS

GRAHAM, DR. D. (BP) 4 DEC 1989
HOW PROTEINS ABSORB TO INTERFACES

* GREENWOOD, PROF. N.N. (UNIVERSITY OF LEEDS) 9 NOV 1989
NOVEL CLUSTER GEOMETRIES IN METALLOBORANE CHEMISTRY

HOLLOWAY, PROF. J.H. (UNIVERSITY OF LEICESTER) 1 FEB 1990
NOBLE GAS CHEMISTRY

HUGHES, DR. M.N. (KINGS COLLEGE, LONDON) 30 NOV 1989
A BUGS EYE VIEW OF THE PERIODIC TABLE

HUISGEN, PROF. R. (UNIVERSITAT MUNCHEN) 15 DEC 1989
RECENT MECHANISTIC STUDIES OF [2+2] ADDITIONS

IDDON, DR. B. (UNIVERITY OF SALFORD) 15 DEC 1989
SCHOOLS LECTURE: THE MAGIC OF CHEMISTRY

KLINOWSKI, DR. J. (CAMBRIDGE UNIVERSITY) 13 DEC 1989
SOLID STATE NMR STUDIES OF ZEOLITIC CATALYSTS

LUNAZZI, PROF. L. (UNIVERSITY OF BOLOGNA) 12 JAN 1990
APPLICATION OF DYNAMIC NMR TO THE STUDY OF CONFORMATIONAL ENANTIOMERISM

* PALMER, DR. F. (NOTTINGHAM UNIVERSITY) 17 OCT 1989
THUNDER AND LIGHTENING

PARKER, DR. D. (DURHAM UNIVERSITY) 16 NOV 1989
MACROCYCLES, DRUGS AND ROCK'N'ROLL

PERUTZ, DR. R.N. (YORK UNIVERSITY) 24 JAN 1990
PLOTTING THE COURSE OF C-H ACTIVATIONS WITH ORGANOMETALLICS

POWELL, DR. R.L. (ICI) 6 DEC 1989
THE DEVELOPMENT OF CFC REPLACEMENTS

POWIS, DR. I. (NOTTINGHAM UNIVERSITY) 21 MAR 1990
SPINNING OFF IN A HUFF: PHOTO DISSOCIATION OF METHYL IODIDE

STODDART, DR. J.F. (SHEFFIELD UNIVERSITY) 1 MAR 1990
MOLECULAR LEGO

SUTTON, PROF. D. (SIMON FRASER UNIVERSITY, B.C.) 14 FEB 1990
SYNTHESIS AND APPLICATIONS OF DINITROGEN AND DIAZO COMPOUNDS OF RHENIUM AND IRIDIUM

THOMAS, DR. R.K. (OXFORD UNIVERSITY) 28 FEB 1990
NEUTRON REFLECTOMETRY FROM SURFACES

THOMPSON, DR. D.P. (NEWCASTLE UNIVERSITY) 7 FEB 1990
THE ROLE OF NITROGEN IN EXTENDING SILICATE CRYSTAL CHEMISTRY